

Elucidating the origin and mechanism of a non-canonical auxin signalling pathway in lateral organ development

by

Chun Hou (Aaron) Ang

January 2024

A thesis submitted to the University of East Anglia for
the degree of
Doctor of Philosophy

University of East Anglia
John Innes Centre

© This copy of the thesis has been supplied on condition that anyone who consults it is understood to recognise that its copyright rests with the author and that use of any information derived there from must be in accordance with current UK Copyright Law. In addition, any quotation or extract must include full attribution.

This thesis is dedicated to my mother Ker Ah Lian.

Abstract

The development of complex body plans in multicellular life from a single pluripotent cell necessitates mechanisms that regulate cell differentiation and tissue patterning. The phytohormone auxin plays an important role in almost every aspect of plant growth and development. While the perception and downstream signalling of auxin has been mainly attributed to a canonical degradation-based pathway, numerous alternative pathways have been described in recent years. One such pathway involves a direct auxin-induced switch in the transcriptional regulatory activity of the Auxin Response Factor (ARF) ETTIN (ETT/ARF3). ETT has a middle region domain that contains motifs associated with direct auxin binding and lacks a conserved C-terminus domain involved in canonical pathway interactions. As the ETT clade only exists in the angiosperms, it remains unknown when the pathway evolved. This thesis reports a two-step origin of the ETT clade and its neofunctionalisation through the gain of auxin perception for the role of gynoecium patterning. Phylogenetic analyses confirmed that ETT and its paralogue ARF4 diverged from an ancestral euphyllophyte ETT/ARF4-like clade in the angiosperms and that these paralogues have diverged in motif sequence and domain structure. Auxin sensitivity was identified as an ETT-specific innovation that likely originated in the last common angiosperm ancestor. Importantly, it was found that the DNA-binding domain of ETT influenced auxin sensing, implicating the complex nature of auxin binding by ETT. Furthermore, *in planta* complementation experiments demonstrated the full genetic redundancy of ETT and ARF4 in leaf and ovary patterning, but a specialised role for the ETT-mediated auxin signalling pathway in style development. Together, this thesis supports the hypothesis that ETT was recruited from an ancestral leaf development role and has undergone neofunctionalisation through the acquisition of direct auxin sensing for a novel role in gynoecium patterning.

Access Condition and Agreement

Each deposit in UEA Digital Repository is protected by copyright and other intellectual property rights, and duplication or sale of all or part of any of the Data Collections is not permitted, except that material may be duplicated by you for your research use or for educational purposes in electronic or print form. You must obtain permission from the copyright holder, usually the author, for any other use. Exceptions only apply where a deposit may be explicitly provided under a stated licence, such as a Creative Commons licence or Open Government licence.

Electronic or print copies may not be offered, whether for sale or otherwise to anyone, unless explicitly stated under a Creative Commons or Open Government license. Unauthorised reproduction, editing or reformatting for resale purposes is explicitly prohibited (except where approved by the copyright holder themselves) and UEA reserves the right to take immediate 'take down' action on behalf of the copyright and/or rights holder if this Access condition of the UEA Digital Repository is breached. Any material in this database has been supplied on the understanding that it is copyright material and that no quotation from the material may be published without proper acknowledgement.

Acknowledgements

Firstly, I would like to thank Prof. Lars Østergaard as the primary supervisor of my PhD. Thank you, Lars, for the support, guidance, and freedom that you have provided me throughout my entire PhD journey, from the drafting of my first proposal to the completion of this thesis. Your enthusiasm, generosity and friendly demeanour allowed me to push on despite the challenges posed by the Covid-19 pandemic. But most of all, thank you for directly influencing the trajectory of my life and career, through your help in establishing a collaboration with the group of Prof. Dolf Weijers in the Netherlands.

I would therefore also like to thank Dolf, Dr. Sumanth Mutte and Ellis van de Laak for the collaboration that generated the *in silico* data of Chapter 2. I would like to thank Sumanth as well for his help in proofreading Chapter 2 of the thesis. Dolf also accepted me for a six-month internship in his lab which allowed me to enhance my technical and analytical skills and expand my social network which made me a better scientist. For that, I express my profound gratitude.

I would also like to thank my secondary supervisor, Dr. Xiaoqi Feng for her helpful comments and advice throughout my PhD project. More importantly, Xiao was the one who inspired me to pursue a career in academia as I had such an amazing experience conducting my undergraduate summer internship in her lab.

In both labs, I have made valuable connections both professionally and personally with my colleagues. In particular, I would like to sincerely thank Dr. Andre Kuhn and Dr. Yuli Ding for their immense support during the first two years of my PhD. The research materials (seeds, vectors, and reagents), technical support and constructive criticisms from the both of you were instrumental in the development of my hypothesis and the completion of this thesis. Thank you as well to Dr. Yuxiang Jiang for helping me with the crossing and maintenance of plant lines while I was

away on internship. More importantly, you three have been there for me for my personal issues, and for that I consider you true friends.

Though some unsuccessful experiments did not make it into this thesis, I am still grateful for the help in attempting them. Thank you, Dr. Pingtao Ding and Juriaan Rienstra for teaching and helping me with DAP-seq respectively. I would also like to thank Sjoerd Woudenberg for his assistance with the *Ceratopteris richardii* transformation. I extend my thanks to Dr. Rebecca Povilus, Dr. Andy Plackett, Dr. Phil Carella and the staff at Cambridge Botanic Gardens for the provision of important plant materials that made the evolutionary analyses possible.

The research also would not have been possible without the generous funding that I have been provided by the Gatsby Charitable Foundation. Furthermore, the training weekends, network meetings and scientific advice from the advisory board have enriched my PhD experience. Hence, I would like to thank the advisers and funders at Gatsby for giving me this life-changing opportunity.

I have also been fortunate enough to have the love and support of my partner, Ruben Massop, that gave me the strength to complete this PhD. Although we could not always be together physically during my PhD, you have always been there for me through the highs and the lows. I am a very lucky man to have you by my side, and I truly appreciate how much you have helped me. Bedankt voor alles, mijn schatje.

Finally, I would like to thank my brother and my mother, for I would not have been the person that I am today without them. Thank you, Jordan, for always being supportive of me since our shared childhoods. And thank you, mum, for all your sacrifice these years to provide for us and ensure that we can be the best person that we can possibly be. 即使世界对你非常不公，你也应该知道我有多在乎你。你是世界上最伟大的妈妈，我会尽我所能让你感到骄傲。

Table of Contents

Abstract.....	I
Acknowledgements.....	II
Table of Contents.....	IV
List of Figures and Tables.....	VII
Chapter 1: General introduction.....	1
1.1 Principles of morphogenesis in multicellular organisms.....	2
1.2 Mechanisms of auxin signalling in plants.....	6
1.2.1 The biosynthesis and transport of auxin.....	6
1.2.2 The canonical TIR1/AFB-dependent pathway.....	7
1.2.3 Rapid auxin responses through alternative pathways.....	14
1.2.4 The ETT-mediated auxin signalling pathway.....	18
1.3 Development and evolution of lateral organs in plants.....	20
1.3.1 Novel roles of ancient regulators in body plan innovations.....	20
1.3.2 The abaxial-adaxial leaf polarity network.....	23
1.3.3 Gynoecium initiation and its apical-basal patterning.....	28
1.4 Scope of the thesis.....	32
Chapter 2: A deep phylogenetical analysis of the Class B ARFs reveals the stepwise evolution of the ETT/ARF4 clade and its associated motifs and domains.	35
2.1 Introduction.....	36
2.2 Results.....	39
2.2.1 The ETT/ARF4-like clade originated after the divergence of the euphyllophytes.....	39
2.2.2 Diverging trajectories of ETT and ARF4 structural evolution in the core angiosperms.....	41
2.2.3 Delineation of ETT and ARF4 through variants in conserved middle region motifs.....	44
2.3 Discussion.....	48
2.3.1 The ETT/ARF4 clade is an euphyllophyte innovation.....	50
2.3.2 Diverging trajectories of ETT and ARF4 clade evolution in core angiosperms.....	52
2.3.3 Delineation of ETT and ARF4 through middle region motifs.....	54
2.4 Concluding Remarks.....	56
2.5 Materials and Methods.....	58
2.5.1 Data acquisition and phylogenetic tree construction.....	58
2.5.2 Middle region motif identification and visualisation.....	58
Chapter 3: The ETT-mediated auxin signalling pathway might have originated in the last common ancestor of flowering plants.....	59

3.1	Introduction	60
3.2	Results	63
3.2.1	Conserved interactions between ETT and abaxial domain transcription factors may be auxin-insensitive	63
3.2.2	The ETT-mediated auxin signalling pathway may have originated in the last common angiosperm ancestor	66
3.2.3	The auxin-sensing property of ETT is strongly associated with a specific region of the ES domain.....	71
3.3	Discussion.....	74
3.3.1	The auxin sensing ability of ETT is a neofunctionalisation of the angiosperms.....	76
3.3.2	The ES domain is not the sole domain influencing the auxin sensitivity of ETT	78
3.3.3	The role of the ETT-mediated auxin signalling pathway in leaf dorsiventral polarity is uncertain.....	79
3.4	Concluding Remarks.....	80
3.5	Materials and Methods.....	82
3.5.1	Orthologue identification	82
3.5.2	Plant material and growth conditions	83
3.5.3	RNA isolation and cDNA synthesis.....	84
3.5.4	Generation of Y2H constructs.....	84
3.5.5	Yeast 2 hybrid interaction assays	85
3.5.6	Leaf area measurements and statistical analyses	85
Chapter 4: The ETT clade was co-opted for gynoecium development from an ancestral vegetative role		86
4.1	Introduction	87
4.2	Results	91
4.2.1	The role of ETT in gynoecium development arose in the last common ancestor of flowering plants	91
4.2.2	The ETT/ARF4-like clade has an ancestral role in vegetative development.....	95
4.2.3	The ETT-mediated auxin signalling pathway influences style development.....	98
4.3	Discussion.....	100
4.3.1	The evolution of the dual roles of ETT in gynoecium development occurred after the divergence of the angiosperms	100
4.3.2	The ETT/ARF4-like clade acquired its function in leaf polarity and development after the origin of seed plants	103
4.3.3	Auxin sensitivity is necessary for proper style morphogenesis.....	105
4.4	Concluding Remarks.....	106

4.5	Materials and Methods	108
4.5.1	CRISPR/Cas9-mediated gene editing	108
4.5.2	Generation of ETT/ARF4 complementation lines	110
4.5.3	Genotyping of transgenic plants	110
4.5.4	Quantitative real-time PCR	111
4.5.5	Scanning Electron Microscopy	112
4.5.6	Phenotyping of complementation lines	112
Chapter 5: General discussion		113
5.1	Introduction	114
5.2	The ETT/ARF4-like clade is conserved within the euphyllophytes	115
5.3	ETT and ARF4 have undergone divergent evolutionary trajectories	117
5.4	Auxin sensing is a neofunctionalisation of the ETT clade	119
5.5	The ETT DBD and MR contributes to its auxin sensitivity	121
5.6	ETT-mediated auxin signalling is an innovation for style development ...	123
5.7	Concluding Remarks	127
Appendix		129
List of Abbreviations		130
Supplementary data from Chapter 2		134
Supplementary data from Chapter 3		140
Supplementary data from Chapter 4		156
References		161

List of Figures and Tables

Figure Number	Page No.
Figure 1.1: Canonical phytohormone signalling pathways	5
Figure 1.2: Canonical and alternative auxin signalling pathways	8
Figure 1.3: Structure and function of canonical auxin signalling components	10
Figure 1.4: Anatomy and gene regulatory networks of the <i>A. thaliana</i> gynoecium and leaf	25
Figure 2.1: Phylogenetic tree of the ETT/ARF4-like clade in land plants	40
Figure 2.2: Copy number of ETT/ARF4-like orthologues in euphyllophyte genomes	43
Figure 2.3: Enriched middle region motifs in ETT and ARF4 orthologues	45
Figure 2.4: Alignment of monilophyte ETT/ARF4-like MR sequences	47
Figure 2.5: Domain changes in ETT/ARF4-like orthologues in the euphyllophytes	49
Figure 3.1: Y2H interaction screen of the KAN and YAB families in the seed plants	65
Figure 3.2: Auxin-sensitivity Y2H interaction assay of ETT/ARF4 orthologues with the KAN and YAB families	67
Figure 3.3: Phylogeny of the TPL/TPR family included in the Y2H assay	69
Figure 3.4: Y2H interaction screen of the TPL/TPR family in the land plants	70
Figure 3.5: Auxin-sensitivity Y2H assay for ETT/ARF4-TPL/TPR interactions	72
Figure 3.6: Domain swapped chimeric constructs to investigate regions contributing to ETT auxin sensitivity	73
Figure 3.7: Auxin sensitivity Y2H screen of the interactions between chimeric ETT/ARF4-like constructs and the TPL/TPR corepressors	75
Figure 4.1: Gynoecium morphology of wild-type, mutant, and ETT/ARF4 genetic complementation lines	92

Figure 4.2: Relative expression levels of PID in wild-type, mutant and ETT/ARF4-like complementation lines	95
Figure 4.3: Leaf phenotypes of the ett-3 arf4GE complementation lines	97
Figure 4.4: Gynoecium phenotypes of genetic complementation lines expressing chimeric ETT/ARF4-like constructs	99
Figure 5.1: Model of the molecular mechanism of ETT and ARF4 during leaf and gynoecium development	125
Figure S2.1: Full Class B ARF phylogeny of land plants	134
Figure S2.2: Biophysical and compositional parameters of ETT/ARF3 and ARF4	135
Table S2.1: Genomes included in the Class B ARF phylogeny	136
Table S3.1: List of KAN, YAB, TPL/TPR and ETT/ARF4-like orthologues used in the Y2H screens	140
Table S3.2. List of oligonucleotides used in Chapter 3	142
Figure S3.1: Leaf phenotypes of the pETT:ETT ^{2CS} auxin-insensitive line	152
Figure S3.2: Y2H auto-activation test for ETT/ARF4-like orthologues	153
Figure S3.3: Y2H screen of chimeric ARF constructs with TPL/TPR orthologues	154
Figure S3.4: Y2H interaction assay to test for ETT and ARF4 interactions with AUX/IAAs	155
Table S4.1: List of oligonucleotides used in Chapter 4	156
Figure S4.1: Expression level of ETT/ARF4-like orthologues in transgenic ett-3 complementation lines	158
Figure S4.2: Lateral view of the gynoecium of wild-type, mutant and ETT/ARF4-like complementation lines	159
Figure S4.3: Rosette phenotypes of wild-type and <i>A. trichopoda</i> ETT-derived complementation lines	160

Chapter 1:

General introduction

Sections 1.2.3 - 1.2.5 on alternative auxin signalling pathways have been published as:

Ang, A.C.H., and Østergaard, L. (2023). Save your TIRs – more to auxin than meets the eye. *New Phytologist* 238, 971-976.

1.1 Principles of morphogenesis in multicellular organisms

The biodiversity of life on Earth is manifested through the myriad forms and shapes exhibited by plants and animals as a product of billions of years of natural selection. This diversity in shape and form can largely be attributed to differences in cell types and cellular organisation. Despite this diversity, every cell within a multicellular organism traces its origins to a single progenitor cell, the zygote, and harbours the same genomic blueprint. Thus, highly orchestrated mechanisms governing cellular differentiation and morphogenesis are required to achieve the spatiotemporal variations in gene expression among cells that ultimately give rise to the complex forms seen in multicellular life (Carroll, 2001; Knoll, 2011).

The coordination and regulation of gene expression across considerable cellular distances are facilitated by intercellular signalling molecules that are perceived in a concentration-dependent manner. These molecules, termed morphogens, establish concentration gradients from their origin to target regions. Cells distributed along these gradients initiate distinct transcriptional programs, giving rise to the various cell types that collectively compose tissues and organs (Ashe and Briscoe, 2006; Stumpf, 1966; Wolpert, 1969). Critically, morphogens do not dictate specific cell fates; instead, they provide positional information that activates a differentiation program dependent on the cell's genotype and developmental history (Wolpert, 1969). This adaptability allows for the same morphogen to be applied in diverse developmental contexts.

The concept of morphogens was mostly developed based on studies on embryogenesis in the fruit fly *Drosophila melanogaster* (Driever and Nüsslein-Volhard, 1988; Steward et al., 1988). The early *Drosophila* embryo is a syncytium where nuclear division takes place thirteen times without cytokinesis. This allows for the free diffusion of morphogens such as Bicoid which patterns the anterior-posterior axis of the embryo. Bicoid is a maternally derived transcription factor that

is highly expressed at the anterior end of the embryo and undergoes exponential decay in concentration as it diffuses towards the posterior end (Frohnhofer and Nüsslein-Volhard, 1986). As a classic morphogen, Bicoid activates its target genes *orthodenticle (otd)* and *hunchback (hb)* at different concentrations: *hb* has high-affinity Bicoid binding sites in its promoter while *otd* has low-affinity sites, thus restricting *otd* expression to about half the range of *hb* at the anterior end (Driever et al., 1989; Gao and Finkelstein, 1998).

Nonetheless, the syncytial nature of the early *Drosophila* embryo is unique, and many morphogen signalling pathways encompasses cytoplasmic signalling cascades that convey the morphogen signal perceived by cell-surface receptors to the nucleus to modulate transcription. A classic example of such a pathway in animals is the wingless/Int-1(Wnt)/ β -catenin signalling pathway which controls multiple aspects of embryogenesis including body axis patterning, cellular differentiation and proliferation, as well as cell migration (Cadigan and Nusse, 1997; Nüsslein-Volhard and Wieschaus, 1980). In the absence of the Wnt protein ligand, β -catenin is ubiquitinated and degraded by the degradosome complex in the cytoplasm (reviewed in Gammons and Bienz, 2018). The binding of Wnt to its receptor Frizzled triggers a signalling cascade culminating in the sequestration of degradosome components at the plasma membrane in a so-called signalosome. The free β -catenin accumulates and enters the nucleus where it binds transcription factors such as the T-Cell Factor (TCF). This causes a conformational change in TCF that displaces the corepressor GROUCHO and facilitates the recruitment of transcriptional coactivators and chromatin remodellers to activate gene expression. Plants, having evolved multicellularity independently of animals, exhibit a body plan reflective of their sessile nature. Unlike animals, plants continuously generate new organs throughout their lifecycle through the maintenance and differentiation of stem cells within their meristems (Weigel and Jürgens, 2002). The rigid cell walls of

plant cells impede cell migration, thus necessitating tight control over the orientation of cell division and expansion for morphogenesis (Scheres, 2007; Scheres et al., 1994). Notably, plants face the challenge of coordinating development and growth in response to various biotic and abiotic stresses. Yet, despite these differences in body plan, the basic principles of morphogen patterning can also be applied to plant development (Abley et al., 2013).

Unlike animals, most plant signalling molecules are small non-peptide metabolites collectively termed phytohormones. Phytohormones are structurally and functionally diverse, but they all act to regulate developmental and physiological processes in coordination with environmental stimuli (Santner et al., 2009; Verma et al., 2016).

The mechanism of cytokinin, ethylene, and brassinosteroid signalling are reminiscent of animal and plant peptide signalling pathways as they involve the binding of the hormones to transmembrane receptors that mediate intracellular signalling cascades (Binder, 2020; Kieber and Schaller, 2018; Planas-Riverola et al., 2019). However, most other phytohormones are perceived by nuclear or cytosolic receptors and often involve the degradation of repressive components by the ubiquitin-proteasome pathway (Fig. 1.1; reviewed in Kelley and Estelle, 2012).

In the auxin, gibberellin, strigolactone and jasmonic acid pathways, the transcription factors that mediate the hormone response are bound by repressor proteins in the absence of the phytohormone (Leyser, 2017; Mashiguchi et al., 2021; Ruan et al., 2019; Schwechheimer, 2012). The binding of the hormone to its receptor stabilises the interactions between the receptors and the repressor proteins. The receptor-bound repressors are ubiquitinated by the Skp1/Cullin/F-box (SCF) ubiquitin ligase complex to mark the repressors for degradation by the 26S proteasome, therefore allowing gene expression from hormone-responsive target genes. Interestingly, a variation on this strategy is observed in the ethylene signalling pathway, where the activator of hormone response is degraded by the SCF complex in the absence of

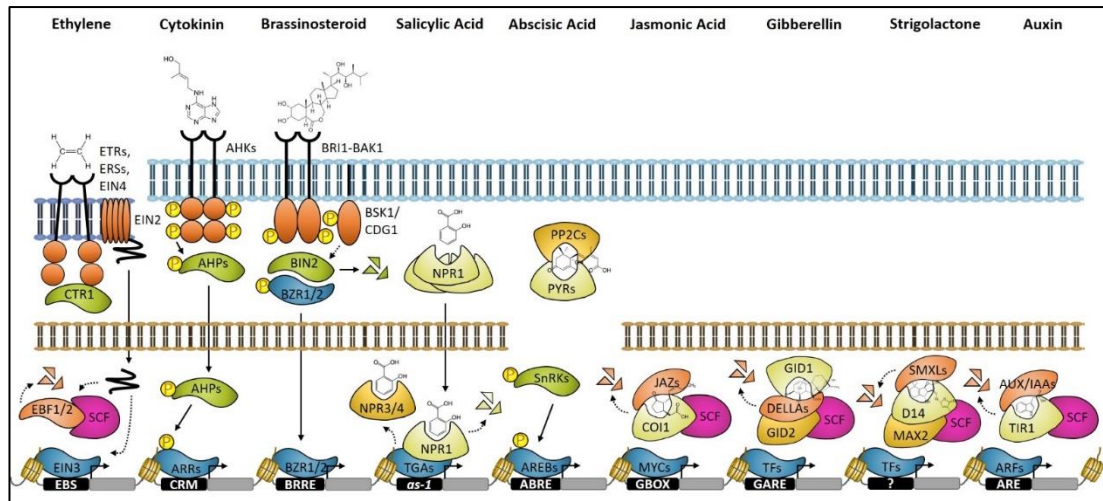


Figure 1.1: Canonical phytohormone signalling pathways. Ethylene binding to ETRs/ERSs/EIN4 deactivates CTR1 and triggers the cleavage of the EIN2 tail to stabilise EIN3 from SCF^{EBF1/2}-mediated degradation. Cytokinin and brassinosteroid perception by AHKs or BRI1-BAK1 induces phosphorylation cascades culminating in the activation of the downstream ARR or BZR1/2 transcription factors. Salicylic acid deactivates the NPR3/4 repressors and induces NPR1 monomerisation and nuclear entry to facilitate TGA-mediated gene expression. Abscisic acid perception by PYR-PP2C causes a SnRK-dependent phosphorylation cascade resulting in AREB activation. Jasmonic acid, gibberellin, strigolactone and auxin stabilises the interactions between their receptors (COI1, GID1, D14, and TIR1) and repressor proteins (JAZs, DELLAs, SMXLs, and AUX/IAAs) ultimately causing SCF-mediated ubiquitination and proteasomal degradation of the repressors. The dark blue membrane represents the endoplasmic reticulum membrane while the light blue and brown membranes are the plasma and nuclear membranes respectively. Dotted arrows indicate indirect steps.

ethylene (Fig. 1.1; Guo and Ecker, 2003).

Of all the phytohormones, auxin most fits the classical definition of a morphogen (Bhalerao and Bennett, 2003). For simplicity, the term 'auxin' in this thesis will refer to the most abundant natural auxin, indole-3-acetic acid (IAA) unless stated otherwise. Since its discovery by Thimann and Koepfli (1935), auxin has been

implicated in almost all developmental processes in plants, from embryogenesis to organogenesis in shoots and roots (Friml et al., 2003; Reinhardt et al., 2003; Sabatini et al., 1999). In almost every developmental context, auxin exerts its effect through the formation of concentration gradients to subdivide tissue into different cell types, often creating distinct regions of high or low concentrations known as auxin maxima or minima (Reinhardt et al., 2003; Sabatini et al., 1999; Sorefan et al., 2009). Furthermore, the flow of auxin from source to sink tissue also plays a role in vascular differentiation and the phenomenon of apical dominance (Bennett et al., 2006; Prusinkiewicz et al., 2009). Therefore, the regulation of auxin biosynthesis and transport is crucial for its role in morphogenesis.

1.2 Mechanisms of auxin signalling in plants

1.2.1 The biosynthesis and transport of auxin

Auxin is synthesised from the amino acid tryptophan in a two-step process. The first step involves the conversion of tryptophan into indole-3-pyruvate (IPA) by the TRYPTOPHAN AMINOTRANSFERASE OF ARABIDOPSIS 1/ TRYPTOPHAN AMINOTRANSFERASE RELATED (TAA1/TAR) enzymes (Stepanova et al., 2008; Tao et al., 2008). IPA then undergoes oxidative decarboxylation mediated by the YUCCA (YUC) flavin monooxygenases to form IAA (Cheng et al., 2006; Cheng et al., 2007). Whereas auxin can diffuse freely as protonated IAAH in the acidic environment of the apoplast, its ionisation in the pH-neutral cytoplasm prevents passive diffusion out of cells (Zazimalová et al., 2010). As auxin biosynthesis is localised to specific groups of cells in shoots and roots (Cheng et al., 2006; Stepanova et al., 2008; Tao et al., 2008), an active transport system is required for the directional transport of auxin critical for the formation of maxima and minima. The PIN-FORMED (PIN) family of auxin efflux carriers are transmembrane proteins localised to the plasma membrane that mediate auxin export from cells for polar auxin transport (Gälweiler et al., 1998; Okada et al., 1991; Petrásek et al., 2006).

The directionality of auxin transport thus depends on the polar localisation of the PINs on the plasma membrane. The phosphorylation of PINs by the PINOID (PID) serine-threonine kinase targets them to the apical plasma membrane while PIN dephosphorylation by PROTEIN PHOSPHATASE 2A (PP2A) shifts their localisation to the basal plasma membrane (Benjamins et al., 2001; Friml et al., 2004; Michniewicz et al., 2007). As the PINs undergo constitutive cycles of endo- and exocytosis (Geldner et al., 2001), their polar localisation can be rapidly altered in response to hormonal or environmental stimuli for developmental processes and tropic responses (Blilou et al., 2005; Friml et al., 2002; Scarpella et al., 2006; Zhang et al., 2020a).

While auxin can diffuse passively into cells from the apoplast, they are also imported into cells by the AUX1/LAX family of plasma membrane permeases (Bennett et al., 1996; Marchant et al., 1999; Péret et al., 2012). Like the PINs, the AUX1/LAX localisation on the plasma membrane is dynamic and can be polarised (Kleine-Vehn et al., 2006; Tidy et al., 2023). In tandem with the PINs, the high-affinity auxin import activities of AUX1/LAX proteins are instrumental in creating auxin sinks that redirect polar auxin transport for the regulation of plant growth and development (Marchant et al., 2002; Swarup et al., 2005; Yang et al., 2006).

1.2.2 The canonical TIR1/AFB-dependent pathway

For auxin to act as a morphogen, there must be mechanisms that perceive cellular auxin levels to induce appropriate changes in gene expression. To date, the best characterised auxin signalling pathway is the so-called canonical pathway involving three major protein families: the TRANSPORT INHIBITOR RESISTANT1/ AUXIN SIGNALING F-BOX (TIR1/AFB) family of auxin receptors, the AUXIN/INDOLE-3-ACETIC ACID (AUX/IAA) transcriptional repressors and the AUXIN RESPONSE FACTOR (ARF) transcription factors (Fig. 1.2a; reviewed in Leyser, 2017).

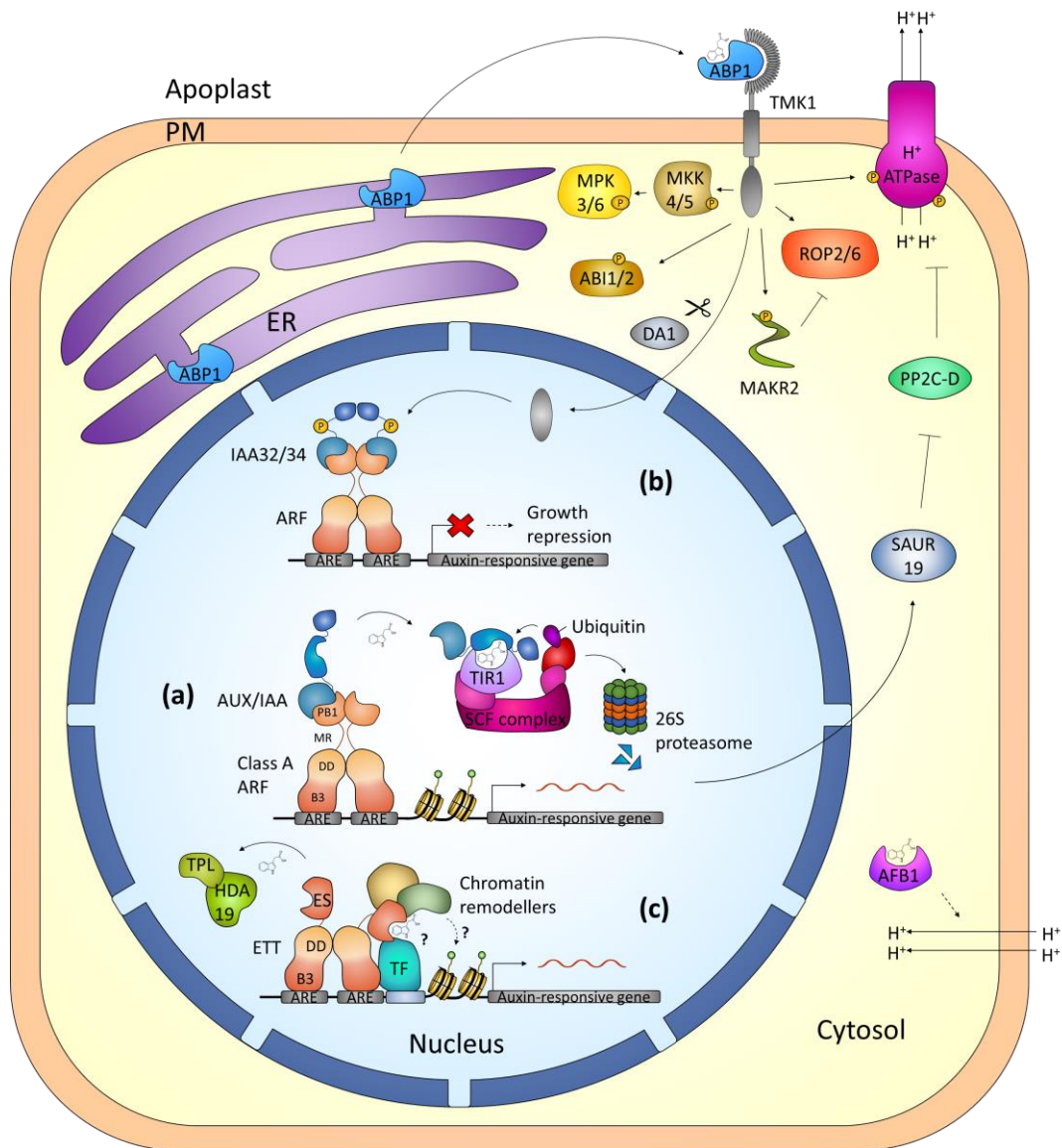


Figure 1.2: Canonical and alternative auxin signalling pathways. (a) The perception of auxin by TIR1/AFBs facilitates the degradation of AUX/IAAs by the 26S proteasome. In acid growth, the canonical pathway induces SAUR19 expression to inhibit PP2C-D phosphatases for apoplast acidification. AFB1 also mediates apoplast alkalisation through an unknown mechanism. **(b)** ABP1 forms a receptor complex with the TMKs and phosphorylates multiple targets upon auxin perception including the ROPs, ABIs, MKKs, H⁺ ATPases and MAKR2. Auxin perception also leads to DA1-dependent cleavage of the TMK C-terminus which enters the nucleus to phosphorylate IAA32/34 to promote growth repression on the concave side of the apical hook. **(c)** The ES domain of ETT interacts with TPL and other transcription factors in an auxin-sensitive manner. The binding of auxin to ETT disrupts these interactions and possibly leads to the recruitment of proteins that positively regulate gene expression.

The ARFs bind to cis-regulatory elements known as AUXIN RESPONSIVE ELEMENTS (AuxREs) found in the promoters of target genes to transcriptionally activate or repress their expression (Boer et al., 2014; Galli et al., 2018; Lieberman-Lazarovich et al., 2019; Ulmasov et al., 1999a). In the absence of auxin, the AUX/IAAs heterodimerise with the ARFs through their C-terminus Phox/Bem1 (PB1) domains (Tiwari et al., 2003; Ulmasov et al., 1997). The AUX/IAAs recruit the TOPLESS/TOPLESS RELATED (TPL/TPR) family of corepressors which in turn attracts histone deacetylases (HDAs), ultimately resulting in chromatin condensation and the transcriptional repression of auxin-responsive genes (Kuhn et al., 2020; Long et al., 2006; Szemenyei et al., 2008; Wang et al., 2013). Auxin acts as a 'molecular glue' to facilitate the interaction between the TIR1/AFB receptors in complex with the SCF E3 ubiquitin ligases and the AUX/IAAs (Dharmasiri et al., 2005; Kepinski and Leyser, 2005; Tan et al., 2007). This results in the polyubiquitination of the AUX/IAAs which marks them for degradation by the 26S proteasome (Gray et al., 2001; Maraschin Fdos et al., 2009). The removal of the AUX/IAAs derepresses the ARFs leading to the expression of auxin-responsive target genes.

In the model plant *Arabidopsis thaliana*, there are six members of the TIR1/AFB auxin receptors. These receptors belong to the F-box protein family that associate with the SCF E3 ligase complex to target proteins for ubiquitination and degradation (Dharmasiri et al., 2005; Gray et al., 2001; Kepinski and Leyser, 2005). The auxin binding pocket of TIR1 is located at the C-terminus leucine-rich-repeat (LRR) domain (Fig. 1.3; Tan et al., 2007). Auxin increases the affinity between TIR1-LRR and the degron domain of AUX/IAAs, thus facilitating their interaction. While all TIR1/AFB members bind auxin, they exhibit different expression patterns, biochemical properties, and developmental roles (Calderón Villalobos et al., 2012; Parry et al., 2009; Prigge et al., 2020). Interestingly, an adenylate cyclase (AC) motif

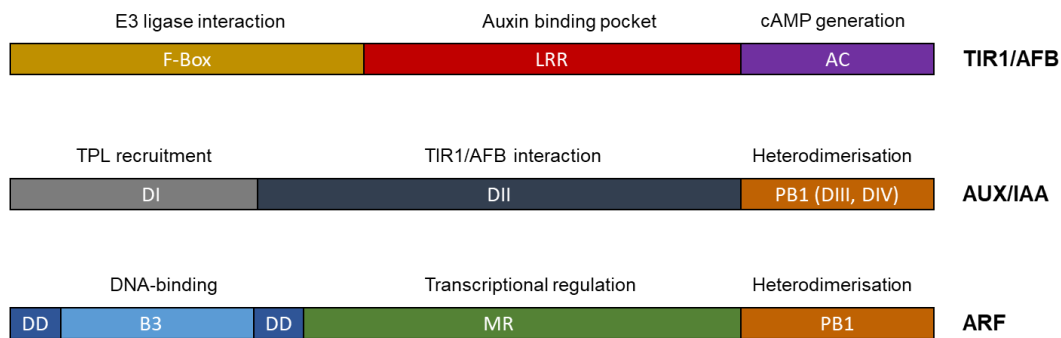


Figure 1.3: Structure and function of canonical auxin signalling components. The TIR1/AFB F-box domain mediates its association with the E3 ligase complex. The LRR domain contains the auxin binding pocket that facilitates auxin-dependent interactions with the AUX/IAAs. Recently it has been shown that TIR1/AFBs contain an AC motif that generates cAMP for transcriptional auxin responses. The AUX/IAAs contain domain I (DI) necessary for the recruitment of TPL/TPR corepressors. DII facilitates auxin-dependent interactions with the TIR1/AFBs, while DIII and DIV form the PB1 domain that is responsible for heterodimerisation with the ARFs. The ARF B3 domain functions to bind AuxREs and is flanked by dimerisation domains that mediate homo- and heterodimerisation of the ARFs. The MR in Class A ARFs are glutamine-rich and generally activate transcription of target genes while the Class B and C ARFs have serine-rich MRs and typically act as transcriptional repressors. The ARF PB1 mediates its interaction with the AUX/IAAs.

has recently been identified in the C-terminus region of the TIR1/AFBs (Qi et al., 2022). This motif is required for the generation of cAMP, an important secondary messenger in mammalian signalling pathways (reviewed in Beavo and Brunton, 2002). AC activity appears to be important for the transcriptional roles of TIR1/AFBs, providing an additional layer of complexity in gene regulation by the canonical auxin signalling pathway.

The TIR1/AFBs originated from a gene duplication event in the ancestral land plant, with the other paralogue encoding the jasmonic acid receptor, CORONATINE INSENSITIVE 1 (COI1) (Bowman et al., 2017; Mutte et al., 2018). However, the

TIR1/AFB/COI1-like orthologues of charophyte algae lack the hormone-contacting residues found in TIR1/AFB and COI1, indicating that these orthologues do not function as auxin or jasmonic acid receptors. As TIR1/AFB-dependent auxin signalling is also functional in the bryophytes *Physcomitrium patens* and *Marchantia polymorpha* (Flores-Sandoval et al., 2015; Prigge et al., 2010; Suzuki et al., 2023), this suggests that canonical auxin signalling originated shortly after the divergence of the ancestral land plant from the charophytes.

Three clades of auxin receptors became established in the last common ancestor of euphyllophytes (monilophytes and seed plants), while another gene duplication event in the angiosperms gave rise to the TIR1/AFB1 and AFB2/AFB3 clades (Mutte et al., 2018; Prigge et al., 2020). Interestingly, AFB1 have undergone extensive structural and functional divergence since its split from TIR1 at the base of the Brassicales (Prigge et al., 2020). Unlike TIR1, AFB1 is localised primarily in the cytoplasm and does not associate readily with the SCF complex. Nonetheless, AFB1 is vital for rapid auxin-induced membrane depolarisation to inhibit root growth (Li et al., 2021; Prigge et al., 2020; Serre et al., 2021). This highlights the fact that closely related paralogues can undergo major changes in terms of expression patterns and biochemistry despite their relatively recent origins.

Further expanding the complexity of the auxin response is the AUX/IAA family, which in *A. thaliana* contains 29 members. In general, the AUX/IAs share three important domains (Fig. 1.3). The N-terminus domain I contains an Ethylene-responsive element binding factor-associated Amphiphilic Repression (EAR) motif which facilitates the recruitment of TPL/TPRs to repress gene expression (Causier et al., 2012; Szemenyei et al., 2008; Tiwari et al., 2004). The degron motif in domain II facilitates AUX/IAA interaction with the TIR1/AFBs in the presence of auxin (Gray et al., 2001; Kepinski and Leyser, 2005; Ramos et al., 2001). Finally, the PB1 domain (made up of domain III and domain IV) at the C-terminus mediates the

heterodimerisation of AUX/IAAs with the ARFs (Tiwari et al., 2003).

Evolutionary analyses of the AUX/IAA family reveal that proto-AUX/IAA orthologues exist in the charophyte algae, but they lack domain I and II (Bowman et al., 2017; Mutte et al., 2018). An ancestral gene duplication event in the land plants gave rise to two clades, one reminiscent of the proto-AUX/IAAs while the other gained domain I and II, becoming the canonical AUX/IAAs. The canonical AUX/IAA clade diverged into three major clades in the euphyllophyte common ancestor and further radiated after the origin of angiosperms (Mutte et al., 2018). The clades containing the *A. thaliana* IAA20, IAA30, IAA31, IAA32, and IAA34 have secondarily lost domain II, thus preventing their interaction with the TIR1/AFB auxin receptors (Cao et al., 2019; Sato and Yamamoto, 2008). While the function of IAA20, IAA30, and IAA31 remains unclear, IAA32 and IAA34 have been shown to participate in an alternative auxin signalling pathway mediated by TRANSMEMBRANE KINASE 1 (TMK1) (Cao et al., 2019; Gu et al., 2022).

The canonical auxin signalling pathway ultimately converges upon the ARFs that transcriptionally regulate auxin-induced gene expression. There are 23 ARFs in the *A. thaliana* genome, each having distinct and dynamic expression patterns throughout plant development and consequently regulate different developmental processes (Guan et al., 2017; Rademacher et al., 2012; Rademacher et al., 2011; Weijers et al., 2006). Furthermore, ARFs are typically not interchangeable, indicating that there are significant differences at the protein level (Finet et al., 2010; Rademacher et al., 2012; Weijers et al., 2005). Nonetheless, all ARFs usually consist of three distinct domains: an N-terminus B3 DNA-binding domain (DBD), a Middle Region (MR) and a C-terminus PB1 domain (Fig. 1.3).

The B3-DBD of ARFs are responsible for the recognition and binding of the AuxRE cis-elements located in the promoters of auxin-responsive genes (Tiwari et al., 2003; Ulmasov et al., 1999b; Ulmasov et al., 1997). The first AuxRE sequence to be

characterised was the canonical TGTCTC sequence (Li et al., 1994; Ulmasov et al., 1995). However, later studies demonstrated that other AuxRE variants (TGTCNN) exist, which can sometimes be bound by ARFs with greater affinity than the canonical sequence (Boer et al., 2014; O'Malley et al., 2016; Zemlyanskaya et al., 2016). The crystal structures of ARF1 and ARF5 reveal that ARFs bind to AuxRE pairs as dimers. Dimerisation is mediated by the dimerisation domains (DDs) flanking the B3-DBD, and mutations in these domains abolish ARF function (Boer et al., 2014; Liu et al., 2015; Ulmasov et al., 1999b). Interestingly, there appears to be little difference in the intrinsic binding specificity between ARFs of distantly related clades (Boer et al., 2014; Galli et al., 2018; O'Malley et al., 2016). Instead, ARFs have differential preferences for the spacing and orientation between AuxRE repeats (Boer et al., 2014; Freire-Rios et al., 2020).

In contrast with the DBD, the MR is highly variable in sequence and regulates the transcriptional activity of ARFs. Based on their MR amino acid composition, ARFs can be divided phylogenetically into three major clades: the glutamine-rich Class A ARFs, and the serine-rich Class B and C ARFs (Finet et al., 2013; Mutte et al., 2018; Tiwari et al., 2003). The Class C ARFs can be distinguished from the Class B ARFs by their post-transcriptional regulation by the microRNA160 (miR160) (Axtell et al., 2007; Mallory et al., 2005). Trans-activation assays of the MRs show that the Class A ARFs function as transcriptional activators while the Class B ARFs are repressors (Tiwari et al., 2003; Ulmasov et al., 1999a). Experimental data on Class C ARF activity is sparse, and there is increasing evidence that the Class C ARFs are not involved in auxin-responsive gene regulation (Flores-Sandoval et al., 2018; Kato et al., 2020; Mutte et al., 2018).

Most ARFs contain a PB1 domain at the C-terminus that mediates the interaction between ARFs and AUX/IAAs (Guilfoyle and Hagen, 2001; Ulmasov et al., 1997). Structural analyses of the ARF5 and ARF7 PB1 domains demonstrate that the PB1

has both acidic and basic faces that mediate homodimerisation between ARFs and heterodimerisation with the AUX/IAAs (Korasick et al., 2014; Nanao et al., 2014). Intriguingly, the *A. thaliana* ETTIN (ETT)/ARF3, ARF13 and ARF17 lack the PB1 domain, and the PB1 has been lost independently multiple times throughout land plant evolution (Finet et al., 2010; Mutte et al., 2018). Moreover, most Class B and Class C ARFs have limited or no interaction with the AUX/IAAs (Piya et al., 2014; Vernoux et al., 2011). Recent evidence suggests that Class B ARFs might regulate the auxin response through competition with the Class A ARFs for binding sites, given that Class B ARFs can interact with the TPL/TPR corepressors directly and bind to similar sites in the genome as the Class A ARFs (Causier et al., 2012; Galli et al., 2018; Kato et al., 2020). Therefore, it appears that the current model of the canonical auxin signalling pathway is mostly relevant to the Class A ARFs and the role of Class B and Class C ARFs in this pathway requires further investigation.

1.2.3 Rapid auxin responses through alternative pathways

While the versatility of the auxin response in plants can be largely attributed to the complicated network of TIR1/AFB, AUX/IAA and ARF interactions, there remains auxin-induced phenomena that are inconsistent with the kinetics of the canonical pathway. Transcriptional responses to auxin typically require minutes (Abel and Theologis, 1996; McClure et al., 1989), whereas certain cellular processes including membrane polarisation, cytoplasmic streaming and proton fluxes can occur within seconds (Friml et al., 2022; Li et al., 2021; Serre et al., 2021). In addition, auxin responses can be found in algae despite the lack of a complete TIR1/AFB-dependent pathway (Jin et al., 2008; Klämbt et al., 1992; Ohtaka et al., 2017). Therefore, alternative mechanisms must exist to explain these phenomena.

Auxin has long been known to trigger rapid apoplast acidification, leading to cell wall modifications that facilitate turgor pressure-mediated cell expansion (Arsuffi and Braybrook, 2018; Hager et al., 1971; Kutschera, 1994; Takahashi et al., 2012). This

phenomenon, termed acid growth, occurs through the auxin-induced activation of H⁺-ATPases, resulting in proton efflux into the apoplast in shoots. In contrast, auxin promotes apoplast alkalisation through the rapid activation of proton influx in roots. Through these two modes of action, auxin promotes growth in shoots while inhibiting root growth (Barbez et al., 2017; Fendrych et al., 2016; Li et al., 2021; Spartz et al., 2014).

As discussed earlier, part of the rapid root growth inhibition response is dependent on the canonical TIR1/AFB receptors, especially AFB1, through a non-transcriptional branch of their function (Fig. 1.2). Reduced apoplast alkalisation, membrane polarisation and root growth inhibition were observed in *tir1* and *afb1* loss-of-function mutants (Fendrych et al., 2018; Prigge et al., 2020; Serre et al., 2021). The mechanism of apoplast alkalisation is yet to be resolved; however, two distinct mechanisms have been characterised for apoplast acidification (Fig. 1.2). Firstly, the canonical pathway upregulates the expression of *SMALL AUXIN UP-RNA19 (SAUR19)* which in turn inhibits the PP2C phosphatases, thus promoting H⁺-ATPase phosphorylation and proton efflux (Ren et al., 2018; Spartz et al., 2014). A second mechanism involves the rapid phosphorylation of H⁺-ATPases by cell surface-localised TMK1 (Li et al., 2021; Lin et al., 2021).

The TMKs are a family of four receptor-like kinases in *A. thaliana*. The TMKs have been proposed as docking proteins for AUXIN-BINDING PROTEIN 1 (ABP1) on the extracellular surface mediating intracellular responses through their cytoplasmic domain (Xu et al., 2014). While the involvement of ABP1 in this pathway has been controversial, the role of the TMKs in mediating auxin responses has been made more strongly.

The perception of extracellular auxin activates the cytosolic C-terminus kinase domain of the TMKs to trigger intracellular signalling cascades. Besides the H⁺-ATPases, the TMKs have numerous downstream targets regulating various aspects

of plant development (Fig. 1.2b). In the context of leaf pavement cell interdigitation, TMKs activate the Rho-like GTPases (ROPs), ROP2 and ROP6, which are required to remodel the cytoskeleton and regulate PIN endocytosis (Nagawa et al., 2012; Xu et al., 2014; Xu et al., 2010). During root gravitropism, ROP6 regulates the asymmetric redistribution of PIN2 and therefore asymmetric distribution of auxin when a shift in the gravity vector occurs. The unstructured protein MEMBRANE-ASSOCIATED KINASE REGULATOR2 (MAKR2) antagonises ROP6 signalling through the inhibition of TMK1 activity (Marques-Bueno et al., 2021). Auxin perception by the TMKs causes the internalisation of MAKR2, freeing ROP6 from inhibition and mediating PIN2 relocalisation.

Development of the apical hook in seedlings of *A. thaliana* requires an asymmetric auxin gradient with the higher auxin concentration located on the concave side (Zadnikova et al., 2010; Zadnikova et al., 2016). Apical hook bending was impaired in the *tmk1* mutant, implicating its role in this process (Cao et al., 2019). Indeed, the high auxin levels on the concave side was shown to promote cleavage of the TMK1 C-terminus domain by the DA1 family of peptidases (Cao et al., 2019; Gu et al., 2022). The cleaved kinase domain enters the nucleus where it interacts with and phosphorylates the non-canonical AUX/IAAs, IAA32 and IAA34. Phosphorylation stabilises IAA32 and IAA34, resulting in their accumulation and allowing them to regulate downstream gene expression for the development of the apical hook.

With the TMKs also being implicated in activating Mitogen-Activated Protein Kinase (MAPK) and abscisic acid signalling pathways (Huang et al., 2019; Yang et al., 2021), their kinase activity is undoubtedly integral throughout plant development, and yet their mechanism of auxin perception remained enigmatic. ABP1 was proposed to function upstream of the TMKs for auxin binding (Xu et al., 2014). With its strong binding affinity to auxin and the *abp1* embryo lethal phenotype (Hertel et al., 1972; Hesse et al., 1989), ABP1 was considered the major auxin receptor in

plants (for a detailed review, see Napier, 2021). Nevertheless, many controversies disputed its role as an auxin receptor. Firstly, ABP1 was found to mainly localise to the endoplasmic reticulum, rather than the plasma membrane, and does not bind auxin efficiently at neutral cytosolic pH (Ramos et al., 2001). Further complicating matters was the discovery that the original *abp1* loss-of-function phenotype was caused by the disruption of a neighbouring gene (Gao et al., 2015; Michalko et al., 2015). After years of being considered a red herring, the recent work of Friml et al. (2022) finally dissipates the ambiguity behind the function of ABP1.

The first line of evidence validating ABP1 function is the finding that ABP1 is partly secreted to the apoplast where it can bind auxin efficiently. Furthermore, it was observed that the rapid auxin-induced phosphorylation of thousands of protein targets in wild-type plants was impaired in confirmed null mutants of *tmk1* and *abp1*. Cytosolic streaming and vasculature regeneration were also impaired in the *tmk1* and *abp1* mutant and the ABP1(M2X) allele that is unable to bind auxin failed to complement the mutant phenotypes (Friml et al., 2022). Another study critically demonstrated that two ABP1-like (ABL) proteins existed in *A. thaliana* and that these proteins also form coreceptor complexes with the TMKs (Yu et al., 2023). Strikingly, strong developmental phenotypes including reduced plant size, curled leaves, and altered leaf pavement cell morphology were observed in the *abp1;abl1/2* triple mutant. Thus, the lack of developmental phenotypes in confirmed *abp1* null mutants can be explained by genetic redundancy with the ABLs.

The ABP1/ABLs are evolutionarily ancient, with orthologues found also in the green algae (Tomas et al., 2010). It is therefore tempting to speculate that the ABP1/ABLs are responsible for the auxin responses observed in algae. Indeed, a new study from Kuhn et al. (2024) has demonstrated that the ABP1-TMK1-mediated pathway is required for a set of deeply conserved rapid auxin responses. As seen in *A. thaliana*, auxin rapidly induced cytoplasmic streaming in the bryophyte *M.*

polymorpha and the streptophyte alga *Klebsormidium nitens* (Friml et al., 2022; Kuhn et al., 2024). The rapid phosphoproteomic shifts induced by auxin in *A. thaliana* were also observed in bryophytes and algae. Mining of the conserved phosphoproteomic datasets identified a set of rapidly accelerated fibrosarcoma (RAF)-like protein kinases that might mediate the auxin-induced phosphoproteomic response. Loss-of-function *raf* mutants in both *A. thaliana* and *M. polymorpha* had numerous developmental defects, reduced auxin-induced growth inhibition and altered phosphoproteomes. Crucially, RAF phosphorylation was perturbed in both *abp1* and *tmk1* null mutants, thus implicating the ABP1-TMK1 pathway in this evolutionarily ancient process, though further studies are required to elucidate the details of this mechanism.

1.2.4 The ETT-mediated auxin signalling pathway

It is clear now that two distinct branches of auxin signalling exist in plants: the transcriptional TIR1/AFB-dependent pathway mediating 'slow' developmental responses and the rapid non-transcriptional physiological responses mediated by AFB1 and the ABP1-TMK pathway. Curiously, yet another transcriptional auxin signalling pathway exists under the control of the atypical Class B ARF, ETT (Kuhn et al., 2020; Simonini et al., 2017; Simonini et al., 2016).

ETT/ARF3 in *A. thaliana* lacks the PB1 domain necessary for interaction with the AUX/IAAs (Finet et al., 2010; Sessions et al., 1997b). Instead, ETT possesses a modified MR termed the ETT-Specific (ES) domain that overall has poor structural conservation within the seed plants but contains phylogenetically well-defined motifs (Finet et al., 2013; Simonini et al., 2018a). Though most Class B ARFs, including ETT, act as transcriptional repressors, ETT has been shown to activate gene expression for a subset of its target genes in an auxin-dependent manner (Kuhn et al., 2020; Simonini et al., 2017). Additionally, the protein-protein interaction between ETT and transcription factors from multiple families are disrupted in the presence of

auxin (Simonini et al., 2016). The auxin-sensitivity of ETT is a property of the ES domain, as mutations in motifs within the ES domain, including a highly conserved tryptophan residue (W505), abolishes the ability of ETT to sense auxin (Kuhn et al., 2020; Simonini et al., 2016; Simonini et al., 2018a).

Kuhn et al. (2020) demonstrated through independent biophysical assays that the ES domain binds auxin directly. In low concentrations of auxin, ETT interacts directly with the TPL/TPR corepressors through the EAR-like motif in the ES domain, resulting in the depletion of the histone H3K27 acetylation in the promoters of target genes, thus preventing gene expression. The binding of auxin to ETT disrupts the ETT-TPL/TPR interaction, restoring H3K27 acetylation and mediating auxin-induced gene expression (Fig. 1.2c). The dual functions of ETT as an activator and repressor of gene expression depending on hormone-induced conformational changes is reminiscent of animal hormone signalling such as the Wnt/ β -catenin pathway (Gammons and Bienz, 2018).

An open question remains as to how important the ETT-mediated pathway is for plant development. Whereas the canonical and non-transcriptional pathways have been studied in a variety of developmental contexts, our understanding of the ETT-mediated pathway is mostly limited to its role in the gynoecium (Kuhn et al., 2020; Simonini et al., 2016; Simonini et al., 2018b). However, an auxin-insensitive allele of ETT, ETT^{2CS}, confers pleiotropic phenotypes in roots, axillary buds, and ovules, implicating a greater role for this pathway beyond gynoecium development (Simonini et al., 2018a). In fact, the role of ETT in patterning the gynoecium has been proposed to be derived from the adaxial-abaxial leaf polarity network, which is perhaps unsurprising given the evolutionary origin of carpels from leaves (Meyerowitz et al., 1989; Nemhauser et al., 2000; Pelaz et al., 2000).

1.3 Development and evolution of lateral organs in plants

1.3.1 Novel roles of ancient regulators in body plan innovations

The transition of the land plants (embryophytes) to a terrestrial habitat from their aquatic origin is marked by numerous morphological innovations (for detailed reviews, see Bowman, 2022; Jill Harrison, 2017). In contrast to their charophyte algal relatives, embryophytes exhibit complex multicellularity in both their haploid gametophyte and diploid sporophyte generations (Hofmeister, 1862). The dominant generation differs in two major lineages of embryophytes: the gametophyte-dominant bryophytes (liverworts, mosses, and hornworts) and the sporophyte-dominant tracheophytes, or vascular plants (lycophytes, ferns/monilophytes, and seed plants). Further elaborations of the sporophyte generation during tracheophyte evolution gave rise to bifurcating shoot systems and indeterminate meristems (Edwards et al., 2014; Philipson, 1990; Sakakibara et al., 2008). Roots might have originated from a shoot-like system and have evolved independently within the lycophytes and euphyllophytes (de Vries et al., 2016; Hetherington and Dolan, 2018). Similarly, leaves are probably modified shoots and have at least three independent origins within the tracheophytes (Harrison et al., 2007; Sanders et al., 2011; Tomescu, 2009; Zimmermann, 1952). Seeds and pollen arose within the seed plants (spermatophytes) as modifications of the gametophyte generation to aid reproduction away from water (Linkies et al., 2010; Lopez-Obando et al., 2022). Finally, the modification of leaf-like structures gave rise to whorls of floral organs in the angiosperms (Meyerowitz et al., 1989; Ó'Maoiléidigh et al., 2018; Theissen and Melzer, 2007).

The increasing availability of algal and plant genomes covering important phylogenetic clades have been instrumental in uncovering the mechanisms behind the development and evolution of these morphological innovations. Like the ARFs, comparative genomics have uncovered the origins of various transcription factor

families in the charophyte algae (Cannell et al., 2020; Catarino et al., 2016; Floyd et al., 2006; Tanabe et al., 2005). A recurring trend observed is the expansion and diversification of these families in lineages with more complex body plans, a trend also observed in animal transcription factor families (Banks et al., 2011; Degnan et al., 2009; Hori et al., 2014; Mutte et al., 2018; Rensing et al., 2008). Genome duplications are common throughout embryophyte evolution, thus potentially driving morphological evolution through the neofunctionalisation of newly acquired paralogues (Cui et al., 2006; Prince and Pickett, 2002). This scenario is further supported through the numerous examples where ancient transcription factor regulatory networks were co-opted for the development of novel morphologies.

In the chlorophyte alga *Chlamydomonas reinhardtii*, the KNOTTED-LIKE HOMEODOMAIN (KNOX) and BEL1-LIKE (BELL) transcription factors are brought together upon mating and heterodimerise to activate zygote formation (Dierschke et al., 2021; Hisanaga et al., 2021; Horst et al., 2016; Lee et al., 2008; Sakakibara et al., 2013). The KNOX family have diverged into two clades, KNOX1 and KNOX2, in the embryophytes (Bharathan et al., 1999; Kerstetter et al., 1994). In angiosperms, KNOX1 plays an important role in regulating cell proliferation in shoot meristems, and this is dependent on their heterodimerisation with the BELLS, while KNOX2 antagonises KNOX1 activity (Bellaoui et al., 2001; Furumizu et al., 2015; Rutjens et al., 2009). Strikingly, bryophyte KNOX-BELL interactions have been shown to regulate both the zygote development programme, similar to *C. reinhardtii*, and sporophyte development, as in angiosperms (Dierschke et al., 2021; Hisanaga et al., 2021; Horst et al., 2016; Sakakibara et al., 2013; Sakakibara et al., 2008). Therefore, it appears that the KNOX-BELL module has been recruited from its original role in initiating the diploid programme to regulating the continuous development of indeterminate sporophytes in the vascular plants.

Another transcription factor family that has been co-opted for the development of a new morphological context is LEAFY (LFY). In the angiosperms, LFY is a pioneer transcription factor that initiates the floral development programme through the activation of MADS-box homeotic genes (Jin et al., 2021; Parcy et al., 1998; Schultz and Haughn, 1991; Weigel et al., 1992; Weigel and Nilsson, 1995). However, the LFY family is present in all embryophytes and related streptophyte algae (Sayou et al., 2014). Gymnosperm LFY orthologues are similar to their angiosperm counterparts as they are highly expressed in reproductive organs and potentially regulate MADS-box genes (Mellerowicz et al., 1998; Moyroud et al., 2017; Shindo et al., 2001). In contrast, the moss LFY orthologue controls the first cell division of the zygote and later sporophyte development (Tanahashi et al., 2005). Silencing of the two *LFY* paralogues in the fern *Ceratopteris richardii* arrests shoot apex development in both the gametophyte and sporophyte stage, suggesting that LFY has evolved a role in maintaining sporophyte indeterminacy (Plackett et al., 2018). This shift in function is correlated with a gradual change in the DNA-binding specificity of LFY (Maizel et al., 2005; Sayou et al., 2014).

In contrast to the ancient origins of the TIR1/AFB- and ABP1-TMK-mediated pathways, the evolutionary history of the ETT-mediated pathway remains unresolved. ETT and its close paralogue, ARF4, originated from a gene duplication event in the last common ancestor of angiosperms, while conflicting data places the origin of the ETT/ARF4-like clade at either the base of the euphyllophytes or seed plants (Finet et al., 2010; Mutte et al., 2018; Sun and Li, 2020). Unlike ETT, ARF4 in *A. thaliana* retains a PB1 domain and is able to interact with the AUX/IAAs (Piya et al., 2014). The loss of the PB1 domain from ETT appears to be of functional significance, as a chimeric ETT construct containing the ARF4 PB1 was unable to fully rescue the gynoecium phenotype of the *ett-1* mutant (Finet et al., 2010). In a developmental context, ETT and ARF4 regulate leaf polarity and outgrowth in a

redundant manner, while only ETT is necessary for proper gynoecium morphogenesis in *A. thaliana* (Guan et al., 2017; Pekker et al., 2005; Sessions et al., 1997b). Taking this all into account, it is tempting to speculate that the ETT/ARF4-like clade had an ancestral role in leaf development, while structural changes and the gain of auxin perception in the ETT clade facilitated the evolution of its role in gynoecium development in the angiosperms. Nonetheless, a thorough examination of the function of ETT, ARF4 and auxin in leaf and gynoecium morphogenesis must be considered before addressing this hypothesis.

1.3.2 The abaxial-adaxial leaf polarity network

The early vascular plants, such as *Cooksonia*, *Rhynia* and *Zosterophyllum*, were leafless, consisting only of naked photosynthetic shoots (Harrison and Morris, 2018; Kenrick and Crane, 1997). Zimmermann (1952) proposed in his teleome theory a progressive evolutionary framework for the origin of 'megaphyll' leaves in the euphyllophytes, beginning with the development of unequal branching, the planation of lateral branches, and the formation of webbing between the branches to form the lamina. The 'microphyll' leaves of lycophytes were recognised as fundamentally different from megaphylls, having evolved possibly from the elaboration of epidermal outgrowths or sterilisation of lateral sporangia (Crane and Kenrick, 1997; Tomescu, 2009). Nevertheless, the extensive fossil record of early leafless lycophyte, monilophyte and spermatophyte lineages indicate that leaves have at least three independent origins, with the possibility of more within the monilophytes (Tomescu, 2009).

From an evolutionary development perspective, there is merit to the hypothesis that leaves are modified axillary shoots as leaf primordia initiation and elaboration is tightly linked with the development and patterning of the shoot apical meristem. In angiosperms, the shoot apical meristem can be organised into three zones: the central zone containing pluripotent stem cells, the peripheral zone where organ

differentiation occurs, and the rib zone from which stem tissues are derived. Leaf primordia initiation in the peripheral zone is dependent on the establishment of auxin maxima at the epidermis directed by PIN-mediated auxin transport (Benková et al., 2003; Heisler et al., 2005; Reinhardt et al., 2003). Remarkably, PIN-mediated auxin transport is also required for phyllid initiation in moss and likely also microphyll initiation in lycophytes despite their non-homology to seed plant leaves, indicating that this mechanism has been independently recruited for the development of leaf-like organs (Bennett et al., 2014; Sanders and Langdale, 2013).

The differentiation of leaves from the shoot meristem reflects a switch from indeterminate growth to a determinate developmental programme. As mentioned earlier, the *KNOX1* genes in angiosperms maintain stem cell fate in shoot meristems (Jackson et al., 1994; Long et al., 1996). Conversely, members of the *ASYMMETRIC LEAVES1*, *ROUGH SHEATH2*, *PHANTASTICA* (*ARP*) transcription factor family are required to initiate the leaf development programme (Byrne et al., 2000; Tsiantis et al., 1999; Waites et al., 1998). The mutual antagonism between the *KNOX1* and *ARP* families maintains the distinct central and peripheral zones in the shoot apical meristem to balance meristem maintenance and organ differentiation (Byrne et al., 2000; Ori et al., 2000; Semiarti et al., 2001). Leaf primordia emerge at points of auxin maxima in the peripheral zone where *KNOX1* expression is downregulated (Reinhardt et al., 2000; Reinhardt et al., 2003). The exact mechanism as to how auxin regulates *KNOX1* expression, and how it functions with the ARPs is still unclear but could involve the spatiotemporal integration of the shoot meristem auxin gradient by ARFs such as ETT (Burian et al., 2022; Galvan-Ampudia et al., 2020; Hay et al., 2006; Zhang et al., 2022).

Following leaf primordia initiation, the establishment of an adaxial-abaxial tissue polarity network is required for growth in the medio-lateral plane to form a flat lamina (Fig. 1.4c). Angiosperm leaves typically demonstrate distinct cell types and tissue

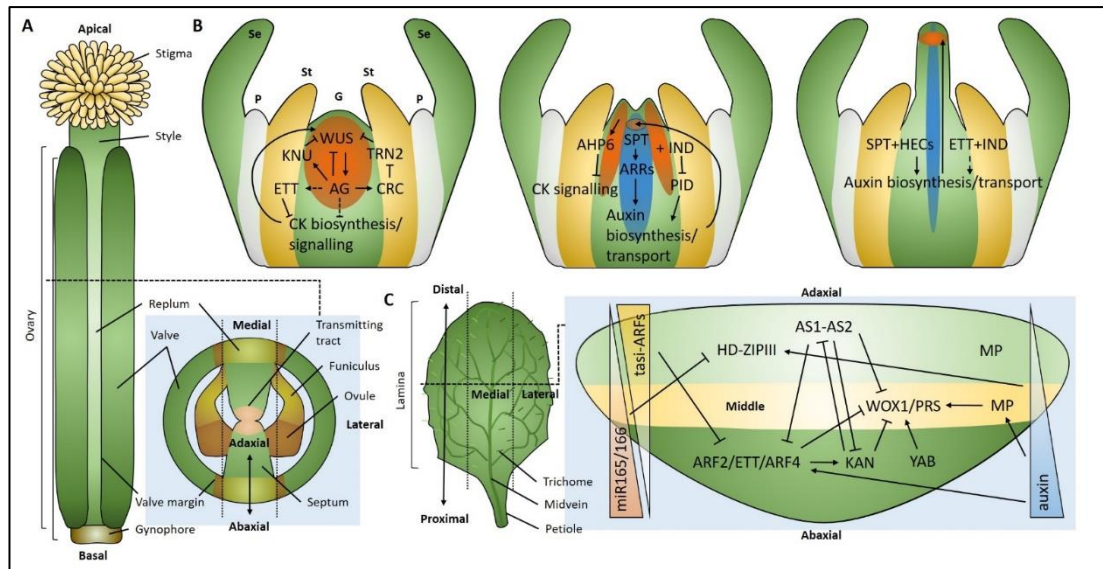


Figure 1.4: Anatomy and gene regulatory networks of the *A. thaliana* gynoecium and leaf. (a) The *A. thaliana* gynoecium consists of multiple tissue types across the apical-basal, medio-lateral and adaxial-abaxial axes. **(b)** The gynoecium tube is initiated by the termination of the floral meristem through the activities of *AG* and *ETT*. *AG* upregulates *ETT*, *CRC* and *KNU* to inhibit *WUS* expression. Part of this mechanism involves the downregulation of cytokinin signalling. As the primordia develops, lateral auxin foci form from *PIN* activity. *SPT* activity in the CMM upregulates cytokinin signalling and together with *IND*, promotes the formation of the medial auxin foci through *PID* repression. In late gynoecium development, *SPT*, *HEC*, *ETT* and *IND* promote auxin biosynthesis and transport for the formation of the auxin ring necessary for radial style symmetry. **(c)** Initiation and maintenance of the leaf adaxial-abaxial polarity for medio-lateral lamina growth is dependent on a complex regulatory network and auxin. The *AS1-AS2* and *HD-ZIP III* promotes adaxial fate while *ARF2/ETT/ARF4*, *KAN* and *YAB* promote abaxial fate. Mutual antagonism of the adaxial-abaxial factors and two small RNA gradients refine the boundaries between the two domains. High auxin levels in the middle domain promote the *MP*-dependent activation of *WOX1* and *PRS* for lamina outgrowth.

organisation in the adaxial and abaxial domains as adaptations for photosynthesis, transpiration and gaseous exchange (Steeves and Sussex, 1989). In *A. thaliana*, adaxial identity is conferred by the ARP member ASYMMETRIC LEAVES1 (AS1), the LATERAL ORGAN BOUNDARIES (LOB)-type transcription factor AS2, and three redundant CLASS III HOMEODOMAIN LEUCINE ZIPPER (HD-ZIP III) transcription factors, REVOLUTA (REV), PHABULOSA (PHB), and PHAVOLUTA (PHV) (Byrne et al., 2000; McConnell et al., 2001; Prigge et al., 2005; Semiarti et al., 2001; Xu et al., 2003). In contrast, the KANADI (KAN) and YABBY (YAB) transcription factor families and the Class B ARFs, ETT, ARF4 and ARF2, promote abaxial identity (Emery et al., 2003; Guan et al., 2017; Kerstetter et al., 2001; Pekker et al., 2005; Sarojam et al., 2010; Siegfried et al., 1999).

Mutual antagonism of the adaxial and abaxial transcription factors maintain the distinct tissue domains to pattern the leaf. For instance, ETT and ARF4 are epigenetically silenced in the adaxial domain by the AS1-AS2 complex while KAN1 represses the transcription of AS2 (Husbands et al., 2015; Iwasaki et al., 2013; Wu et al., 2008). The boundaries between the domains are further reinforced by small RNA gradients: *miR165/166* restricts HD-ZIP III expression to the adaxial domain while trans-acting short interfering RNAs (tasiARFs) restrict the expression of the Class B ARFs to the abaxial side (Chitwood et al., 2009; Juarez et al., 2004; Nogueira et al., 2007).

The juxtaposition of adaxial and abaxial domains in the leaf primordia creates a middle domain where the *WUS*-like meristematic genes *WUSCHEL-RELATED HOMEODOMAIN1* (*WOX1*) and *PRESSED FLOWER* (*PRS*)/*WOX3* are expressed to mediate leaf flattening (Guan et al., 2017; Nakata et al., 2012; Vandenbussche et al., 2009). Auxin signalling mediated by ETT and the Class A ARF *MONOPTEROS* (*MP*)/*ARF5* plays a key role in regulating the expression of *WOX1* and *PRS*. *ARF2*, *ETT* and *ARF4* repress *WOX1* and *PRS* expression in the abaxial domain, while

MP-mediated activation of *WOX1* and *PRS* is likely restricted in the adaxial domain by low auxin levels, thus limiting *WOX1* and *PRS* expression to the margins of the middle domain for mediolateral outgrowth (Guan et al., 2017; Qi et al., 2014).

While the maintenance of the adaxial-abaxial polarity network is relatively well understood, the mechanism of its initiation is less apparent. It is unclear whether polarity is established from a transient auxin gradient in initiating primordia, or from the inheritance of prepatterned domains from the shoot apical meristem that promote adjacent cells into acquiring adaxial or abaxial cell fate (Bhatia et al., 2019; Caggiano et al., 2017; Guan et al., 2018; Qi et al., 2014). A recent study from Burian et al. (2022) reconciles the two viewpoints by demonstrating that the delineation of the adaxial and abaxial boundary is driven by an asymmetric auxin transcriptional output from a uniform auxin field through spatial information from the AS2-KAN1 meristem prepattern. AS2 and KAN1 domains, despite having similar auxin levels in the early primordia, exhibit distinct auxin responsiveness. Surprisingly, ETT was shown to drive the high auxin transcriptional activity observed on the adaxial side of incipient primordia and likely promotes the acquisition of adaxial founder cell fate (Burian et al., 2022). It is possible that the ETT-mediated auxin signalling pathway is responsible for this response, though this remains speculative for now.

Many of the components of the adaxial-abaxial polarity network have ancient origins preceding the evolution of leaves. The HD-ZIP IIIs regulate phyllid development in moss, but the KAN orthologue of *M. polymorpha* does not regulate tissue polarity (Briginshaw et al., 2022; Yip et al., 2016). The HD-ZIP III, KAN and YAB families appear to have generally conserved polarised expression patterns within the seed plants (Arnault et al., 2018; Finet et al., 2016; Floyd et al., 2006; Zumajo-Cardona and Ambrose, 2020). However, *HD-ZIP III* expression in lycophytes is non-polar and limited to younger leaf primordia, reflecting the independent origins of microphyll leaves (Floyd et al., 2006; Prigge and Clark, 2006; Vasco et al., 2016). Interestingly,

the *ARP* family appears to repress *KNOX* activity in both lycophyte microphylls and seed plant leaves, indicating the convergent evolution of this pathway in regulating organogenesis (Harrison et al., 2005). Monilophyte orthologues share similar localisation patterns of *ARP*, *HD-ZIP III* and *KAN* despite the presumed non-homology between fern fronds and seed plant leaves (Harrison et al., 2005; Vasco et al., 2016; Zumajo-Cardona et al., 2019). A recent study also observed abaxial expression of an *ETT/ARF4*-like gene in the monilophyte *Ceratopteris pteridioides* (Sun and Li, 2020). Nonetheless, the lack of the YABBY family in monilophytes indicates a divergent mechanism of lamina expansion, and functional studies will be required to elucidate the similarities and differences between fern frond and seed plant leaf developmental programmes (Finet et al., 2016; Li et al., 2018).

1.3.3 Gynoecium initiation and its apical-basal patterning

The adaxial-abaxial polarity network is not limited to leaf patterning, but also regulates the development of other lateral organs such as flowers. Defects in floral organ polarity and growth can be observed in mutants of the *KAN*, *YAB*, *HD-ZIP III* and *ARF* gene families (Pekker et al., 2005; Prigge et al., 2005; Sessions et al., 1997b; Siegfried et al., 1999). In addition, the polarised nuclear auxin response in the middle region of developing leaf primordia was also observed in bracts and sepals (Burian et al., 2022). Expression patterns and heterologous expression studies of *KAN*, *YAB* and *ARF* orthologues from basal angiosperms suggest that the role of auxin and the adaxial-abaxial polarity network in floral organ development has been present in the last common ancestor of extant angiosperms (Arnault et al., 2018; Fourquin et al., 2007; Lora et al., 2011; Yamada et al., 2011). These data support a scenario in which the ancestral polarity network was co-opted for the development of floral organs in coordination with the MADS-box organ identity genes after the evolution of flowers.

The gynoecium is the defining trait of the angiosperms and is found in the innermost whorls of flowers. In *A. thaliana*, the gynoecium is formed from the congenital fusion of two carpels that grows out as a hollow tube after the termination of the floral meristem (Fig. 1.4a; Reyes-Olalde et al., 2013; Sessions et al., 1997b). The carpel margin meristem (CMM) forms on the inner (adaxial) side of the tube giving rise to inner tissues. The stigma consisting of elongated papilla cells is located at the apex of the gynoecium and is important for pollen collection, germination, and pollen tube growth. Below the stigma is the style that surrounds the central transmitting tract. The ovary, consisting of the replum, valves, valve margins, ovules and septum, form the largest part of the *A. thaliana* gynoecium. The two lateral valves, separated by the medial repla, protect the developing seeds. The valve margins connect the repla and the valves and are vital for the dehiscence of the mature fruits (also known as siliques). The inner septum connects the repla within the ovary and contains placenta that give rise to ovules. The most basal structure is the gynophore which connects the fruit with the rest of the plant.

The termination of the floral meristem and the initiation of the gynoecium primordium is dependent on the Class C MADS-box gene *AGAMOUS* (*AG*). *AG* terminates the floral meristem through a variety of pathways that converges upon the repression of the meristem maintenance gene *WUS*. *AG* becomes expressed in the floral meristem through the actions of *WUS* and *LFY* during stage 3 when sepal primordia emerge (Lohmann et al., 2001; Uemura et al., 2018). As the developing sepals begin to cover the meristem at stage 4 and 5, *AG* directly represses *WUS* (Liu et al., 2011; Prunet et al., 2008). During stage 6 when the gynoecium primordium becomes established, *AG* promotes the expression of *KNUCKLES* (*KNU*) to further repress *WUS* (Sun et al., 2009). *AG* also modulates the hormone response in the gynoecium primordium to mediate *WUS* repression. The direct *AG* target gene *CRABSCLAW* (*CRC*), a member of the YAB family, inhibits the

TORNADO2 (*TRN2*) gene involved in auxin homeostasis for the formation of an auxin maxima (Yamaguchi et al., 2017). AG also activates the expression of *ETT*, and in synergy with *ETT*, promotes the auxin-dependent repression of cytokinin biosynthesis and signalling (Zhang et al., 2018b).

Following the establishment of the gynoecium primordium (Fig. 1.4b), two auxin maxima, or foci, are formed at the lateral regions while cytokinin signalling becomes restricted to the adaxial side of the medial domain (Larsson et al., 2014; Moubayidin and Østergaard, 2014; Müller et al., 2017; Reyes-Olalde et al., 2017). The transcription factor gene *SPATULA* (*SPT*) becomes expressed in this high cytokinin signalling domain and is necessary for the proper formation of the CMM (Heisler et al., 2001; Reyes-Olalde et al., 2017). *SPT* activates the cytokinin signalling components *ARABIDOPSIS RESPONSE REGULATOR1* (*ARR1*) and *ARR12* to activate auxin biosynthesis and transport for gynoecium growth. In the high auxin lateral domains, *ARABIDOPSIS HISTIDINE PHOSPHOTRANSFERASE 6* (*AHP6*) represses cytokinin signalling to maintain the distinct auxin and cytokinin signalling domains (Reyes-Olalde et al., 2017).

As the gynoecium continues to develop at stage 9, two additional medial auxin foci appear and fuse with the lateral foci to form an auxin ring at stage 10. The formation of this ring is dependent on the activities of *SPT* and *INDEHISCENT* (*IND*) which directly repress *PID* to mediate auxin redistribution (Moubayidin and Østergaard, 2014). The *HECATE* (*HEC*) transcription factors also function with *SPT* to regulate auxin biosynthesis and transport for the formation of the auxin ring (Gremski et al., 2007; Schuster et al., 2015). Finally, the *ETT*-mediated auxin signalling pathway contributes to the formation of the auxin ring through its auxin-sensitive interaction with *IND* and the auxin-dependent regulation of *PID* and *HEC1* expression (Kuhn et al., 2020; Simonini et al., 2017; Simonini et al., 2016). With the formation of the ring, a radial style develops from the initial bilateral gynoecium primordium (Moubayidin

and Østergaard, 2014). By stage 12, the gynoecium tube closes with the development of stigmatic papillae cells and the maturation of the transmitting tract. Lastly, the valve margins are defined by an auxin minimum prior to fruit dehiscence at Stage 17 (Sorefan et al., 2009).

Unlike the wild-type gynoecium, *ett* gynoecia exhibit over-proliferation of the medial and apical tissues (Nemhauser et al., 2000; Sessions et al., 1997b). Furthermore, the gynoecium fails to close properly, giving rise to a 'split-style' phenotype. An enlarged gynophore and reduced ovary size is also observed, likely due to the role of ETT in mediating valve growth through upregulation of pectin methylesterases (Andres-Robin et al., 2018). Curiously, the phenotype of wild-type gynoecium with auxin transport inhibitors resemble that of *ett* null mutants, strongly indicating ETT as an essential integrator of the auxin signal (Nemhauser et al., 2000).

As seen in leaf development, the juxtaposition of the adaxial-abaxial boundary is necessary for the establishment of a domain of high auxin response and mediolateral outgrowth. It has been proposed that the adaxial-abaxial boundary of the gynoecium primordium lies at the apical ridge which separates the outer and inner tissues (Hawkins and Liu, 2014; Larsson et al., 2013). Loss of ETT disrupts this boundary, resulting in partially adaxialised carpels with enlarged adaxial tissues such as the stigma and style. This model is supported by the similarity of the gynoecium phenotype in higher order *kan* mutants and the complete loss of abaxial tissue in gynoecia of the *ett arf4* double mutant (Pekker et al., 2005).

Given the multiple and integral roles of ETT in gynoecium development, only a small part of its function has been attributed to the non-canonical auxin signalling pathway that it mediates (Kuhn et al., 2020; Simonini et al., 2016). It has been shown that ETT interacts with the *KAN* gene *ABERRANT TESTA SHAPE (ATS)* in an auxin-sensitive manner, so the ETT-mediated auxin signalling pathway might be important for adaxial-abaxial polarity in lateral organs (Simonini et al., 2016). Furthermore, the

A. thaliana gynoecium is highly derived, so the degree of conservation of the ETT-mediated pathway in other angiosperms is unclear. In the ANA grade angiosperms (Amborellales, Nymphaeales and Austrobaileyales), three lineages that form a sister clade to the rest of the core angiosperms, the gynoecium is ascidiate or tube-shaped, typically with incomplete closure and lacking distinct styles (Endress and Igersheim, 2000). As ETT is also expressed in a similar pattern in the gynoecium of the ANA grade angiosperm *Amborella trichopoda* (Arnault et al., 2018; Finet et al., 2010), it is possible that ETT and its auxin signalling pathway may have played a role in gynoecium development in the last common ancestor of extant angiosperms despite the vastly different morphologies.

1.4 Scope of the thesis

The long history of auxin research, encompassing its biosynthesis, transport, signalling pathways, developmental functions, and evolution, has solidified its status as the primary morphogen in plants. Beyond the canonical auxin signalling pathway, various alternative pathways have emerged to explain aspects of auxin signalling not accommodated by the canonical route. Notably, one such pathway involves the direct modulation of ETT transcriptional activity by auxin. The recent evolutionary emergence of ETT and its paralogue ARF4 in land plants, along with their widespread roles in lateral organ polarity and development, opens up questions on the mechanisms underpinning the ETT-mediated pathway's influence on lateral organ morphogenesis and its evolutionary origin. Therefore, this thesis aims to elucidate the mechanism and origin of the ETT-mediated auxin signalling pathway in leaf and gynoecium development.

Chapter 2 investigates the evolutionary history of the Class B ARFs with emphasis on the ETT/ARF4-like clade. Prior studies have shown that the ETT/ARF4-like clade exist in the gymnosperms and a gene duplication event at the base of the angiosperm clade resulted in the divergence of the ETT and ARF4 clades (Finet et

al., 2013; Mutte et al., 2018). However, there is increasing evidence that the ETT/ARF4-like clade preceded the seed plants and exists in monilophytes (Sun and Li, 2020; Xia et al., 2017). ETT and ARF4 have also undergone extensive structural changes, such as the loss of the PB1 domain, during the radiation of extant angiosperm clades which complicates the delineation of ETT and ARF4 orthologues in non-eudicot lineages (Finet et al., 2010). With the creation of our updated Class B ARF phylogeny encompassing numerous previously underrepresented lineages, we confirm the existence of the ETT/ARF4-like clade in monilophytes and further clarify the structural divergence of ETT and ARF4 within the magnoliids and monocots. Through a machine learning algorithm, we also identified ETT- or ARF4-enriched motif variants of the ARF middle region domain that might be important for the differential functions of both ARFs with regards to auxin sensing and plant development.

To complement the *in silico* data obtained in Chapter 2, the auxin sensitivity of ETT/ARF4-like orthologues from chosen species representing key phylogenetic lineages in the land plants were tested in **Chapter 3**. A yeast-2-hybrid screen of these ETT/ARF4-like orthologues were conducted against the KAN and YAB abaxial polarity transcription factor families to assess the contribution of the ETT-mediated auxin sensing pathway in mediating lateral organ polarity. The results of the screen was inconclusive due to the failure of the positive auxin-sensitive *ATS* control that was previously shown to interact with ETT in an auxin-dependent manner (Simonini et al., 2016), although it remains a possibility that the results are biologically relevant meaning that ETT-mediated auxin signalling is not important for lateral organ polarity. Nonetheless, another yeast-two-hybrid screen with the TPL/TPR family of corepressors indicate that auxin sensing is a property specific to ARF4 and has originated since the last common angiosperm ancestor. Furthermore,

chimeric constructs between auxin-sensitive and auxin-insensitive ETT/ARF4-like orthologues identifies contributions of the DNA-binding domain to auxin binding.

In **Chapter 4**, the developmental roles of the various ETT/ARF4-like orthologues assessed in Chapter 2 were investigated through their heterologous expression in the *ett-3* mutant background. All ETT orthologues from angiosperm species complemented the *ett-3* phenotype while all angiosperm ARF4 orthologues provided partial complementation. Strikingly, none of the non-angiosperm ETT/ARF4-like orthologues were able to complement the *ett-3* gynoecium defect, indicating the evolutionary origin of ETT's gynoecium development function in the last common ancestor of the angiosperms. Moreover, heterologous expression of the ETT/ARF4-like orthologues in the *ett-3 arf4^{GE}* background revealed the origin of ETT's role in leaf morphogenesis. Full complementation of the *ett-3 arf4^{GE}* leaf polarity defect was observed for all angiosperm ETT and ARF4 orthologues, while a gymnosperm ETT/ARF4-like orthologue was able to partially complement the phenotype. To assess the contribution of the ETT-mediated pathway in gynoecium development, the chimeric ETT constructs from Chapter 3 were expressed in *ett-3* plants. These lines supported a link between the auxin responsiveness of ETT/ARF4-TPL/TPR interactions and complementation of style development.

Finally, **Chapter 5** provides a summary of the results of this thesis and how the data relates to the current model of ETT action and evolution. Future directions to better understand the mechanisms of this pathway are also discussed.

Chapter 2:

A deep phylogenetical analysis of the Class B ARFs reveals the stepwise evolution of the ETT/ARF4 clade and its associated motifs and domains.

The Class B ARF phylogenetic tree and motif alignments (Figure 1.1 – 1.3) were generated by Dr. Sumanth Mutte and Ellis van de Laak (Weijers Lab, Wageningen University and Research, the Netherlands).

2.1 Introduction

As discussed in Chapter 1, the ARFs can be divided into three major clades in the land plants (Finet et al., 2013; Mutte et al., 2018). The Class A ARFs play a major role in the canonical TIR1/AFB-dependent auxin signalling pathway where they activate gene expression upon perception of auxin by the TIR1/AFB F-box receptors (Kepinski and Leyser, 2005; Tiwari et al., 2003; Ulmasov et al., 1999a). In contrast, the Class B and Class C ARFs were classified as repressors based on biochemical assays and have limited interactions with the AUX/IAA repressors involved in canonical auxin signalling (Piya et al., 2014; Ulmasov et al., 1999a; Vernoux et al., 2011). In the bryophyte *Marchantia polymorpha*, the sole Class B ARF was shown to act in an auxin-independent manner to negatively regulate Class A ARF activity through the competitive binding of downstream target genes (Kato et al., 2020).

In *Arabidopsis thaliana*, the Class B ARF known as ARF3/ETT completely lacks the Phox/Bem1 (PB1) domain necessary for AUX/IAA heterodimerisation and thus cannot participate in the canonical auxin signalling pathway. Nonetheless, it has been demonstrated that ETT can regulate a subset of genes in gynoecium development in an auxin-dependent manner, independently from the TIR1/AFB-dependent pathway (Kuhn et al., 2020; Simonini et al., 2017). This auxin-sensing ability of ETT was shown to be dependent on key residues in its middle region, hereby referred to as the ETT-specific (ES-) domain (Kuhn et al., 2020; Simonini et al., 2018a). The direct binding of auxin to ETT triggers a conformational change that disrupts the protein-protein interaction between ETT and the TPL/TPR corepressors, as well as the interactions with numerous transcription factors from various families (Kuhn et al., 2020; Simonini et al., 2016). These findings suggest that ETT has neofunctionalised to participate in a novel TIR1/AFB-independent auxin signalling pathway.

The origins of the canonical TIR1/AFB-dependent pathway can be traced to the streptophyte algae, where ARF precursors known as proto-ARFs have been identified (Martin-Arevalillo et al., 2019; Mutte et al., 2018). Nevertheless, the complete TIR1/AFB-dependent signalling pathway as described in *A. thaliana* only exists within the embryophytes where it is deeply conserved (Kato et al., 2020; Prigge et al., 2010). As ETT originated through a relatively recent gene duplication event in the last common ancestor of extant angiosperms (Finet et al., 2013; Finet et al., 2010), it is currently unknown whether the ETT-mediated auxin signalling pathway is conserved within the angiosperms and whether this auxin-sensing property originated prior to or after its divergence from the ETT/ARF4-like clade.

As mentioned earlier, ETT in *A. thaliana* completely lacks the PB1 domain which precludes it from the canonical auxin signalling pathway. However, its close paralogue, ARF4, contains a functional PB1 domain that can interact with AUX/IAA proteins (Piya et al., 2014). Interestingly, the PB1 truncation pattern is reversed in the ANA grade basal angiosperms, *A. trichopoda* and *Cabomba aquatica*; the ETT orthologues of both species contain the full PB1 domain, while truncated ARF4 transcripts due to alternative splicing (in *A. trichopoda*) or a premature stop codon (in *C. aquatica*) have been detected (Finet et al., 2010). Thus, PB1 absence/presence patterns cannot be used to delineate ETT or ARF4 identities outside the core eudicots. The poor conservation of the intrinsically disordered domains of ETT and ARF4 also presents a challenge in identifying domains or motifs that could be useful for delineating both clades for functional characterisation (Roosjen et al., 2017; Simonini et al., 2018a).

Beyond the angiosperms, there has been some confusion on the evolutionary origin of the ETT/ARF4-like clade that predates the ETT and ARF4 divergence. The scientific consensus accepts the presence of the ETT/ARF4-like clade in gymnosperms but data has previously been lacking on the presence of the clade in

the monilophytes (Finet et al., 2013; Mutte et al., 2018). Until very recently, the availability of monilophyte genomes have been poor due to their typically immense genome sizes (on average 12.3 Gb) (Li et al., 2018; Sessa and Der, 2016).

Therefore, discrepancies between studies could be attributed to missing data in the transcriptomes used in phylogeny construction. Recent transcriptomics-based studies however have provided compelling evidence for the origin of the ETT/ARF4-like clade in the last common ancestor of the euphyllophytes (Gao et al., 2020; Sun and Li, 2020; Xia et al., 2017). To complement these studies and to reduce sampling artefacts, genomics-based resources should be utilised in phylogeny construction and orthologue identification for further characterisation.

This chapter thus aims to address the limitations from previous phylogenetic analyses on the evolution of the Class B ARFs with a strong focus on the ETT and ARF4 clades. Firstly, we construct a phylogeny of the Class B ARFs with greater taxon sampling from previously underrepresented groups such as the monilophytes and magnoliids (Table S1.1). Using this phylogeny, we confirm the presence of the ETT/ARF4-like clade in monilophytes and identify important orthologues for further characterisation.

Through the greater sampling of the monocots and magnoliids, we detect two instances where ARF4 has been lost: once in the last common ancestor of the monocots, and once after the divergence of the Laurales from the Magnoliales within the magnoliids. Importantly, we show that the PB1 domain has been lost in multiple species within the monocots, in contrary to the findings of Finet et al. (2013).

Finally, we carried out an *in silico* analysis to identify biochemical properties and cryptic motifs in the ETT and ARF4 middle regions that could be used for delineating both clades. Through this method, we identify ETT- or ARF4-enriched variants of the NLS, W505 and EAR-like motifs.

2.2 Results

2.2.1 The ETT/ARF4-like clade originated after the divergence of the euphyllophytes

The recent availability of multiple genomes from underrepresented clades in the monilophytes, ANA grade angiosperms, non-Poaceae monocots, magnoliids and basal eudicots (Table S2.1) opens the possibility of resolving the contradictions regarding the origin of the ETT/ARF4 clade (Finet et al., 2013; Finet et al., 2010; Mutte et al., 2018; Sun and Li, 2020; Xia et al., 2017). In addition, the increased taxonomic sampling allows us to investigate the evolution of protein motifs and domains that delineate ETT and ARF4 at a higher resolution. Therefore, to address these problems, we constructed a comprehensive phylogeny of the Class B ARFs with improved sampling of previously underrepresented clades using published whole genome sequencing data (Fig. 2.1, Fig. S2.1).

In accordance with previous studies, the bryophytes and lycophytes only contain a single Class B ARF clade, with no orthologues falling within the *Arabidopsis thaliana* ARF2, ETT/ARF4 or ARF1/rest (all other Class B ARFs) clades (Fig. S2.1) (Mutte et al., 2018; Xia et al., 2017). However, our phylogeny clusters a subset of Class B ARF sequences from the monilophytes *Ceratopteris richardii*, *Azolla filiculoides* and *Salvinia cucullata* with the ETT/ARF4 clade of the spermatophytes, indicating that the ETT/ARF4 clade is also present in the monilophytes (Fig. 2.1, Fig. S2.1). Our results indicate that the ETT/ARF4 clade evolved after the divergence of the euphyllophytes and lycophytes rather than after the divergence of monilophytes and spermatophytes, thus supporting the findings of Xia et al. (2017) and Sun and Li (2020) and rejecting the conclusion of Mutte et al. (2018).

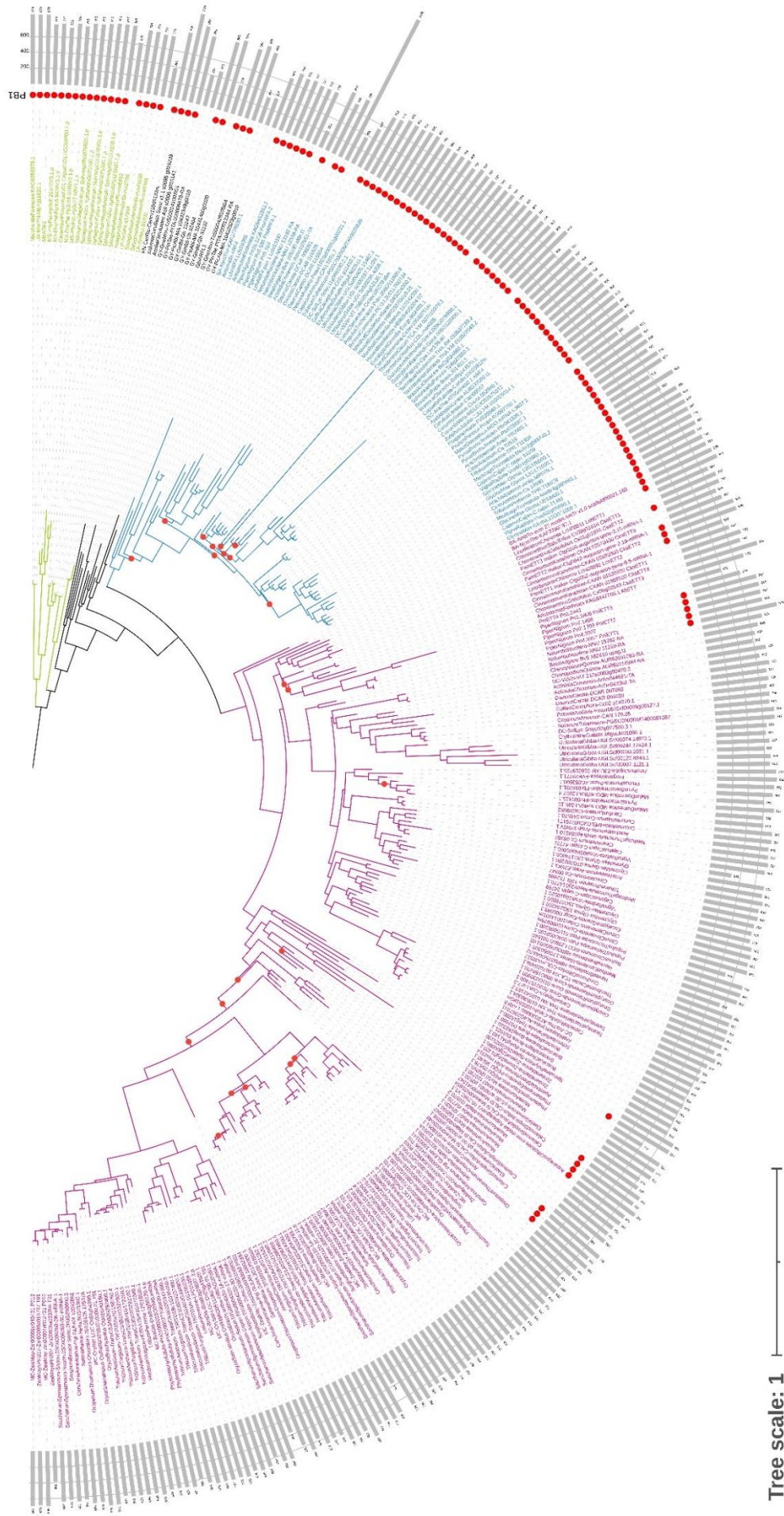


Figure 2.1: Phylogenetic tree of the ETT/ARF4-like clade in land plants (previous page). Sequences in green text belong to the sole Class B ARF clade in the bryophytes and lycophytes. Sequences in black represent the ETT/ARF4-like in monilophytes and gymnosperms. Angiosperm ETT sequences are represented in magenta while ARF4 sequences are represented in cyan. Red circles next to the taxa names indicate the presence of a PB1 domain, and the grey bars indicate the length of the protein sequence. Red circles on the branches indicate the poor bootstrap support (<75) for that split.

2.2.2 Diverging trajectories of ETT and ARF4 structural evolution in the core angiosperms

After the divergence of the ETT/ARF4 clade from the rest of the Class B ARFs in the euphyllophytes, the ETT/ARF4 clade subsequently underwent a gene duplication event prior to the last common ancestor of extant angiosperms to give rise to the separate ETT and ARF4 clades (Finet et al., 2013; Finet et al., 2010). We confirm this finding through the detection of ETT and ARF4 orthologues from the genomes of the ANA grade angiosperms, *Amborella trichopoda* and *Nymphaea thermarum* (Fig. 2.1, Fig. 2.2). However, our improved phylogeny also allowed us to further investigate the evolutionary trajectories of ETT and ARF4 in the core angiosperms after their divergence from the basal angiosperms beyond the scope of Finet et al. (2013).

We show that ARF4 has been lost independently twice in the core angiosperms (Fig. 2.1, Fig. 2.2). One event occurred on the branch leading to the last common monocot ancestor, as no ARF4 orthologue can be found in any sampled monocot species. This includes the species *Zostera marina* and *Spirodela polyrhiza* within the Alismatales order that is sister to all other monocots except the Acorales. Another ARF4 loss event occurred in the magnoliids after the divergence of the Laurales from the Magnoliales, as no ARF4 orthologue can be found from the

genomes of *Persea americana*, *Cinnamomum kanehirae* and *Chimonanthus salicifolius* while ARF4 is found in the genome of *Liriodendron chinense*.

Interestingly, the ETT clade is usually kept as a single copy in the genomes of most core eudicots despite the ancestral gamma whole genome triplication event in the last common ancestor of the core eudicots and subsequent lineage-specific Whole Genome Duplications (WGDs) (Jiao et al., 2012; Qin et al., 2021). In contrast, the ETT clade has expanded greatly in the commelinid monocots, ranging from two copies in *Ananas comosus* and *Hordeum vulgare* to 12 copies in the hexaploid *Triticum aestivum* genome. High copy numbers of ETT are also observed in the diploid *Oryza sativa* (4 copies) and the double-haploid *Musa acuminata* (6 copies) genomes, suggesting that high copy numbers are not only due to recent polyploidisation events in the commelinid monocots.

While ETT and ARF4 are closely related paralogues, a defining trait of ETT in *A. thaliana* is the absence of the PB1 domain (Sessions et al., 1997a; Simonini et al., 2016). Gymnosperm ETT/ARF4-like orthologues were found to contain the PB1 domain, indicating that the presence of the PB1 domain is ancestral to the ETT and ARF4 clades (Finet et al., 2010). We detect the presence of the PB1 domain not only in most gymnosperm ETT/ARF4-like orthologues, but also in the monilophyte orthologues, thus supporting this hypothesis (Fig. 2.1). Additionally, we observe the loss of the PB1 domain from the ARF4 but not the ETT orthologue of *N. thermarum*, in line with the observations of Finet et al. (2010) regarding the ANA grade.

The PB1 domain of ETT was proposed to have been lost at least twice after the divergence of the core angiosperms from the ANA grade, once within the magnoliids and once prior to the last common ancestor of both monocots and eudicots (Finet et al., 2013). Our extensive sampling of monocot genomes from multiple orders demonstrates that the full PB1 domain is retained in the ETT orthologues of *Z. marina*, *Asparagus officinalis*, *Calamus simplicifolius* and *Elaeis*

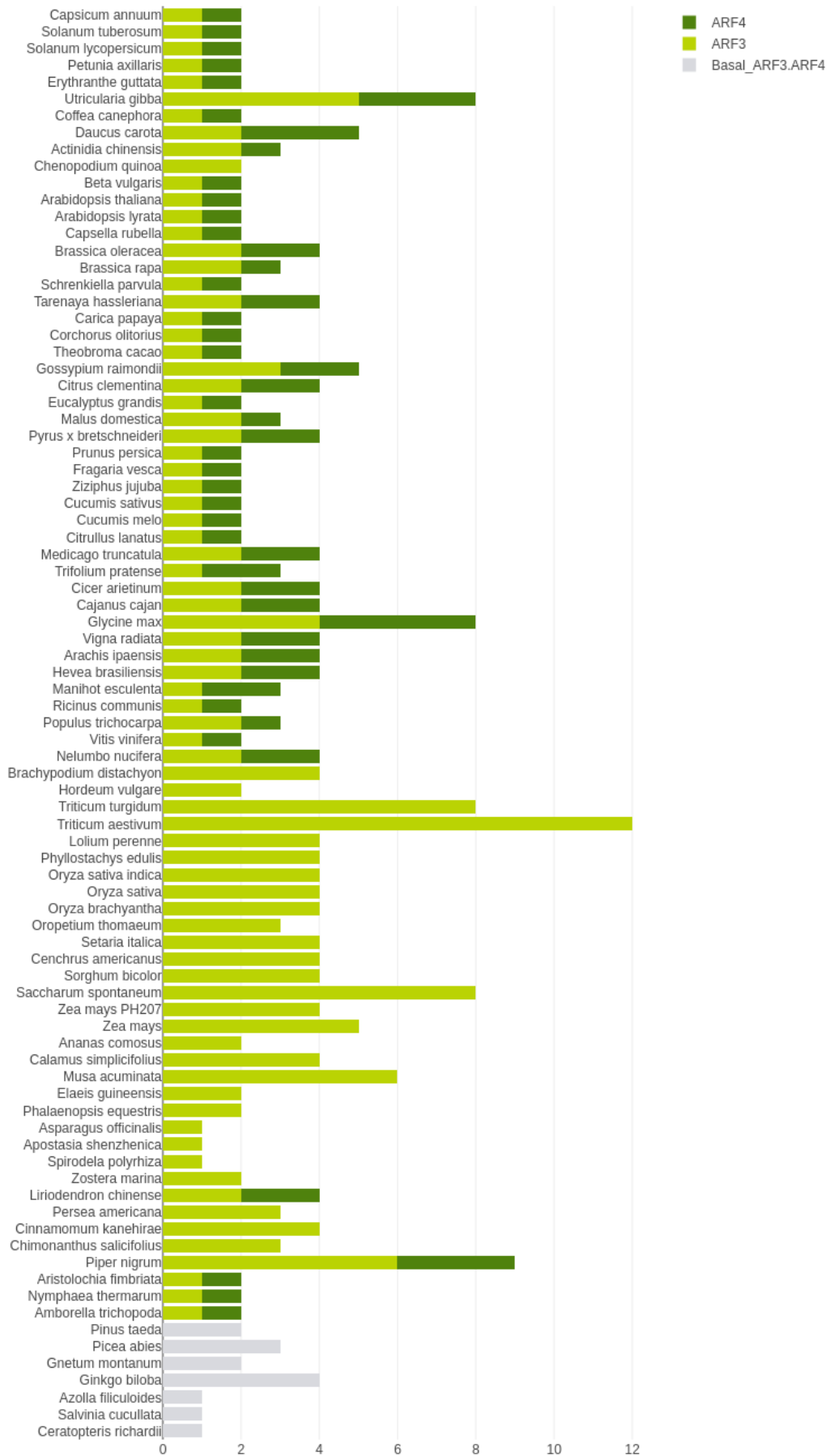


Figure 2.2: Copy number of ETT/ARF4-like orthologues in euphyllophyte genomes (previous page). Grey bars indicate the number of ETT/ARF4-like paralogues in non-angiosperm lineages. Light and dark green bars correspond to the number of ETT and ARF4 paralogues, respectively, in angiosperm genomes.

guineensis, suggesting that the PB1 domain has been independently lost within the monocots at least thrice (Fig. 2.1).

2.2.3 Delineation of ETT and ARF4 through variants in conserved middle region motifs

As discussed above, the major difference between ETT and ARF4 in the core eudicots is the absence or presence of the PB1 domain, and except for a few primary sequence motifs, the intrinsically-disordered middle region is poorly conserved between species (Simonini et al., 2018a). This presents a problem in non-eudicot angiosperm species where the absence/presence pattern of the PB1 domain in ETT or ARF4 orthologues is not as clearcut. Therefore, we attempted to identify cryptic motifs specific to ETT, ARF4 or the ETT/ARF4-like clades through a machine learning approach (Fig. 2.3).

The middle region of the Class B ARFs from our sampled genomes were grouped according to their phylogenetic clades and analysed in R to assess biophysical properties and motifs that are enriched in each clade. Among the parameters assessed by the algorithm were the amino acid composition, basic primary sequence characteristics, intrinsic disorder properties and conserved di- or tripeptide motifs. We included the F3 parameter for protein bulkiness, the arginine-lysine (RK)-ratio and asparagine (N) content as measures of protein stickiness, and the isoelectric point (pI) (Figure S2.2). In general, ETT orthologues possess longer middle regions, a lower proportion of bulky amino acids, a higher RK-ratio, lower N-enrichment and a lower pI than ARF4 orthologues.

The N-terminus of the ETT middle region contains a KRx(K/R) nuclear localisation signal (NLS) motif that have also been identified in 14 other *A. thaliana* ARFs (Simonini et al., 2018a). Our analysis reveals that the motif is also found in the ARF4, ARF1/rest and ARF2 clades (Fig. 2.3C). However, a subset of monocot ARF4 orthologues contains the variant KKxR motif and it is uncertain whether this motif is functionally equivalent to the KRx(K/R) motif. Furthermore, the NLS motif in ARF2 is typically preceded by a NPLP motif (Fig. 2.3C), but nothing is known about the significance of this motif.

The ARF2 and ETT/ARF4 clades in angiosperms are well defined by the presence of tasiARF binding sites necessary for the post-transcriptional regulation of the ARFs (Garcia et al., 2006; Xia et al., 2017; Yifhar et al., 2012). In angiosperms, ARF2 orthologues contain only a single tasiARF site whereas ETT/ARF4 orthologues have two tasiARF sites. The result of our alignment not only independently confirms this finding when analysing the translated, conserved amino acid sequence, but we also identify a conserved IC diamino acid motif adjacent to the second tasiARF site specific in ARF4 (Fig. 2.3A).

Our alignment of the monilophyte ETT/ARF4-like orthologues uncovers the highly variable nature of monilophyte tasiARF sites relative to angiosperm ETT or ARF4 sequences (Fig. 2.4). The *A. filiculoides* and *S. cucullata* orthologues completely lack a tasiARF site, while the *C. richardii* orthologue contains only one tasiARF site that is divergent in sequence to the canonical site that translates into a VLQGQE motif found in angiosperm ETT or ARF4 orthologues (Fig. 2.3A), suggesting that monilophyte ETT/ARF4-like orthologues might not be post-transcriptionally regulated by the tasiARF pathway.

The (R/K)LFG EAR-like motif at the C-terminus of the middle region in ETT is necessary for the interaction of ETT with the TPL/TPR corepressors (Kuhn et al., 2020). This motif has also been shown to be important for TPL/TPR recruitment by

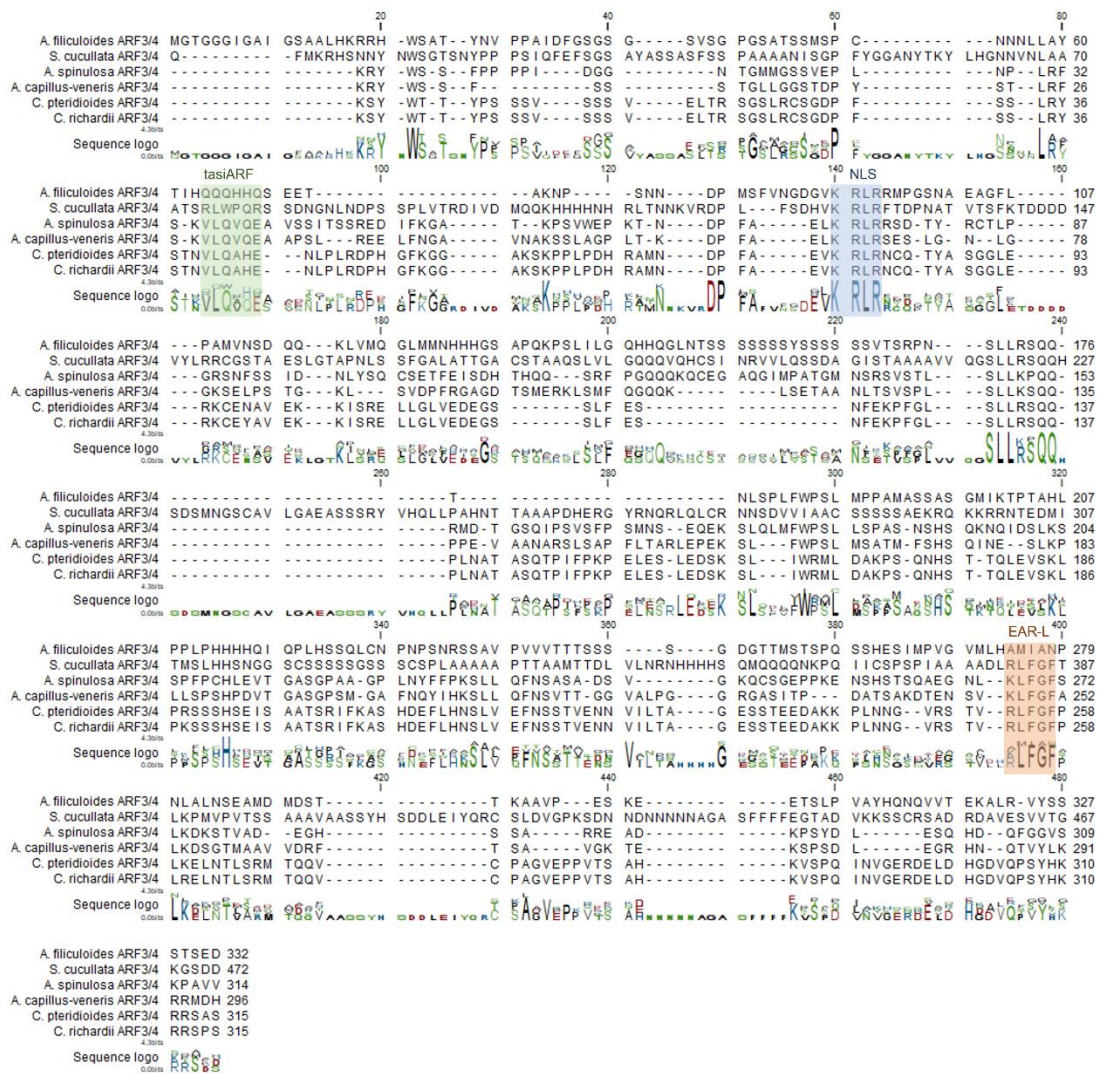


Figure 2.4: Alignment of monilophyte ETT/ARF4-like MR sequences. Species included in the alignment are *Azolla filiculoides*, *Salvinia cucullata* and *Ceratopteris richardii* from our phylogeny, *Ceratopteris pteridioides* (Sun and Li, 2020), and *Adiantum capillus-veneris* and *Alsophila spinulosa* whose orthologues were identified from BLAST searches of the recently released genomes (Fang et al., 2022; Huang et al., 2022). The tasiARF binding site, NLS and EAR-like motifs are highlighted by the green, blue and orange boxes respectively.

A. thaliana ARF2 and *M. polymorpha* ARF2 (Choi et al., 2018; Kato et al., 2020).

The result of our analysis shows that the ARF4 EAR-like motif is predominantly (C)KLFG while the eudicot ETT EAR-like motif is usually (C)RLFG (Fig. 2.3B).

Interestingly, the monocot ETT EAR-like motifs are more variable with a consensus

motif of (C)(R/K/M)(L/I)FG. By extending our analysis to the whole Class B ARF clade, we also identify the (C)RLFG sequence as the dominant variant in the ARF1/rest clade while the (C)K(L/I)FG is dominant in the ARF2 clade. Curiously, the EAR-like motif has been lost from the ETT/ARF4-like orthologue of the monilophyte *A. filiculoides* although the motif is found in the closely related species *S. cucullata* (Fig. 2.4)

The W505 residue in the *A. thaliana* ETT sequence has been shown to contribute to the auxin sensitivity and direct auxin binding properties of ETT (Kuhn et al., 2020). Nonetheless, it is unknown whether this tryptophan residue is conserved beyond *A. thaliana* and if it is also present in other Class B ARFs. We find that the W505 residue is widely conserved in eudicot ETT sequences, but not in monocot ETT sequences where it is sometimes substituted with a leucine residue (Fig. 2.3D). In addition, we detect the presence of a tryptophan in an equivalent position as well in most ARF4 sequences, where it is typically preceded by an LGA motif and followed by a G+K motif (Fig. 2.3D).

2.3 Discussion

This chapter attempts to further our understanding of Class B ARF evolution with an emphasis on the structural changes in the ETT and ARF4 clades after their divergence in angiosperms. With recent technological innovations reducing sequencing costs and improving large genome assemblies, many genomes beyond those of model or crop species have become available (Chen et al., 2018; Marks et al., 2021). Taking advantage of this, we were able to investigate ETT and ARF4 evolution throughout the land plants in greater detail than was possible before. Our phylogenetical analysis confirms the existence of monilophyte ETT/ARF4-like orthologues, further elucidates the structural divergence of ETT and ARF4 within the core angiosperms, and uncovers patterns of motif evolution within each clade (Fig. 2.5).

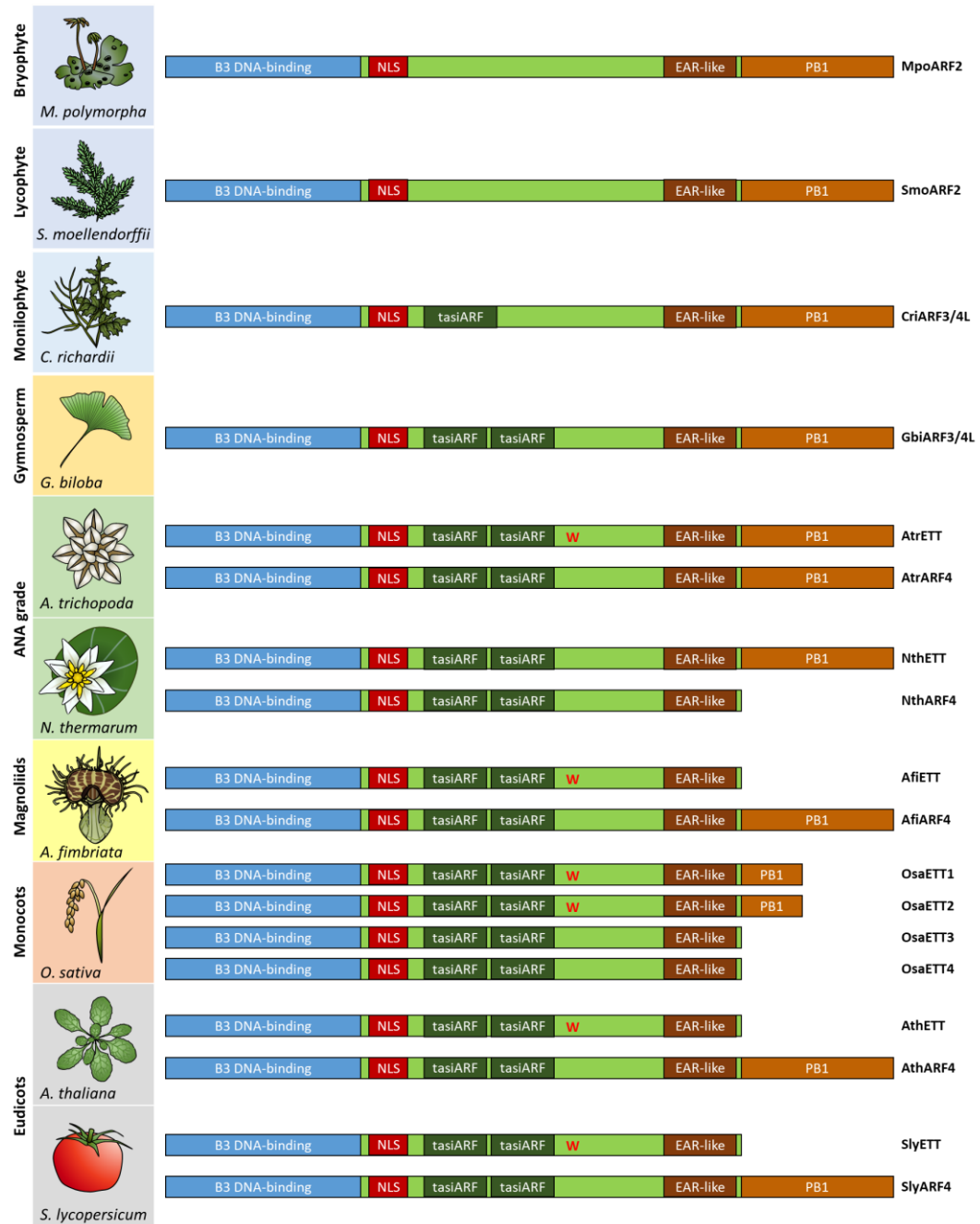


Figure 2.5: Domain changes in ETT/ARF4-like orthologues in the euphyllophytes. The sole Class B ARF clade of the bryophytes and lycophytes contain the EAR-like domain but lack tasiARF binding sites. The tasiARF site is present as a single copy in monilophytes and as tandem repeats in spermatophytes. The W505 residue has been detected in the ETT orthologues of most, but not all, angiosperms. ARF4 is missing in all monocots while ETT is usually present as multiple copies in the commelinid monocots. The PB1 domain has been independently lost in the ARF4 orthologues of the Nymphaeales and the ETT orthologues of some monocots, magnoliids and all core eudicots.

2.3.1 The ETT/ARF4 clade is an euphyllophyte innovation

Earlier studies in ARF evolution were limited by the lack of genomic resources in certain recalcitrant clades such as the monilophytes (Finet et al., 2013). Thus, transcriptomic data, either from publicly available databases such as the OneKP initiative (Leebens-Mack et al., 2019), or from *de novo* RNAseqs were utilised (Mutte et al., 2018; Sun and Li, 2020; Xia et al., 2017). Discrepancies between these studies can therefore be explained by missing data caused by the technical limitations of a transcriptome-based approach (Guo et al., 2023). Furthermore, these studies were not focused on the evolution of the domains and motifs related to auxin signalling. Therefore, we updated Class B ARF phylogeny focused on the ETT/ARF4-like clade and its structural evolution which supported the hypothesis that the ETT/ARF4-like clade originated in the last common ancestor of the euphyllophytes.

The study by Sun and Li (2020) demonstrated that the ETT/ARF4-like orthologues of the polypod ferns *Ceratopteris pteridioides*, *Cyrtomium guizhouense*, and *Parathelypteris nipponica* lacked the canonical tasiARF sites as seen in spermatophyte orthologues (Fig. 2.3), with the implication that monilophyte ETT/ARF4-like orthologues are not post-transcriptionally regulated by the *miR390-TAS3-ARF* pathway (Marin et al., 2010; Xia et al., 2017). We observe a similar trend in the ETT/ARF4-like orthologues of our included monilophyte species, either as the complete lack of a site in the Salviniales representatives *A. filiculoides* and *S. cucullata*, or as a divergent motif sequence (Fig. 2.4). Interestingly, Xia et al. (2017) found that the fern *Anemia tomentosa* contained two tasiARF sites with the canonical motif sequence. As this is the only species from their analysis to exhibit such a pattern, there is doubt as to whether this is biologically true or an experimental artefact resulting from sample contamination. More in-depth studies and sampling of diverse fern species are required to fully understand the patterns of

tasiARF evolution, as well as those of the other motifs that make up the ETT/ARF4-like middle region.

Curiously, Sun and Li (2020) found that expression of the *C. pteridioides* ETT/ARF4-like orthologue was localised in the abaxial domain of frond primordia, similar to how ETT and ARF4 orthologues are localised in the abaxial domain of leaf primordia in the seed plants, despite the lack of tasiARF regulation (Garcia et al., 2006; Guan et al., 2017). This pattern of localisation follows the trends of other well-characterised leaf polarity transcription factor families such as the Class III HD-ZIPs and the KANADIs (KANs), where the expression patterns of monilophyte orthologues in frond primordia match those of seed plant orthologues in leaf primordia (Vasco et al., 2016; Zumajo-Cardona et al., 2019).

The *miR390-TAS3-ARF* pathway is critical for tissue specificity and function of the ARF2/3/4 clade in angiosperms, and leaf developmental defects have been described in mutants deficient in this pathway for various species including maize, rice, *Medicago*, and tomato (Douglas et al., 2010; Song et al., 2012; Yifhar et al., 2012; Zhou et al., 2013). Hence, it appears that monilophyte fronds do not require the *miR390-TAS3-ARF* pathway for proper polarity establishment and growth. Given that monilophyte fronds and seed plant leaves are of independent evolutionary origin, it is perhaps unsurprising that their developmental mechanisms differ (Tomescu, 2009). Nonetheless, the shared localisation patterns of the leaf polarity transcription factors in fronds imply a high degree of convergent evolution and further studies will be required to elaborate the role of the ETT/ARF4-like orthologue in monilophytes.

2.3.2 Diverging trajectories of ETT and ARF4 clade evolution in core angiosperms

While the distinctive feature of ETT in *A. thaliana* is the lack of a PB1 domain, this trait is an apomorphy of the core eudicots and ETT orthologues of the ANA grade angiosperms contain the full PB1 domain (Finet et al., 2013; Finet et al., 2010).

Intriguingly, truncations in the PB1 domain were observed for the ARF4 orthologue of both *A. trichopoda* and *C. aquatica*. Our analysis confirms the conservation of this pattern, particularly in the Nymphaeales, as the *N. thermarum* ARF4 orthologue also lacks a PB1 domain. This begs the question as to why this parallel loss of the PB1 had occurred and whether this loss is merely stochastic or functional, given that the lack of the PB1 domain have profound implications for ARF dimerisation and AUX/IAA interactions (Mutte and Weijers, 2020; Piya et al., 2014).

Furthermore, the loss of the ETT PB1 domain is a repeated event throughout the evolution of the core angiosperms (Finet et al., 2013). Our alignment data demonstrates that the loss of the ETT PB1 had occurred independently more often than previously thought, as ETT orthologues with the full PB1 domain have been identified within the Alismatales, Asparagales, Poales and Arecales (Fig. 2.1, Fig. 2.2). Considering the apparently random patterns of PB1 loss within the magnoliids and monocots, it is possible that the PB1 is non-functional or only has a negligible effect in organismal fitness and thus the domain is truncated through stochastic processes. Nonetheless, Finet et al. (2010) showed that the PB1 domain of ARF4 altered the ability of chimeric ETT constructs to complement *ett-1* loss-of-function gynoecium defects. A possible explanation is that the loss of the ETT PB1 is important for the proper regulation and activity of ETT orthologues only in the core eudicots and not in other angiosperm lineages. Further work involving *in vitro* biochemical assays and *in planta* rescue lines in both heterologous and native

systems will be necessary to disentangle the role of the ETT and ARF4 PB1 domains and explain their evolutionary patterns.

Another pattern that we discovered from our phylogeny is that ARF4 has been lost twice in angiosperm evolution, once in the last common ancestor of extant monocots and another event after the split of the Laurales from the Magnoliales (Fig. 2.1, Fig. 2.2). This implies that ARF4 provides little in terms of fitness during plant development in those lineages. Indeed, *A. thaliana* ARF4 does not appear to have a major role in leaf and flower development as single loss-of-function mutants are indistinguishable from the wild-type (Guan et al., 2017; Pekker et al., 2005). Interestingly, the loss-of-function of ARF4 in *ett* mutant backgrounds results in leaf polarity defects and an exacerbation of the *ett* gynoecium phenotype. In addition, ARF4 has been shown to regulate flowering time and drought resistance in strawberry and tomato (Chen et al., 2021; Dong et al., 2021). Therefore, it is plausible that ARF4 is retained in certain genomes due to cryptic physiological roles and lineage-specific functions while it is lost in others (e.g. the monocots) due to compensation by ETT or other ARFs.

In contrast, the ETT clade has undergone a significant expansion in gene copy number within the commelinid monocots, with gene copies as high as 12 in hexaploid wheat (Fig. 2.2). While the high ETT copy number in polyploid species can be attributed to their recent genome duplication events, the high copy number in genetically diploid or double haploid species such as banana and rice suggests that the ETT paralogues might be functionally non-redundant. In rice, the four ETT paralogues are distinct and have evolved specific roles in the different whorls of the complex grass floret; while the rice ETT1 and ETT2 genes redundantly regulate carpel development, ETT1 also has prominent roles in lemma development while ETT2 is involved specifically in awn development (Khanday et al., 2013; Si et al., 2022; Toriba and Hirano, 2014). Thus, though it is also possible that ETT copy

numbers may be falsely inflated in some genomes due to the inconsistent inclusion of isoforms, careful lineage-specific analysis of the ETT paralogues such as in rice will allow us to understand the biological relevance of the expansion of ETT in the commelinid monocots and their potential role in the evolution of complex floral structures.

2.3.3 Delineation of ETT and ARF4 through middle region motifs

The middle region of ARFs is poorly conserved as it is intrinsically disordered (Roosjen et al., 2017; Simonini et al., 2018a). This presents a challenge for the identification of ETT- or ARF4-specific primary sequence characteristics that might be useful for clade delineation and functional analyses. Using our computational approach where ETT and ARF4 sequences were grouped and aligned according to phylogenetical relationships (Fig. 2.1), we were able to determine ETT- and ARF4-specific motif variants of the NLS, W505 and EAR-like motifs common to both clades. While we were able to also detect general biophysical differences between the ETT and ARF4 clades (Fig. S2.2), the high variability between samples necessitates more in-depth studies before conclusions can be drawn about each assessed parameter on ETT or ARF4 function.

While we could detect clade-enriched motif variants for the shared middle region motifs of ETT and ARF4, it is imperative to note that any single motif on its own is insufficient in delineating ETT or ARF4 sequences, as exceptions can be observed within each clade (Fig. 2.3). Instead, a combination of character states for each motif plus the aforementioned physical and biochemical properties should provide better support for delineating ETT and ARF4 sequences.

The NLS and EAR-like motifs are important for ARF nuclear localisation and its interaction with the TPL/TPR family of corepressors, respectively (Kuhn et al., 2020). It is currently unclear whether the variants enriched in ETT or ARF4 orthologues function similarly in terms of biochemistry, or whether there is functional

divergence that is specifically important for each clade for their proper regulation and activity. Conversely, with the exception of the monilophyte sequences, the tasiARF sites is extremely well-conserved even at the nucleotide sequence level in all sampled angiosperms (Fig. 2.3). As discussed earlier, the divergence in monilophyte tasiARF sequence implies an alternative regulatory mechanism in fern fronds that is perhaps indicative of their independent origins from spermatophyte leaves. Nevertheless, it remains a mystery as to why two sites are present in spermatophyte sequences and why there are no alternative complementary pairs between the *TAS3*-derived small RNAs and their *ETT/ARF4*-like transcript targets. A potential explanation is that the two tasiARF sites perform a protein-level role in the spermatophytes, which would greatly constrain any shift in sequence and copy number.

Finally, we show that the W505 residue is conserved in most ETT orthologues, including that of *A. trichopoda* (Fig. 2.3). This suggests that the residue has been present and possibly functional in non-canonical auxin signalling since the last common ancestor of extant angiosperms. As the W505 residue has been demonstrated to be necessary for ETT-mediated auxin signalling (Kuhn et al., 2020), the loss of the residue in some monocot sequences imply that this ability is lost from those orthologues. Furthermore, the W505 residue has been detected in an equivalent position on most ARF4 orthologues but flanked by an upstream LGA motif (Fig. 2.3). A thorough biochemical assay of orthologue auxin sensitivity with respect to the presence or absence of the W505 residue will be crucial to elucidate the importance of the W505 and flanking residues in the ETT-mediated auxin signalling pathway.

2.4 Concluding Remarks

Our findings support the hypothesis that ETT and ARF4 originated as the ETT/ARF4-like clade in the euphyllophyte common ancestor prior to their subsequent divergence and specialisation in the angiosperms. Despite the availability of studies on the evolutionary history of certain ETT/ARF4 motifs and domains, little is known about their character state variations for effective delineation and functional analyses of ETT and ARF4 (Finet et al., 2013; Simonini et al., 2018a; Xia et al., 2017). Our data provides insight into ETT and ARF4 middle region motif variants that, taken as a whole, will be useful for delineating the clades in non-eudicot species. Nonetheless, the phylogeny presented in this chapter is not necessarily without flaws as the quality of an alignment depends on the quality of the input dataset.

While our investigation confirms the phylogenetical placement of the ETT/ARF4-like clade and refines our understanding of PB1 truncations within the angiosperms by utilising currently available public genomic resources, there are still major clades that are underrepresented or not represented in our study due to the lack of well-annotated genomes. For example, there is only one lycophyte representative in our study (*S. moellendorffii*), and there are no representatives for the phylogenetically significant clades of the Austrobaileyales, Chloranthales and Ceratophyllales within the angiosperms. In addition, we cannot discount for the possibility that some of the sequences included in the study are pseudogenes or mis-annotations. Conversely, genes that are present in a species might be missing from our dataset if they are not annotated. For example, the Liu et al. (2021) were unable to detect ETT/ARF4-like orthologues in the *G. biloba* genome but we identified one orthologue that was split across contigs in the sequencing data. Therefore, careful curation of the dataset with expression data from the native species will be required to obtain a more accurate phylogeny.

In silico data is, by nature, purely descriptive and does not explain the biological relevance or function of any of the motives and domain variants. Therefore, further work must be done in order to validate any correlations observed in the data presented here. One approach would be to test the biochemical properties of ETT and/or ARF4 orthologues with mutations or variations in their NLS, tasi-ARF binding site, EAR-like motif or PB1 domain *in vivo* with regards to their subcellular or tissue-level localisation patterns, their degradation rates or protein-protein interaction dynamics.

In Chapter 3, I will test the auxin-sensitivity of ETT, ARF4 and ETT/ARF4-like orthologues from representative species of key phylogenetic importance with respect to their TPL/TPR interactions to investigate the conservation of this non-canonical auxin signalling pathway. Furthermore, domain swap experiments between orthologues of different species will inform us of the contributions of the different motifs and domains to ETT's auxin signalling ability. The *in planta* developmental role of these orthologues and their domains will also be investigated in Chapter 4. As ETT and ARF4 are known to have different degrees of redundancy in leaf and gynoecium development, I will generate complementation lines of the *ett-3* and *ett-3 arf4* loss-of-function single and double mutant via heterologous expression of the orthologues tested in Chapter 3.

To summarise, the results of this chapter provide a basic framework to investigate the evolution of the non-canonical auxin signalling pathway mediated by ETT through the accurate identification of orthologues and their associated motifs. The focus of this thesis will be on the sub- and/or neofunctionalisation of ETT and ARF4 with relation to their auxin-sensing ability and their roles in leaf and gynoecium development. However, our data will also be useful for future studies on the other Class B ARFs and their functional roles in other species-of-interest.

2.5 Materials and Methods

2.5.1 Data acquisition and phylogenetic tree construction

A total of 104 proteomes from sequenced genomes available mainly through PLAZA (Van Bel et al., 2021) and Phytozome (Goodstein et al., 2011) were searched for ARF homologs using HMMER (v3.3; Finn et al., 2011) with HMM made from the alignment of *Arabidopsis* and *Marchantia* ARF homologs as query sequences. The initial fast alignment was made using the MAFFT FFT-NS-1 algorithm (v7.505; Katoh et al., 2002) and a tree was built with IQtree (v2.2.0; Minh et al., 2020) with a maximum of 100 rapid bootstraps. From this tree, only the sequences in the Class B ARF clade were selected along with a few Class A ARF sequences that were used as outgroups for the later phylogenetic tree construction. These selected Class B ARF sequences were further aligned using MAFFT E-INS-i algorithm (v7.505; Katoh et al., 2002). Regions with more than 60% gaps were removed from the alignment using trimAl (Capella-Gutiérrez et al., 2009). IQtree2 was used with JTT+F+R10 as the evolutionary model selected from ModelFinder (Kalyaanamoorthy et al., 2017) with 1000 rapid bootstraps. Phylogenetic trees were visualised using iTOL (v5; Letunic and Bork, 2021)

2.5.2 Middle region motif identification and visualisation

From our alignment, the ARF middle region (MR) was selected in JalView (v2; Waterhouse et al., 2009) using sequences of the DNA-binding domain as published before in Boer et al. (2014) and the PB1 domain as published in (Mutte and Weijers, 2020). The R packages 'protr' and 'Peptides' were used to compute sequence features of the MR (Osorio et al., 2015; Xiao et al., 2015). Sequence logos for visualising conserved peptides were made using WebLogo v3.7.4 (Crooks et al., 2004). Monilophyte ETT/ARF4-like orthologues (Fig. 2.4) were aligned and visualised in CLC Workbench.

Chapter 3:

The ETT-mediated auxin signalling pathway might have originated in the last common ancestor of flowering plants

3.1 Introduction

In the previous chapter, we confirmed that the ETT/ARF4-like clade have already existed in the last common ancestor of euphyllophytes and that clade-specific differences in ES domain motifs can be identified from ETT and ARF4 orthologues. As the *A. thaliana* ETT has been demonstrated to participate in a novel auxin signalling pathway independent of the TIR1/AFBs (Kuhn et al., 2020; Simonini et al., 2016), an open question remains as to whether ARF4 and the non-angiosperm ETT/ARF4-like orthologues behave in a similar manner.

The canonical TIR1/AFB-dependent auxin signalling pathway is ancient and can be traced back to the last common ancestor of all land plants (Mutte et al., 2018). Unsurprisingly, the role of the TIR1/AFB-dependent pathway in plant development is indispensable, with well-characterised roles in cellular differentiation and organogenesis from bryophytes to angiosperms (Gorelova, 2023; Prigge et al., 2010; Prigge et al., 2020). In contrast, the ETT clade is specific to the angiosperms, having evolved from the greater ETT/ARF4-like clade after the divergence of the angiosperms from extant gymnosperms (Chapter 2; Finet et al., 2013; Mutte et al., 2018). Given that the most significant developmental role of ETT in *A. thaliana* is gynoecium development (Nemhauser et al., 2000; Sessions et al., 1997b), there appears to be a correlation between the evolution of the ETT clade and the appearance of the carpel in angiosperms.

Nevertheless, ETT is also involved in the development and tissue polarity of other lateral organs such as leaves and lateral roots (Guan et al., 2017; Marin et al., 2010; Pekker et al., 2005; Simonini et al., 2016). A peculiar trend observed in single and double loss-of-function mutants of ETT and ARF4 is that *arf4* single mutants are indistinguishable from the wild-type, while *ett* single mutants have a strong gynoecium phenotype. Additionally, phenotypic defects in vegetative organs are only apparent in higher order mutants, while the gynoecium defect of *ett* is greatly

exacerbated in the *ett arf4* background (Pekker et al., 2005). The heterologous expression of *ARF4* under the *ETT* promoter was also unable to fully rescue the *ett* gynoecium phenotype (Finet et al., 2010). Taking all this into account, I hypothesise that the non-canonical auxin signalling pathway mediated by ETT is a neofunctionalisation specific to the ETT clade that is necessary for its role in gynoecium development. Under this scenario, ARF4 and ETT/ARF4-like orthologues from non-angiosperm clades lack the ability to sense auxin directly and therefore cannot fully replace the function of ETT in gynoecium morphogenesis.

The ETT-mediated auxin signalling pathway has mostly been studied in the context of gynoecium development (Kuhn et al., 2020; Simonini et al., 2017; Simonini et al., 2016; Simonini et al., 2018b). However, the *pETT:ETT^{2CS}* line suggests that the ETT-mediated auxin signalling pathway might also play roles in other developmental processes (Simonini et al., 2016). The ETT^{2CS} protein has had two non-conserved cysteine residues in its ES domain substituted with serine residues and behaves in an auxin-insensitive manner with regards to its TF interactions in a Y2H assay. The *pETT:ETT^{2CS}* exhibits numerous pleiotropic phenotypes, including overgrowth of the outer integument and stigmatic tissue, increased lateral root number and abnormal primary branch fusion (Simonini et al., 2016). This suggests that ETT-mediated auxin signalling may also be involved in developmental contexts beyond the gynoecium.

Our lab has previously shown that ETT interacts with the members of many TF families in an auxin-sensitive manner (Simonini et al., 2016). Some of these TFs are involved in the development of organs that are defective in the *pETT:ETT^{2CS}* line, such as PLETHORA5 (PLT5) for root development, ABBERANT TESTA SHAPE (ATS) for integument development and TCP18 for stem-pedicel fusion. ATS belongs to the KANADI (KAN) TF family that is broadly involved the abaxial polarity of lateral organs (Kelley et al., 2012). A weak auxin-sensitive interaction between ETT and

FILAMENTOUS FLOWER (FIL), a member of the YABBY (YAB) abaxial polarity TF family, was also found by Simonini et al. (2016). Considering these data and my own observations of a previously undescribed leaf epinasty phenotype in the *pETT:ETT^{2CS}* line (Fig. S3.1), I speculate that the ETT-mediated auxin signalling pathway might also be important for leaf polarity and outgrowth.

ETT also interacts with the TPL/TPR family of transcriptional corepressors in an auxin-dependent manner (Kuhn et al., 2020). In the context of the canonical TIR1/AFB-dependent pathway, the AUX/IAA proteins that heterodimerise with the activating ARFs through their PB1 domains recruit the TPL/TPR corepressors to prevent auxin-induced gene expression in the absence of auxin (Long et al., 2006; Szemenyei et al., 2008). ETT lacks the PB1 domain, but like other Class B ARFs, can interact with TPL directly through its EAR-like motif in the ES domain (Choi et al., 2018; Kato et al., 2020; Kuhn et al., 2020). The auxin-dependent interaction between ETT and the TPL/TPRs forms the core mechanism of the ETT-mediated signalling pathway, where the direct binding of auxin to ETT switches its activity from a transcriptional repressor to an activator (Kuhn et al., 2020). While this mechanism was primarily studied in the context of two genes with prominent roles in gynoecium development, *PINOID (PID)* and *HECATE1 (HEC1)*, transcriptomic profiling of auxin-treated gynoecia revealed a large subset of genes that are activated by ETT only in the presence of auxin (Simonini et al., 2017). It is likely that these genes are regulated by the ETT-TPL module in a similar manner.

The ES domain of ETT has been shown to be sufficient for its auxin sensing function in biochemical assays (Kuhn et al., 2020; Simonini et al., 2018a). NMR, Y2H and protein pull-down data suggest a major contribution of the W505 residue in the ES auxin sensitivity (Kuhn et al., 2020). However, it is plausible that other ARF domains can influence the auxin sensitivity of ETT. The ETT PB1 domain has been lost multiple times in core angiosperm evolution and the fusion of the ARF4 PB1 to

ETT impeded its ability to rescue the *ett* gynoecium phenotype (Chapter 2; Finet et al., 2013; Finet et al., 2010). The presence of the PB1 in the ETT orthologues of the ANA grade angiosperms raises the question as to whether they are also able to bind and sense auxin. In contrast with the well-resolved 3D structure of TIR1 (Tan et al., 2007), the intrinsically disordered nature of the ES domain makes it difficult to predict the contributions of allosteric effects to auxin sensing. Thus, direct experimental data would be necessary to address these questions.

In this chapter, I attempt to answer the questions raised above through Y2H screens of auxin sensitive ETT and ARF4 interactions. Firstly, a screen of the KAN and YAB leaf polarity TFs was conducted to identify conserved interactions with ETT/ARF4-like orthologues from the seed plants that might uncover the role of the ETT-mediated pathway in leaf development. Unfortunately, the data obtained were inconclusive, as the positive control ATS appeared to lack auxin sensitivity. Nonetheless, the second screen involving the TPL/TPR corepressor family suggested a likely origin of the ETT-mediated pathway in the last common ancestor of angiosperms as the *A. trichopoda* ETT orthologue was found to be responsive to auxin. Finally, a screen with domain-swapped ARF constructs imply that the ES-dependent auxin sensing is unaffected by the presence of the PB1 domain but can be repressed by currently unknown motifs found in the DNA-binding domain (DBD) of ETT/ARF4-like orthologues.

3.2 Results

3.2.1 Conserved interactions between ETT and abaxial domain

transcription factors may be auxin-insensitive

To elucidate the conservation and origin of the auxin-sensing property of ETT, the auxin sensitivity of ETT/ARF4-like orthologues from different species representing key phylogenetic lineages had to be assessed. A Y2H approach was chosen to test this due to the ease of large-scale screening and the establishment of this technique

in our lab. Candidate species from the bryophytes, monilophytes, gymnosperms, ANA grade basal angiosperms, magnoliids, monocots and core eudicots were selected based on the availability of ETT/ARF4-like orthologue information from Chapter 2 and the ease of acquisition of plant material for molecular cloning (Table S3.1). These ETT/ARF4-like orthologues were tested for auto-activation prior to the Y2H screen (Fig. S3.2).

As ETT interacts with a wide range of transcription factors, a suitable candidate partner had to be identified for the auxin sensitivity assay. Ideally, the chosen partner should form direct auxin-sensitive interactions with ETT, be widely conserved in the land plants, and have similar developmental phenotypes as *ett* and/or *ett arf4* loss-of-function mutants. Given that the interaction between ATS and FIL with ETT have been found to be auxin sensitive, and the leaf epinasty phenotype of the *pETT:ETT^{2CS}* line (Fig. S3.1), a Y2H screen of the KAN and YAB families was conducted (Fig. 3.1).

In *A. thaliana*, the KAN family comprises four members (KAN1, KAN2, KAN3 and ATS) while the YAB family contains six members (FIL, YAB2, YAB3, INNER NO OUTER (INO), YAB5 and CRABSCLAW (CRC)). Both ETT and ARF4 interacts with all members of the KAN family (Fig. 3.1a). ARF4 also interacts with all YAB paralogues while ETT only interacts with FIL, YAB2, YAB3 and INO. Through both literature studies and *de novo* BLAST searches of their respective genomes, all well-annotated members of the KAN and YAB families from the asterid *S. lycopersicum*, the ANA grade angiosperm *A. trichopoda* and the gymnosperm *G. biloba* were identified, categorised and cloned (Fig S3.2; Arnault et al., 2018; Finet et al., 2016; Huang et al., 2013b; Yamada et al., 2011).

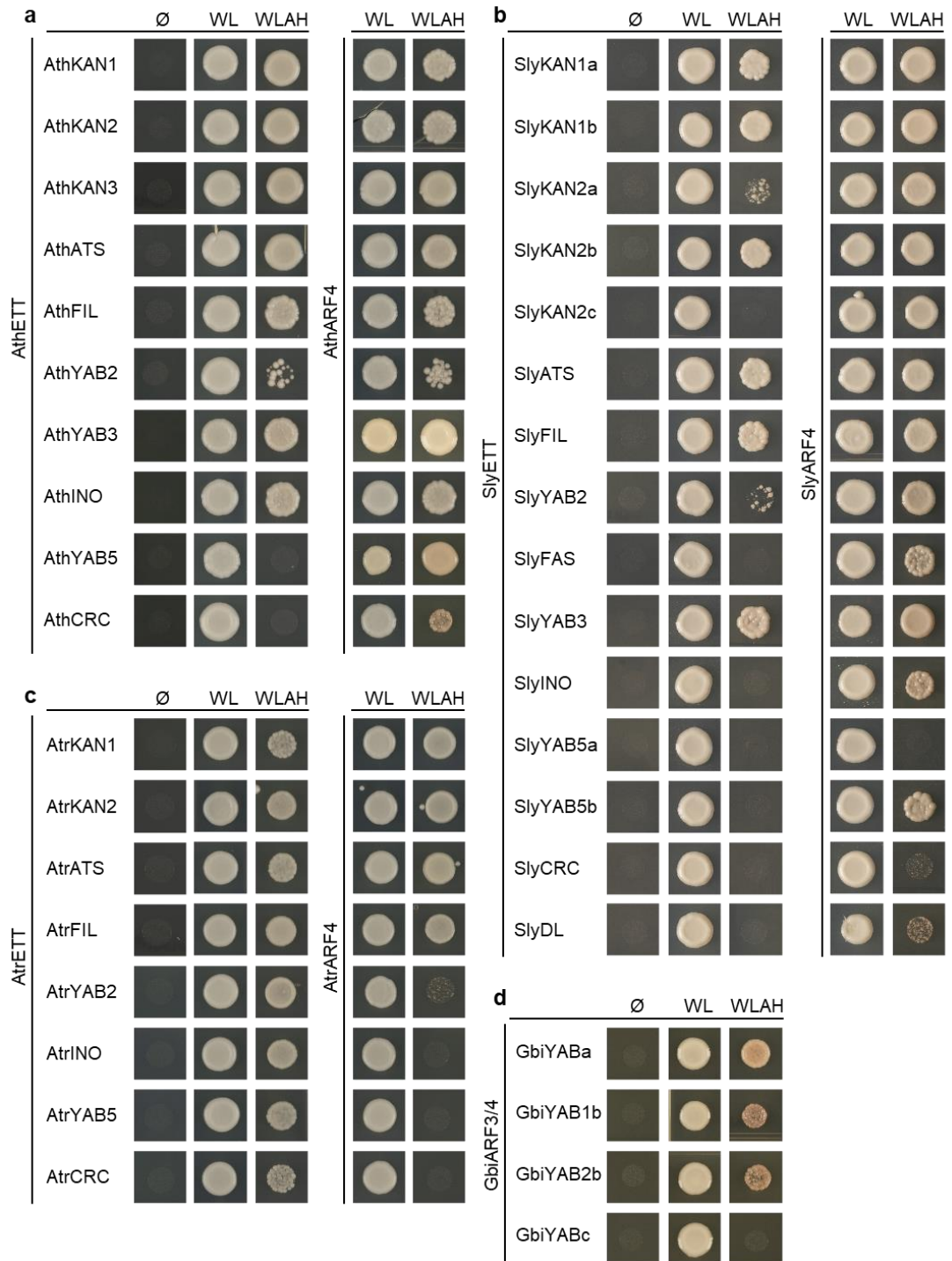


Figure 3.1: Y2H interaction screen of the KAN and YAB families in the seed plants

(previous page). The interaction between ETT/ARF4-like orthologues from *A. thaliana* (a), *S. lycopersicum* (b), *A. trichopoda* (c), and *G. biloba* (d) with their respective KAN and/or YAB transcription factors were assessed. Ø indicates the empty vector control for testing auto-activation of KAN and YAB constructs. WL represents growth on tryptophan and leucine-deficient media for selection of positive yeast co-transformants while WLAH represents growth on media lacking tryptophan, leucine, adenine and histidine to test for protein-protein interactions.

The *S. lycopersicum* ETT and ARF4 orthologues behaved similarly to those of *A. thaliana*, with ARF4 interacting with more members of the YAB family than ETT (Fig. 3.1b). Interestingly, an opposite pattern was observed for the *A. trichopoda* orthologues where ETT interacted with all YAB members while ARF4 only interacted with the FIL orthologue (Fig. 3.1c). As there were issues with auto-activation of the *G. biloba* KANs in yeast, only the YAB family was screened where it was shown that all YABs except YABc interacted with the selected *G. biloba* ETT/ARF4-like orthologue (Fig. 3.1d). The positive interactors identified from the KAN and YAB screen were tested for auxin sensitivity by plating of the transformed yeast strains on auxin-containing media (Fig. 3.2). However, none of the interactions were found to be auxin sensitive, including ATS which was previously identified as an auxin-sensitive interactor of ETT (Simonini et al., 2016).

3.2.2 The ETT-mediated auxin signalling pathway may have originated in the last common angiosperm ancestor

As ETT also interacts with the TPL/TPR corepressors in an auxin-sensitive manner as part of its non-canonical signalling pathway in gynoecium development, the TPL/TPR family was chosen as an alternative candidate partner to test for auxin sensitive protein-protein interactions of the ETT/ARF4-like orthologues. Similar to

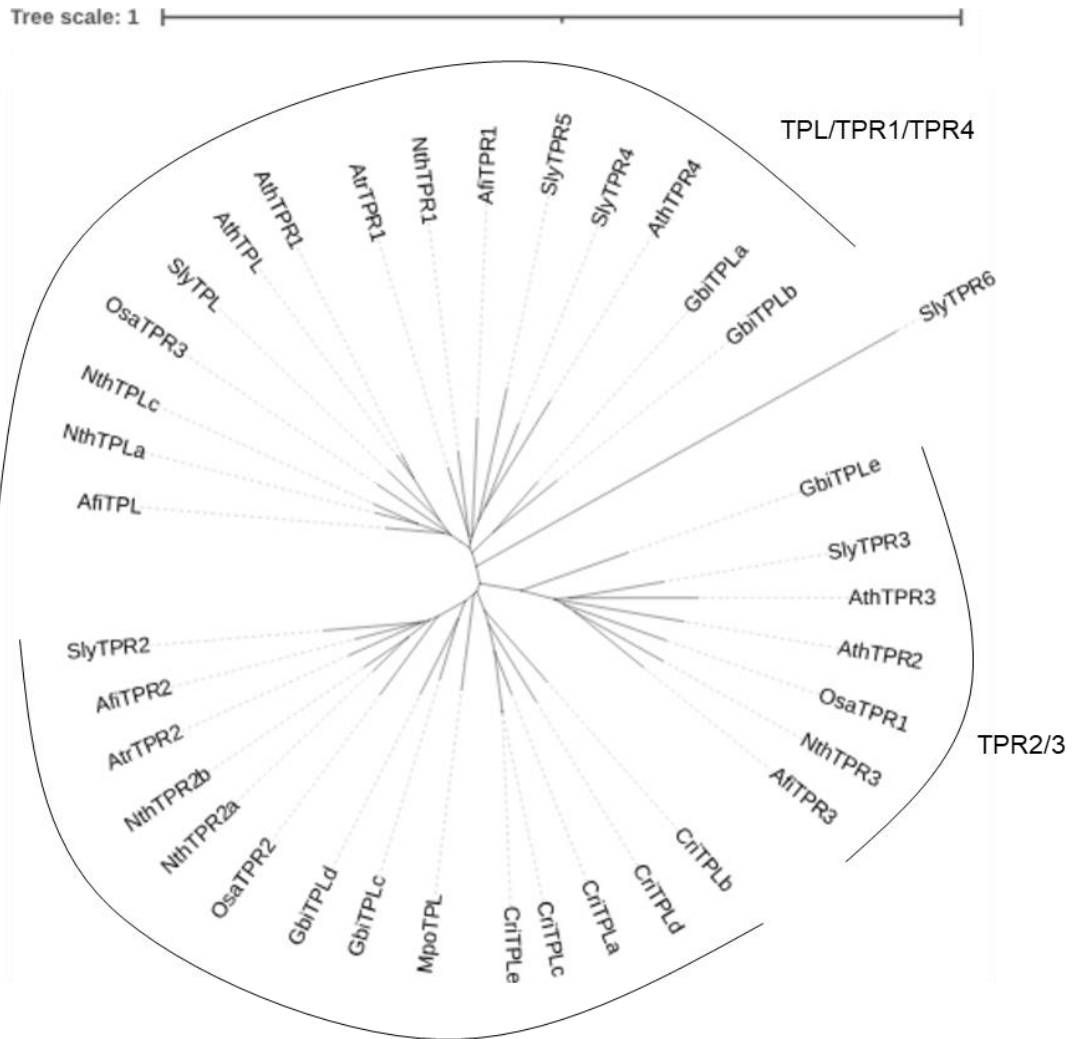


Figure 3.2: Auxin-sensitivity Y2H interaction assay of ETT/ARF4 orthologues with the KAN and YAB families. Numbers at the bottom of the figure indicate the serial dilution series of the assayed yeast colonies. None of the interactions were disrupted by auxin.

the KAN and YAB Y2H screen, TPL and TPR orthologues from representative species were identified through literature survey and BLAST searches of genomes and cloned into yeast vectors (Table S3.1). The TPL and TPR orthologues were aligned and categorised into clades. In agreement with Plant et al. (2021), the TPL/TPR family in the land plants can be roughly divided into three major clades, one encompassing the *A. thaliana* TPL/TPR1/TPR4, the TPR2/3 clade and a clade that is not found in *A. thaliana* (Fig. 3.3).

The Y2H screen of the TPL/TPR family from diverse land plant species identified members that interacted with their ETT/ARF4-like orthologues (Fig. 3.4). In *A. thaliana*, it is known that ETT interacts with TPL, TPR2 and TPR4 (Kuhn et al., 2020). Interestingly, the *S. lycopersicum* ETT does not appear to interact with any of the six TPL/TPR orthologues (Fig. 3.4a). Furthermore, while the *A. thaliana* ARF4 interacted with TPL, the *S. lycopersicum* ARF4 did not interact with SlyTPL but with SlyTPR2 and SlyTPR4 instead. This suggests that the interaction pairs between ETT/ARF4-like orthologues and their TPL/TPR orthologues are not well-conserved even in closely related species. In fact, the Y2H data suggests that none of the three *O. sativa* TPL/TPR orthologues interacted with any of its four ETT paralogues (Fig. 3.4b). Whether this observation could be an artefact of the experimental setup or of biological relevance has not been pursued.

Nonetheless, positive ETT-TPL/TPR interactions were identified in the sampled ANA grade angiosperm and magnoliid species (Fig. 3.4c). The ETT orthologues of the ANA grade angiosperms *A. trichopoda* and *N. thermarum*, and the magnoliid *A. fimbriata* all interacted with at least one member of the TPL/TPR family. It is however interesting to note that the ARF4 of both ANA grade species did not interact with any of their TPL/TPR paralogues. With regards to the non-angiosperm species, protein-protein interactions between the ETT/ARF4-like orthologues of the gymnosperm *G. biloba* and the monilophyte *C. richardii* were also identified (Fig. 3.4d). However, no interaction was detected between the sole *M. polymorpha* Class B ARF (ARF2) and its sole TPL orthologue. This is strange as the *M. polymorpha* ARF2 contains the EAR-like domain necessary for TPL/TPR interaction and has been demonstrated to interact with TPL in a FRET-FLIM assay (Kato et al., 2020). It is therefore likely that this negative result is an artefact of the experimental system.



Land plant TPL/TPR clade missing in *A. thaliana*

Figure 3.3: Phylogeny of the TPL/TPR family included in the Y2H assay. The gene identifiers of each orthologue is given in Table S3.1. The designation of TPL/TPR clades is based on Plant et al. (2021).

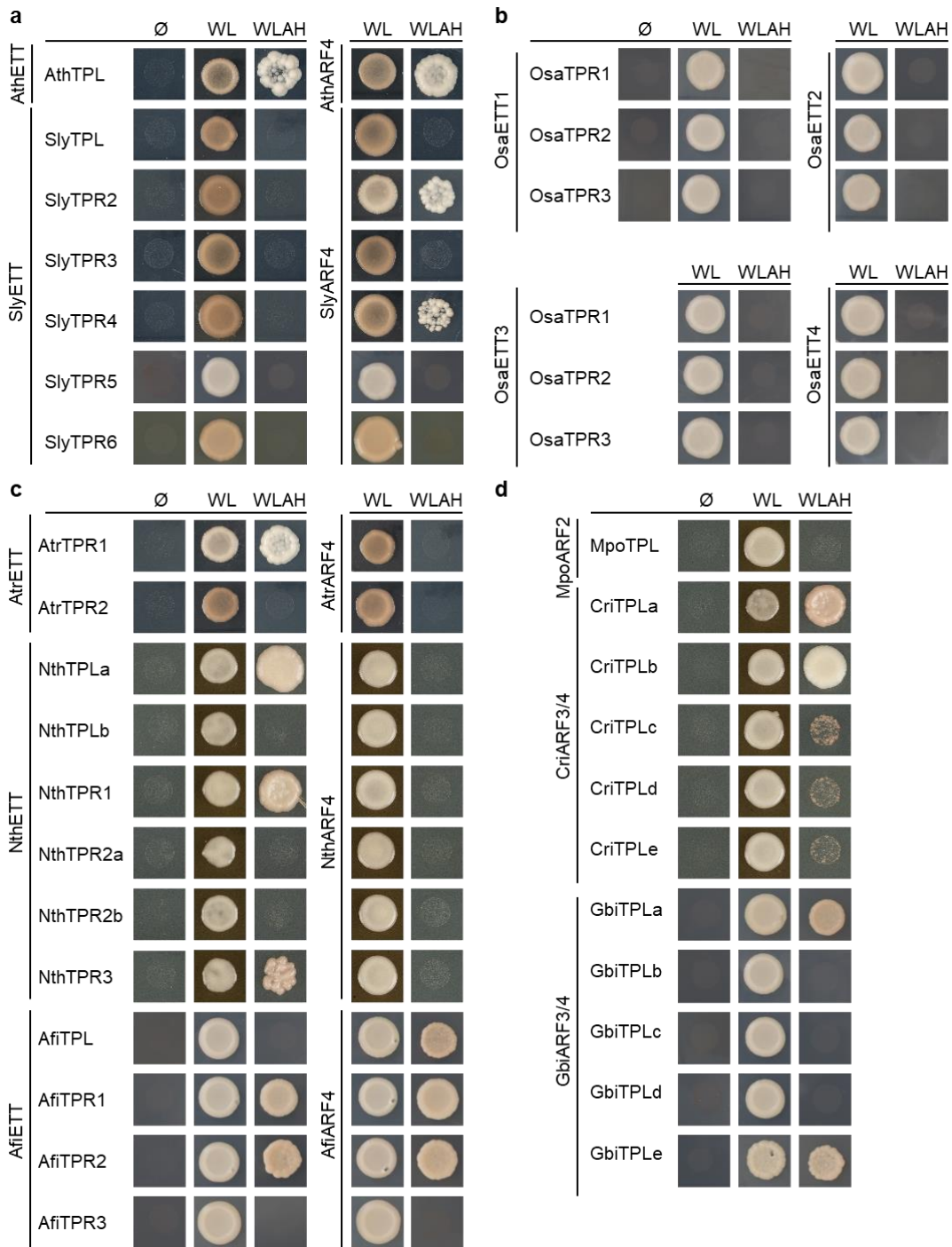


Figure 3.4: Y2H interaction screen of the TPL/TPR family in the land plants (previous page). Core eudicot (a), monocot (b), ANA grade and magnoliid (c) and non-angiosperm (d) ETT/ARF4-like interactions with TPL/TPR orthologues were tested.

Having identified positive TPL/TPR interactors for the ANA grade, magnoliid, gymnosperm and monilophyte models, these interactions were then tested for their auxin sensitivity via plating of yeast strains onto media containing auxin (Fig. 3.5). The *A. thaliana* ETT-TPL interaction was used as a positive control for the auxin sensitivity assay while the ARF4-IAA19 interaction was used as a negative control for auxin sensitivity as the yeast system used lacked the canonical TIR1/AFB-dependent pathway necessary for the auxin-induced disruption of ARF-AUX/IAA interactions.

In accordance with previous studies, the *A. thaliana* ETT-TPL interaction was disrupted by auxin (Fig. 3.5). On the other hand, the *A. thaliana* ARF4-TPL interaction was insensitive to auxin, implying that auxin sensing is a neofunctionalisation of ETT and not the entire ETT/ARF4-like clade. Strikingly, the *A. trichopoda* ETT-TPR1 interaction was also sensitive to auxin which suggests that ETT may have gained its novel auxin-sensing property before evolution of the last common ancestor of all extant flowering plants. The lack of auxin-sensitivity of the *G. biloba* and *C. richardii* ETT/ARF4-like orthologues further supports the hypothesis that the ETT-mediated auxin signalling pathway is an innovation of the angiosperms and not ancestral to the ETT/ARF4-like clade. Nevertheless, the ETT orthologues of *N. thermarum* and *A. fimbriata* do not exhibit auxin sensitivity in this assay. This implies that the ETT-mediated auxin signalling pathway is not as well-conserved as the canonical TIR1/AFB-dependent pathway and can be lost in some lineages.

3.2.3 The auxin-sensing property of ETT is strongly associated with a specific region of the ES domain

It has been shown that the auxin-sensing property of ETT is dependent on its modified middle region that was termed the ES domain (Kuhn et al., 2020; Simonini et al., 2016; Simonini et al., 2018a). To investigate which region of the ES domain



Figure 3.5: Auxin-sensitivity Y2H assay for ETT/ARF4-TPL/TPR interactions. Only the *A. thaliana* and *A. trichopoda* ETT orthologues exhibited auxin sensitivity in this assay.

might contribute to the conserved auxin-sensitivity of the *A. thaliana* and *A. trichopoda* ETT orthologues, domain swapped chimeric constructs of the *A. thaliana* and *A. trichopoda* ETTs as well as the auxin-insensitive *G. biloba* ETT/ARF4-like orthologue were generated (Fig. 3.6). The domains swapped between the three orthologues include the B3 DNA-binding domain, the first half of the ES domain encompassing the NLS and first tasiARF motif (MR1), the second half of the ES

domain including the W505 residue and EAR-like motif (MR2), and the PB1 domain if present. The constructs were then tested for auto-activation and their interactions with the *A. thaliana*, *A. trichopoda* and *G. biloba* TPL/TPRs (Fig. S3.3).

Positive ARF-TPL/TPR interacting pairs were replica plated on auxin-containing plates to assess for ARF auxin-sensitivity (Fig. 3.7). The DS1 construct, containing the *A. thaliana* DBD and the *G. biloba* MR and PB1 domains, was auxin insensitive while the DS2 construct, comprising the *A. thaliana* DBD and *A. trichopoda* MR and PB1, exhibits mild auxin sensitivity. This is in line with previous data suggesting that the ES domain is the auxin-sensing domain (Kuhn et al., 2020; Simonini et al., 2018a). However, the DS3 and DS4 constructs, which are the *A. thaliana* and *A. trichopoda* ETTs with the *G. biloba* DBD, do not exhibit auxin-sensitivity. This shows that the *G. biloba* DBD can interfere with the auxin-sensing ability of the angiosperm

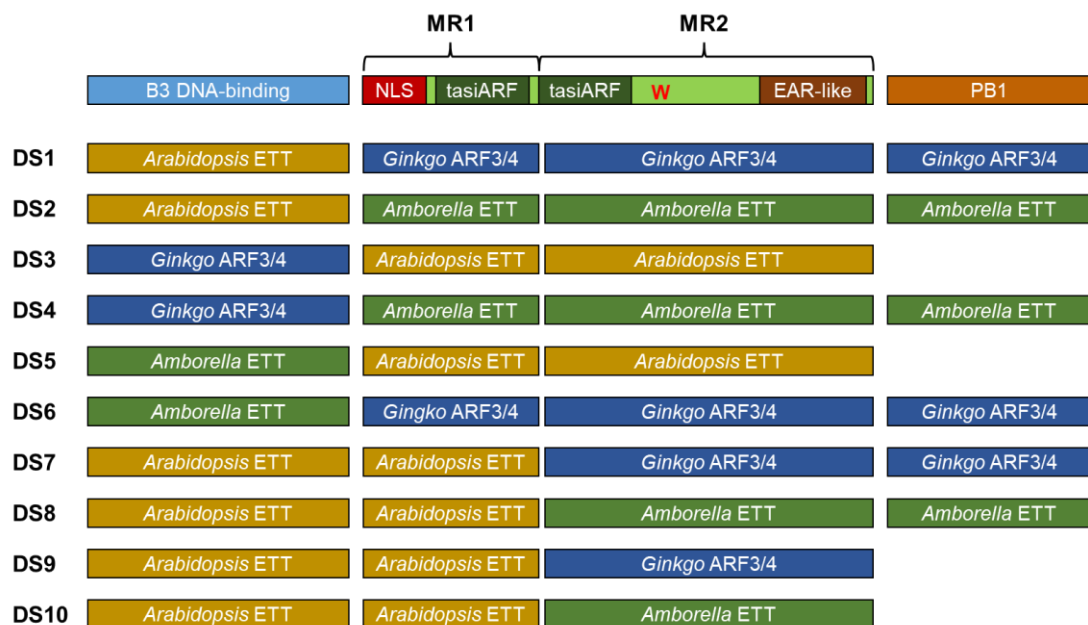


Figure 3.6: Domain swapped chimeric constructs to investigate regions contributing to ETT auxin sensitivity. A schematic of ETT domains and motifs is illustrated at the top of the figure.

ETT. In contrast, the DS5 and DS6 constructs containing the *A. trichopoda* DBD appear to exhibit auxin-sensitivity although their interactions with TPL/TPR partners are weaker. Therefore, it is possible that there are motifs or residues within the DBD that contribute to the auxin sensitivity of ETT as well.

Finally, the DS7, DS8, DS9 and DS10 constructs revealed the contributions of the MR2 region of the ES domain and the PB1 domain to the auxin-sensing property of ETT (Fig 3.7). DS7 and DS9 which contained the *G. biloba* ETT/ARF4-like MR2 were insensitive to auxin, while DS8 and DS10 which had the *A. trichopoda* ETT MR2 were auxin sensitive. The PB1 of the *A. trichopoda* ETT is known to be functional at least with respect to AUX/IAA interactions (Fig. S3.4). Nonetheless, these results suggest that the PB1 domain does not interfere with the non-canonical auxin-signalling pathway and that MR2 contributes strongly to auxin sensing.

3.3 Discussion

In Chapter 2, we confirmed that the ETT/ARF4-like clade originated in the euphyllophytes and diverged into separate clades after the evolution of angiosperms. In addition, we identified motif variants that were more enriched in either ETT or ARF4 orthologues. Nonetheless, how this translates to the ability of ETT and/or ARF4 to sense and respond to auxin remains uncertain. In the present chapter, I investigated the auxin sensitivity of ETT/ARF4-like orthologues from key land plant lineages to elucidate the conservation and origin of the ETT-mediated auxin signalling pathway. Using Y2H assays, I pinpointed the likely origin of this novel auxin-signalling pathway to the last common ancestor of the flowering plants. Moreover, I identified regions within and beyond the ES domain that contribute to the auxin sensitivity of ETT.

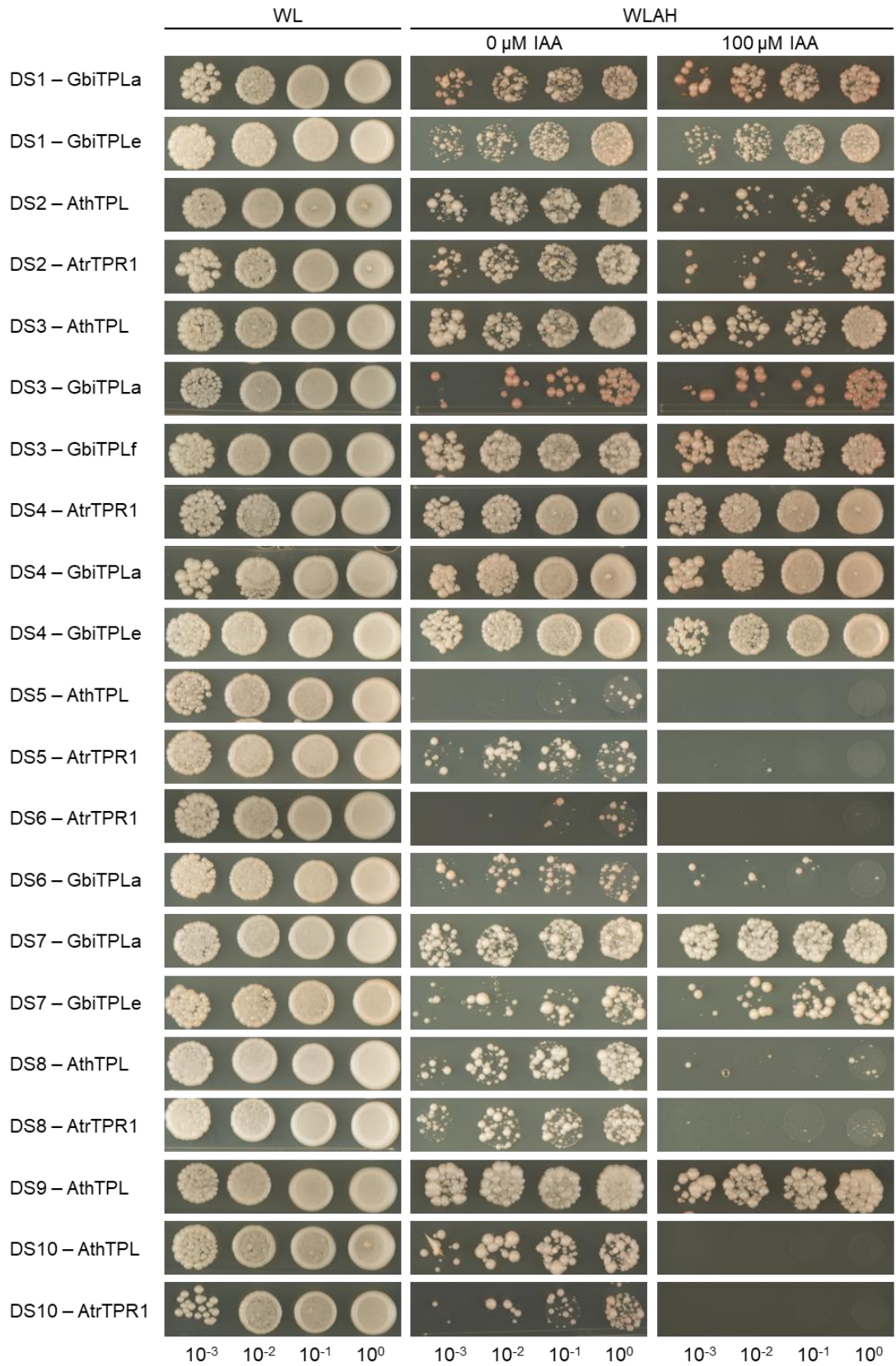


Figure 3.7: Auxin sensitivity Y2H screen of the interactions between chimeric ETT/ARF4-like constructs and the TPL/TPR corepressors (previous page). Mild auxin-sensitivity is observed for DS2 while strong auxin-sensitivity is observed for DS5, DS6, DS8 and DS10.

3.3.1 The auxin sensing ability of ETT is a neofunctionalisation of the angiosperms

The results of the Y2H auxin sensitivity screen show that ETT but not ARF4 respond to auxin with respect to its TPL/TPR protein-protein interactions (Fig. 3.5). From previous studies and our independent analysis in Chapter 2, we know that ETT and ARF4 share multiple motifs within their middle region domains (Simonini et al., 2018a). On the other hand, our data from Chapter 2 demonstrated that there are clade-enriched variants of the NLS, W505 and EAR-like motifs. Additionally, a major difference in *A. thaliana* between its ETT and ARF4 orthologues is the absence or presence of the PB1 domain respectively (Finet et al., 2013). It is therefore a possibility that the ETT-enriched variants of the middle region motifs and/or the absence of the PB1 domain facilitates its ability to sense auxin. However, the discovery that the full-length *A. trichopoda* ETT containing a functional PB1 domain is auxin sensitive suggests that the PB1 domain exerts little to no influence on ETT's auxin-sensing ability (Fig. 3.5, Fig. S3.4).

The ability of the *A. trichopoda* ETT orthologue to sense auxin also implies that the ETT-mediated auxin signalling pathway is a neofunctionalisation of the ETT clade that originated in the last common angiosperm ancestor, as *A. trichopoda* belongs to a lineage that is sister to all other extant angiosperms (Project et al., 2013). This hypothesis is further supported by the inability of the *C. richardii* and *G. biloba* ETT/ARF4-like orthologues to respond to auxin in the Y2H assay (Fig. 3.5).

In *A. thaliana*, ETT has a more important role than ARF4 in gynoecium development as *ett* loss-of-function single mutants have impaired gynoecium growth and tissue

polarity while *arf4* loss-of-function mutants have normal gynoecia (Pekker et al., 2005). The heterologous expression of ARF4 in the *ett* loss-of-function background is also unable to fully rescue the gynoecium phenotype (Finet et al., 2010). Moreover, the *pETT:ETT^{CS}* line previously published in our lab exhibited various pleiotropic phenotypes including the over-proliferation of stigmatic tissue (Simonini et al., 2016). Taking all this into account, it is tempting to speculate that the evolution of this novel auxin-signalling pathway specific to the ETT clade is linked to the development and possibly the origin of the carpel in angiosperms.

Nevertheless, the lack of auxin sensitivity of the *N. thermarum* and *A. fimbriata* implies that the ETT-mediated auxin signalling pathway is not as well-conserved within the angiosperms as the canonical TIR1/AFB-mediated pathway. Due to the limitations of the experimental system, it is possible that the ETT orthologues of these species interact with other unknown partners in an auxin-sensitive manner.

Alternatively, if the ETT orthologues of these species are truly auxin insensitive, then ETT might not be necessary for carpel development in these species. ETT in the *A. thaliana* and *Brassica rapa* is strongly associated with the development of the radial style (Simonini et al., 2018b). The ANA grade angiosperms, including *N. thermarum*, have ascidiate carpels without styles, while the carpels and stamens of *A. fimbriata* are fused into a gynostemium structure without a distinct style (Endress and Doyle, 2015; Pabón-Mora et al., 2015; Pérez-Mesa et al., 2020; Povilus et al., 2015). The non-canonical auxin signalling function of ETT in these species might be irrelevant then and thus lost from their orthologues. However, this scenario opens more questions as to what the original function of this non-canonical auxin signalling pathway is, such as in the ascidiate carpels of *A. trichopoda*.

3.3.2 The ES domain is not the sole domain influencing the auxin sensitivity of ETT

The ES domain has been repeatedly shown to be the domain responsible for auxin sensing in ETT with regards to its auxin-sensitive interactions with protein partners (Kuhn et al., 2020; Simonini et al., 2016; Simonini et al., 2018a). Important motifs that have been implicated include two non-conserved cysteine residues in the ETT^{2CS} variant, the W505 residue, and a serine-rich patch. Nonetheless, these data do not exclude the possibility of other domains influencing the auxin binding capacity of the ES domain. In addition, it is unknown whether the same motifs contribute to auxin sensitivity in the orthologues of other species where the ETT-mediated auxin signalling pathway is active.

The data from the Y2H assay with domain swapped constructs strongly suggest that MR2 of the ES domain is necessary for the auxin sensing ability of ETT, as replacement of the *A. thaliana* ETT with the auxin-insensitive *G. biloba* MR2 completely abolishes its auxin sensitivity but not with the auxin-sensitive *A. trichopoda* MR2 (Fig. 3.7). Given that MR2 in both *A. thaliana* and *A. trichopoda* is known to contain all motifs associated with auxin sensing in ETT (Fig. 3.6), this is perhaps unsurprising, but it implies that the same motifs might be involved in the auxin sensing process since the evolution of this pathway in the last common angiosperm ancestor.

These assays also demonstrate the irrelevance of the PB1 domain in the role of ETT-mediated auxin signalling, as neither the presence of the PB1 in the full-length *A. trichopoda* ETT and the DS8 construct, nor its removal in the DS10 construct, affects its auxin sensitivity (Fig. 3.5, Fig. 3.7). It has been proposed that the repeated truncations of the PB1 domain of ETT orthologues within the core angiosperms is functional, as the heterologous expression of a chimeric ETT construct carrying the ARF4 PB1 failed to fully rescue the *ett* gynoecium phenotype

(Finet et al., 2010). The data presented here does not necessarily contradict this finding, but rather implies that the non-canonical auxin signalling role of ETT and its PB1-dependent functions are unlinked.

Finally, the data presented here suggest a level of allosteric inhibition of the MR2 auxin sensing function by the ETT/ARF4-like DNA binding domain (Fig. 3.7). The *G. biloba* ETT/ARF4-like DBD was able to completely disrupt the auxin-sensitivity of the TPL/TPR interactions of both *A. thaliana* and *A. trichopoda* ES domains. The DBD of ARFs within the same clade are known to be highly similar and similar DNA-binding residues are conserved between clades (Boer et al., 2014; Galli et al., 2018), so this was an unexpected discovery. However, it is a possibility that there are cryptic motifs within the DBD that are also involved in auxin sensing. Therefore, it is important in future studies to consider the contribution of this domain to the non-canonical auxin signalling function of ETT.

3.3.3 The role of the ETT-mediated auxin signalling pathway in leaf dorsiventral polarity is uncertain

The initial Y2H auxin sensitivity screen was conducted with the KAN and YAB TF families as it appeared that the ETT-mediated auxin signalling pathway might be important for leaf polarity (Fig. 3.1). Firstly, the *pETT:ETT^{2CS}* auxin insensitive line exhibited leaf epinasty and other organ polarity defects (Fig. S3.1; Simonini et al., 2016). Furthermore, ATS, and to a lesser extent FIL, have been shown to interact in an auxin-dependent manner with ETT (Simonini et al., 2016). Therefore, the lack of auxin sensitivity of all KAN and YAB interactions with ETT in the initial screen was unexpected.

The lack of auxin sensitivity of the KAN or YAB interactions with ETT might be an artefact of the experimental system. The Y2H expression system utilised by Simonini et al. (2016) and this study differs, and therefore there might have been

protein abundance differences that affected the auxin sensitivity assays. The expression system might also explain the lack of interactions of the *M. polymorpha* ARF2 with TPL when it has been demonstrated by Kato et al. (2020). Alternatively, it is possible that the auxin sensing function of ETT is not important for leaf polarity and development, which is in line with the fact that the gymnosperm and monilophyte ETT/ARF4-like orthologues are also auxin insensitive.

3.4 Concluding Remarks

Contrary to the TIR1/AFB-dependent pathway, whose origins can be traced back to the early land plants (Mutte et al., 2018), little is known about the conservation and evolution of the ETT-mediated auxin signalling pathway. The data presented in this chapter provides evidence that the ability of ETT to sense auxin arose through neofunctionalisation of the clade after its divergence from ARF4 in the last common ancestor of flowering plants. Furthermore, while the auxin sensitivity of ETT has been attributed as a function of motifs within the ES domain (Kuhn et al., 2020; Simonini et al., 2016; Simonini et al., 2018a), I showed that the DBD also contributes to the auxin-sensing function of ETT.

Nonetheless, the data here is preliminary and further work must be done to understand better how the ETT-mediated auxin signalling pathway functions in terms of biochemistry and development. While it appears that the ETT-mediated auxin signalling pathway is specific to the angiosperms, there is still limited data regarding its conservation within the angiosperms (Fig. 3.5). This is in part due to the lack of taxon sampling, as only one or two species are used to represent an entire clade. As seen with the two ANA grade angiosperms included in the study, there is the possibility of the loss of the ETT-specific pathway from certain lineages. Similarly, the possibility that there exists non-angiosperm ETT/ARF4-like orthologues that are auxin sensitive cannot be completely discounted. Thus, a more

accurate picture of the evolutionary history of ETT can only be uncovered through means of increased sampling.

Another caveat of the experimental system is the standard technical limitations imposed by the Y2H approach. False negatives have been described in Y2H systems due to multiple factors including steric hindrance by the reporter tags, lack of essential post-translational modifications or different protein sub-cellular compartmentalisation (Brückner et al., 2009). Conversely, false positives can also occur due to non-specific protein interactions. These experimental artefacts could possibly explain the discrepancy between studies such as with the ETT-ATS interaction (Simonini et al., 2016). Therefore, alternative approaches must be utilised to validate these results. Both co-immunoprecipitation and FRET-FLIM experiments were trialled, but unfortunately due to protein expression issues and time limitations for troubleshooting, they were unsuccessful. These techniques should be followed up on to provide support for the data presented in this chapter.

Another issue with the Y2H approach is the targeted, and therefore biased, nature of the setup. It is unfeasible to screen every member of every TF family that interacts with ETT, let alone other non-TF protein interactors. There remains the possibility for auxin sensitive interactions between the ETT/ARF4-like orthologues (supposedly not facilitating auxin sensitive interactions) with currently unknown partners. An unbiased proteome-wide approach, such as Turbo-ID, should be considered (Branon et al., 2018). Transgenic *A. thaliana* lines expressing ETT or ARF4 fused with the MiniTurbo tag were planned to address this but unfortunately due to issues with the generation of the plants within the timeframe of the study, they were abandoned. Nevertheless, the Turbo-ID approach should be prioritised in future studies to fully understand the landscape of auxin-dependent interactions mediated by ETT and/or ARF4.

This study also uncovered the unexpected contribution of the DBD of ETT to its auxin sensitivity, while strengthening the evidence for MR2 as a major contributor to auxin sensing (Fig. 3.7). Hence, future studies to identify specific motifs or combinations of motifs that mediate conserved ETT-mediated auxin signalling must consider the entire protein instead of just the ES domain. While structural biology is beyond the scope of this thesis, the 3D structure of ETT, perhaps in complex with auxin, would be highly informative to elucidate how the different domains interact with one another for the auxin sensing role of ETT and the consequences on its protein-protein interactions.

With the evolutionary origin of the ETT/ARF4-like clade clarified in Chapter 2, and the auxin sensitivity of selected orthologues tested in the present chapter, the question remains as to whether this auxin sensing role of ETT evolved to facilitate carpel development. Thus, I will investigate the *in planta* developmental roles of these orthologues with respect to both vegetative and reproductive contexts in Chapter 4.

3.5 Materials and Methods

3.5.1 Orthologue identification

The KAN, YAB, TPL/TPR and AUX/IAA orthologues included in this study were identified from public databases (NCBI and Phytozome) using the Basic Local Alignment Search Tool (BLAST) with the *A. thaliana* orthologue sequences as queries. All putative orthologues were aligned in CLC Workbench (Qiagen) and a phylogenetic tree was constructed using the Neighbour-Joining method and Jukes-Cantor model with a maximum of 1000 bootstraps. Trees were visualised with iTOL as in Chapter 2.

3.5.2 Plant material and growth conditions

All *A. thaliana* plants were derived from the Col-0 ecotype. The *pETT:ETT^{2CS}* line was previously published by Simonini et al. (2016). Seeds were surface sterilised, sown in petri dishes containing MS media with 0.8 % agar and 1 % sucrose, and stratified in the dark at 4 °C for three days. The seedlings were grown for 10 days under long-day conditions (16 h light/8 h dark) before they were transplanted into soil (Levington F2 compost with insecticide) under long-day conditions at 22 °C.

The *C. richardii* ferns were of the Hn-n ecotype. Spores were obtained from Andrew Plackett (University of Birmingham), surface sterilised using bleach solution (4 % sodium hypochlorite, 0.1 % Tween) for 5 minutes, washed twice and resuspended in dH₂O before plating on ½ MS media. The spores were grown at 25 °C under long-day conditions for two weeks until the gametophytes have formed fertile archegonia and antheridia. Water was added to the plates to facilitate gametophyte fertilisation, and the developing sporophytes were transplanted into soil (Levington F2 compost with insecticide) and grown under long-day conditions at 80 % relative humidity and 28 °C.

N. thermarum seeds were obtained from Rebecca Povilus (Whitehead Institute) and sown in Aquatic Compost (Vitax Ltd.). Pots were placed in a tank with the water level approximately 50 to 100 mm above compost level. The tanks were placed in a greenhouse under 12 h light/12 h dark conditions, at 28 °C and 80 % relative humidity. *Daphnia pulex* and *Planorbarius corneus* were introduced into the tanks as biological control against algae. Plants were fertilised every 10 days with commercial pond tablets or chicken manure pellets.

M. polymorpha TAK-1, *S. lycopersicum* 'MicroTom' and *O. sativa* 'Kiitake' plants were obtained from the lab of Xiaoqi Feng when at the John Innes Centre (now at Institute of Science and Technology, Austria) while *A. fimbriata* seeds were purchased from Chiltern Seeds. Gemmae and seeds were sown directly in compost

under the same conditions as *C. richardii*. *A. trichopoda* shoot and leaf samples were collected from Cambridge University Botanic Gardens, while *G. biloba* shoot and leaf tissue were collected from a tree in the John Innes Centre courtyard.

3.5.3 RNA isolation and cDNA synthesis

The RNeasy Plant Mini Kit (Qiagen) was used according to the manufacturer's instructions to isolate RNA from *A. thaliana* inflorescences and shoots. For all other species, the CTAB pre-treatment protocol from Kim et al. (2004) was utilised. The on-column RNase free DNase kit (Qiagen) was added according to the manufacturer's instructions to remove genomic DNA. RNA was eluted from the columns in 40 µl RNase free water. The SuperScript™ IV First-Strand Synthesis kit (ThermoFisher) was used according to manufacturer's instructions to synthesise cDNA from 1 µg of total RNA.

3.5.4 Generation of Y2H constructs

The coding regions of ARF, KAN, YAB, TPL/TPR, and AUX/IAA orthologues were cloned using the Phusion Flash High-Fidelity PCR Master Mix kit (Thermo Scientific). The list of primers used are shown in Table S3.2. The pB1880 Gal4-BD and pB1881 Gal4-AD Y2H vectors from Ding et al. (2018) were obtained from Yuli Ding (John Innes Centre) and digested using Sall and NotI restriction enzymes. The coding sequence of the orthologues were inserted into the linearised vectors using In-Fusion (Takara Bio) according to the manufacturer's instructions. The constructs were transformed into *E. coli* Stellar™ Competent Cells (Takara Bio) and plated on LB plates containing 100 µg/ml carbenicillin. Positive colonies were identified using colony PCR and grown overnight in 10 ml liquid LB at 37 °C and 200 rpm shaking. Plasmids were extracted according to manufacturer's instructions with the NucleoSpin Plasmid EasyPure kit (Macherey-Nagel) and sequences were validated via Sanger sequencing with Macrogen Europe.

3.5.5 Yeast 2 hybrid interaction assays

The AH109 yeast strain (Clontech) was used for all Y2H experiments. Yeast cells were transformed using the co-transformation method described by Egea-Cortines et al. (1999). Yeast cells were grown at 28 °C for 3-4 days on WL YSD minimal media lacking tryptophan and leucine to select for positive transformants. The transformed yeast colonies were then plated on WLAH media lacking tryptophan, leucine, adenine, and histidine to assay for protein-protein interactions. To test for auxin sensitivity, yeast cells were serially diluted (10^0 , 10^{-1} , 10^{-2} and 10^{-3}) and spotted on WLAH media supplemented with 100 μ M indole-3-acetic acid (IAA). Images were taken after 5 days of growth at 28 °C.

3.5.6 Leaf area measurements and statistical analyses

Leaves 8-10 of Col-0, *ett-3*, *arf4-2* and *ETT^{2CS}* were collected and glued to a sheet of paper. Cuts were made at leaf margins to flatten out the leaves. Photographs of the leaves were taken with a ruler for scale. Images were converted to 8 bits and the leaf areas were measured using the Analyse Particles tool in ImageJ and plotted in RStudio 1.1.463.

The 8th, 9th and 10th leaves of *A. thaliana* Col-0 and *pETT:ETT^{2CS}* plants were collected and flattened on a sheet of paper, making cuts in the lamina where necessary. Images of the leaves with a ruler for scale were taken and converted to 8 bits. The leaf areas were measured using the Analyse Particles tool in ImageJ. The boxplots were plotted in RStudio 1.1.463 using the ggplot2 package (Wickham, 2011) and the statistical significance between leaf areas were calculated and visualised using the ggsignif package (Ahlmann-Eltze and Patil, 2021).

Chapter 4:

**The ETT clade was co-opted for
gynoecium development from an
ancestral vegetative role**

4.1 Introduction

In the previous chapters, I have demonstrated that the ETT/ARF4-like clade originated in the euphyllophytes and diverged into the ETT and ARF4 clades at the base of the angiosperm lineage. Following this divergence, ETT and ARF4 have undergone numerous structural changes, and ETT appears to have acquired the novel ability to sense auxin. Considering the differential redundancy of ETT and ARF4 in leaf and gynoecium development (Guan et al., 2017; Pekker et al., 2005; Sessions et al., 1997b), and the importance of the ETT-mediated auxin signalling pathway in proper gynoecium morphogenesis (Kuhn et al., 2020; Simonini et al., 2016), I hypothesise that auxin sensing by ETT is an important neofunctionalisation instrumental for its specialised role in gynoecium development after its recruitment from the ancient leaf polarity network.

The technological progress of recent years in whole genomic sequencing infrastructure and bioinformatic tools, as well as increasing international collaborations, have resulted in a massive increase in plant genome availability, including those from non-model or crop species (Marks et al., 2021). Through the investigation of genomes from distantly related plant lineages, it is becoming apparent that a so-called 'ancestral developmental tool kit' existed in the last common ancestor of the embryophytes (Floyd and Bowman, 2007). Numerous key transcription families that regulate important developmental processes in angiosperms are also present in bryophyte or algal genomes, including the lateral organ polarity factors or components of hormone signalling pathways (Briginshaw et al., 2022; Briones-Moreno et al., 2023; Li et al., 2020a; Mutte et al., 2018; Prigge and Clark, 2006; Sakakibara et al., 2008).

Nevertheless, many of these tool kit genes exist at lower copy numbers in algae and bryophytes compared to tracheophyte lineages (Bowman et al., 2017; Hori et al., 2014; Mutte et al., 2018; Rensing et al., 2008). Whole genome duplication events

are common throughout the evolutionary history of the land plants, such as the ancient duplication predating the diversification of extant angiosperms (Cui et al., 2006; Project et al., 2013). The three duplication events preceding the evolution of the Brassicales has been estimated to generate approximately ninety percent of the gene families in *A. thaliana* (Maere et al., 2005). In many cases, the redundant gene copies may be reduced through gene loss (Clark, 2023; Ibarra-Laclette et al., 2013). However, the presence of redundant copies allows the possibility for the division of original function between copies (subfunctionalisation), or the acquisition of novel functions (neofunctionalisation) (Birchler and Yang, 2022; Prince and Pickett, 2002). It is likely that the expansion of these tool kit genes drove the invention of morphological novelties in the land plant body plan through the recruitment of these duplicated paralogues in new developmental contexts.

The evolutionary gain of function in these gene families are oftentimes stepwise, as exemplified by the PIN auxin efflux transporters. The sole PIN orthologue of the alga *K. nitens* is able to drive auxin export but is non-polar and could not rescue the shoot/root defects of the *A. thaliana pin1/3/4/7* quadruple mutant in genetic complementation experiments (Skokan et al., 2019; Zhang et al., 2020b). While bryophyte orthologues complemented the shoot/root defects, they were unable to rescue the bare inflorescences of the *pin1* mutant unlike vascular plant orthologues. However, only angiosperm orthologues were able to fully restore fertile flowers with high seed set to the *pin1* line. These lines reveal that the PINs first acquired shoot and root function after the divergence of embryophytes from the charophytes, followed by the gain of inflorescence function in tracheophytes and floral roles in the angiosperms.

Similarly, the ARF gene family has greatly diversified across land plant lineages since their origins in the last common embryophyte ancestor (Finet et al., 2013; Mutte et al., 2018). Structural analyses of algal proto-ARFs suggest that they share

DNA binding preferences with their land plant orthologues (Martin-Arevalillo et al., 2019; Mutte et al., 2018). However, these proto-ARFs were not under auxin regulation by the canonical pathway due to the lack of functional TIR1/AFB and AUX/IAA orthologues in alga. In contrast, the complete canonical pathway is fully functional in bryophytes, as seen in the model liverwort *M. polymorpha* (Kato et al., 2020). In this minimal system, the sole Class A ARF interacts with the AUX/IAA orthologue and activates auxin-induced gene expression similar to the angiosperm system. However, the *M. polymorpha* Class B ARF behaves in an auxin-independent manner as a transcriptional repressor (Kato et al., 2015; Kato et al., 2020). As the ARFs have distinct and overlapping expression patterns, it is likely that regions of different auxin sensitivities are created through the antagonism of the Class A ARF activity by target site competition from the Class B ARF.

While angiosperm Class B ARFs are also transcriptional repressors and are unlikely to be regulated by the TIR1/AFB system (Piya et al., 2014; Tiwari et al., 2003; Ulmasov et al., 1999a; Vernoux et al., 2011), ETT has acquired a novel role in activating auxin-dependent gene expression through its direct binding and response to auxin (Kuhn et al., 2020; Simonini et al., 2016; Simonini et al., 2018a). In contrast, its closest paralogue ARF4 retains a functional PB1 domain and is unable to functionally complement ETT function in gynoecium development (Chapter 3; Finet et al., 2010). With respect to its developmental roles, ETT coordinates numerous processes in gynoecium initiation, polarity, and growth. ETT terminates the floral meristem in synergy with the MADS-box transcription factor AG and stimulates valve growth through its positive regulation of pectin methylesterase activity (Andres-Robin et al., 2018; Liu et al., 2014c). Importantly, it was shown that ETT interacts with the transcription factor IND in an auxin-sensitive manner, and that this interaction regulates *PID* expression to mediate the development of the radial style (Moubayidin and Østergaard, 2014; Simonini et al., 2016).

In *A. thaliana*, both ETT and ARF4, and also ARF2, redundantly regulate abaxial tissue identity through their protein-protein interactions with the KAN transcription factors and their antagonism of the adaxial polarity factors (Guan et al., 2017; Kelley et al., 2012; Pekker et al., 2005). While expression of the auxin insensitive ETT^{2CS} allele resulted in leaf epinasty (Chapter 3; Simonini et al., 2016), I was unable to demonstrate that auxin regulated the interactions between ETT and the KAN/YAB families. Given the full redundancy between ETT and ARF4 in this context, the ETT-mediated auxin signalling pathway might not be necessary for leaf polarity and growth, and the *pETT:ETT^{2CS} ett-3* phenotype might reflect auxin-independent changes in ETT function. In this scenario, the ETT/ARF4-like clade which emerged in the last euphyllophyte ancestor might have possessed an ancestral auxin-independent role in mediating leaf development before the recruitment and neofunctionalisation of ETT in the angiosperms for carpel development. Nonetheless, the discovery of monilophyte ETT/ARF4-like orthologues and the independent evolution of fern fronds opens up the question as to whether these orthologues are functionally equivalent to those of the seed plants (Chapter 2; Sun and Li, 2020; Xia et al., 2017).

Therefore, this chapter aims to address the evolutionary origin of the vegetative and reproductive roles of ETT and ARF4, and the potential contribution of the ETT-mediated auxin signalling pathway in leaf and gynoecium development. Genetic complementation experiments of the *ett-3* null mutant were performed to investigate the functional equivalence of the ETT/ARF4-like orthologues tested in Chapter 3 in gynoecium development. Only angiosperm ETT and ARF4 orthologues were able to complement the gynoecium defects of *ett-3* fully or partially, indicating the origin of the carpel development role in the last common angiosperm ancestor. Furthermore, there is a correlation between auxin sensitivity and full complementation of the style. Heterologous expression of the orthologues in the *ett-3 arf4^{GE}* background supports

an ancestral leaf development function for the ETT/ARF4-like clade and the non-homology of monilophyte fronds and spermatophyte leaves. Finally, expression of the chimeric ETT constructs in *ett-3* further supports the hypothesis that the ETT-mediated auxin signalling pathway was vital for the origin of the carpel.

4.2 Results

4.2.1 The role of ETT in gynoecium development arose in the last common ancestor of flowering plants

To uncover the functional origin of the gynoecium development role of ETT, interspecies genetic complementation lines were generated in the *A. thaliana ett-3* background (Fig. 4.1). ETT/ARF4-like orthologues from the phylogenetically important species included in Chapter 3 were expressed under the 5 kb *A. thaliana ETT* promoter, and independent lines were assessed and selected for transgene expression levels that were comparable to the endogenous ETT expression in wild-type gynoecia (Fig. S4.1). As the *ett-3* loss-of-function mutant exhibits reduced valve growth, medial outgrowths and a bilateral 'split-style' phenotype (Sessions et al., 1997b; Simonini et al., 2016), the heterologous complementation lines were assessed for their style and ovary morphology (Fig. 4.1, Fig. S4.2).

The heterologous expression of ETT orthologues from all sampled angiosperms except *N. thermarum* and *A. fimbriata* fully rescue the gynoecium defects of the *ett-3* background (Fig. 4.1a-c). The valve length, medial outgrowth and style symmetry of the *A. trichopoda* and *S. lycopersicum* complementation lines were comparable to that of the wild type. On the other hand, ARF4 expression in the *ett-3* background provided only partial rescue of the *ett-3* phenotype: the silique length is mostly restored (Fig. 4.1c) but slight medial outgrowths and mild style asymmetry can be observed in the gynoecia of the ARF4 complementation lines (Fig. 4.1a, b). These results suggest that ETT and ARF4 regulate certain

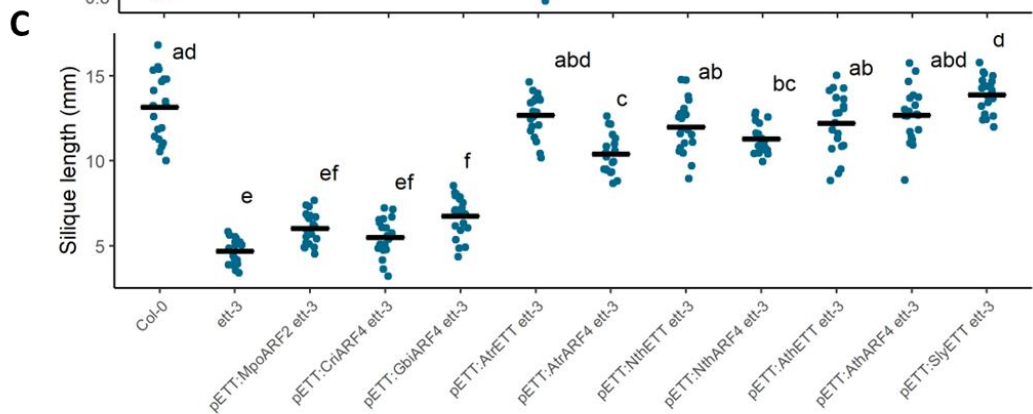
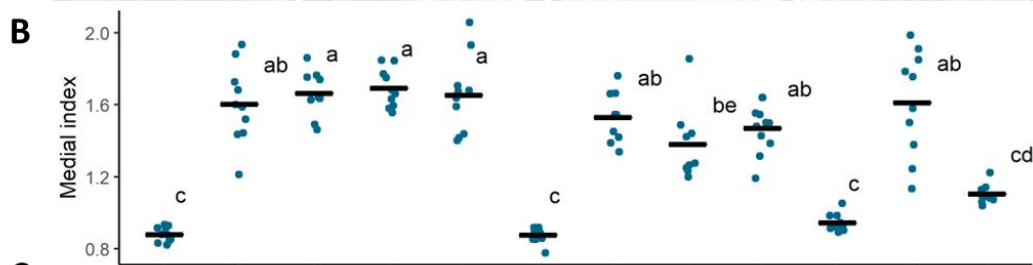
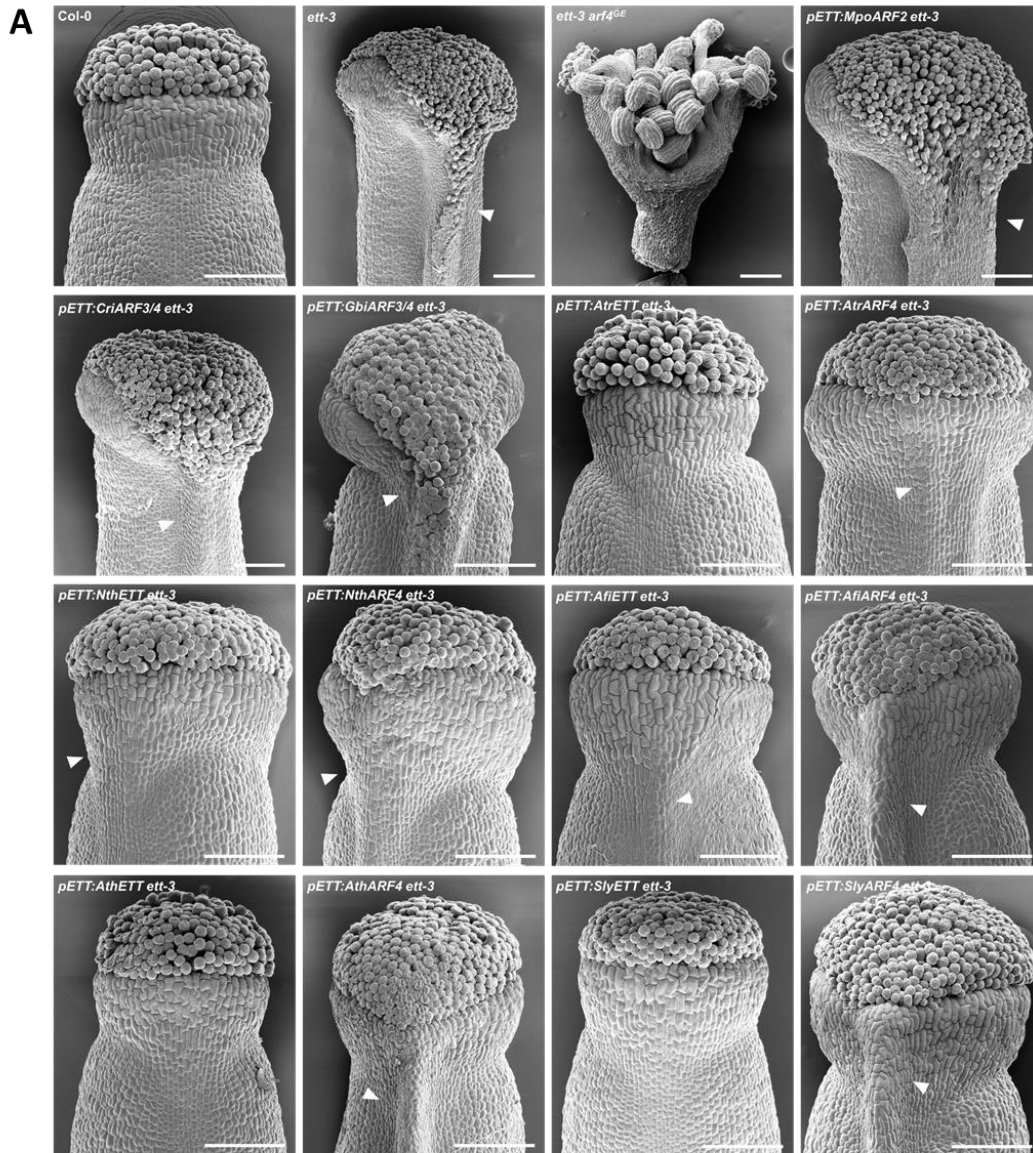


Figure 4.1: Gynoecium morphology of wild-type, mutant, and ETT/ARF4 genetic complementation lines (previous page). (A) SEM images of the gynoecium apex of Col-0, *ett-3*, *ett-3 arf4^{GE}* and complementation lines. Scale bar represents 100 μm . **(B)** The medial index (maximum style width / valve width) of tested lines demonstrates the complementation of the *ett-3* medial outgrowths by eudicot and *A. trichopoda* ETT orthologues ($n = 10$). **(C)** Lengths of fully-elongated green siliques indicate the rescue of the *ett-3* valve growth defect by all angiosperm ETT and ARF4 orthologues ($n = 20$). In **(B)** and **(C)**, black bars indicate the mean, and the letters indicate statistical differences between groups after one-way analysis of variance and Tukey's HSD post-hoc test ($p < 0.05$).

developmental processes in gynoecium morphogenesis, mainly in ovary and silique growth, in a redundant manner but ETT has evolved a specialised role for proper style development. Furthermore, as even the ETT and ARF4 orthologues of *A. trichopoda* were able to provide partial to full rescue of the *ett-3* phenotype, this indicates that the role of ETT and ARF4 in gynoecium development is widely conserved and was present since the last common angiosperm ancestor.

In line with the above hypothesis, none of the non-angiosperm ETT/ARF4-like orthologues were able to complement the *ett-3* gynoecium defects (Fig. 4.1). The *G. biloba*, *C. richardii*, and *M. polymorpha* rescue lines exhibited reduced ovary lengths, prominent medial outgrowths and the 'split style' phenotype characteristic of the *ett-3* background. This is especially interesting for the *G. biloba* ETT/ARF4-like orthologue which more closely resembles the angiosperm ETT and ARF4 orthologues in terms of domain and motif structure than the monilophyte or bryophyte orthologues (Chapter 2; Finet et al., 2013). This observation implies that the ETT/ARF4 clade only evolved their roles in gynoecium morphogenesis after the divergence of extant angiosperms from the gymnosperms, rather than it being a stepwise process throughout euphyllophyte evolution.

Interestingly, the *N. thermarum* ETT and ARF4 were both unable to fully complement the gynoecium phenotype of *ett-3* (Fig. 4.1a, b). While the silique lengths were comparable to those of the wild-type and other angiosperm ETT and ARF4 lines (Fig. 4.1c), medial outgrowths can be observed for both lines expressing the *N. thermarum* ETT and ARF4. Considering that the *A. trichopoda* ETT provided full complementation, it is likely that the *N. thermarum* ETT has lost some functionality in style development, perhaps through the loss of its auxin sensitivity (see Chapter 3).

ETT is known to regulate style morphogenesis in part through its auxin-sensitive and stage-dependent transcriptional control of its target genes *PID* (Kuhn et al., 2020; Simonini et al., 2017). In the absence of auxin, the expression of *PID* and *HEC1* are repressed in an ETT-dependent manner, while these genes are upregulated upon the perception of auxin. Therefore, the expression level of *PID* in the gynoecia of the complementation lines were measured through qPCR to assess the ability of the ETT/ARF4-like orthologues in regulating downstream target genes through the non-canonical auxin signalling pathway.

As shown in previous studies (Kuhn et al., 2020; Simonini et al., 2016), the expression of *PID* in *ett-3* was constitutively upregulated relative to the wild-type (Fig. 4.2). However, none of the complementation lines exhibited significantly different expression of *PID* compared to the wild type, including those from non-angiosperm lineages that failed to complement the gynoecium phenotype (Fig. 4.1). Taking these observations into account, the regulation of *PID* by ETT/ARF4-like orthologues cannot be the only factor behind the gynoecium phenotypes of the genetic complementation lines. However, it is important to note that high variability is seen between individual replicates and perhaps increased sampling, or alternate methodology is necessary for more statistical power.

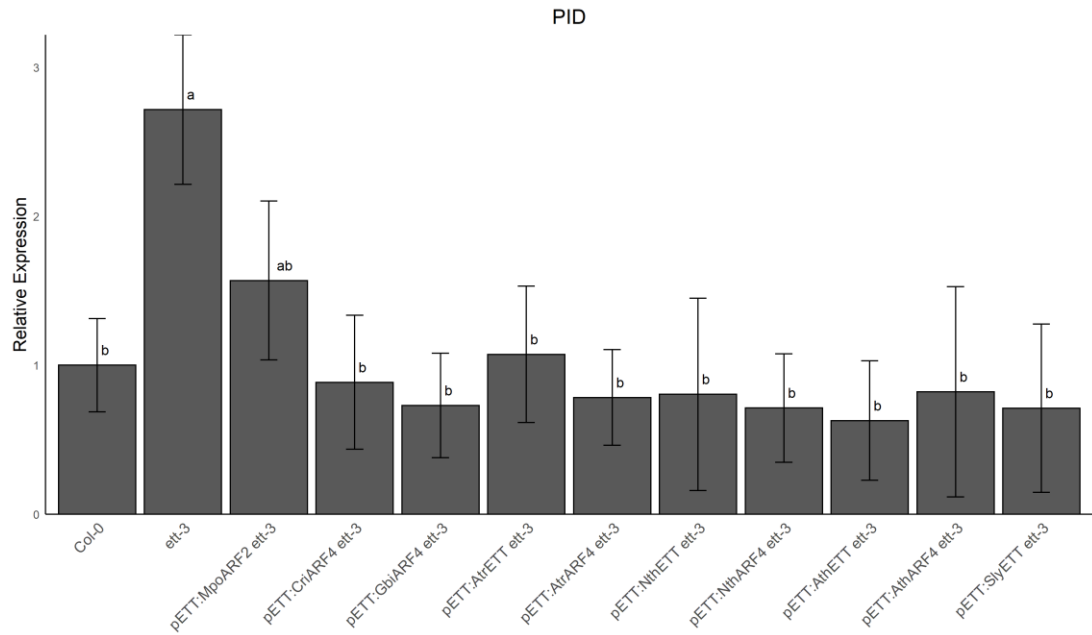


Figure 4.2: Relative expression levels of *PID* in wild-type, mutant and ETT/ARF4-like complementation lines. *PID* expression is misregulated in the *ett-3* background, but is not significantly different from the wild-type in all ETT/ARF4-like complementation lines. The bars plot the mean value while the error bars represent standard deviation of the mean ($p < 0.05$, $n = 3$).

4.2.2 The ETT/ARF4-like clade has an ancestral role in vegetative development

Besides their roles in gynoecium development, ETT and ARF4 also contribute to leaf polarity and growth (Guan et al., 2017; Pekker et al., 2005). The complete genetic redundancy of ETT and ARF4 in leaf development could indicate an ancestral role of the ETT/ARF4-like clade in vegetative development that was retained fully in both ETT and ARF4 clades after their divergence in the last common ancestor of the flowering plants. In addition, the ETT/ARF4-like orthologue of the monilophyte *C. pteridioides* exhibited an expression pattern in fronds similar to that of the ETT and ARF4 orthologues in seed plant leaves (Sun and Li, 2020). Therefore, the *ett-3* complementation lines generated were crossed with the *ett-3*

arf4^{GE} line to assess the ability of the ETT/ARF4-like orthologues to rescue the leaf polarity defects of the *ett-3 arf4^{GE}* background.

While the relative proximal-distal and medio-lateral curvature of leaves were not significantly different between most lines (Fig. 4.3B, C), uncomplemented lines could be distinguished by the presence of a cup-like indentation in their leaves (Fig. 4.3A). In line with the hypothesis and other studies (Guan et al., 2017; Pekker et al., 2005), the *A. thaliana* ETT and ARF4 are functionally equivalent in leaf development as both paralogues could complement the leaf hyponasty phenotype of *ett-3 arf4^{GE}* (Fig. 4.3A). Furthermore, the ANA grade ETT orthologues were able to complement the *ett-3 arf4^{GE}* leaf defects, implicating that the role of ETT in leaf development was present since the last common angiosperm ancestor. Unfortunately, the crosses of the ANA grade ARF4 lines in the *ett-3* background with the *ett-3 arf4^{GE}* background were unsuccessful, and due to time constraints, were unable to be repeated. Thus, it is unknown if the ARF4 of the ANA grade are also functionally equivalent to ETT and ARF4 from the core eudicots in leaf development.

As predicted from my hypothesis, the sole *M. polymorpha* Class B orthologue was unable to rescue leaf development in *A. thaliana*, indicative of a strong functional divergence (Fig. 4.3A, B). Furthermore, despite the origins of the ETT/ARF4-like clade in the euphyllophytes, the *C. richardii* ETT/ARF4-like orthologue could not complement the *ett-3 arf4^{GE}* phenotype. Given that the ETT/ARF4-like orthologue of monilophytes are under divergent post-transcriptional regulation by the tasiARFs (Sun and Li, 2020; Xia et al., 2017), and the independent origins of monilophyte fronds (Tomescu, 2009), it is clear that the role of the ETT/ARF4-like clade in true leaf development came after the divergence of the monilophytes from the seed plants. This is further supported by the partial complementation of the *ett-3 arf4^{GE}* phenotype by the *G. biloba* ETT/ARF4-like orthologue, exhibiting reduced leaf hyponasty and fewer occurrences of the cup-shaped indentations (Fig. 4.3A).

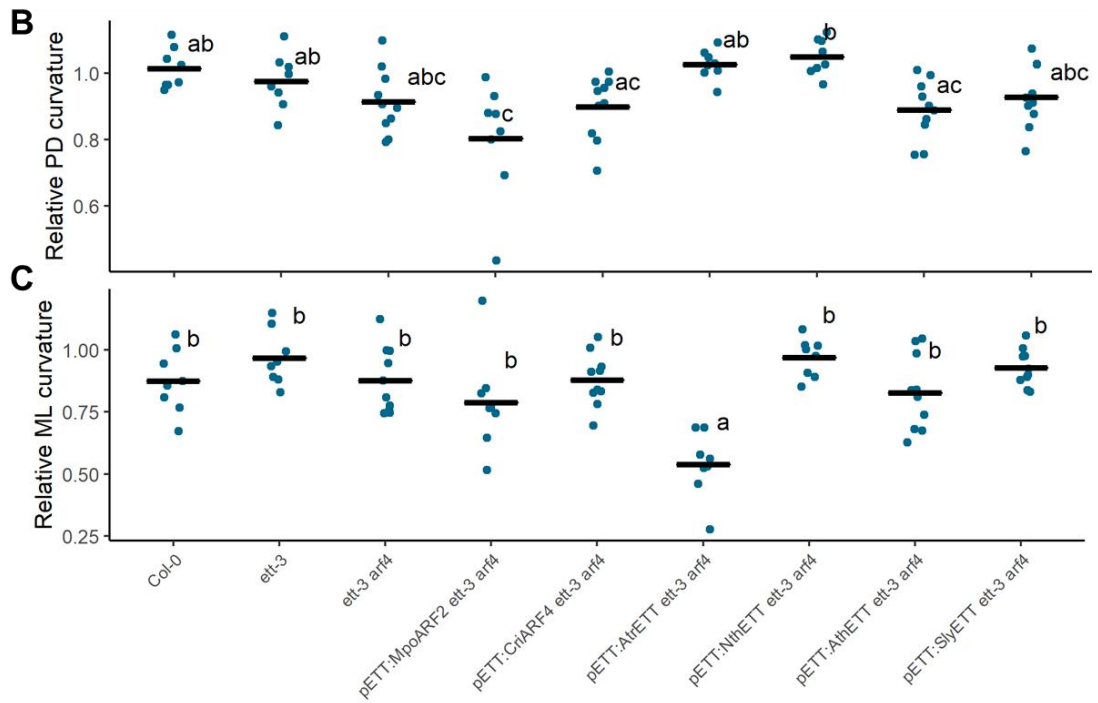
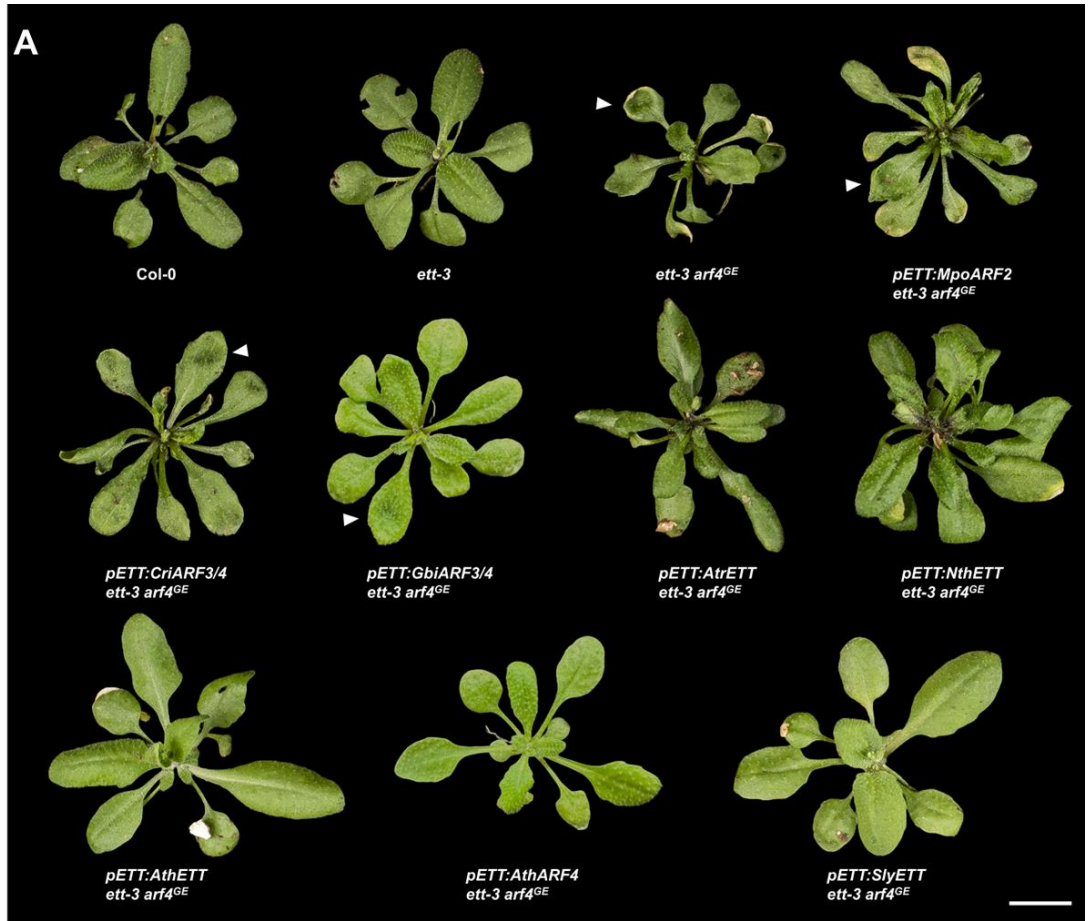


Figure 4.3: Leaf phenotypes of the *ett-3 arf4^{GE}* complementation lines (previous page).

(A) Rosette phenotypes of wild-type, mutant and complementation lines. Error bar represents 10 mm. White arrows highlight cup-like leaf indentations. Relative leaf proximal-distal **(B)** and medio-lateral **(C)** curvature were calculated as a ratio of the apparent unflattened leaf length/width to the actual flattened length/width ($n = 8$). The black bars and letters have the same meaning as in Fig. 4.1.

An interesting observation of both *ett-3* and *ett-3 arf4^{GE}* expressing the *A. trichopoda* *ETT* is a gain-of-function leaf epinasty phenotype reminiscent of the *pETT:ETT^{2CS} ett-3* line (Fig. 4.3A, C, Fig. S4.2, Chapter 3). As the *A. trichopoda* *ETT* has been shown to be auxin sensitive in Chapter 3, and fully complements the *ett-3* gynoecium (Fig. 4.1), it is likely that this reflects a divergence in function of the *A. trichopoda* *ETT* unrelated to the *ETT*-mediated auxin signalling pathway.

4.2.3 The *ETT*-mediated auxin signalling pathway influences style development

The chimeric constructs used in Chapter 3 revealed the strong contributions of MR2 and the DBD to the auxin sensing ability of *ETT*. As there appears to be a correlation between the auxin sensitivity of *ETT/ARF4*-like orthologues and the genetic rescue of the *ett-3* medial outgrowth phenotype (Fig. 4.1), *ett-3* complementation lines expressing the chimeric *ETT/ARF4*-like constructs were generated to further test the hypothesis that the *ETT*-mediated auxin signalling pathway is necessary for proper development of the radial style.

The DS1, DS5, DS6 and DS7 lines were able to rescue the reduced valve length phenotype of *ett-3*, but not the medial outgrowths of the style (Fig. 4.4). This is similar to the phenotypes of the *ARF4* and *N. thermarum* *ETT* complementation lines (Fig. 4.1). In contrast, the DS2, DS3, DS8 and DS10 lines exhibited normal

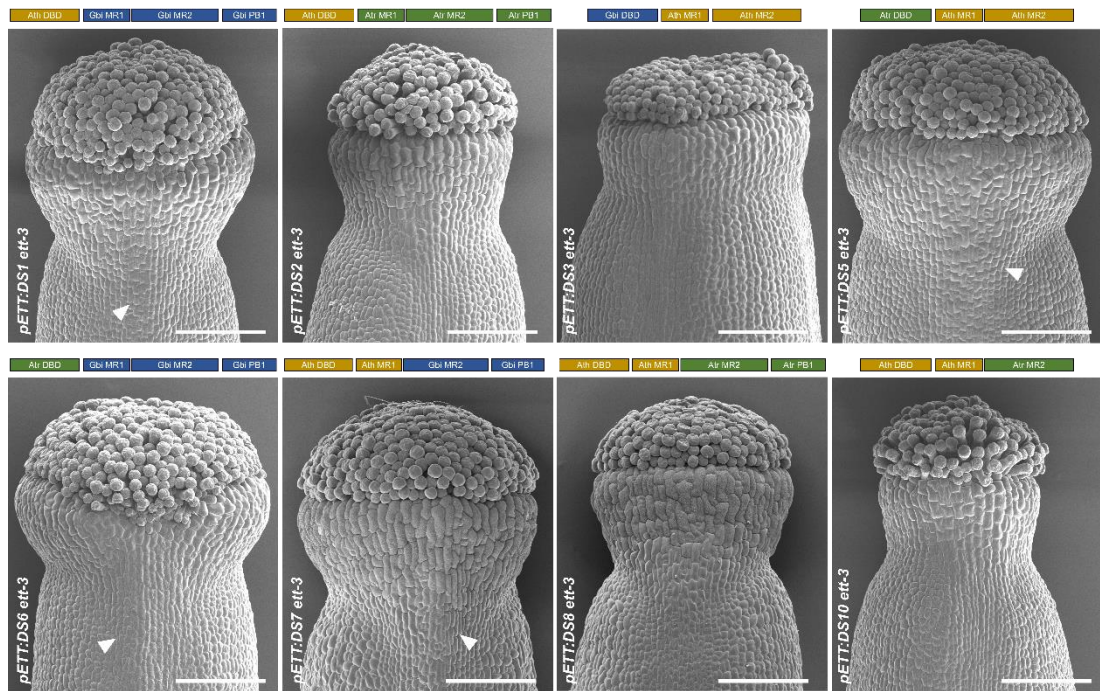


Figure 4.4: Gynoecium phenotypes of genetic complementation lines expressing chimeric ETT/ARF4-like constructs. The white arrows highlight medial outgrowths of the style. The construct schematic (DBD, MR1, MR2, and PB1 if present) is displayed above each SEM image, colour-coded according to species (brown – *A. thaliana*, blue – *G. biloba*, green – *A. trichopoda*). Scale bar represents 100 μ m.

radial styles (Fig. 4.4). With the exception of DS5, all of the complementation lines that did not fully rescue style development contained the *G. biloba* MR2 which has been shown to be auxin-insensitive (Chapter 3). This suggests that the auxin sensitivity of ETT is important for the proper development of the style. However, the chimeric constructs containing the auxin insensitive *G. biloba* MR is able to complement valve growth unlike the full-length *G. biloba* ETT/ARF4-like orthologue (Fig. 4.1), indicating that there are functional differences between the DBD of *G. biloba* and angiosperm ETT orthologues.

Interestingly, all *G. biloba* complementation lines expressing chimeric constructs containing the *A. trichopoda* MR domains (DS2, DS8 and DS10) had epinastic leaves, similar

to the *A. trichopoda* ETT and *pETT:ETT^{2CS} ett-3* lines (Fig. S4.3, Chapter 3). This suggests that the MR2 of the *A. trichopoda* ETT is sufficient to confer the leaf epinasty phenotype and that this is independent of ETT's auxin sensing role, although the mechanism behind this phenotype is still unknown.

4.3 Discussion

In Chapter 3, I discovered that the novel auxin sensing ability of ETT is likely specific to the ETT clade and was probably already present when the ETT and ARF4 clades diverged in the last common ancestor of flowering plants.

Nonetheless, it remains unclear as to whether this ability is important in leaf development, and whether ETT's role in gynoecia and leaves are conserved in the ETT/ARF4-like orthologues from diverse embryophyte lineages. Thus, this chapter focused on investigating the *in planta* developmental roles of the ETT/ARF4-like orthologues through genetic complementation lines, revealing the two-step origins of ETT function and the contributions of its different domains to lateral organ morphogenesis.

4.3.1 The evolution of the dual roles of ETT in gynoecium development occurred after the divergence of the angiosperms

The gynoecium phenotypes of the ETT/ARF4-like complementation lines clearly demonstrate that ETT acquired its role in gynoecium development in the last common ancestor of extant flowering plants, as full complementation of the *ett-3* gynoecium defects was observed for the *pETT:AtrETT ett-3* line (Fig. 4.1). This is further supported by the failure of all three non-angiosperm Class B ARF or ETT/ARF4-like orthologues to rescue gynoecium development in *A. thaliana*. The sole Class B ARF of *M. polymorpha* (ARF2), like other bryophyte and lycophyte Class B ARFs, lack multiple motifs in the MR that likely contribute to both ETT's auxin-dependent and auxin-independent functions (see Chapter 2). Likewise, the fern ETT/ARF4-like orthologues do not closely resemble ETT or ARF4 from the

spermatophytes, typically having only one tasiARF binding site instead of tandem repeats (Chapter 2; Xia et al., 2017). Therefore, it is unsurprising that both orthologues fail to complement *A. thaliana* gynoecium development. However, the *G. biloba* orthologue used in this experiment shares relatively high sequence similarities with the ETT and ARF4 orthologues of the angiosperms. Therefore, its failure to complement gynoecium development suggests that further functional divergence in protein biochemistry occurred after the acquisition of ETT/ARF4-like motifs.

All ARF4 orthologues from angiosperm species were able to partially complement the *ett-3* gynoecium phenotype with respect to ovary/valve development (Fig. 4.1c). Nevertheless, all ARF4 lines were unable to complement the medial outgrowths observed in the *ett-3* background, although there was a high degree of variability between gynoecia of the same line (Fig. 4.1b). These observations imply that ETT regulates two different aspects of gynoecium patterning with differing levels of redundancy with ARF4: ETT and ARF4 are interchangeable in function for the role of valve elongation, but ETT has specific functions related to style development that cannot be compensated by ARF4. It is known that ETT regulates valve growth through the activation of pectin methylesterases which reduces cell wall stiffness in the valves (Andres-Robin et al., 2018). It is likely that ARF4 is able to fulfil this role as well, but that this function of ARF4 may be masked by the different expression pattern of ARF4 in *ett* loss-of-function mutants.

Intriguingly, it was previously shown that the presence of the PB1 domain in chimeric ETT constructs interfered with ETT's ability to rescue the phenotype of null mutants (Finet et al., 2010). While the ETT orthologues of both ANA grade angiosperms sampled in this study possessed the PB1 domain, the *A. trichopoda* ETT rescued both valve growth and radial style formation in the *ett-3* background, whereas the *N. thermarum* ETT only complemented valve growth like the ARF4

lines (Fig. 4.1). The chimeric ETT construct from Finet et al. (2010) contained the *A. thaliana* ARF4 PB1. Therefore, it is possible that there are biochemical differences between the ANA grade ETT PB1 and the ARF4 PB1 from the core eudicots.

Additionally, the differences in the style complementation ability between paralogues (ETT vs ARF4) and orthologues (*A. trichopoda* vs *N. thermarum*) correlate with the auxin-sensitivity exhibited by the orthologues as demonstrated in Chapter 3. Therefore, it is possible that valve growth is independent of the ETT-mediated auxin signalling pathway while style formation requires this pathway. It was previously demonstrated that the ETT-mediated pathway is necessary for style formation through the regulation of the *PID* gene (Kuhn et al., 2020; Simonini et al., 2016). The repression of *PID* by the auxin-sensitive ETT-IND interacting pair prevents PIN1 phosphorylation, resulting in the redistribution of auxin into a ring formation at the gynoecium apex that mediates the bilateral-to-radial symmetry switch in the style (Moubayidin and Østergaard, 2014; Simonini et al., 2016). Thus, a possible explanation for the medial outgrowths of the *pETT:NthETT ett-3* and ARF4 lines is the misregulation of *PID*.

Surprisingly, the relative expression levels of *PID* in all complementation lines, including those that displayed medial outgrowths, were comparable to the wild type (Fig. 4.2). Therefore, it appears that the auxin-dependent regulation of *PID* is not the defining factor establishing radial style symmetry. Nevertheless, the high variability between biological replicates necessitates higher statistical power through increased sampling. Furthermore, an unbiased transcriptome-wide approach such as RNAseq might be more informative, as ETT regulates numerous gynoecium development genes such as *HEC1* and *TEC1* in an auxin-dependent manner (Kuhn et al., 2020; Simonini et al., 2017).

4.3.2 The ETT/ARF4-like clade acquired its function in leaf polarity and development after the origin of seed plants

The heterologous expression of *ETT* orthologues from all sampled angiosperms fully complemented the leaf hyponasty and epidermal outgrowth phenotype of the *ett3 arf4^{GE}* double mutant (Fig. 4.3). This result supports the deep conservation of ETT function throughout the angiosperms in the leaf polarity network. As the auxin-insensitive *N. thermarum* ETT and the ARF4 complementation lines also rescued leaf development, this provides further evidence that ETT-mediated auxin signalling is not necessary for the polarity network and leaf flattening.

Recent work on the leaf polarity network initiation in incipient primordia suggests that ETT defines adaxial fate through its activation of transcriptional auxin responses that converts a uniform auxin concentration into polarised signalling outputs (Burian et al., 2022). As ETT typically behaves as a transcriptional repressor in the absence of auxin (Kuhn et al., 2020; Simonini et al., 2017; Simonini et al., 2016), I speculated that the ETT-mediated pathway might be responsible for the auxin signalling output in the adaxial domain. However, given the data in Fig. 4.3, an alternative mechanism might be regulating ETT's auxin-dependent role in leaf polarity.

The *M. polymorpha* ARF2 was unable to rescue the leaf development defects of *ett3 arf4^{GE}*, which is in line with the hypothesis that the ETT/ARF4-like clade emerged in the euphyllophytes for roles in the leaf polarity and lamina flattening programme (Fig. 4.3). In contrast, the role of the monilophyte ETT/ARF4-like orthologues in leaf development is more contentious. The presence of this clade in the monilophytes, and their reported conserved abaxial localisation of orthologues in fronds (Sun and Li, 2020), supports a homologous role in frond development as seen in the seed plants. In agreement with this scenario, most other seed plant leaf polarity factors, including the HD-ZIP III, KAN and ARP families, have conserved

adaxial-abaxial expression domains in monilophyte fronds (Harrison et al., 2005; Vasco et al., 2016; Zumajo-Cardona et al., 2019).

However, the failure of the *C. richardii* ETT/ARF4-like orthologue to complement leaf development in *A. thaliana* implies that there is functional divergence between monilophyte and angiosperm orthologues. Monilophyte orthologues possess only one tasiARF binding site in the ARF MR domain, unlike the seed plant orthologues. Moreover, the tasiARF binding site sequence is divergent from the widely conserved seed plant motif and tasiARF regulation was not observed for the *C. pteridioides* ETT/ARF4-like orthologue (Sun and Li, 2020; Xia et al., 2017). In angiosperms, failure of the tasiARF regulatory system that maintains the abaxial localisation of the ARF2 and ETT/ARF4 clades results in abaxialised lateral organs and/or an impairment in medio-lateral expansion (Ding et al., 2020; Douglas et al., 2010; Fahlgren et al., 2006; Yifhar et al., 2012). Therefore, the lack of complementation by the *C. richardii* orthologue could in part be due to a misregulation of expression in addition to possible protein level differences. Nonetheless, this result does not prove that monilophyte ETT/ARF4-like orthologues are not involved in frond polarity and development, but it supports the non-homology between fronds and true leaves.

Interestingly, the *G. biloba* ETT/ARF4-like orthologue appears to partially complement the *ett3 arf4^{GE}* leaf phenotype, with reduced hyponasty (Fig. 4.3). This result indicates that some aspects of ETT function in leaf development have already originated in the gymnosperms. As the fossil record supports the homology of all seed plant leaves (Tomescu, 2009), the ETT/ARF4-like clade might have already been recruited for the leaf polarity network in the last common ancestor of the seed plants. However, the lack of full complementation implies that there are differences between the leaf polarity network of angiosperms and gymnosperms. Nonetheless, the *G. biloba* orthologue is not necessarily representative of the ancestral seed plant

state or of all gymnosperms, and it is possible that other gymnosperm orthologues possess greater functional similarities with those of the angiosperms.

A peculiar phenotype observed for the *A. trichopoda* ETT line is leaf epinasty (Fig. S4.3). This phenotype is shared by lines expressing chimeric constructs containing *A. trichopoda* ETT domains, and closely resembles the *pETT:ETT^{2CS} ett-3* phenotype as described in Chapter 3. As the *A. trichopoda* ETT has previously been shown to be auxin sensitive and fully complements the gynoecium defects of *ett-3* (Fig. 4.1), this implies that leaf epinasty is a gain-of-function phenotype unrelated to its auxin signalling function. It is likely that the *A. trichopoda* ETT interacts with other members of the leaf polarity network in a sufficiently dissimilar manner to the *A. thaliana* ETT but not in the context of the gynoecium development programme.

4.3.3 Auxin sensitivity is necessary for proper style morphogenesis

The phenotypes of the *ett-3* complementation lines expressing chimeric ETT/ARF4-like constructs support the hypothesis that the ETT-mediated auxin signalling pathway is important for style development (Fig. 4.4). In Chapter 3, it was revealed through Y2H assays that the *A. thaliana* and *A. trichopoda* ETT MR2 domains were auxin sensitive whereas the *G. biloba* ETT/ARF4-like MR2 was not. However, the presence of the *G. biloba* DBD in the constructs interfered with the auxin sensitivity of the angiosperm ETT MR2 domain. Consistent with these observations, only the chimeric constructs carrying the *A. thaliana* and *A. trichopoda* ETT MR2 were able to fully complement the medial outgrowth phenotype of *ett-3*.

Interestingly, the DS5 construct containing the *A. thaliana* DBD and the *A. trichopoda* MR1 and MR2 was not able to fully complement style development. It was seen in Chapter 3 that the DS5 construct had poor interactions with both *A. thaliana* TPL and *A. trichopoda* TPR1. Therefore, it is possible that there are steric effects caused by the interaction of the *A. thaliana* ETT DBD and the *A. trichopoda* ETT MR that interferes with TPL/TPR recruitment and potentially other protein

interactors that are necessary for style development. This result highlights the importance of future structural studies to understand how the topology of ETT influences its protein biochemistry and developmental roles.

While the full-length ETT/ARF4-like orthologue of *G. biloba* was unable to complement any aspect of the *ett-3* gynoeceium phenotype (Fig. 4.1), the chimeric constructs containing the *G. biloba* MR (DS1, DS6, DS7) were able to rescue valve growth to a similar extent as the angiosperm ARF4 lines (Fig. 4.4). The DS1, DS6 and DS7 lines contain either the *A. thaliana* or *A. trichopoda* ETT DBD. Thus, it appears that the *G. biloba* ETT/ARF4-like DBD has undergone a significant functional divergence from the angiosperm ETT orthologues. Whether this is due to a change in target site binding affinity and specificity, dimerisation ability or other protein-protein interactions remains a mystery. Further investigations into the DNA binding ability and interactome of the *G. biloba* ETT/ARF4-like DBD will be necessary to distinguish between these possibilities.

4.4 Concluding Remarks

Advances in genomics and the development of novel model systems representing key phylogenetic lineages have demonstrated that many ancient transcription factor families acquired their characteristic roles in angiosperms through gradual changes in ancestral expression patterns and/or protein biochemistry after their recruitment in novel morphological or physiological contexts (Briones-Moreno et al., 2023; Maizel et al., 2005; Plackett et al., 2018; Sakakibara et al., 2013; Zhang et al., 2020b). The data in this chapter supports a similar scenario for ETT in which ETT has undergone two major functional innovations at the protein level for its roles in leaf polarity and gynoeceium patterning.

The complementation lines reveal that ETT has specific functions in style development that cannot be compensated by ARF4, and this ability appears to be linked to the auxin-sensitivity demonstrated by the orthologues. Nonetheless, as

discussed in Chapter 3, greater sampling of species from each key lineage is required to strengthen this correlation, as only one representative each from the bryophytes, monilophytes and gymnosperms were included in this study. While the regulation of *PID* expression has been demonstrated to be important for the establishment of the radial style (Kuhn et al., 2020; Moubayidin and Østergaard, 2014; Simonini et al., 2016), *PID* regulation by the ETT/ARF4-like orthologues is not the causal factor for style complementation (Fig. 4.2). The redundancy of ETT and ARF4 in leaf development also implies that ETT and ARF4 share greater functional overlap in the context of leaf polarity, possibly through common target genes or protein interactors.

Thus, to understand the mechanistic basis of ETT and ARF4's common and divergent functions in the ancestral leaf network and the derived carpel network, an unbiased transcriptome-wide approach through RNAseq experiments of lines exhibiting full, partial, or no complementation of the style and leaf should be considered to elucidate the causal factor or factors. Additionally, direct targets of ETT and ARF4 can be elucidated through chromatin immunoprecipitation (ChIP) or Cut&Tag-based methods (Gade and Kalvakolanu, 2012; Kaya-Okur et al., 2020). A Cut&Tag experiment to distinguish the shared and unique targets of ETT and ARF4, in both leaves and gynoecia, was planned but like the Turbo-ID lines planned in Chapter 3, this was unable to be completed within the time constraints of the study. However, this approach should be prioritised in future studies to elucidate the mechanism behind ETT and ARF4's genetic redundancy.

As seen with the transcription factor LFY (Maizel et al., 2005), evolutionary shifts in DNA binding affinity can influence protein function for novel developmental roles. While Class A and Class B ARFs have similar DNA binding domains and preferences (Boer et al., 2014; Galli et al., 2018; Mutte et al., 2018), it cannot fully be discounted that DNA binding affinity or specificity differ between ETT/ARF4-like

orthologues, which is supported by the rescue of the valve growth in the *pETT:DS7 ett-3* line (Chapter 3, Fig. 4.4). As many important phylogenetic lineages are recalcitrant to functional genetics due to material rarity, long generation times and/or lack of transformation techniques, ChIP or Cut&Tag in the native system is not feasible. However, DNA affinity purification sequencing (DAP-seq) is a potential method to overcome this barrier as it works with *in vitro*-expressed transcription factors and purified genomic DNA (Bartlett et al., 2017; Galli et al., 2018). While DAP-seq experiments were attempted in this study, I was unable to optimise the protocol within the time constraints. Given the time and budget, this method merits a revisit to investigate shifts in targets throughout the ETT/ARF4-like clade.

Finally, while the heterologous complementation of *A. thaliana* null mutants provides information regarding the conservation and origin of ETT and ARF4 function in angiosperm leaf and flower development, it is uninformative on the roles of the orthologues in the context of their native species. For example, the *C. richardii* ETT/ARF4-like, or the *N. thermarum* ETT orthologues could be necessary for frond or carpel development respectively in those species. It is also possible that the *G. biloba* ETT/ARF4-like orthologue plays a role in reproductive development in cones but lack the necessary functions to complement carpels. Therefore, it is important to focus attention on novel model systems that represent important land plant clades to discern the evolutionary origins of transcription factor function, especially with the recent development of transformation pipelines in formerly recalcitrant species (Bui et al., 2015; Dupré et al., 2000; Han et al., 2023; Plackett et al., 2015; Yu et al., 2018) .

4.5 Materials and Methods

4.5.1 CRISPR/Cas9-mediated gene editing

The *arf4^{GE}* line was generated using CRISPR/Cas9-mediated gene editing as described in Castel et al. (2019). The genomic sequence of the *A. thaliana* *ARF4*

was inputted into the online CHOPCHOP tool (Labun et al., 2019) to identify CRISPR/Cas9 target sites with little to no off-targets. Four single guide RNA (sgRNA) were selected, and guide sequences were designed to contain 20 nucleotides prior to the 3' Protospacer Adjacent Motif (PAM). The forward primers for sgRNA guides contain a Golden Gate cloning site, while the reverse primer shared homology with the gRNA template plasmid (AddGene #46966). All primers used are listed in Table S4.1.

Golden Gate cloning was conducted as described by Engler and Marillonnet (2014). All vectors were obtained from TSL Synbio (<http://synbio.tsl.ac.uk>). For the digestion and ligation of Level 0 reactions, 15 µl final mix (100 ng L0 backbone plasmid, 100 ng insert fragment, 1.5 µl 10 x Bovine Serum Albumin (BSA, 1 mg/ml), 1.5 µl 10 x T4 Ligase Buffer (New England Biolabs), 1 µl Bpil (New England Biolabs), 1 µl T4 DNA ligase (New England Biolabs), water) was incubated for 25 cycles of 3 min at 37 °C and 4 min at 16°C, followed by 5 min at 50°C. The Level 1 reaction mix and cycling conditions were similar to the Level 0 but using 1 µl Bsal (New England Biolabs) instead of Bpil. The Level 2 mix and cycling conditions were identical to the Level 0 mix but incorporated 100 ng of the L2 binary vector and 100 ng of each L1 plasmid.

Ligated products were transformed into *E. coli* Stellar™ Competent Cells (Takara Bio) and selected on LB plates as follows: Level 0 – spectinomycin (50 µg/ml), X-Gal (5-bromo-4-chloro-3-indolyl-beta-D-galacto-pyranoside, 40 µg/ml) and IPTG (Isopropyl β- d-1-thiogalactopyranoside, 0.5 mM), Level 1 – carbenicillin (100 µg/ml), X-Gal (40 µg/ml) and IPTG (0.5 mM), Level 2 – kanamycin (50 µg/ml). Positive colonies were confirmed through colony PCR and Sanger sequencing (Macrogen Europe).

The Level 2 construct was introduced into *Agrobacterium tumefaciens* GV3101 containing the pSoup plasmid (rifampicin and gentamycin resistance) and selected on LB plates containing rifampicin (100 µg/ml), gentamycin (10 µg/ml) and kanamycin (50 µg/ml). Positive *A. tumefaciens* colonies were cultured overnight and used to

transform *A. thaliana* plants through the floral dip method (Clough and Bent, 1998). Transformed plants were selected on MS plates containing phosphinothricin (PPT/BASTA; 15 µg/ml) and survivors were transplanted into soil after 10 days. Plants were genotyped in the T1 and T2 generations for the presence of genomic deletions.

4.5.2 Generation of ETT/ARF4 complementation lines

All lines were generated in the *ett-3* background. The 5 kb *A. thaliana* ETT promoter and 5' UTR (Simonini et al., 2016) was used to drive the expression of ETT/ARF4-like orthologues from the species chosen in Chapter 3. The promoter and ARF coding sequence were inserted into the pCambia1305 vector (obtained from Yuli Ding, John Innes Centre) carrying kanamycin resistance through In-Fusion cloning (Takara Bio) according to the manufacturer's instructions. The list of primers used can be found in Table S4.1. As described for the *arf4^{GE}* line, validated constructs were inserted into *A. tumefaciens* GV3101 cells for the transformation of *A. thaliana* plants.

The *ett-3 arf4^{GE}* double mutant was generated through the cross-pollination of *ett-3* and *arf4^{GE}* plants as described by Weigel and Glazebrook (2006). The *ett-3 arf4^{GE}* line is maintained as the *ett-3 (-/-) arf4^{GE}(+/-)* sesquimutant due to the sterility of *ett-3 (-/-) arf4^{GE}(-/-)* plants. To assess leaf phenotypes, the *ett-3* complementation lines were crossed with the *ett-3 (-/-) arf4^{GE}(+/-)* line and the presence of ETT/ARF4 transgenes and the null *arf4^{GE}* allele were confirmed through genotyping in the F1 and F2 generations.

4.5.3 Genotyping of transgenic plants

A paper-based nucleic acid extraction protocol was employed for the genotyping of plant lines. Young leaves were collected and imprinted onto FTA™ PlantSaver (Whatman) cards. Small paper discs containing sample DNA were punched out and transferred into PCR plates. The discs were incubated with 50 µl of FTA buffer (10 mM Tris-HCL (pH 7.5), 2 mM EDTA (pH 8.0)) for at least 1 hour. After incubation, the

FTA buffer was removed completely and 180 µl of TE⁻¹ buffer (10 mM Tris-Cl (pH 8.0), 0.1 mM EDTA (pH 8.0)) was added to each well to wash the discs. After removing the TE⁻¹ buffer, 10 µl of PCR master mix (1 µl 10X DreamTaq™ Buffer (Thermo Scientific), 0.2 µl dNTP mix, 0.2 µl forward primer (10 µM), 0.2 µl reverse primer (10 µM), 0.05 µl DreamTaq polymerase (Thermo Scientific), and 8.35 µl water) was added to each well. Genotyping PCRs were carried out using the following programme: 95 °C for 3 min followed by 30 cycles at 95 °C for 30 s, 56 °C for 30 s and 72 °C for 1 min per kilobase of PCR product, with a final extension step of 3 min at 72 °C. The PCR products were visualised by gel electrophoresis on a 1 % agarose gel.

4.5.4 Quantitative real-time PCR

RNA extraction and cDNA synthesis for qPCR analyses were conducted as described in Chapter 3. All qPCR primers (Table S4.1) were tested for their amplification efficiency using a cDNA dilution series (1/4 to 1/65536), and their specificity through analyses of the melting curves (65 °C to 95 °C). The qPCRs were set up in 96-well white plates with a final reaction volume of 10 µl (5 µl 2 x qPCRBIO SyGreen Blue Mix (PCR Biosystems), 0.4 µl forward primer (10 µM), 0.4 µl reverse primer (10 µM), 1 µl 1:5 diluted cDNA, 3.2 µl water). The reactions were conducted in CFX96 thermal cyclers (Bio-Rad) using the following programme: 95 °C for 2 min followed by 40 cycles at 95°C for 10 s, 60 °C for 10 s and 72 °C for 30 s. The relative expression value of the reactions were analysed using the 2^{-ΔCT} method (Livak and Schmittgen, 2001). The expression level of the *POLYUBIQUITIN 10 (UBQ10/AT4G05320)* gene was used for data normalisation. Data visualisation was conducted using RStudio 1.1.463 as described in Chapter 3, and statistical analyses of expression levels were conducted a one-way ANOVA with post-hoc Tukey multiple comparison test.

4.5.5 Scanning Electron Microscopy

Inflorescences were collected in vials and fixed in FAA solution (3.7 % formaldehyde, 3 % acetic acid and 50 % ethanol) at room temperature overnight. After the removal of the fixative, 70 % ethanol was added to the vials and left to incubate overnight. A dehydration series consisting of 90 % ethanol for 1 hour, 100 % ethanol for 1 hour and two washes of 100 % dry ethanol for 30 min each was used to prepare the samples prior to critical point drying using the Leica CPD300. The dried gynoecia were dissected and mounted on stubs for gold coating using an Agar high resolution sputter coater. The Zeiss Supra 55VP Field Emission Scanning Electron Microscope (3kV acceleration voltage) was used to image the samples.

4.5.6 Phenotyping of complementation lines

The maximum style width to style height ratio was measured and calculated from SEM images of gynoecia using the ImageJ software. Fully elongated but unripe siliques were collected, lined on a piece of paper, and measured for silique lengths. Leaf measurements for *ett-3 arf4^{GE}* complementation lines were taken just as the plants were beginning to bolt. The 7th to 9th leaves were collected and placed on a piece of paper to be photographed with a ruler for scale. The same leaves were then flattened on masking tape and photographed again. ImageJ was used to measure the length and width of the leaves before and after flattening. The relative medio-lateral and proximal-distal curvature was then calculated as a ratio of the apparent unflattened width/length to the actual flattened width/length.

Chapter 5:

General discussion

5.1 Introduction

A long-standing question in developmental biology is how multicellular body plans are elaborated from a single progenitor cell. Through decades of research in plant and animal model systems, the morphogen concept has been devised to explain the patterning of higher order structures (Bhalerao and Bennett, 2003; Driever and Nüsslein-Volhard, 1988; Heisler et al., 2005; Nellen et al., 1996). The best known example of a plant morphogen is the phytohormone auxin, which regulates almost every aspect of plant growth and development (Vanneste and Friml, 2009). The morphogenetic property of auxin is highlighted by its ability to trigger differential transcriptional responses in a concentration and cell-type dependent manner (Guan et al., 2017; Reinhardt et al., 2003; Sabatini et al., 1999). Nonetheless, it remains poorly understood how the diversity and specificity of auxin responses are generated.

As discussed in Chapter 1, the canonical TIR1/AFB-dependent pathway, and the diversification of its individual components in land plant evolution, accounts for the majority of auxin responses seen in angiosperm models (Calderón Villalobos et al., 2012; Leyser, 2017; Mutte et al., 2018; Prigge et al., 2020). Despite this, the presence of rapid non-transcriptional auxin responses, including in lineages lacking the canonical pathway, implies that the canonical pathway is neither the only auxin signalling pathway in plants, nor the most ancient. Instead, recent works on alternative signalling pathways have uncovered a deeply conserved mechanism involving the controversial ABP1 protein and transmembrane kinases that predates canonical auxin signalling (Cao et al., 2019; Friml et al., 2022; Kuhn et al., 2024; Xu et al., 2014).

In contrast to both TIR1/AFB- and ABP1-mediated pathways, a relatively young auxin signalling pathway involving the atypical ARF ETT has previously been described by our lab (Simonini et al., 2016). The ETT clade is specific to the

angiosperms and is indispensable for proper gynoecium patterning in *A. thaliana* (Finet et al., 2010; Nemhauser et al., 2000; Sessions et al., 1997b). It was shown that ETT directly binds auxin which alters its protein-protein interactions and downstream target gene regulation (Kuhn et al., 2020; Simonini et al., 2017; Simonini et al., 2016). Nonetheless, it is unknown whether auxin sensing evolved prior to or after the divergence of ETT and its paralogue ARF4 from the ancestral ETT/ARF4-like clade. Furthermore, the different degrees of genetic redundancy between ETT and ARF4 during leaf and gynoecium development implies that ETT has neofunctionalised, likely through the gain of this novel auxin signalling pathway, for its gynoecium patterning roles (Guan et al., 2017; Pekker et al., 2005). Therefore, the aim of this thesis was to elucidate the origins and mechanism of the ETT-mediated auxin signalling pathway and its implications for the evolutionary development of leaves and carpels.

5.2 The ETT/ARF4-like clade is conserved within the euphyllophytes

Conflicting data places the origin of the ancestral ETT/ARF4-like clade at either the base of the euphyllophytes, or at the base of the seed plants (Finet et al., 2013; Mutte et al., 2018; Sun and Li, 2020; Xia et al., 2017). Resolving this conundrum is important for accurate inferences on the origin of ETT and ARF4's role in the leaf polarity and medio-lateral growth network. In Chapter 2, our collaborative work with the Weijers Lab (Wageningen University and Research) set out to achieve this through the construction of a Class B ARF phylogeny with greater sampling of genomes from the bryophytes, monilophytes, gymnosperms, magnoliids and monocots to ameliorate past sampling limitations and biases.

Our phylogeny provides unequivocal support for the presence of ETT/ARF4-like orthologues in monilophytes, indicating that the ETT/ARF4-like clade is a euphyllophyte innovation. The alignment of monilophyte orthologues however reveal a structural divergence from the angiosperm or gymnosperm ETT/ARF4-like

sequences. The post-transcriptional regulation of the ARF2 and ETT/ARF4 clades by small RNAs called tasiARFs is widely conserved in the seed plants and have important roles in maintaining their abaxial localisation for proper leaf development (Douglas et al., 2010; Marin et al., 2010; Xia et al., 2017; Yifhar et al., 2012). Our data indicates that the tasiARF binding site is present only as a single copy instead of the tandem repeats found in seed plant ETT/ARF4-like orthologues and does not contain the conserved seed plant sequence. This implies that monilophyte ETT/ARF-like orthologues do not undergo tasiARF regulation, supporting the conclusion of Sun and Li (2020).

Furthermore, I showed in Chapter 4 that the ETT/ARF4-like orthologue of the monilophyte *C. richardii* was unable to complement the adaxialised leaves of the *ett-3 arf4^{GE}* double mutant, indicating significant functional divergence from angiosperm orthologues. As the *G. biloba* orthologue provided partial complementation, this finding supports the non-homology of fern fronds and seed plant leaves as surmised from the fossil record (Tomescu, 2009), despite the fact that multiple seed plant polarity factors share conserved expression patterns in the monilophytes (Harrison et al., 2005; Vasco et al., 2016; Zumajo-Cardona et al., 2019).

The native role of the ETT/ARF4-like clade in monilophytes therefore remains unresolved by the results of this thesis. Nonetheless, monilophyte ETT/ARF4-like orthologues do interact with the TPL/TPR family (Chapter 3) suggesting that they behave similarly as other Class B ARFs as transcriptional repressors. With the recent releases of well-annotated fern genomes, the optimisation of DAP-seq for ARFs and the development of *C. richardii* as a genetically amendable model system (Bui et al., 2015; Galli et al., 2018; Li et al., 2018; Marchant et al., 2022; Marchant et al., 2019), future work should consider the endogenous target genes and protein-protein interactions of monilophyte ETT/ARF4-like orthologues and their role in frond development to gain a better understanding of how leaf-like organs evolved.

5.3 ETT and ARF4 have undergone divergent evolutionary trajectories

ETT and ARF4 clades originated at the base of the angiosperms following the genome duplication event that preceded angiosperm radiation (Finet et al., 2013; Finet et al., 2010; Mutte et al., 2018). Our phylogeny from Chapter 2 provides further support for this scenario through the detection of ETT and ARF4 orthologues in the *N. thermarum* genome (Povilus et al., 2020). ETT orthologues of the ANA grade angiosperms retain the PB1 domain missing from eudicot sequences, while their ARF4 orthologues have truncated PB1 domains through alternative splicing or premature translational termination (Finet et al., 2010). The loss of the PB1 domain in the *N. thermarum* ARF4 suggests that PB1 truncation is conserved within the Nymphaeales, but its functional relevance is unclear. While it was shown that the PB1 domain interfered with ETT's role in gynoecium patterning (Finet et al., 2010), the *A. trichopoda* ETT containing a functional PB1 domain (Chapter 3) could rescue both valve growth and style development in the *ett-3* background. In contrast, the *N. thermarum* orthologue only provided partial rescue (Chapter 4). This suggests that the PB1 domain does not affect ETT's function in style development, which depends on other regions that differ between the *A. trichopoda* and *N. thermarum* orthologues. While this difference appears to correlate with auxin sensitivity, further domain swaps between the ETT orthologues of both ANA grade species will be needed to strengthen the hypothesis.

As the PB1 domain appears irrelevant to ETT's role in the gynoecium, it is puzzling as to why it has been lost multiple times throughout angiosperm evolution (Finet et al., 2013). Our alignments revealed that independent losses of the PB1 domain are more common than previously thought, as multiple monocot and magnoliid genomes reveal a seemingly stochastic pattern of loss between and within angiosperm orders. It is possible that the PB1 domain has no biological relevance for ETT function and thus the patterns of loss and retainment in the angiosperms

reflect stochastic processes, but proteomic assays such as Turbo-ID or IP-MS in genetically amenable species expressing full and truncated ETT forms should be conducted to validate this.

In a similar vein, the ARF4 orthologue itself has been lost twice in angiosperm evolutionary history, once in the last monocot ancestor and another in the ancestor of the Laurales. The ETT clade however has expanded greatly in the commelinid monocots. It is interesting to note that loss of ARF4 itself does not confer any obvious phenotype in *A. thaliana* (Pekker et al., 2005), although subtle physiological and developmental effects do exist in tomato (Chen et al., 2021; Sagar et al., 2013). Meanwhile, ETT paralogues in grasses appear to have sub- or neo-functionalised further for the development of specific floral whorls (Khanday et al., 2013; Si et al., 2022; Toriba and Hirano, 2014). Therefore, it appears that the evolution of the ETT and ARF4 clades is highly dynamic and differential patterns of losses occur easily perhaps due to significant functional redundancies between paralogues in certain lineages, while expansions in the ETT clade could bring about further morphological specialisations. Like the monilophyte orthologues, this hypothesis needs to be tested through thorough investigations of ETT and ARF4 function from divergent angiosperm lineages in both native and heterologous systems. While *ett-3* complementation lines of the four rice orthologues as well as rice and tomato CRISPR lines were generated, they were not ready for phenotypic analysis within the timeframe of this thesis. Nevertheless, further work should continue on analysing these lines to understand the changes in ETT and ARF4 function within the angiosperms.

The ETT-specific (ES) domain of ETT was termed so due to its lack of similarities to other ARF domains (Simonini et al., 2016; Simonini et al., 2018a). However, the results of our machine learning-based motif analyses indicate that the ES domain is an ARF MR domain that shares multiple conserved motifs with ARF4, including the

NLS, tasiARF sites, EAR-like domain and auxin-interacting W505 residue.

Nevertheless, clade-enriched variants of these motifs do exist and were sufficient to delineate ETT and ARF4 independently of PB1 absence/presence. The functional significance of these variants however remains unexplored within the scope of this thesis. As seen in Chapters 3 and 4, ETT and ARF4 differ in their auxin sensing property and *in planta* developmental roles. Therefore, to understand the structural and biochemical basis of the ETT-mediated pathway, a multifaceted approach involving motif swaps, predictive modelling and *in planta* complementation between ETT and ARF4 should be conducted to understand the mechanism behind ETT's neofunctionalisation.

5.4 Auxin sensing is a neofunctionalisation of the ETT clade

Due to the lack of the PB1 domain and its characterised role as a transcriptional repressor (Tiwari et al., 2003; Ulmasov et al., 1999a), ETT does not participate in the canonical auxin signalling pathway. However, our lab has previously identified an alternative auxin signalling pathway mediated by ETT that involves a direct auxin-induced switch in ETT's transcriptional regulation of target genes and its protein-protein interactions (Kuhn et al., 2020; Simonini et al., 2017; Simonini et al., 2016). Y2H and NMR-based assays implicate multiple ES domain motifs or amino acid residues that might play a role in mediating the perception of auxin, including a serine-rich region, two non-conserved cysteines and most convincingly the W505 tryptophan residue. The data in Chapter 2 revealed that the W505 is also present in most ARF4 orthologues but is flanked by an LGA motif. The presence of a motif however does not indicate functionality, as allosteric inhibition of interaction or function by other protein regions is possible. This is observed in the *M. polymorpha* Class A ARF orthologue which does not interact with TPL unlike its Class B and Class C ARFs despite the presence of the EAR-like domain in all three ARFs (Kato

et al., 2020). Therefore, it is unknown whether auxin sensing is specific only to ETT or also present in ARF4.

The Y2H data in Chapter 3 demonstrates that auxin sensing is specific to ETT and likely evolved in the last common ancestor of the angiosperms, as both *A. trichopoda* and *A. thaliana* ETT orthologues exhibited auxin sensitivity in their interaction with the TPL/TPR corepressors. Moreover, the lack of auxin-sensitivity in ETT/ARF4-like orthologues from the gymnosperms and monilophytes suggest that auxin sensing was gained by the ETT clade after its divergence from ARF4, rather than its loss in ARF4 from an ancestral auxin-sensitive state in the ETT/ARF4-like clade. Contrary to the canonical auxin signalling pathway, which is deeply conserved and functional in all land plant lineages (Kato et al., 2020; Prigge et al., 2010), the ETT-mediated pathway does not appear to be present in all angiosperms as the *N. thermarum* and *A. fimbriata* ETT orthologues were auxin-insensitive in their TPL/TPR interactions. Considering the uncomplemented medial outgrowths by the heterologous expression of the *N. thermarum* ETT (Chapter 4), the ETT-mediated pathway might be specialised for style development and may have been lost in species that do not develop distinctive styles.

Unfortunately, a major limitation of this study is the lack of alternative methodology to assess the auxin sensitivity of ETT orthologues in an unbiased manner. The TPL/TPR, KAN and YAB families were picked based on previously established results from our lab and others, or the similarities between the *ett-3* and *ett-3 arf4^{GE}* mutants to those defective in the adaxial-abaxial polarity network. While Co-IP and FRET-FLIM assays were trialled to validate the Y2H data in a quantitative manner, protein expression levels were too variable and oftentimes resulted in poor signal detection even for the positive ETT-TPL control. Further optimisations of these techniques should therefore be followed up on to address this limitation.

Additionally, Turbo-ID experiments should be planned to identify the local ETT and

ARF4 interactome that is directly altered by auxin in both leaves and gynoecia, as this will provide more insight into the mechanism of ETT function in both contexts.

5.5 The ETT DBD and MR contributes to its auxin sensitivity

It was previously shown that the ES/MR domain of ETT was sufficient for its auxin-dependent interactions with IND and TPL (Kuhn et al., 2020; Simonini et al., 2016; Simonini et al., 2018a). The Y2H domain swap experiments in Chapter 3 confirm this as the DS1, DS7 and DS9 constructs containing the *A. thaliana* ETT DBD and the partial or full *G. biloba* ETT/ARF4-like MR do not exhibit auxin sensitivity whereas the DS2, DS8 and DS10 constructs with the *A. trichopoda* ETT MR do. The results also show that the second half of the MR, MR2, exhibits a strong link with auxin sensing. This region contains the W505 residue and other putative residues that may influence auxin binding (Kuhn et al., 2020; Simonini et al., 2018a). However, it is still vital to conduct additional fine-scale domain swaps or direct mutagenesis of these motifs and analyse their effects on ETT's auxin-sensitive interactions to prove their direct involvement in auxin sensing.

The domain swap data however also revealed the contributions of regions beyond the ES to the auxin sensing property of ETT. The DS3 and DS4 constructs containing the *G. biloba* ETT/ARF4-like DBD were insensitive to auxin despite the presence of the *A. thaliana* and *A. trichopoda* ETT MR. Interestingly, the *ett-3* complementation line expressing the DS7 construct (*A. thaliana* ETT DBD and *G. biloba* ETT/ARF4-like MR + PB1) phenocopied ARF4 complementation lines, with restored valve growth but uncomplemented medial outgrowths (Chapter 4). This phenotype is less severe than the *pETT:GbiARF3/4 ett-3* line, indicating that differences in the DBD contribute to ETT's function in gynoecium patterning.

While ARF DBDs exhibit high similarities in both protein structure and binding preferences (Boer et al., 2014; Galli et al., 2018; Kato et al., 2020), it is possible that differences in the DBD, and therefore DNA-binding affinity or specificity, of the

angiosperm and non-angiosperm orthologues may affect their functional complementation of gynoecium and/or leaf patterning. Nonetheless, it is important to note that the region defined as the DBD in this study also encompasses the dimerisation domains, the Tudor-like ancillary domain and potentially other cryptic domains that are yet to be described. A recent unpublished result from our lab uncovered the presence of a conserved TPL/TPR-interacting motif in the N-terminus end of the ETT/ARF4-like orthologues (B. Natarajan, unpublished). Therefore, further studies should separate the DBD from these adjacent domains and investigate their biochemical properties *in vitro* and *in vivo* through DNA-binding assays such as ChIP-seq, DAP-seq, or Cut&Tag and the phenotypic assessment of mutagenised domains in heterologous complementation lines.

These results highlight the complex structural basis of ETT-mediated auxin sensing relative to the TIR1/AFB receptors. The auxin binding mechanism of TIR1 was resolved through the availability of high-resolution crystal structures in complex with auxin and an AUX/IAA coreceptor (Tan et al., 2007). In contrast, the full-length ETT protein is poorly soluble and is difficult to express in bacterial systems (Simonini et al., 2018a). Furthermore, the ES domain is intrinsically disordered which hampers the crystallisation process and *in silico* predictions through AlphaFold (Jumper et al., 2021). Nonetheless, the influence of domains beyond the ES domain implicates the existence of cross-domain interactions for auxin binding and the regulation of ETT's transcriptional activity. This suggestion is supported by recent results in our laboratory (B. Natarajan, unpublished). Thus, future work should be carried out on unravelling the ETT structure, perhaps in a stabilised form with TPL, auxin and other transcription factors.

5.6 ETT-mediated auxin signalling is an innovation for style development

While originally described for its roles in gynoecium development (Sessions et al., 1997b), ETT and also its close paralogue ARF4 controls the patterning of virtually every lateral organ, including leaves, integuments, axillary branches, and lateral roots (Kelley et al., 2012; Marin et al., 2010; Pekker et al., 2005; Simonini et al., 2016). Interestingly, ARF4 and ETT appears to be fully redundant in all developmental contexts except for the gynoecium, which exhibits decreased valve elongation and seed yield, as well as an overproliferation of stigmatic and medial tissue in *ett* loss-of-function mutants. These phenotypes imply that ETT and ARF4 have overlapping biological activities in other lateral organs but not the gynoecium. As the gynoecium is a late morphological innovation that only arose in the angiosperms (Becker, 2020), this led to the hypothesis that the ETT/ARF4-like clade had an ancestral function in vegetative development that was retained in both ETT and ARF4 clades after their divergence in the angiosperms. Following the radiation of angiosperms, ETT acquired a novel auxin sensing function (Chapter 3) that may explain its specialised ability in gynoecium patterning.

The genetic complementation lines in Chapter 4 demonstrate that all angiosperm ETT, with the exception of the *N. thermarum* orthologue, fully rescue the *ett-3* gynoecium defects. In line with the hypothesis, neither ARF4 nor the ETT/ARF4-like orthologues of the non-angiosperm species were able to fully complement the *ett-3* phenotype. The chimeric ETT/ARF4-like constructs that were found to be auxin-sensitive in Chapter 3 also fully rescued the *ett-3* gynoecium while auxin-insensitive constructs only provided partial complementation, providing further support for this hypothesis. Moreover, all sampled ETT and ARF4 orthologues from the angiosperms complemented leaf development in the *ett-3 arf4^{GE}* background, while only the *G. biloba* ETT/ARF4-like orthologue provided partial complementation from

the non-angiosperm lineages. Taking this all into account, a possible scenario is that the ETT/ARF4-like clade developed functions in the adaxial-abaxial polarity network that regulates the development of all seed plant leaves in the last seed plant ancestor before both paralogues became co-opted for the development of the carpel. Interestingly, the lack of full complementation by the *G. biloba* ETT/ARF4-like orthologue indicates that there is a significant difference in the leaf development mechanism between *A. thaliana* and *G. biloba*. An increased sampling of gymnosperm orthologues, and ideally functional genetics in gymnosperm models, are required before this conclusion can be applied to all gymnosperms.

The full-length and domain swapped ETT/ARF4-like complementation lines also reveal that leaf development, and aspects of gynoecium morphogenesis, do not require the auxin sensing ability of ETT. The Y2H screen in Chapter 3 of the KAN and YAB families indicate that the leaf polarity factors do not interact with ETT in an auxin-dependent manner, in contradiction to the findings of Simonini et al. (2016). Although differences in yeast expression systems could explain this discrepancy, the plant phenotypes support the scenario in which the ETT-mediated auxin signalling pathway plays little to no role in leaf polarity, as all angiosperm ETT and ARF4 orthologues complemented the *ett-3 arf4^{GE}* phenotype regardless of their auxin sensitivity. Furthermore, the lines reveal the functional overlap between ETT and ARF4 in aspects of gynoecium patterning. Valve growth likely does not depend on the ETT-mediated pathway as expression of *ARF4* under the *ETT* promoter complements this phenotype. The rescue of style development however correlates strongly with the assessed auxin sensitivity of these orthologues from Chapter 3.

Therefore, a shift in both of expression pattern and protein biochemistry between ETT and ARF4 could explain their differential redundancies in leaves and gynoecia. In the developing leaf primordia (Fig. 5.1a), there might be a large overlap in the target genes regulated by ETT and ARF4 that are involved in abaxial tissue identity

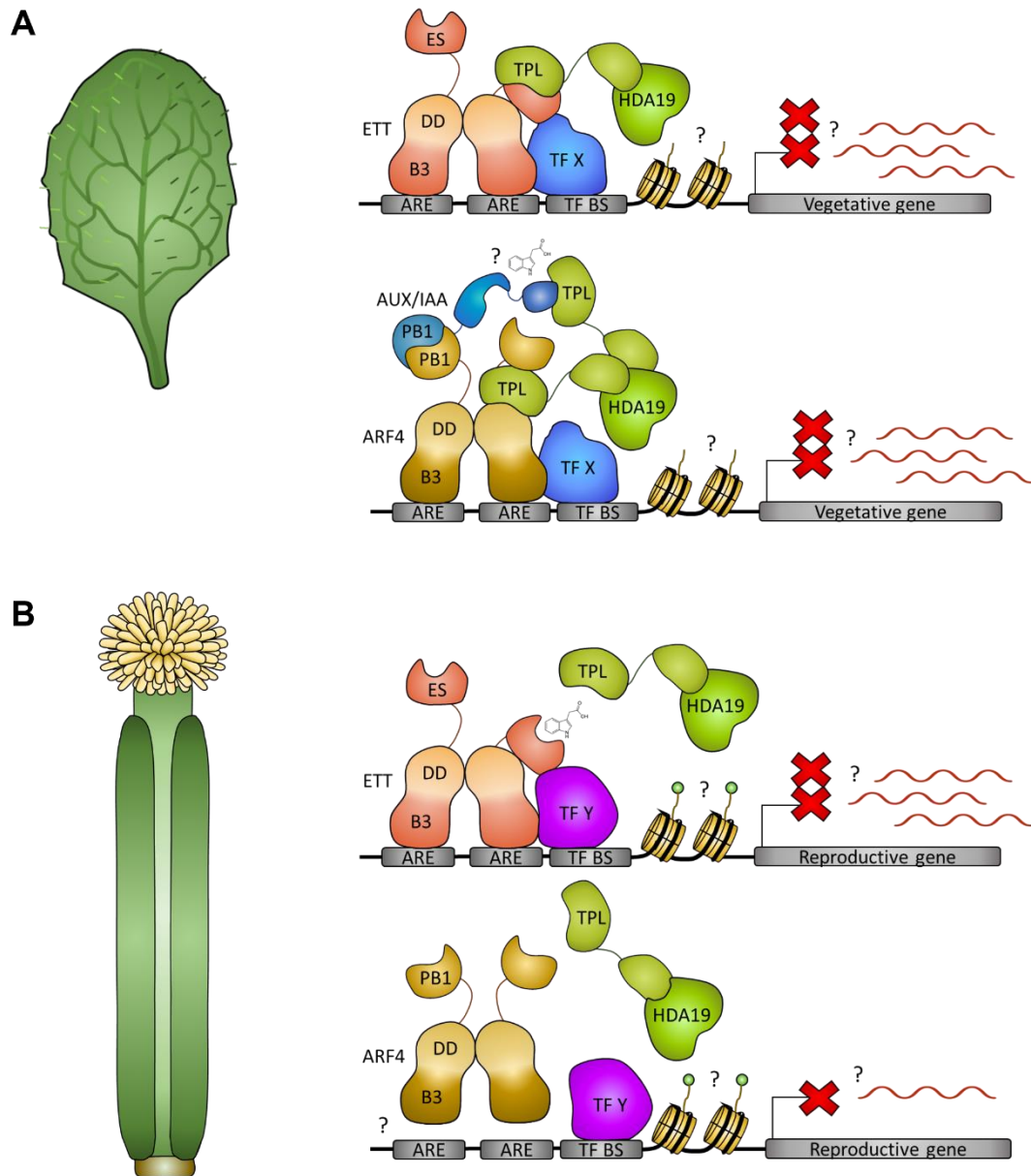


Figure 5.1: Model of the molecular mechanism of ETT and ARF4 during leaf and gynoecium development. (A) During leaf development, ETT and ARF4 bind to the promoters of similar target genes involved in abaxial polarity and medio-lateral growth and exhibit similar interaction dynamics with other transcription factors or chromatin regulators. It is unknown if this process is regulated by auxin, although it is unlikely to be mediated by the ETT-dependent pathway. **(B)** In the developing style, ARF4 is unable to bind to the promoters of a large subset of ETT-regulated genes or might not interact with crucial protein partners with the same specificity and affinity. These processes might depend on the ETT-mediated auxin signalling pathway. Therefore ARF4 cannot fully compensate for the loss of ETT.

and medio-lateral expansion such as *WOX3* and *PRS* (Vandenbussche et al., 2009; Zhang et al., 2020c). ETT and ARF4 also likely exhibit similar expression patterns and protein-protein interaction dynamics with other transcription factors within the abaxial domain of leaf primordia, allowing them to fully compensate for each other in single mutant backgrounds. A parallel scenario probably operates within the gynoecium during valve expansion, but the ARF4 expression domain might not have sufficient overlap with that of ETT resulting in the failure of the endogenous ARF4 to complement valve growth in the *ett-3* single mutant. However, during the formation of the style (Fig. 5.1b), ETT and ARF4 do not regulate downstream target genes that influence auxin redistribution and style growth such as *PID*, *HEC1* and *TEC1* to a similar degree, resulting in the failure of ARF4 to rescue the split-style and medial outgrowth phenotype of *ett-3*. This is possibly due to a divergence in binding site preferences, or protein-protein interactions that are influenced by auxin in the ETT-mediated pathway. Through an evolutionary perspective, the behaviour of ETT and ARF4 protein in leaf primordia might represent the ancestral state of the ETT/ARF4-like clade before ETT acquired its auxin sensing property to properly regulate style development genes.

While this model provides a starting point to investigate the molecular mechanisms behind the differences in ETT and ARF4's function in leaf and gynoecium development, there are still many open questions that have to be addressed to support the model. The model assumes that ETT and ARF4 exhibit greater expression pattern overlaps in leaves than in gynoecia, so fluorescent reporter lines have to be generated to prove this. The model also assumes that ETT and ARF4 share a larger subset of target genes and protein interactors in leaves than in the style, so a multiomics approach such as Cut&Tag for binding site assessment and Turbo-ID for interactome profiling is required. These assays should also be conducted at different auxin concentrations and with auxin-insensitive variants of

ETT to understand the contribution of the ETT-mediated pathway in both contexts. Lastly, these experiments should be carried out in a wide range of species with their corresponding orthologues to understand if the mechanisms are conserved within all angiosperms or if they are specific to *A. thaliana* and/or the Brassicales.

5.7 Concluding Remarks

The work that has been described in this thesis presents evidence for the two-step origin of a novel auxin signalling pathway in the angiosperms and its role in patterning the gynoecium. Through collaborative efforts, we demonstrated that the ETT/ARF4-like clade arose in the euphyllophytes. Although the ancestral function of this clade in the monilophytes is unclear, the ETT/ARF4-like clade likely acquired its role in regulating abaxial domain identity and medio-lateral growth in lateral organs after the divergence of the seed plants.

We also revealed that widespread changes in ETT and ARF4 domain structure and motif sequence have occurred after the radiation of the core angiosperms, and it is likely that some of these changes correlate with the gain of auxin sensitivity and style development function in the ETT clade. While the ES/MR domain of ETT was described as sufficient for auxin sensing (Kuhn et al., 2020; Simonini et al., 2018a), I uncovered a role for the ETT DBD in contributing to modulating the auxin sensitivity of ETT. This discovery highlights the complexity of auxin sensing by ETT and implicates the need for full-length protein analyses in structural and mechanistic studies.

Through Y2H assays of ETT/ARF4-like orthologues representing major land plant lineages, I demonstrate that ETT and ARF4's interactions with the TPL/TPR, KAN and YAB families are generally conserved. However, the KAN and YAB polarity factors do not display auxin-sensitivity in their ETT interactions, implying that the leaf polarity network does not require the ETT-mediated auxin signalling pathway.

On the other hand, auxin sensitivity of the ETT-TPL/TPR interaction in *A. trichopoda*

indicates that the pathway originated in the last common angiosperm ancestor, although this pathway has been lost in other angiosperm lineages. The auxin sensitivity of ETT/ARF4-like orthologues correlate with the phenotypic complementation of style development in *ett-3* mutants, suggesting a potential neofunctionalisation role in the angiosperms for the evolution of the carpel.

Finally, I developed a model to integrate the results of this thesis in explaining ETT and ARF4's divergent roles in lateral organ development. Potential shifts in the ancestral binding site preferences and protein-protein interactions of the ETT/ARF4-like clade after the split of the ETT and ARF4 clades could have led to the inability of ARF4 to fully compensate for the loss of ETT. It is likely that ETT acquired new regulatory targets or interactions in the gynoecium that is dependent on its novel auxin sensing role. However, a plethora of open questions remains on the universality and precise mechanisms of this model. This model should serve as a starting point for future work in addressing the parallel divergence of the two ARFs and the potential ramifications for the evolution and development of lateral organs.

Appendix

List of Abbreviations

Abbreviation	Full Name
3D	3-Dimensional
ABI	ABSCISIC ACID INSENSITIVE
ABP1/ABL	AUXIN-BINDING PROTEIN1/ABP1-LIKE
AC	Adenylate cyclase
AD	Activation domain
AG	AGAMOUS
AHK	Arabidopsis Histidine Kinase
ANA	Amborellales, Nymphaeales, Austrobaileyales
ANOVA	Analysis of variance
AREB1	ABSCISIC ACID-RESPONSIVE ELEMENT BINDING PROTEIN1
ARF	Auxin Response Factor
ARP	ASYMMETRIC LEAVES1/ROUGH SHEATH2/PHANTASTICA
ARR	Arabidopsis Response Regulator
AS1/2	ASYMMETRIC LEAVES1/2
ATS	ABERRANT TESTA SHAPE
AUX/IAA	AUXIN/INDOLE ACETIC ACID
AUX1/LAX	AUXIN1/LIKE AUXIN RESISTANT
AuxRE	Auxin Response Element
BAK1	BRI1-ASSOCIATED RECEPTOR KINASE
BD	Binding domain
BEL	BELL-LIKE
BRI1	BRASSINOSTEROID INSENSITIVE1
BZR1/2	BRASSINAZOLE-RESISTANT1/2
cAMP	Cyclic adenosine 3',5'-monophosphate
cDNA	complementary DNA
ChIP	Chromatin immunoprecipitation
CK	Cytokinin
CMM	Carpel margin meristem
COI1	CORONATINE INSENSITIVE1
Col-0	<i>Arabidopsis thaliana</i> Columbia ecotype
CoIP	Co-immunoprecipitation
CRC	CRABSCLAW
CTAB	Cetyltrimethylammonium bromide

CTR1	CONSTITUTIVE TRIPLE RESPONSE1
D14	DWARF14
DAP-seq	DNA Affinity Purification Sequencing
DBD	DNA-binding domain
DI/II/III/IV	Domain I/II/III/IV
DNA	Deoxyribonucleic acid
dNTP	deoxynucleotide triphosphate
EAR	ERF-associated amphiphilic repression
EBF1/2	EIN3-BINDING F-BOX PROTEIN1/2
EDTA	Ethylenediaminetetraacetic acid
EIN2/3/4	ETHYLENE INSENSITIVE2/3/4
ERS	ETHYLENE RESPONSE SENSOR
ES	ETTIN-specific
ETR	ETHYLENE RECEPTOR 1
ETT	ETTIN
FAA	Formaldehyde Alcohol Acetic Acid
FIL	FILAMENTOUS FLOWER
FRET-FLIM	Förster resonance energy transfer and fluorescence lifetime imaging microscopy
GAL4	Galectin 4
GID1	GIBBERELLIN INSENSITIVE DWARF1
H ⁺ ATPase	Proton ATPase
H3K27	Lysine 27 on histone H3
hb	hunchback
HD-ZIP III	Class III homeodomain-leucine zipper
HEC1	HECATE1
IAA	Indole-3-acetic acid
IND	INDEHISCENT
INO	INNER NO OUTER
IPA	Indole-3-pyruvic acid
IPTG	Isopropyl β-D-Thiogalactopyranoside
JAZ	JASMONATE-ZIM-DOMAIN PROTEIN
KAN	KANADI
KNOX	KNOTTED-like homeobox
KNU	KNUCKLES
LB	Lysogeny broth

LFY	LEAFY
LOB	LATERAL ORGAN BOUNDARIES
LRR	Leucine-rich repeat
MAKR2	MEMBRANE-ASSOCIATED KINASE REGULATOR2
MAPK	MITOGEN-ACTIVATED PROTEIN KINASE
miR160/165/166/ 390	microRNA160/165/166/390
MKK	MITOGEN-ACTIVATED PROTEIN KINASE KINASE
MP	MONOPTEROS
MR	Middle region
MS	Murashige and Skoog medium
NLS	Nuclear localisation signal
NMR	Nuclear Magnetic Resonance
NPR1/3/4	NONEXPRESSOR OF PATHOGENESIS-RELATED GENES1/3/4
∅	Empty vector
oneKP	1000 Plants initiative
otd	Orthodenticle
PAM	Protospacer Adjacent Motif
PB1	Phox/Bem1
PCR	Polymerase chain reaction
PHB	PHABULOSA
PHV	PHAVOLUTA
pI	Isoelectric point
PID	PINOID
PIN	PIN-FORMED
PLT5	PLETHORA5
PP2A/C	Protein phosphatase 2A/C
PPT	Phosphinothricin
PYR	PYRABACTIN RESISTANCE
RAF	Rapidly Accelerated Fibrosarcoma
REV	REVOLUTA
RNA	Ribonucleic acid
RNASeq	RNA Sequencing
ROP	Rho-type GTPases
SAUR19	SMALL AUXIN UP RNA19
SCF	Skp, Cullin, F-box containing complex

SEM	Scanning electron microscopy
sgRNA	Single guide RNA
SMXL	SUPPRESSOR OF MAX2-LIKE
SnRK	Snf1-Related protein Kinase
SPT	SPATULA
TAA1/TAR	TRYPTOPHAN AMINOTRANSFERASE OF ARABIDOPSIS1/TRYPTOPHAN AMINOTRANSFERASE RELATED
TAS3	TRANS-ACTING SIRNA3
tasiARF	Trans-acting ARF-targeting small interfering RNA
TCF	T-Cell Factor
TCP18	TEOSINTE BRANCHED1/CYCLOIDEA/PROLIFERATING CELL FACTOR18
TEC1	TARGET UNDER ETTIN CONTROL1
TGA	TGACG-binding
TIR1/AFB	TRANSPORT INHIBITOR RESPONSE1/AUXIN-SIGNALING F-BOX
TMK	TRANSMEMBRANE KINASE
TPL/TPR	TOPLESS/TOPLESS RELATED
TRN2	TORNADO2
W505	Tryptophan at position 505
WGD	Whole genome duplication
Wnt	Wingless/Int-1
WOX1/PRS	WUSCHEL-RELATED HOMEBOX1/PRESSED FLOWER
WUS	WUSCHEL
X-Gal	5-bromo-4-chloro-3-indolyl-beta-D-galacto-pyranoside
Y2H	Yeast-2-Hybrid
YAB	YABBY
YSD	Yeast Soytone Dextrose
YUC	YUCCA

Supplementary data from Chapter 2

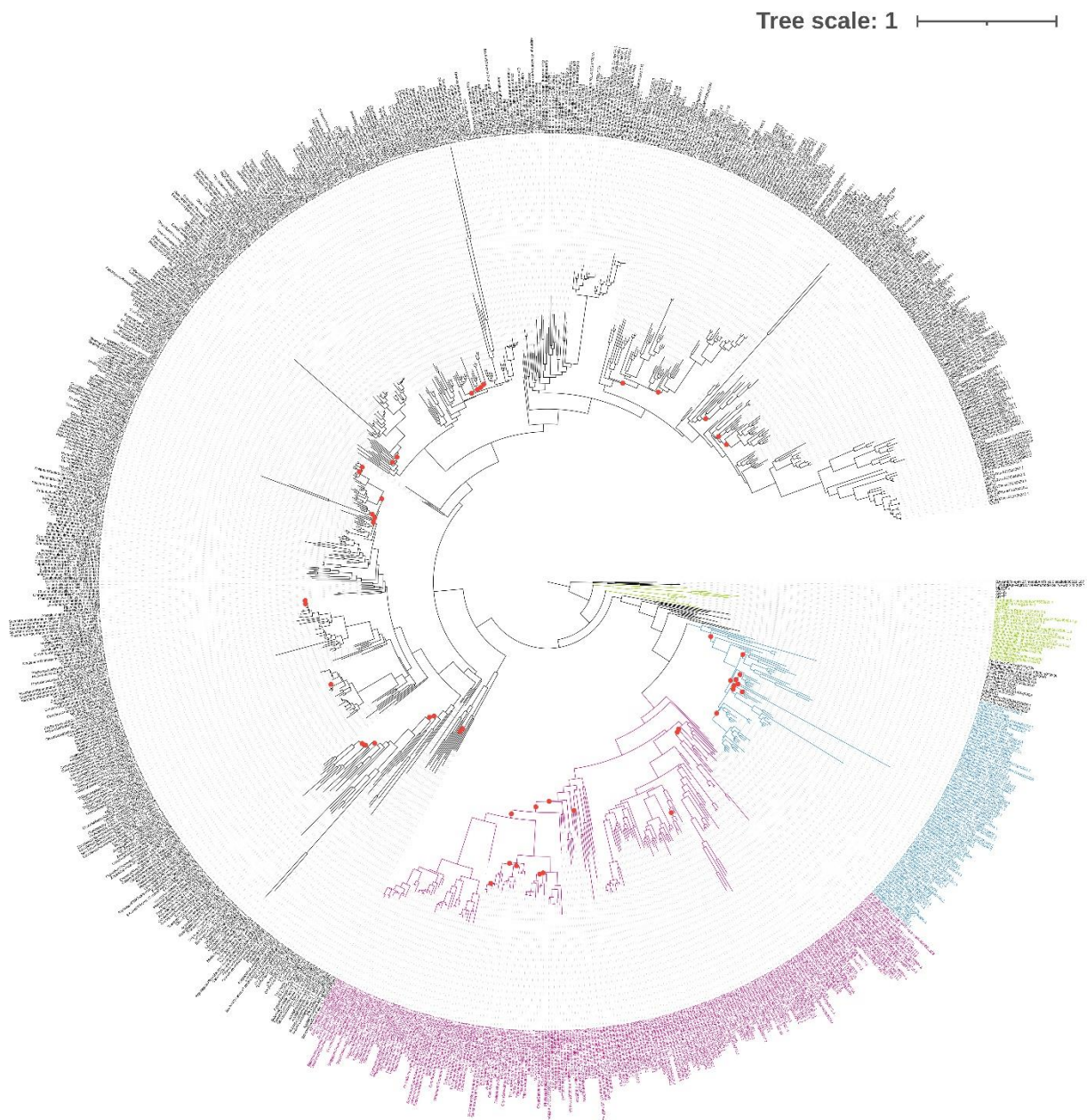


Figure S2.1: Full Class B ARF phylogeny of land plants. The colour-coded segment on the lower right is identical to Fig. 1.1. The ARF2 and ARF1/rest clades are represented by the black segment on the upper left side.

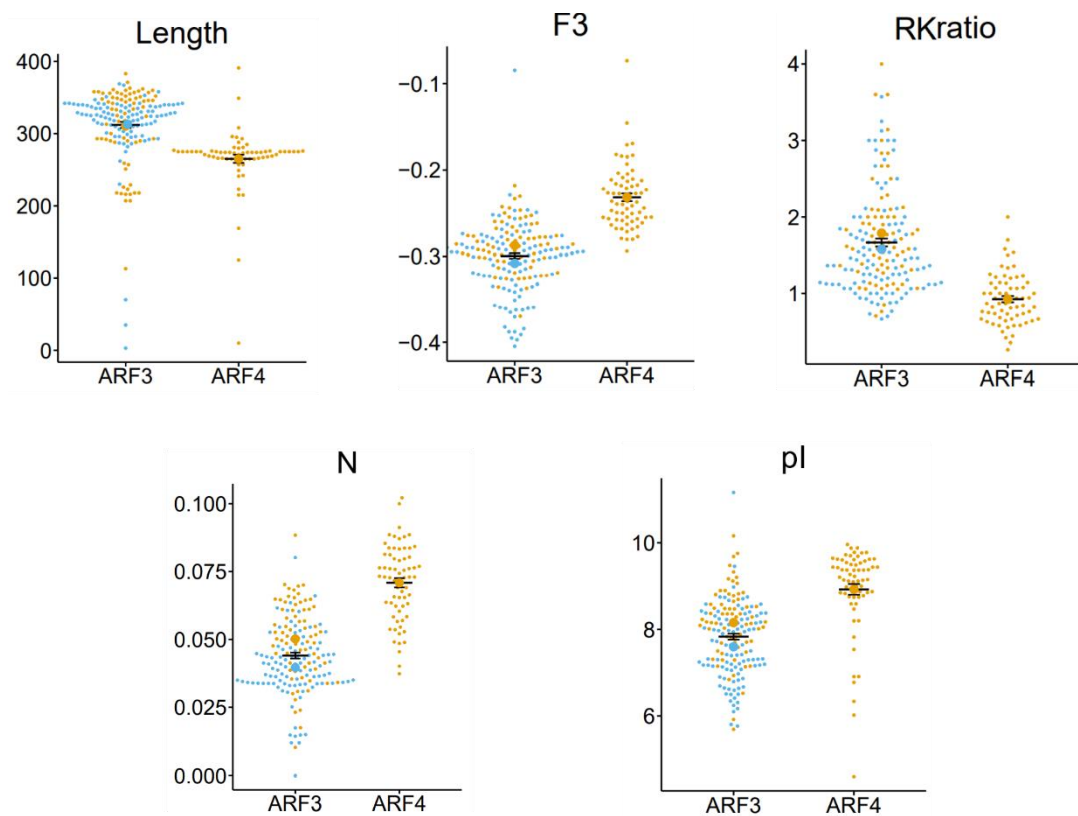


Figure S2.2: Biophysical and compositional parameters of ETT/ARF3 and ARF4. Blue datapoints represent monocot sequences while orange datapoints indicate eudicot sequences. Protein length is represented in number of residues. The F3 is a measure of the protein bulkiness (Liang and Li, 2007). The RK-ratio and N parameters measures the stickiness and aggregation properties of proteins (Dubreuil et al., 2019; Gil-Garcia et al., 2021).

Table S2.1: Genomes included in the Class B ARF phylogeny. Manually sourced genomes were downloaded from links provided in the referenced publication.

Species	Clade	Source	Reference
<i>Chlamydomonas reinhardtii</i>	Alga: Chlorophyte	PLAZA	Merchant et al. (2007)
<i>Micromonas commoda</i>	Alga: Chlorophyte	PLAZA	Worden et al. (2009)
<i>Mesotaenium endlicherianum</i>	Alga: Charophyte	Manual	Cheng et al. (2019)
<i>Chara braunii</i>	Alga: Charophyte	Manual	Nishiyama et al. (2018)
<i>Mesostigma viride</i>	Alga: Charophyte	Manual	Wang et al. (2020)
<i>Chlorokybus atmophyticus</i>	Alga: Charophyte	Manual	Wang et al. (2020)
<i>Coleochaete scutata</i>	Alga: Charophyte	Manual	de Vries et al. (2018)
<i>Klebsormidium nitens</i>	Alga: Charophyte	Manual	Hori et al. (2014)
<i>Spirogløea muscicola</i>	Alga: Charophyte	Manual	Cheng et al. (2019)
<i>Penium margaritaceum</i>	Alga: Charophyte	Manual	Jiao et al. (2020)
<i>Marchantia palacea</i>	Bryophyte: Liverwort	Manual	Diop et al. (2020)
<i>Marchantia polymorpha</i>	Bryophyte: Liverwort	Manual	Bowman et al. (2017)
<i>Physcomitrium patens</i>	Bryophyte: Moss	Manual	Lang et al. (2018)
<i>Ceratodon purpureus</i>	Bryophyte: Moss	Phytozome	Carey et al. (2021)
<i>Sphagnum fallax</i>	Bryophyte: Moss	Phytozome	Healey et al. (2023)
<i>Sphagnum magellanicum</i>	Bryophyte: Moss	Phytozome	Healey et al. (2023)
<i>Anthoceros agrestis</i>	Bryophyte: Hornwort	Manual	Li et al. (2020b)
<i>Selaginella moellendorffii</i>	Lycophyte	Manual	Banks et al. (2011)
<i>Azolla filiculoides</i>	Monilophyte	Manual	Li et al. (2018)
<i>Salvinia cucullata</i>	Monilophyte	Manual	Li et al. (2018)
<i>Ceratopteris richardii</i>	Monilophyte	Manual	Marchant et al. (2022)
<i>Ginkgo biloba</i>	Gymnosperm	Manual	Liu et al. (2021)
<i>Pinus taeda</i>	Gymnosperm	Manual	Zimin et al. (2017)
<i>Picea abies</i>	Gymnosperm	Manual	Nystedt et al. (2013)
<i>Gnetum montanum</i>	Gymnosperm	Manual	Wan et al. (2018)
<i>Amborella trichopoda</i>	Angiosperm: ANA Grade	Manual	Project et al. (2013)
<i>Nymphaea thermarum</i>	Angiosperm: ANA Grade	Manual	Povilus et al. (2020)
<i>Aristolochia fimbriata</i>	Angiosperm: Magnoliid	Manual	Qin et al. (2021)

<i>Piper nigrum</i>	Angiosperm: Magnoliid	Manual	Hu et al. (2019)
<i>Liriodendron chinense</i>	Angiosperm: Magnoliid	Manual	Chen et al. (2019)
<i>Chimonanthus salicifolius</i>	Angiosperm: Magnoliid	Manual	Lv et al. (2020)
<i>Persea americana</i>	Angiosperm: Magnoliid	Manual	Rendón-Anaya et al. (2019)
<i>Cinnamomum kanehirae</i>	Angiosperm: Magnoliid	Phytozome	Chaw et al. (2019)
<i>Zostera marina</i>	Angiosperm: Monocot	PLAZA	Olsen et al. (2016)
<i>Spirodela polyrhiza</i>	Angiosperm: Monocot	PLAZA	Wang et al. (2014b)
<i>Apostasia shenzhenica</i>	Angiosperm: Monocot	PLAZA	Zhang et al. (2017)
<i>Phalaenopsis equestris</i>	Angiosperm: Monocot	PLAZA	Cai et al. (2015)
<i>Asparagus officinalis</i>	Angiosperm: Monocot	PLAZA	Harkess et al. (2017)
<i>Elaeis guineensis</i>	Angiosperm: Monocot	PLAZA	Singh et al. (2013)
<i>Calamus simplicifolius</i>	Angiosperm: Monocot	PLAZA	Zhao et al. (2018b)
<i>Musa acuminata</i>	Angiosperm: Monocot	PLAZA	D'Hont et al. (2012)
<i>Ananas comosus</i>	Angiosperm: Monocot	PLAZA	Ming et al. (2015)
<i>Zoysia japonica</i>	Angiosperm: Monocot	PLAZA	Tanaka et al. (2016)
<i>Oropetium thomaeum</i>	Angiosperm: Monocot	PLAZA	VanBuren et al. (2018)
<i>Brachypodium distachyon</i>	Angiosperm: Monocot	Manual	Vogel et al. (2010)
<i>Triticum turgidum</i>	Angiosperm: Monocot	PLAZA	Maccaferri et al. (2019)
<i>Triticum aestivum</i>	Angiosperm: Monocot	PLAZA	Consortium et al. (2014)
<i>Lolium perenne</i>	Angiosperm: Monocot	PLAZA	Nagy et al. (2022)
<i>Hordeum vulgare</i>	Angiosperm: Monocot	PLAZA	Mascher et al. (2017)
<i>Phyllostachys edulis</i>	Angiosperm: Monocot	PLAZA	Zhao et al. (2018a)
<i>Saccharum spontaneum</i>	Angiosperm: Monocot	PLAZA	Zhang et al. (2018a)
<i>Zea mays</i>	Angiosperm: Monocot	Manual	Schnable et al. (2009)
<i>Zea mays</i> PH207	Angiosperm: Monocot	PLAZA	Hirsch et al. (2016)
<i>Setaria italica</i>	Angiosperm: Monocot	PLAZA	He et al. (2023)
<i>Sorghum bicolor</i>	Angiosperm: Monocot	PLAZA	Paterson et al. (2009)
<i>Cenchrus americanus</i>	Angiosperm: Monocot	PLAZA	Varshney et al. (2017)
<i>Oryza brachyantha</i>	Angiosperm: Monocot	PLAZA	Chen et al. (2013)
<i>Oryza sativa</i> ssp. <i>indica</i>	Angiosperm: Monocot	PLAZA	Yu et al. (2002)

<i>Oryza sativa ssp. japonica</i>	Angiosperm: Monocot	Manual	Sasaki and International Rice Genome Sequencing (2005)
<i>Nelumbo nucifera</i>	Angiosperm: Eudicot	PLAZA	Ming et al. (2013)
<i>Vitis vinifera</i>	Angiosperm: Eudicot	Manual	Jaillon et al. (2007)
<i>Pyrus bretschneideri</i>	Angiosperm: Eudicot	PLAZA	Wu et al. (2013)
<i>Malus domestica</i>	Angiosperm: Eudicot	PLAZA	Daccord et al. (2017)
<i>Fragaria vesca</i>	Angiosperm: Eudicot	PLAZA	Shulaev et al. (2011)
<i>Prunus persica</i>	Angiosperm: Eudicot	PLAZA	Verde et al. (2013)
<i>Ziziphus jujuba</i>	Angiosperm: Eudicot	PLAZA	Liu et al. (2014a)
<i>Citrullus lanatus</i>	Angiosperm: Eudicot	PLAZA	Guo et al. (2013)
<i>Cucumis melo</i>	Angiosperm: Eudicot	PLAZA	Garcia-Mas et al. (2012)
<i>Cucumis sativus</i>	Angiosperm: Eudicot	PLAZA	Hu et al. (2019)
<i>Trifolium pratense</i>	Angiosperm: Eudicot	PLAZA	De Vega et al. (2015)
<i>Arachis ipaensis</i>	Angiosperm: Eudicot	PLAZA	Lu et al. (2018)
<i>Cajanus cajan</i>	Angiosperm: Eudicot	PLAZA	Varshney et al. (2012)
<i>Vigna radiata</i>	Angiosperm: Eudicot	PLAZA	Kang et al. (2014)
<i>Medicago truncatula</i>	Angiosperm: Eudicot	PLAZA	Young et al. (2011)
<i>Cicer arietinum</i>	Angiosperm: Eudicot	PLAZA	Varshney et al. (2013)
<i>Glycine max</i>	Angiosperm: Eudicot	PLAZA	Schmutz et al. (2010)
<i>Populus trichocarpa</i>	Angiosperm: Eudicot	PLAZA	Tuskan et al. (2006)
<i>Ricinus communis</i>	Angiosperm: Eudicot	PLAZA	(Chan et al., 2010)
<i>Manihot esculenta</i>	Angiosperm: Eudicot	PLAZA	Wang et al. (2014a)
<i>Hevea brasiliensis</i>	Angiosperm: Eudicot	PLAZA	Tang et al. (2016)
<i>Citrus clementina</i>	Angiosperm: Eudicot	PLAZA	Wu et al. (2014)
<i>Eucalyptus grandis</i>	Angiosperm: Eudicot	PLAZA	Myburg et al. (2014)
<i>Gossypium raimondii</i>	Angiosperm: Eudicot	PLAZA	Wang et al. (2012)
<i>Corchorus olitorius</i>	Angiosperm: Eudicot	PLAZA	Islam et al. (2017)
<i>Theobroma cacao</i>	Angiosperm: Eudicot	PLAZA	Argout et al. (2011)
<i>Carica papaya</i>	Angiosperm: Eudicot	PLAZA	Ming et al. (2008)
<i>Tarenaya hassleriana</i>	Angiosperm: Eudicot	PLAZA	Cheng et al. (2013)
<i>Brassica rapa</i>	Angiosperm: Eudicot	PLAZA	Wang et al. (2011)

<i>Brassica oleracea</i>	Angiosperm: Eudicot	PLAZA	Liu et al. (2014b)
<i>Schrenkiella parvula</i>	Angiosperm: Eudicot	PLAZA	Dassanayake et al. (2011)
<i>Capsella rubella</i>	Angiosperm: Eudicot	PLAZA	Slotte et al. (2013)
<i>Arabidopsis lyrata</i>	Angiosperm: Eudicot	PLAZA	Hu et al. (2011)
<i>Arabidopsis thaliana</i>	Angiosperm: Eudicot	PLAZA	The Arabidopsis Genome (2000)
<i>Beta vulgaris</i>	Angiosperm: Eudicot	PLAZA	Dohm et al. (2014)
<i>Chenopodium quinoa</i>	Angiosperm: Eudicot	PLAZA	Jarvis et al. (2017)
<i>Actinidia chinensis</i>	Angiosperm: Eudicot	PLAZA	Huang et al. (2013a)
<i>Daucus carota</i>	Angiosperm: Eudicot	PLAZA	Iorizzo et al. (2016)
<i>Erythranthe guttata</i>	Angiosperm: Eudicot	PLAZA	Hellsten et al. (2013)
<i>Utricularia gibba</i>	Angiosperm: Eudicot	PLAZA	Ibarra-Laclette et al. (2013)
<i>Coffea canephora</i>	Angiosperm: Eudicot	PLAZA	Denoeud et al. (2014)
<i>Capsicum annuum</i>	Angiosperm: Eudicot	PLAZA	Kim et al. (2014)
<i>Solanum lycopersicum</i>	Angiosperm: Eudicot	Manual	Sato et al. (2012)
<i>Solanum tuberosum</i>	Angiosperm: Eudicot	PLAZA	Xu et al. (2011)
<i>Petunia axillaris</i>	Angiosperm: Eudicot	PLAZA	Bombarely et al. (2016)

Supplementary data from Chapter 3

Table S3.1: List of KAN, YAB, TPL/TPR and ETT/ARF4-like orthologues used in the Y2H screens.

Species	Gene	ID	Reference
<i>Marchantia polymorpha</i>	<i>MpoARF2</i>	Mapoly0011s0167	Bowman et al. (2017)
	<i>MpoTPL</i>	Mapoly0051s0078	
<i>Ceratopteris richardii</i>	<i>CriARF3/4</i>	Ceric.21G089900	Marchant et al. (2022); Phytozome
	<i>CriTPLa</i>	Ceric.08G073000	
	<i>CriTPLb</i>	Ceric.07G013800	
	<i>CriTPLc</i>	Ceric.1Z260400	
	<i>CriTPLd</i>	Ceric.14G074400	
	<i>CriTPLe</i>	Ceric.10G065300	
<i>Ginkgo biloba</i>	<i>GbiARF3/4</i>	Gb_17830/Gb_17831	Guan et al. (2016); Liu et al. (2021)
	<i>GbiTPLa</i>	Gb_37153	
	<i>GbiTPLb</i>	Gb_32130	
	<i>GbiTPLc</i>	Gb_04053	
	<i>GbiTPLd</i>	Gb_26928	
	<i>GbiTPLe</i>	Gb_39002	
	<i>GbiYABa</i>	Gb_36880	
	<i>GbiYAB1b</i>	Gb_22423	
	<i>GbiYAB2b</i>	evm.model.chr12.471	
	<i>GbiYABc</i>	Gb_08229	
<i>Amborella trichopoda</i>	<i>AtrETT</i>	AMTR_s00021p00200760	Project et al. (2013)
	<i>AtrARF4</i>	AMTR_s00034p00110140	
	<i>AtrTPR1</i>	AMTR_s00051p00079490	
	<i>AtrTPR2</i>	AMTR_s00048p00159380	
	<i>AtrKAN1</i>	AMTR_s00024p00053860	
	<i>AtrKAN2</i>	AMTR_s00048p00125480	
	<i>AtrATS</i>	AMTR_s00059p00206130	
	<i>AtrFIL</i>	AMTR_s00085p00032940	
	<i>AtrYAB2</i>	AMTR_s00004p00165390	
	<i>AtrINO</i>	AMTR_s00096p00054100	
	<i>AtrYAB5</i>	AMTR_s00078p00029420	
	<i>AtrCRC</i>	AMTR_s00047p00199030	
	<i>AtrIAA4</i>	AMTR_s00002p00266860	
	<i>AtrIAA9</i>	AMTR_s00184p00030540	
	<i>AtrIAA16</i>	AMTR_s00002p00266760	
<i>Nymphaea thermarum</i>	<i>NthETT</i>	EJ110_NYTH15956	Povilus et al. (2020)
	<i>NthARF4</i>	EJ110_NYTH47885	
	<i>NthTPLa</i>	EJ110_NYTH22400	
	<i>NthTPLb</i>	EJ110_NYTH18194	
	<i>NthTPR1</i>	EJ110_NYTH02857	
	<i>NthTPR2a</i>	EJ110_NYTH44705	
	<i>NthTPR2b</i>	EJ110_NYTH49689	
	<i>NthTPR3</i>	EJ110_NYTH09053	
<i>Aristolochia fimbriata</i>	<i>AfiETT</i>	KAG9447765	Qin et al. (2021)
	<i>AfiARF4</i>	KAG9453363	
	<i>AfiTPL</i>	KAG9450248	
	<i>AfiTPR1</i>	KAG9450199	
	<i>AfiTPR2</i>	KAG9454397	
	<i>AfiTPR3</i>	KAG9459547	
<i>Oryza sativa</i>	<i>OsaETT1</i>	Os05g48870	Yu et al. (2002)
	<i>OsaETT2</i>	Os01g48060	
	<i>OsaETT3</i>	Os01g54990	
	<i>OsaETT4</i>	Os05g43920	
	<i>OsaTPR1</i>	Os01g15020	

	<i>OsaTPR2</i>	Os08g06480	
	<i>OsaTPR3</i>	Os03g14980	
<i>Arabidopsis thaliana</i>	<i>AthETT</i>	AT2G33860	The Arabidopsis Genome (2000); TAIR
	<i>AthARF4</i>	AT5G60450	
	<i>AthTPL</i>	AT1G15750	
	<i>AthKAN1</i>	AT5G16560	
	<i>AthKAN2</i>	AT1G32240	
	<i>AthKAN3</i>	AT4G17695	
	<i>AthATS</i>	AT5G42630	
	<i>AthFIL</i>	AT2G45190	
	<i>AthYAB2</i>	AT1G08465	
	<i>AthYAB3</i>	AT4G00180	
	<i>AthINO</i>	AT1G23420	
	<i>AthYAB5</i>	AT2G26580	
	<i>AthCRC</i>	AT1G69180	
	<i>AthIAA2</i>	AT3G23030	
	<i>AthIAA9</i>	AT5G65670	
	<i>AthIAA16</i>	AT3G04730	
<i>Solanum lycopersicum</i>	<i>SlyETT</i>	Solyc02g077560	Sato et al. (2012); Phytozome
	<i>SlyARF4</i>	Solyc11g069190	
	<i>SlyTPL</i>	Solyc03g117360	
	<i>SlyTPR2</i>	Solyc08g076030	
	<i>SlyTPR3</i>	Solyc01g100050	
	<i>SlyTPR4</i>	Solyc03g116750	
	<i>SlyTPR5</i>	Solyc07g008040	
	<i>SlyTPR6</i>	Solyc08g029050	
	<i>SlyKAN1a</i>	Solyc05g051060	
	<i>SlyKAN1b</i>	Solyc11g011770	
	<i>SlyKAN2a</i>	Solyc08g005260	
	<i>SlyKAN2b</i>	Solyc06g066340	
	<i>SlyKAN2c</i>	Solyc08g076400	
	<i>SlyATS</i>	Solyc04g079600	
	<i>SlyFIL</i>	Solyc01g091010	
	<i>SlyYAB2</i>	Solyc06g073920	
	<i>SlyFAS</i>	Solyc11g071810	
	<i>SlyYAB3</i>	Solyc08g079100	
	<i>SlyINO</i>	Solyc05g005240	
	<i>SlyYAB5a</i>	Solyc07g008180	
	<i>SlyYAB5b</i>	Solyc12g009580	
	<i>SlyCRC</i>	Solyc05g012050	
	<i>SlyDL</i>	Solyc01g010240	

Table S3.2. List of oligonucleotides used in Chapter 3.

ID	Orientation	Gene	Sequence	Use
AA 0606	Forward	<i>MpoARF2</i>	ACGACAAGGGGTCGACCATGTC AGAAGCATCTTCCATCAC	Y2H: pB1880/81
AA 0607	Reverse	<i>MpoARF2</i>	ACCGCGGTGGCGGCCGCCTAC ATGTCGTCGCCGCG	Y2H: pB1880
AA 0608	Reverse	<i>MpoARF2</i>	ACTTACTTAGCGGCCGCCTACAT GTCGTCGCCGCG	Y2H: pB1881
AA 0691	Forward	<i>CriARF3/4</i>	ACGACAAGGGGTCGACCATGCA TCTCGACTCGCAGC	Y2H: pB1880/81
AA 0692	Reverse	<i>CriARF3/4</i>	ACCGCGGTGGCGGCCGCTTAAC CTGAGATGGAGTTCCTG	Y2H: pB1880
AA 0693	Reverse	<i>CriARF3/4</i>	ACTTACTTAGCGGCCGCTTAACC TGAGATGGAGTTCCTG	Y2H: pB1881
AA 0167	Forward	<i>GbiARF3/4</i>	ACGACAAGGGGTCGACCATGGA AATTGATCTCAACAGTCC	Y2H: pB1880/81
AA 1068	Reverse	<i>GbiARF3/4</i>	ACCGCGGTGGCGGCCGCTTAAA TTCTTGTTGCTGGTGGAG	Y2H: pB1880
AA 0169	Reverse	<i>GbiARF3/4</i>	ACTTACTTAGCGGCCGCTTAAAT TCTTGTTGCTGGTGGAG	Y2H: pB1881
AA 0114	Forward	<i>AtrETT</i>	ACGACAAGGGGTCGACCATGGG CATTGATCTGAACCGG	Y2H: pB1880/81
AA 0103	Reverse	<i>AtrETT</i>	ACCGCGGTGGCGGCCGCTTACA CAGCTCTAGCAAGGCC	Y2H: pB1880
AA 0104	Reverse	<i>AtrETT</i>	ACTTACTTAGCGGCCGCTTACAC AGCTCTAGCAAGGCC	Y2H: pB1881
AA 0132	Forward	<i>AtrARF4</i>	ACGACAAGGGGTCGACCATGGA AATTGATCTCAACTGCG	Y2H: pB1880/81
AA 0133	Reverse	<i>AtrARF4</i>	ACCGCGGTGGCGGCCGCCTATT CGAGTCCTCTTGTATGG	Y2H: pB1880
AA 0134	Reverse	<i>AtrARF4</i>	ACTTACTTAGCGGCCGCTATTC GAGTCCTCTTGTATGG	Y2H: pB1881
AA 0733	Forward	<i>NthETT</i>	ACGACGACAAGGGGTCGACCAT GGAGATCGATCTAAACAGGG	Y2H: pB1880/81
AA 0736	Reverse	<i>NthETT</i>	ACCGCGGTGGCGGCCGCTCAA GTCCTTGTTACCGTCAC	Y2H: pB1880
AA 0737	Reverse	<i>NthETT</i>	ACTTACTTAGCGGCCGCTCAAG TCCTTGTTACCGTCAC	Y2H: pB1881
AA 0738	Forward	<i>NthARF4</i>	ACGACAAGGGGTCGACCATGGA AATTGATCTCAACAGTGCAC	Y2H: pB1880/81
AA 0741	Reverse	<i>NthARF4</i>	ACCGCGGTGGCGGCCGCCTAG ATGTTGTTTTCTTAGTCAAC	Y2H: pB1880
AA 0742	Reverse	<i>NthARF4</i>	ACTTACTTAGCGGCCGCCTAGA TGTTGTTTTCTTAGTCAAC	Y2H: pB1881
AA 0902	Forward	<i>AfiETT</i>	ACGACAAGGGGTCGACCATGGA AATCGATCTGAACGCCA	Y2H: pB1880/81
AA 0903	Reverse	<i>AfiETT</i>	ACCGCGGTGGCGGCCGCTCAAT GGCCCTGCCTACAACA	Y2H: pB1880
AA 0904	Reverse	<i>AfiETT</i>	ACTTACTTAGCGGCCGCTCAAT GGCCCTGCCTACAACA	Y2H: pB1881
AA 0905	Forward	<i>AfiARF4</i>	ACGACAAGGGGTCGACCATGGA AATTGATCTGAATGATGATG	Y2H: pB1880/81
AA 0906	Reverse	<i>AfiARF4</i>	ACCGCGGTGGCGGCCGCTTAAG GCCTCGTTACTGTCAAAG	Y2H: pB1880
AA 0907	Reverse	<i>AfiARF4</i>	ACTTACTTAGCGGCCGCTTAAG GCCTCGTTACTGTCAAAG	Y2H: pB1881
AA 0852	Forward	<i>OsaETT1</i>	ACGACAAGGGGTCGACCATGAC CGGGATCGACCTC	Y2H: pB1880/81

AA 0853	Reverse	<i>OsaETT1</i>	ACCGCGGTGGCGGCCGCTCAG ATCATCATATCCATAGTTGAA	Y2H: pB1880
AA 0854	Reverse	<i>OsaETT1</i>	ACTTACTTAGCGGCCGCTCAGA TCATCATATCCATAGTTGAA	Y2H: pB1881
AA 0855	Forward	<i>OsaETT2</i>	ACGACAAGGGGTGACCATGGT GGGCATCGACCTC	Y2H: pB1880/81
AA 0856	Reverse	<i>OsaETT2</i>	ACCGCGGTGGCGGCCGCTCAG ATCATCGTATTCACTGCTG	Y2H: pB1880
AA 0857	Reverse	<i>OsaETT2</i>	ACTTACTTAGCGGCCGCTCAGA TCATCGTATTCACTGCTG	Y2H: pB1881
AA 0858	Forward	<i>OsaETT3</i>	ACGACAAGGGGTGACCATGGC GTGTCGCCGATCC	Y2H: pB1880/81
AA 0859	Reverse	<i>OsaETT3</i>	ACCGCGGTGGCGGCCGCTCATA TCCCAAAGGAGCAGC	Y2H: pB1880
AA 0860	Reverse	<i>OsaETT3</i>	ACTTACTTAGCGGCCGCTCATAT TCCCAAAGGAGCAGC	Y2H: pB1881
AA 0861	Forward	<i>OsaETT4</i>	ACGACAAGGGGTGACCATGGG GATTGACCTGAACACGG	Y2H: pB1880/81
AA 0862	Reverse	<i>OsaETT4</i>	ACCGCGGTGGCGGCCGCTCAC ATTCCCAGGGGAGC	Y2H: pB1880
AA 0863	Reverse	<i>OsaETT4</i>	ACTTACTTAGCGGCCGCTCACAT TCCCAGGGGAGC	Y2H: pB1881
AA 0117	Forward	<i>AthETT</i>	ACGACAAGGGGTGACCATGGG TGGTTTAATCGATCTGAACG	Y2H: pB1880/81
AA 0077	Reverse	<i>AthETT</i>	ACCGCGGTGGCGGCCGCTAG AGAGCAATGTCTAGCAACATG	Y2H: pB1880
AA 0054	Reverse	<i>AthETT</i>	ACTTACTTAGCGGCCGCTAGA GAGCAATGTCTAGCAACATG	Y2H: pB1881
AA 0128	Forward	<i>AthARF4</i>	ACGACAAGGGGTGACCATGGA ATTTGACTTGAATACTGAGA	Y2H: pB1880/81
AA 0088	Reverse	<i>AthARF4</i>	ACCGCGGTGGCGGCCGCTCAAA CCCTAGTGATTGTAGGAGA	Y2H: pB1880
AA 0076	Reverse	<i>AthARF4</i>	ACTTACTTAGCGGCCGCTCAAA CCCTAGTGATTGTAGGAGA	Y2H: pB1881
AA 0115	Forward	<i>SlyETT</i>	ACGACAAGGGGTGACCATGAT GTGTGGACTTATTGATCTG	Y2H: pB1880/81
AA 0106	Reverse	<i>SlyETT</i>	ACCGCGGTGGCGGCCGCTAC AGAGCAATATCAAGAAGCAC	Y2H: pB1880
AA 0107	Reverse	<i>SlyETT</i>	ACTTACTTAGCGGCCGCTACA GAGCAATATCAAGAAGCAC	Y2H: pB1881
AA 0253	Forward	<i>SlyARF4</i>	ACGACAAGGGGTGACCATGGA AATTGATCTGAATCATGCA	Y2H: pB1880/81
AA 0254	Reverse	<i>SlyARF4</i>	ACCGCGGTGGCGGCCGCTCAAA TCCTGATTACAGTTGGAGA	Y2H: pB1880
AA 0255	Reverse	<i>SlyARF4</i>	ACTTACTTAGCGGCCGCTCAAT CCTGATTACAGTTGGAGA	Y2H: pB1881
AA 0129	Forward	<i>AthIAA2</i>	ACGACAAGGGGTGACCATGGC GTACGAGAAAGTCAACG	Y2H: pB1880/81
AA 0095	Reverse	<i>AthIAA2</i>	ACCGCGGTGGCGGCCGCTCATA AGGAAGAGTCTAGAGCAGG	Y2H: pB1880
AA 0090	Reverse	<i>AthIAA2</i>	ACTTACTTAGCGGCCGCTCATA GGAAGAGTCTAGAGCAGG	Y2H: pB1881
AA 0130	Forward	<i>AthIAA9</i>	ACGACAAGGGGTGACCATGTC CCCGAAGAGGAGC	Y2H: pB1880/81
AA 0096	Reverse	<i>AthIAA9</i>	ACCGCGGTGGCGGCCGCTTAAG CTCTCATCTTCGATTTCTCC	Y2H: pB1880
AA 0092	Reverse	<i>AthIAA9</i>	ACTTACTTAGCGGCCGCTTAAG CTCTCATCTTCGATTTCTCC	Y2H: pB1881

AA 0131	Forward	<i>AthIAA16</i>	ACGACAAGGGGTGACCATGAT TAATTTTGAGGCCACGGAGC	Y2H: pB1880/81
AA 0097	Reverse	<i>AthIAA16</i>	ACCGCGGTGGCGGCCGCTCAA CTTCTGTTCTTGCACTTTTC	Y2H: pB1880
AA 0094	Reverse	<i>AthIAA16</i>	ACTTACTTAGCGGCCGCTCAACT TCTGTTCTTGCACTTTTC	Y2H: pB1881
AA 0244	Forward	<i>AtrIAA4</i>	ACGACAAGGGGTGACCATGGA GAAGGCAAGAAGTTATGAG	Y2H: pB1880/81
AA 0245	Reverse	<i>AtrIAA4</i>	ACCGCGGTGGCGGCCGCTCAAT AGGATGAAATGTGTGAAGC	Y2H: pB1880
AA 0246	Reverse	<i>AtrIAA4</i>	ACTTACTTAGCGGCCGCTCAATA GGATGAAATGTGTGAAGC	Y2H: pB1881
AA 0247	Forward	<i>AthIAA9</i>	ACGACAAGGGGTGACCATGTC TCCACCTCTTGCC	Y2H: pB1880/81
AA 0248	Reverse	<i>AthIAA9</i>	ACCGCGGTGGCGGCCGCTAG TTCCGGTTCCTGCAC	Y2H: pB1880
AA 0249	Reverse	<i>AthIAA9</i>	ACTTACTTAGCGGCCGCTAGTT CCGGTTCCTGCAC	Y2H: pB1881
AA 0250	Forward	<i>AthIAA16</i>	ACGACAAGGGGTGACCATGGC GACTGATCTGAGTC	Y2H: pB1880/81
AA 0251	Reverse	<i>AthIAA16</i>	ACCGCGGTGGCGGCCGCTTAG CTTCTGTTCTTGCACTTTCTCC	Y2H: pB1880
AA 0252	Reverse	<i>AthIAA16</i>	ACTTACTTAGCGGCCGCTTAGCT TCTGTTCTTGCACTTTCTCC	Y2H: pB1881
AA 0170	Forward	<i>GbiYABa</i>	ACGACAAGGGGTGACCATGTC TAGCGCATCGAACTCG	Y2H: pB1880/81
AA 0171	Reverse	<i>GbiYABa</i>	ACCGCGGTGGCGGCCGCTTTAT TGCAGAGAGATTCTGCATTC	Y2H: pB1880
AA 0172	Reverse	<i>GbiYABa</i>	ACTTACTTAGCGGCCGCTTTATT GCAGAGAGATTCTGCATTC	Y2H: pB1881
AA 0173	Forward	<i>GbiYAB1b</i>	ACGACAAGGGGTGACCATGTC GAGCAGTTGCATTGACC	Y2H: pB1880/81
AA 0174	Reverse	<i>GbiYAB1b</i>	ACCGCGGTGGCGGCCGCTAG CCATCGTTAGTAGCAGAAT	Y2H: pB1880
AA 0175	Reverse	<i>GbiYAB1b</i>	ACTTACTTAGCGGCCGCTAGC CATCGTTAGTAGCAGAAT	Y2H: pB1881
AA 0176	Forward	<i>GbiYAB2b</i>	ACGACAAGGGGTGACCATGTC TAGCAGCTGCGTT	Y2H: pB1880/81
AA 0177	Reverse	<i>GbiYAB2b</i>	ACCGCGGTGGCGGCCGCTCAG TATGGAATTCGATGGTAGAGT	Y2H: pB1880
AA 0178	Reverse	<i>GbiYAB2b</i>	ACTTACTTAGCGGCCGCTCAGT ATGGAATTCGATGGTAGAGT	Y2H: pB1881
AA 0179	Forward	<i>GbiYABc</i>	ACGACAAGGGGTGACCATGTC TACATGTATTGAGTTCAGTT	Y2H: pB1880/81
AA 0180	Reverse	<i>GbiYABc</i>	ACCGCGGTGGCGGCCGCTCAA CATGGATTGCTGCC	Y2H: pB1880
AA 0181	Reverse	<i>GbiYABc</i>	ACTTACTTAGCGGCCGCTCAAC ATGGATTGCTGCC	Y2H: pB1881
AA 0143	Forward	<i>AtrKAN1</i>	ACGACAAGGGGTGACCATGCC TACACAGGGGGTTTTTC	Y2H: pB1880/81
AA 0144	Reverse	<i>AtrKAN1</i>	ACCGCGGTGGCGGCCGCTCAAT CACGGTCTTTGCCATGC	Y2H: pB1880
AA 0145	Reverse	<i>AtrKAN1</i>	ACTTACTTAGCGGCCGCTCAATC ACGGTCTTTGCCATGC	Y2H: pB1881
AA 0146	Forward	<i>AtrKAN2</i>	ACGACAAGGGGTGACCATGGA GCTTTCTCCTGCACCAC	Y2H: pB1880/81
AA 0147	Reverse	<i>AtrKAN2</i>	ACCGCGGTGGCGGCCGCTTAGT CTGGCCGGCCCAAC	Y2H: pB1880

AA 0148	Reverse	<i>AtrKAN2</i>	ACTTACTTAGCGGCCGCTTAGTC TGGCCGGCCCAAC	Y2H: pB1881
AA 0149	Forward	<i>AtrATS</i>	ACGACAAGGGGTTCGACCATGGA CATGAGGGGCTGGG	Y2H: pB1880/81
AA 0150	Reverse	<i>AtrATS</i>	ACCGCGGTGGCGGCCGCTTAG CATTTAAGAAGTGCGAGTTC	Y2H: pB1880
AA 0151	Reverse	<i>AtrATS</i>	ACTTACTTAGCGGCCGCTTAGC ATTTAAGAAGTGCGAGTTC	Y2H: pB1881
AA 0152	Forward	<i>AtrFIL</i>	ACGACAAGGGGTTCGACCATGTC ATCCTCATCCTCTTTTGCC	Y2H: pB1880/81
AA 0153	Reverse	<i>AtrFIL</i>	ACCGCGGTGGCGGCCGCCTAG TATGGAGTGACCCCATG	Y2H: pB1880
AA 0154	Reverse	<i>AtrFIL</i>	ACTTACTTAGCGGCCGCCTAGT ATGGAGTGACCCCATG	Y2H: pB1881
AA 0155	Forward	<i>AtrYAB2</i>	ACGACAAGGGGTTCGACCATGTC CCTCGAAAACCCGTGC	Y2H: pB1880/81
AA 0156	Reverse	<i>AtrYAB2</i>	ACCGCGGTGGCGGCCGCTTACA CAGCTTGGTGGATGATTGG	Y2H: pB1880
AA 0157	Reverse	<i>AtrYAB2</i>	ACTTACTTAGCGGCCGCTTACAC AGCTTGGTGGATGATTGG	Y2H: pB1881
AA 0158	Forward	<i>AtrINO</i>	ACGACAAGGGGTTCGACCATGTC TTCATGTGAGCACATATTTG	Y2H: pB1880/81
AA 0159	Reverse	<i>AtrINO</i>	ACCGCGGTGGCGGCCGCTCACT CATTGTTTTCCATGAGTAC	Y2H: pB1880
AA 0160	Reverse	<i>AtrINO</i>	ACTTACTTAGCGGCCGCTCACT CATTGTTTTCCATGAGTAC	Y2H: pB1881
AA 0161	Forward	<i>AtrYAB5</i>	ACGACAAGGGGTTCGACCATGTC GAATGCAACAGCAGC	Y2H: pB1880/81
AA 0162	Reverse	<i>AtrYAB5</i>	ACCGCGGTGGCGGCCGCTCATT CAATGCAAACAGCAGCC	Y2H: pB1880
AA 0163	Reverse	<i>AtrYAB5</i>	ACTTACTTAGCGGCCGCTCATTC AATGCAAACAGCAGCC	Y2H: pB1881
AA 0164	Forward	<i>AtrCRC</i>	ACGACAAGGGGTTCGACCATGGA TTTTCTTCCGGGATCC	Y2H: pB1880/81
AA 0165	Reverse	<i>AtrCRC</i>	ACCGCGGTGGCGGCCGCCTAC GTAATTTGCGACCTAGC	Y2H: pB1880
AA 0166	Reverse	<i>AtrCRC</i>	ACTTACTTAGCGGCCGCCTACG TAATTTGCGACCTAGC	Y2H: pB1881
AA 0118	Forward	<i>AthKAN1</i>	ACGACAAGGGGTTCGACCATGTC TATGGAAGGTGTTTTTCTAG	Y2H: pB1880/81
AA 0078	Reverse	<i>AthKAN1</i>	ACCGCGGTGGCGGCCGCTCATT TCTCGTGCCAATCTGG	Y2H: pB1880
AA 0056	Reverse	<i>AthKAN1</i>	ACTTACTTAGCGGCCGCTCATTT CTCGTGCCAATCTGG	Y2H: pB1881
AA 0119	Forward	<i>AthKAN2</i>	ACGACAAGGGGTTCGACCATGGA GCTGTTTCCTGCTCA	Y2H: pB1880/81
AA 0079	Reverse	<i>AthKAN2</i>	ACCGCGGTGGCGGCCGCTTAGT GAGATCGACCCAGAGT	Y2H: pB1880
AA 0058	Reverse	<i>AthKAN2</i>	ACTTACTTAGCGGCCGCTTAGT GAGATCGACCCAGAGT	Y2H: pB1881
AA 0120	Forward	<i>AthKAN3</i>	ACGACAAGGGGTTCGACCATGGA GCTTTTCCCTTCAACAACC	Y2H: pB1880/81
AA 0080	Reverse	<i>AthKAN3</i>	ACCGCGGTGGCGGCCGCTTAG GGAGAGAGGTTTGGTGTAGC	Y2H: pB1880
AA 0060	Reverse	<i>AthKAN3</i>	ACTTACTTAGCGGCCGCTTAGG GAGAGAGGTTTGGTGTAGC	Y2H: pB1881
AA 0121	Forward	<i>AthATS</i>	ACGACAAGGGGTTCGACCATGAT GATGTTAGAGTCAAGAAACA	Y2H: pB1880/81

AA 0081	Reverse	<i>AthATS</i>	ACCGCGGTGGCGGCCGCTTAG CACTTGAGAAGGGTTAAATCA	Y2H: pB1880
AA 0062	Reverse	<i>AthATS</i>	ACTTACTTAGCGGCCGCTTAGC ACTTGAGAAGGGTTAAATCA	Y2H: pB1881
AA 0122	Forward	<i>AthFIL</i>	ACGACAAGGGGTGCGACCATGTC TATGTCGTCTATGTCCTCC	Y2H: pB1880/81
AA 0082	Reverse	<i>AthFIL</i>	ACCGCGGTGGCGGCCGCTTAAT AAGGAGTCACACCAACG	Y2H: pB1880
AA 0064	Reverse	<i>AthFIL</i>	ACTTACTTAGCGGCCGCTTAATA AGGAGTCACACCAACG	Y2H: pB1881
AA 0123	Forward	<i>AthYAB2</i>	ACGACAAGGGGTGCGACCATGTC TG TAGATTCTCATCTGAGC	Y2H: pB1880/81
AA 0083	Reverse	<i>AthYAB2</i>	ACCGCGGTGGCGGCCGCTTAGT AATAGCCATTAGACTTTTGG	Y2H: pB1880
AA 0066	Reverse	<i>AthYAB2</i>	ACTTACTTAGCGGCCGCTTAGTA ATAGCCATTAGACTTTTGG	Y2H: pB1881
AA 0124	Forward	<i>AthYAB3</i>	ACGACAAGGGGTGCGACCATGTC GAGCATGTCCATGTCG	Y2H: pB1880/81
AA 0084	Reverse	<i>AthYAB3</i>	ACCGCGGTGGCGGCCGCCTAG TTATGGGCCACCCCAACG	Y2H: pB1880
AA 0068	Reverse	<i>AthYAB3</i>	ACTTACTTAGCGGCCGCCTAGTT ATGGGCCACCCCAACG	Y2H: pB1881
AA 0125	Forward	<i>AthINO</i>	ACGACAAGGGGTGCGACCATGAC AAAGCTCCCCAACATGAC	Y2H: pB1880/81
AA 0085	Reverse	<i>AthINO</i>	ACCGCGGTGGCGGCCGCTTACT CAAATGGAGATTTTCCCC	Y2H: pB1880
AA 0070	Reverse	<i>AthINO</i>	ACTTACTTAGCGGCCGCTTACTC AAATGGAGATTTTCCCC	Y2H: pB1881
AA 0126	Forward	<i>AthYAB5</i>	ACGACAAGGGGTGCGACCATGGC TAACTCTGTGATGGCAAC	Y2H: pB1880/81
AA 0086	Reverse	<i>AthYAB5</i>	ACCGCGGTGGCGGCCGCTTAG GCTATCTTAGCTTGCTTGTT	Y2H: pB1880
AA 0072	Reverse	<i>AthYAB5</i>	ACTTACTTAGCGGCCGCTTAGG CTATCTTAGCTTGCTTGTT	Y2H: pB1881
AA 0127	Forward	<i>AthCRC</i>	ACGACAAGGGGTGCGACCATGAA CCTAGAAGAGAAACCAACC	Y2H: pB1880/81
AA 0087	Reverse	<i>AthCRC</i>	ACCGCGGTGGCGGCCGCTCACT TCTTCTCACCGAATCCC	Y2H: pB1880
AA 0074	Reverse	<i>AthCRC</i>	ACTTACTTAGCGGCCGCTCACTT CTTCTCACCGAATCCC	Y2H: pB1881
AA 0208	Forward	<i>SlyKAN1a</i>	ACGACAAGGGGTGCGACCATGCT CTTAGAAGGGGTTTTTGT	Y2H: pB1880/81
AA 0209	Reverse	<i>SlyKAN1a</i>	ACCGCGGTGGCGGCCGCTTAGT CATGGTTCTTTTCTACCCA	Y2H: pB1880
AA 0210	Reverse	<i>SlyKAN1a</i>	ACTTACTTAGCGGCCGCTTAGTC ATGGTTCTTTTCTACCCA	Y2H: pB1881
AA 0211	Forward	<i>SlyKAN1b</i>	ACGACAAGGGGTGCGACCATGCC CTTAGAAGGGGTTTTCA	Y2H: pB1880/81
AA 0212	Reverse	<i>SlyKAN1b</i>	ACCGCGGTGGCGGCCGCTCATT CATGATCCTTTTCAATCCAA	Y2H: pB1880
AA 0213	Reverse	<i>SlyKAN1b</i>	ACTTACTTAGCGGCCGCTCATT ATGATCCTTTTCAATCCAA	Y2H: pB1881
AA 0214	Forward	<i>SlyKAN2a</i>	ACGACAAGGGGTGCGACCATGGA GTTATTCCACCA	Y2H: pB1880/81
AA 0215	Reverse	<i>SlyKAN2a</i>	ACCGCGGTGGCGGCCGCCTAT GAAATATTAGGAATTCCTA	Y2H: pB1880
AA 0216	Reverse	<i>SlyKAN2a</i>	ACTTACTTAGCGGCCGCCTATG AAATATTAGGAATTCCTA	Y2H: pB1881

AA 0217	Forward	<i>SlyKAN2b</i>	ACGACAAGGGGTGACCATGGA GCTATTCCCAGCACAACC	Y2H: pB1880/81
AA 0218	Reverse	<i>SlyKAN2b</i>	ACCGCGGTGGCGGCCGCTCAA GGCCTTCCCAAAGTGAAC	Y2H: pB1880
AA 0219	Reverse	<i>SlyKAN2b</i>	ACTTACTTAGCGGCCGCTCAAG GCCTTCCCAAAGTGAAC	Y2H: pB1881
AA 0220	Forward	<i>SlyKAN2c</i>	ACGACAAGGGGTGACCATGGA ACTATTCCCAGCACAACCAG	Y2H: pB1880/81
AA 0221	Reverse	<i>SlyKAN2c</i>	ACCGCGGTGGCGGCCGCTTATA TCAATTTAGACTTTGGATC	Y2H: pB1880
AA 0222	Reverse	<i>SlyKAN2c</i>	ACTTACTTAGCGGCCGCTTATAT CAATTTAGACTTTGGATC	Y2H: pB1881
AA 0223	Forward	<i>SlyATS</i>	ACGACAAGGGGTGACCATGAC GAAGGATACACTACTTTCA	Y2H: pB1880/81
AA 0224	Reverse	<i>SlyATS</i>	ACCGCGGTGGCGGCCGCTTAAC ACTTGAGAAGAGTCAAATCA	Y2H: pB1880
AA 0225	Reverse	<i>SlyATS</i>	ACTTACTTAGCGGCCGCTTAACA CTTGAGAAGAGTCAAATCA	Y2H: pB1881
AA 0182	Forward	<i>SlyFIL</i>	ACGACAAGGGGTGACCATGTC GTCTTCATCTGCTGCT	Y2H: pB1880/81
AA 0183	Reverse	<i>SlyFIL</i>	ACCGCGGTGGCGGCCGCTCAG TAAGGAGATACACCAATGT	Y2H: pB1880
AA 0184	Reverse	<i>SlyFIL</i>	ACTTACTTAGCGGCCGCTCAGT AAGGAGATACACCAATGT	Y2H: pB1881
AA 0229	Forward	<i>SlyYAB2</i>	ACGACAAGGGGTGACCATGTC ACTTGACATGACATATTCCT	Y2H: pB1880/81
AA 0230	Reverse	<i>SlyYAB2</i>	ACCGCGGTGGCGGCCGCTTAAT AGAGACCAATTGTTTTCTGA	Y2H: pB1880
AA 0231	Reverse	<i>SlyYAB2</i>	ACTTACTTAGCGGCCGCTTAATA GAGACCAATTGTTTTCTGA	Y2H: pB1881
AA 0185	Forward	<i>SlyFAS</i>	ACGACAAGGGGTGACCATGTC ATTCGATATGACTTTTTCTT	Y2H: pB1880/81
AA 0186	Reverse	<i>SlyFAS</i>	ACCGCGGTGGCGGCCGCTTATT TGTTGCCCTCCAGCTT	Y2H: pB1880
AA 0187	Reverse	<i>SlyFAS</i>	ACTTACTTAGCGGCCGCTATTT GTTGCCCTCCAGCTT	Y2H: pB1881
AA 0226	Forward	<i>SlyYAB3</i>	ACGACAAGGGGTGACCATGTC CTCTTCAAATAGCTTATCAT	Y2H: pB1880/81
AA 0227	Reverse	<i>SlyYAB3</i>	ACCGCGGTGGCGGCCGCTCAG TAAGGAGACACACTAACA	Y2H: pB1880
AA 0228	Reverse	<i>SlyYAB3</i>	ACTTACTTAGCGGCCGCTCAGT AAGGAGACACACTAACA	Y2H: pB1881
AA 0232	Forward	<i>SlyINO</i>	ACGACAAGGGGTGACCATGTC AACATTGAATAACCATTTGT	Y2H: pB1880/81
AA 0233	Reverse	<i>SlyINO</i>	ACCGCGGTGGCGGCCGCTCAA GGAATCAAACCGTTGCT	Y2H: pB1880
AA 0234	Reverse	<i>SlyINO</i>	ACTTACTTAGCGGCCGCTCAAG GAATCAAACCGTTGCT	Y2H: pB1881
AA 0235	Forward	<i>SlyYAB5a</i>	ACGACAAGGGGTGACCATGGC AGCTGCATTTTCAGTCC	Y2H: pB1880/81
AA 0236	Reverse	<i>SlyYAB5a</i>	ACCGCGGTGGCGGCCGCTTATA GTTTTCTGCTCCCACAAGC	Y2H: pB1880
AA 0237	Reverse	<i>SlyYAB5a</i>	ACTTACTTAGCGGCCGCTTATAG TTTTCTGCTCCCACAAGC	Y2H: pB1881
AA 0238	Forward	<i>SlyYAB5b</i>	ACGACAAGGGGTGACCATGTC ATCAAGCTACATTGATTCT	Y2H: pB1880/81
AA 0239	Reverse	<i>SlyYAB5b</i>	ACCGCGGTGGCGGCCGCTTAGA AGGTGAAGGTCTTTATTTTT	Y2H: pB1880

AA 0240	Reverse	<i>SlyYAB5b</i>	ACTTACTTAGCGGCCGCTTAGAA GGTGAAGGTCTTTATTTTT	Y2H: pB1881
AA 0188	Forward	<i>SlyCRC</i>	ACGACAAGGGGTGACCATGGA TTATGTTCAATCTTCTGAG	Y2H: pB1880/81
AA 0189	Reverse	<i>SlyCRC</i>	ACCGCGGTGGCGGCCGCTAAA CATTGTTGGTATTTCC	Y2H: pB1880
AA 0190	Reverse	<i>SlyCRC</i>	ACTTACTTAGCGGCCGCTAAA CATTGTTGGTATTTCC	Y2H: pB1881
AA 0241	Forward	<i>SlyDL</i>	ACGACAAGGGGTGACCATGTC TTCCTCATCTCCTAATTCC	Y2H: pB1880/81
AA 0242	Reverse	<i>SlyDL</i>	ACCGCGGTGGCGGCCGCTCAG CCAAGGTCCCATTTGG	Y2H: pB1880
AA 0243	Reverse	<i>SlyDL</i>	ACTTACTTAGCGGCCGCTCAGC CAAGGTCCCATTTGG	Y2H: pB1881
AA 0609	Forward	<i>MpoTPL</i>	ACGACAAGGGGTGACCATGTC ATCGTTAAGCAGGGAGC	Y2H: pB1880/81
AA 0610	Reverse	<i>MpoTPL</i>	ACCGCGGTGGCGGCCGCTCATC TCGGAGCTTGATCAG	Y2H: pB1880
AA 0611	Reverse	<i>MpoTPL</i>	ACTTACTTAGCGGCCGCTCATCT CGGAGCTTGATCAG	Y2H: pB1881
AA 0612	Forward	<i>CriTPLa</i>	ACGACAAGGGGTGACCATGTC GTCACTCAGTCGTGAAC	Y2H: pB1880/81
AA 0613	Reverse	<i>CriTPLa</i>	ACCGCGGTGGCGGCCGCTCAC CTTGACAGCTTGCTCAG	Y2H: pB1880
AA 0614	Reverse	<i>CriTPLa</i>	ACTTACTTAGCGGCCGCTCACC TTGACAGCTTGCTCAG	Y2H: pB1881
AA 0615	Forward	<i>CriTPLb</i>	ACGACAAGGGGTGACCATGTC CTCTCTCAGCCGGGA	Y2H: pB1880/81
AA 0616	Reverse	<i>CriTPLb</i>	ACCGCGGTGGCGGCCGCTTACT TTGGAGCCTCCAATTTACA	Y2H: pB1880
AA 0617	Reverse	<i>CriTPLb</i>	ACTTACTTAGCGGCCGCTTACTT TGGAGCCTCCAATTTACA	Y2H: pB1881
AA 0618	Forward	<i>CriTPLc</i>	ACGACAAGGGGTGACCATGTC CTCGCTCAGCCGTG	Y2H: pB1880/81
AA 0619	Reverse	<i>CriTPLc</i>	ACCGCGGTGGCGGCCGCTAC CTTGTTGGCCTGCTCTGAG	Y2H: pB1880
AA 0620	Reverse	<i>CriTPLc</i>	ACTTACTTAGCGGCCGCTTACC TTGTGGCCTGCTCTGAG	Y2H: pB1881
AA 0621	Forward	<i>CriTPLd</i>	ACGACAAGGGGTGACCATGTC ATCGTTGAGTAGGGAGC	Y2H: pB1880/81
AA 0622	Reverse	<i>CriTPLd</i>	ACCGCGGTGGCGGCCGCTATC TTGGAGCTTGCTCTGTAAC	Y2H: pB1880
AA 0623	Reverse	<i>CriTPLd</i>	ACTTACTTAGCGGCCGCTATCT TGGAGCTTGCTCTGTAAC	Y2H: pB1881
AA 0624	Forward	<i>CriTPLe</i>	ACGACAAGGGGTGACCATGTC CTCGCTCAGCCGTG	Y2H: pB1880/81
AA 0625	Reverse	<i>CriTPLe</i>	ACCGCGGTGGCGGCCGCTAC CTTGTTGGCCTGCTCTGAG	Y2H: pB1880
AA 0626	Reverse	<i>CriTPLe</i>	ACTTACTTAGCGGCCGCTTACC TTGTGGCCTGCTCTGAG	Y2H: pB1881
AA 0926	Forward	<i>GbiTPLa</i>	ACGACAAGGGGTGACCATGTC TTCCTCAGCAGAGAGC	Y2H: pB1880/81
AA 0927	Reverse	<i>GbiTPLa</i>	ACCGCGGTGGCGGCCGCTCAC CTTGGGGTTTGCTCTG	Y2H: pB1880
AA 0928	Reverse	<i>GbiTPLa</i>	ACTTACTTAGCGGCCGCTCACC TTGGGGTTTGCTCTG	Y2H: pB1881
AA 0929	Forward	<i>GbiTPLb</i>	ACGACAAGGGGTGACCATGTC TTCGCTTAGTAGAGAGCTTG	Y2H: pB1880/81

AA 0930	Reverse	<i>GbiTPLb</i>	ACCGCGGTGGCGGCCGCTCAC CTAGGACCTTGTCTGAGC	Y2H: pB1880
AA 0931	Reverse	<i>GbiTPLb</i>	ACTTACTTAGCGGCCGCTCACC TAGGACCTTGTCTGAGC	Y2H: pB1881
AA 0932	Forward	<i>GbiTPLc</i>	ACGACAAGGGGTTCGACCATGTC CTCTTTAAGCAGGGAAGTCTG	Y2H: pB1880/81
AA 0933	Reverse	<i>GbiTPLc</i>	ACCGCGGTGGCGGCCGCTCAC CTTGGAGGTGGTTCTGAACC	Y2H: pB1880
AA 0934	Reverse	<i>GbiTPLc</i>	ACTTACTTAGCGGCCGCTCACC TTGGAGGTGGTTCTGAACC	Y2H: pB1881
AA 0935	Forward	<i>GbiTPLd</i>	ACGACAAGGGGTTCGACCATGTC TTCTTTGAGCAGGGAAGTGG	Y2H: pB1880/81
AA 0936	Reverse	<i>GbiTPLd</i>	ACCGCGGTGGCGGCCGCTCAC CTTGGAGGTAATTCTGATCCT	Y2H: pB1880
AA 0937	Reverse	<i>GbiTPLd</i>	ACTTACTTAGCGGCCGCTCACC TTGGAGGTAATTCTGATCCT	Y2H: pB1881
AA 0938	Forward	<i>GbiTPLe</i>	ACGACAAGGGGTTCGACCATGTC TTCCCTCAGTAGGGAATTGG	Y2H: pB1880/81
AA 0939	Reverse	<i>GbiTPLe</i>	ACCGCGGTGGCGGCCGCTTAAT TGCTAGTTGGTGGTGCATG	Y2H: pB1880
AA 0940	Reverse	<i>GbiTPLe</i>	ACTTACTTAGCGGCCGCTTAAT GCTAGTTGGTGGTGCATG	Y2H: pB1881
AA 0390	Forward	<i>AtrTPR1</i>	ACGACAAGGGGTTCGACCATGTC TTCTCTGAGCAGGGAGC	Y2H: pB1880/81
AA 0391	Reverse	<i>AtrTPR1</i>	ACCGCGGTGGCGGCCGCTTACC GGAGGCTGCTCTGATTG	Y2H: pB1880
AA 0392	Reverse	<i>AtrTPR1</i>	ACTTACTTAGCGGCCGCTTACC GAGGCTGCTCTGATTG	Y2H: pB1881
AA 0393	Forward	<i>AtrTPR2</i>	ACGACAAGGGGTTCGACCATGTC TTCTTTGAGCAGGGAGC	Y2H: pB1880/81
AA 0394	Reverse	<i>AtrTPR2</i>	ACCGCGGTGGCGGCCGCTTACC TGAGAGGGTTCAGAGGG	Y2H: pB1880
AA 0395	Reverse	<i>AtrTPR2</i>	ACTTACTTAGCGGCCGCTTACC GAGAGGGTTCAGAGGG	Y2H: pB1881
AA 0743	Forward	<i>NthTPLa</i>	ACGACAAGGGGTTCGACCATGTC GTCTCTTAGTAGAGAACTCG	Y2H: pB1880/81
AA 0746	Reverse	<i>NthTPLa</i>	ACCGCGGTGGCGGCCGCTCATC TTTGCGGCTGGTC	Y2H: pB1880
AA 0747	Reverse	<i>NthTPLa</i>	ACTTACTTAGCGGCCGCTCATCT TTGCGGCTGGTC	Y2H: pB1881
AA 0748	Forward	<i>NthTPLb</i>	ACGACAAGGGGTTCGACCATGTC GTCGCTTAGTAGAGAACTC	Y2H: pB1880/81
AA 0751	Reverse	<i>NthTPLb</i>	ACCGCGGTGGCGGCCGCTCATC TCTGAGGCTGATCCGTG	Y2H: pB1880
AA 0752	Reverse	<i>NthTPLb</i>	ACTTACTTAGCGGCCGCTCATCT CTGAGGCTGATCCGTG	Y2H: pB1881
AA 0753	Forward	<i>NthTPR1</i>	ACGACAAGGGGTTCGACCATGTC GTCTCTCAGTAGAGAACTCG	Y2H: pB1880/81
AA 0756	Reverse	<i>NthTPR1</i>	ACCGCGGTGGCGGCCGCTTACC TTGGTGGCTGCTCAGAG	Y2H: pB1880
AA 0757	Reverse	<i>NthTPR1</i>	ACTTACTTAGCGGCCGCTTACC TGGTGGCTGCTCAGAG	Y2H: pB1881
AA 0763	Forward	<i>NthTPR2a</i>	ACGACAAGGGGTTCGACCATGTC ATCCTTAAGCAGGGAAGT	Y2H: pB1880/81
AA 0766	Reverse	<i>NthTPR2a</i>	ACCGCGGTGGCGGCCGCTCAC CTGGAAGGAGGTTCTGATACC	Y2H: pB1880
AA 0767	Reverse	<i>NthTPR2a</i>	ACTTACTTAGCGGCCGCTCACC TGGAAGGAGGTTCTGATACC	Y2H: pB1881

AA 0768	Forward	<i>NthTPR2b</i>	ACGACAAGGGGTGACCATGTC ATCCTTAAGCAGGGAGCTTG	Y2H: pB1880/81
AA 0771	Reverse	<i>NthTPR2b</i>	ACCGCGGTGGCGGCCGCTCAC CTGGAAGCAGGTTCTGAAG	Y2H: pB1880
AA 0772	Reverse	<i>NthTPR2b</i>	ACTTACTTAGCGGCCGCTCACC TGGAAGCAGGTTCTGAAG	Y2H: pB1881
AA 0758	Forward	<i>NthTPR3</i>	ACGACAAGGGGTGACCATGTC ATCTTTAAGCAGAGAATTGG	Y2H: pB1880/81
AA 0761	Reverse	<i>NthTPR3</i>	ACCGCGGTGGCGGCCGCTCATC TTGAAGTCTGCTCAGAGGC	Y2H: pB1880
AA 0762	Reverse	<i>NthTPR3</i>	ACTTACTTAGCGGCCGCTCATCT TGAAGTCTGCTCAGAGGC	Y2H: pB1881
AA 0908	Forward	<i>AfiTPL</i>	ACGACAAGGGGTGACCATGTC TTCTCTCAGTAGGGAGCTC	Y2H: pB1880/81
AA 0909	Reverse	<i>AfiTPL</i>	ACCGCGGTGGCGGCCGCTCAC CTCTGGGGCTGATCTG	Y2H: pB1880
AA 0910	Reverse	<i>AfiTPL</i>	ACTTACTTAGCGGCCGCTCACC TCTGGGGCTGATCTG	Y2H: pB1881
AA 0911	Forward	<i>AfiTPR1</i>	ACGACAAGGGGTGACCATGAC TTCGCTCAGCAGGGA	Y2H: pB1880/81
AA 0912	Reverse	<i>AfiTPR1</i>	ACCGCGGTGGCGGCCGCTCAC CTTGGTGGTTGATCTGAAAC	Y2H: pB1880
AA 0913	Reverse	<i>AfiTPR1</i>	ACTTACTTAGCGGCCGCTCACC TTGGTGGTTGATCTGAAAC	Y2H: pB1881
AA 0914	Forward	<i>AfiTPR2</i>	ACGACAAGGGGTGACCATGTC TTCCTTAGTAGGGAAC	Y2H: pB1880/81
AA 0915	Reverse	<i>AfiTPR2</i>	ACCGCGGTGGCGGCCGCTCAC CTCTGAGGTGGTTCTGATG	Y2H: pB1880
AA 0916	Reverse	<i>AfiTPR2</i>	ACTTACTTAGCGGCCGCTCACC TCTGAGGTGGTTCTGATG	Y2H: pB1881
AA 0917	Forward	<i>AfiTPR3</i>	ACGACAAGGGGTGACCATGTC GTCACTGAGCAGAGAATTGG	Y2H: pB1880/81
AA 0918	Reverse	<i>AfiTPR3</i>	ACCGCGGTGGCGGCCGCTCATC TTTGGGTTTGTCTGCAGC	Y2H: pB1880
AA 0919	Reverse	<i>AfiTPR3</i>	ACTTACTTAGCGGCCGCTCATCT TTGGGTTTGTCTGCAGC	Y2H: pB1881
AA 0864	Forward	<i>OsaTPR1</i>	ACGACAAGGGGTGACCATGTC GTCGCTCAGCCGG	Y2H: pB1880/81
AA 0865	Reverse	<i>OsaTPR1</i>	ACCGCGGTGGCGGCCGCCTATC TTTGGATTTGGTCTGCAGC	Y2H: pB1880
AA 0866	Reverse	<i>OsaTPR1</i>	ACTTACTTAGCGGCCGCCTATCT TTGGATTTGGTCTGCAGC	Y2H: pB1881
AA 0867	Forward	<i>OsaTPR2</i>	ACGACAAGGGGTGACCATGTC GTCGCTTAGCAGGG	Y2H: pB1880/81
AA 0868	Reverse	<i>OsaTPR2</i>	ACCGCGGTGGCGGCCGCTCAG ACTTCTGGTTTGTAGCTGC	Y2H: pB1880
AA 0869	Reverse	<i>OsaTPR2</i>	ACTTACTTAGCGGCCGCTCAGA CTTCTGGTTTGTAGCTGC	Y2H: pB1881
AA 0870	Forward	<i>OsaTPR3</i>	ACGACAAGGGGTGACCATGTC GTCGCTGAGCCGG	Y2H: pB1880/81
AA 0871	Reverse	<i>OsaTPR3</i>	ACCGCGGTGGCGGCCGCTTATC TTTCTGGTTGATCAGAAC	Y2H: pB1880
AA 0872	Reverse	<i>OsaTPR3</i>	ACTTACTTAGCGGCCGCTTATCT TTCTGGTTGATCAGAAC	Y2H: pB1881
AA 0360	Forward	<i>AthTPL</i>	ACGACAAGGGGTGACCATGTC TTCTCTTAGTAGAGAGCTC	Y2H: pB1880/81
AA 0361	Reverse	<i>AthTPL</i>	ACCGCGGTGGCGGCCGCTCATC TCTGAGGCTGATCAGAT	Y2H: pB1880

AA 0362	Reverse	<i>AthTPL</i>	ACTTACTTAGCGGCCGCTCATCT CTGAGGCTGATCAGAT	Y2H: pB1881
AA 0396	Forward	<i>SlyTPL</i>	ACGACAAGGGGTTCGACCATGTC ATCTCTCAGTAGAGAGC	Y2H: pB1880/81
AA 0397	Reverse	<i>SlyTPL</i>	ACCGCGGTGGCGGCCGCTCTTG GTGCTTGATCGGAGCC	Y2H: pB1880
AA 0398	Reverse	<i>SlyTPL</i>	ACTTACTTAGCGGCCGCTCTTG GTGCTTGATCGGAGCC	Y2H: pB1881
AA 0399	Forward	<i>SlyTPR2</i>	ACGACAAGGGGTTCGACCATGTC TTCCTTGAGTAGGGAAGTGG	Y2H: pB1880/81
AA 0400	Reverse	<i>SlyTPR2</i>	ACCGCGGTGGCGGCCGCCCTT GAAGGTGTTTCTGATGGC	Y2H: pB1880
AA 0401	Reverse	<i>SlyTPR2</i>	ACTTACTTAGCGGCCGCCCTTG AAGGTGTTTCTGATGGC	Y2H: pB1881
AA 0402	Forward	<i>SlyTPR3</i>	ACGACAAGGGGTTCGACCATGTC TTCTCTTAGCAGAGAATT	Y2H: pB1880/81
AA 0403	Reverse	<i>SlyTPR3</i>	ACCGCGGTGGCGGCCGCTCTTT GAACTTGGTCAGCAGC	Y2H: pB1880
AA 0404	Reverse	<i>SlyTPR3</i>	ACTTACTTAGCGGCCGCTCTTTG AACTTGGTCAGCAGC	Y2H: pB1881
AA 0405	Forward	<i>SlyTPR4</i>	ACGACAAGGGGTTCGACCATGAC TTCTTTAAGCAGAGAGCT	Y2H: pB1880/81
AA 0406	Reverse	<i>SlyTPR4</i>	ACCGCGGTGGCGGCCGCCCTT GATGCTTGATCAAGACC	Y2H: pB1880
AA 0407	Reverse	<i>SlyTPR4</i>	ACTTACTTAGCGGCCGCCCTTG ATGCTTGATCAAGACC	Y2H: pB1881
AA 0600	Forward	<i>SlyTPR5</i>	ACGACAAGGGGTTCGACCATGAG GCATTTTGATGAAATGGTGG	Y2H: pB1880/81
AA 0601	Reverse	<i>SlyTPR5</i>	ACCGCGGTGGCGGCCGCCTAC CTTTGAGGTTGATCTG	Y2H: pB1880
AA 0602	Reverse	<i>SlyTPR5</i>	ACTTACTTAGCGGCCGCCTACC TTTGAGGTTGATCTG	Y2H: pB1881
AA 0603	Forward	<i>SlyTPR6</i>	ACGACAAGGGGTTCGACCATGTC TCTTAGTAAGGACCTT	Y2H: pB1880/81
AA 0604	Reverse	<i>SlyTPR6</i>	ACCGCGGTGGCGGCCGCCTATA TTGGTTGCTCATTGGTAAGA	Y2H: pB1880
AA 0605	Reverse	<i>SlyTPR6</i>	ACTTACTTAGCGGCCGCCTATAT TGGTTGCTCATTGGTAAGA	Y2H: pB1881
AA 1188	Reverse	<i>AthETT- GbiARF3/4</i>	CTGCAACTGAACCAGATGGTTC GATCTCCCATGG	Y2H Domain Swaps
AA 1189	Forward	<i>AthETT- GbiARF3/4</i>	ACCATCTGGTTTCAGTTGCAGGAT TGAATGTTTC	Y2H Domain Swaps
AA 1190	Reverse	<i>AthETT- AtrETT</i>	CAGACCCCAAACCAGATGGTTC GATCTCCCATGG	Y2H Domain Swaps
AA 1191	Forward	<i>AthETT- AtrETT</i>	ACCATCTGGTTTGGGGTCTGTTC CAGTATTTAGC	Y2H Domain Swaps
AA 1192	Reverse	<i>GbiARFL1- AthETT</i>	TGGAGATGGAAATACATGGCTC AATTTCCCAT	Y2H Domain Swaps
AA 1193	Forward	<i>GbiARFL1- AthETT</i>	GCCATGTATTTCCATCTCCAATT CAGGCAGC	Y2H Domain Swaps
AA 1194	Reverse	<i>GbiARFL1- AtrETT</i>	CAGACCCCAAATACATGGCTC AATTTCCCAT	Y2H Domain Swaps
AA 1195	Forward	<i>GbiARFL1- AtrETT</i>	GCCATGTATTTGGGGTCTGTTC CAGTATTTAGC	Y2H Domain Swaps
AA 1196	Reverse	<i>AtrETT- AthETT</i>	TGGAGATGGAAAGGTCGATCTC CCATGG	Y2H Domain Swaps
AA 1197	Forward	<i>AtrETT- AthETT</i>	GATCGACCTTTCCATCTCCAATT CAGGCAGC	Y2H Domain Swaps

AA 1198	Reverse	<i>AtrETT-GbiARFL1</i>	CTGCAACTGAAAGGTCGATCTC CCATGG	Y2H Domain Swaps
AA 1199	Reverse	<i>AtrETT-GbiARFL1</i>	GATCGACCTTTTCAGTTGCAGGAT TGAATGTTTC	Y2H Domain Swaps
AA 1200	Reverse	<i>AthETT-GbiARFL1</i>	AAGACACAATTTCTTGACCTTGC AAGACCTTATGG	Y2H Domain Swaps
AA 1201	Reverse	<i>AthETT-GbiARFL1</i>	AGGTCAAGAAATTGTGTCTTTGA AGGCACCCC	Y2H Domain Swaps
AA 1206	Reverse	<i>AthETT-AtrETT</i>	AATGGAAAATTTCTTGACCTTGC AAGACCTTATGG	Y2H Domain Swaps
AA 1207	Forward	<i>AthETT-AtrETT</i>	AGGTCAAGAAATTTCCATTTGA AATCACAGAACA	Y2H Domain Swaps

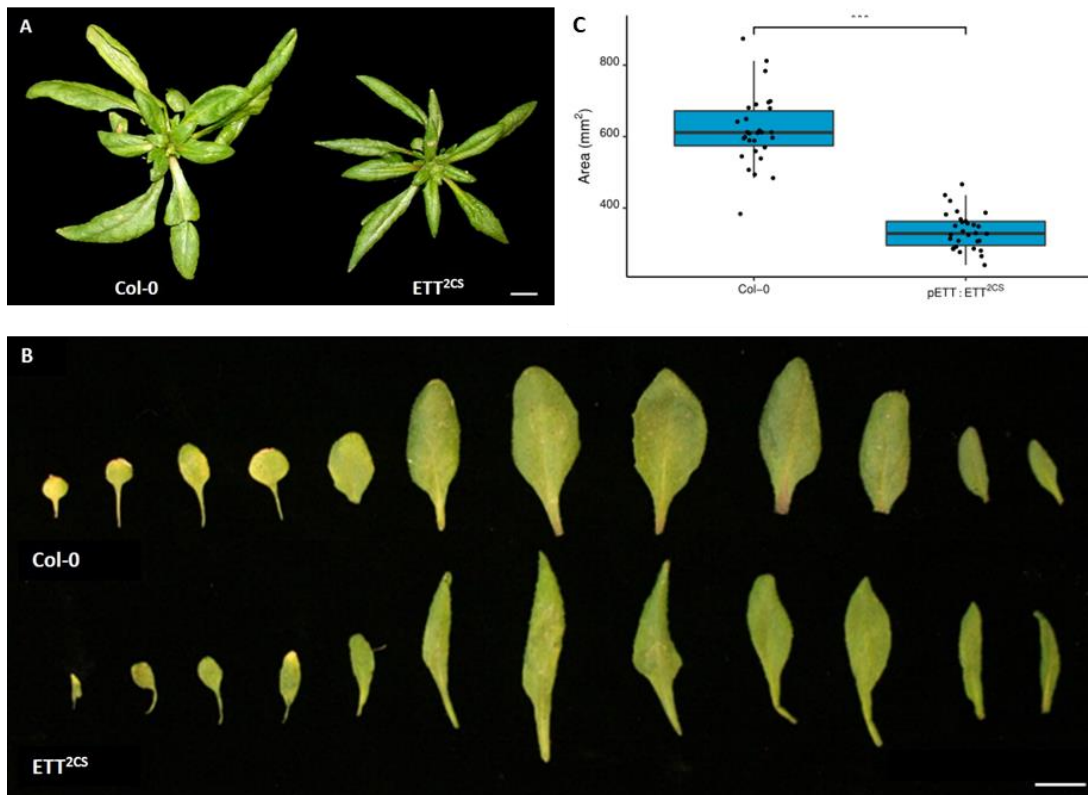


Figure S3.1: Leaf phenotypes of the *pETT:ETT^{2CS}* auxin-insensitive line. Whole plant rosettes (a) and leaf stage series from leaf 1-12 (b) of Col-0 and *pETT:ETT^{2CS}* lines. Scale bars represent 10mm. (c) Statistical analysis of leaf size supports significantly smaller leaves of the *pETT:ETT^{2CS}* line ($p < 0.001$, $n = 30$).

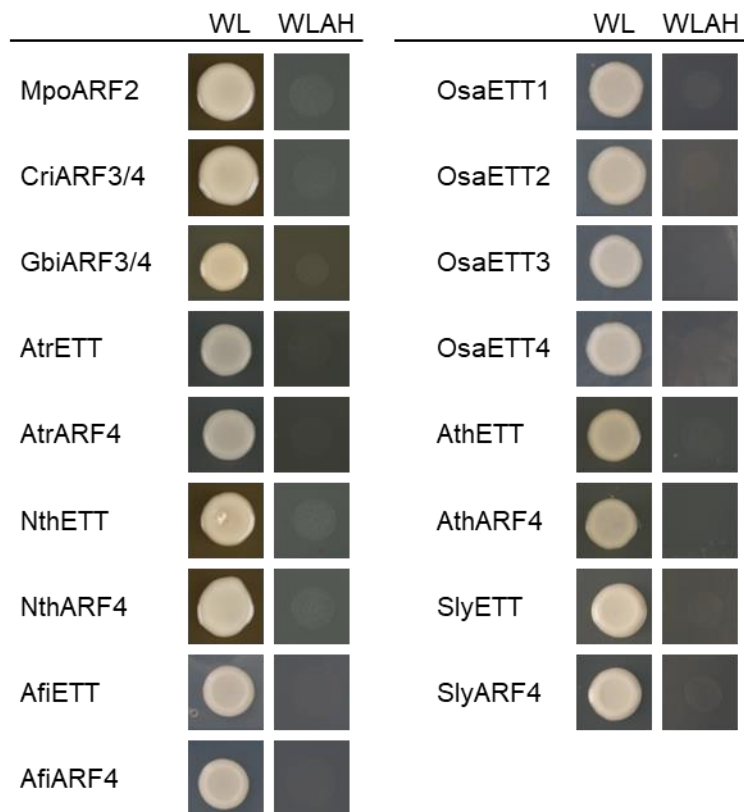


Figure S3.2: Y2H auto-activation test for ETT/ARF4-like orthologues. Constructs were co-transformed with ARF and empty vector constructs, either pB1880 or pB1881 depending on the ARF vector.

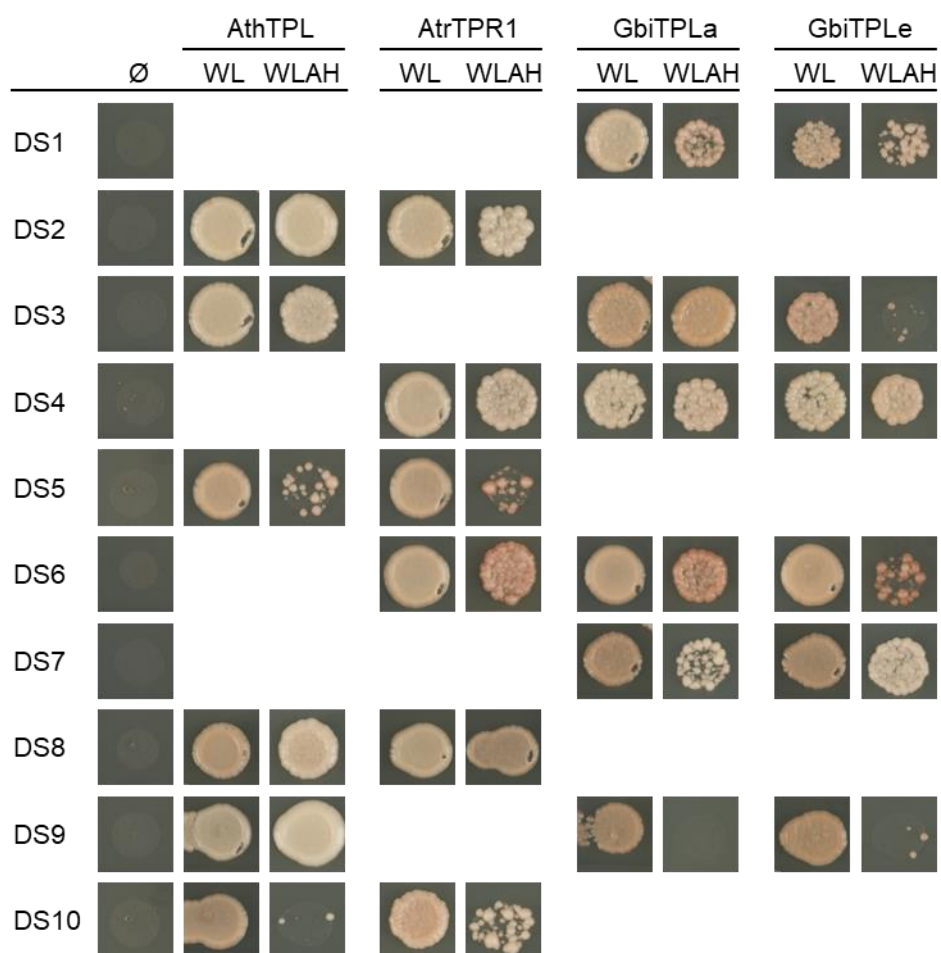


Figure S3.3: Y2H screen of chimeric ARF constructs with TPL/TPR orthologues. TPL/TPR orthologues from species that were included in the chimeric constructs were chosen for the interaction assays. ∅ represents the empty vector control to test for auto-activation of the chimeric constructs.

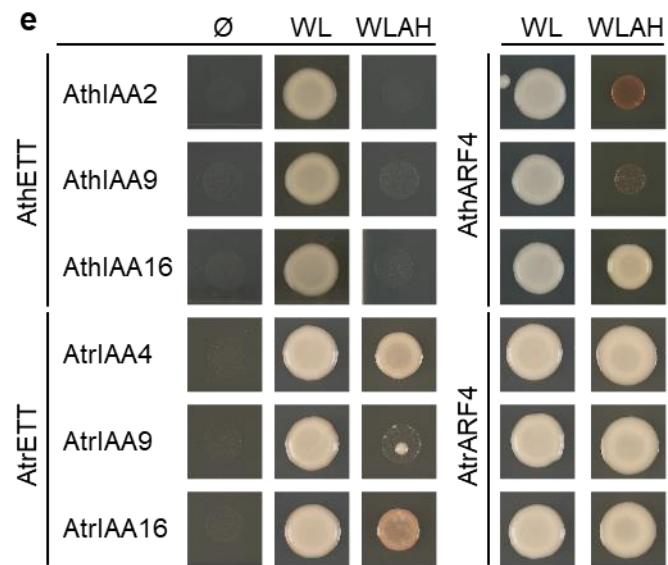


Figure S3.4: Y2H interaction assay to test for ETT and ARF4 interactions with AUX/IAAs. The ARF4 of both *A. thaliana* and *A. trichopoda* interacted with the AUX/IAAs to varying degrees of strength, but only the ETT of *A. trichopoda* was able to interact with the AUX/IAAs.

Supplementary data from Chapter 4

Table S4.1: List of oligonucleotides used in Chapter 4.

ID	Orientation	Gene	Sequence	Use
AA 0256	Forward	<i>pAthETT</i>	GAGCTCGGTACCCGGGGATCCG AGCAATCCTATACGGAGTTCT	Plasmid – Promoter
AA 0512	Reverse	<i>pAthETT-MpoARF2</i>	CTTCTGACATTAAGAGAGAGAA ACAGAGATAAAG	Promoter – CDS
AA 0494	Reverse	<i>pAthETT-CriARF3/4</i>	CGAGATGCATTAAGAGAGAGA AACAGAGATAAAG	Promoter – CDS
AA 0435	Reverse	<i>pAthETT-GbiARF3/4</i>	CAATTTCCATTAAGAGAGAGAA ACAGAGATAAAG	Promoter – CDS
AA 0427	Reverse	<i>pAthETT-AtrETT</i>	CAATGCCCATTAAGAGAGAGA AACAGAGATAAAG	Promoter – CDS
AA 0429*	Reverse	<i>pAthETT-AtrARF4</i>	CAATTTCCATTAAGAGAGAGAA ACAGAGATAAAG	Promoter – CDS
AA 0487	Reverse	<i>pAthETT-NthETT</i>	CGATCTCCATTAAGAGAGAGAA ACAGAGATAAAG	Promoter – CDS
AA 0429*	Reverse	<i>pAthETT-NthARF4</i>	CAATTTCCATTAAGAGAGAGAA ACAGAGATAAAG	Promoter – CDS
AA 1001	Reverse	<i>pAthETT-AfiETT</i>	CGATTTCCATTAAGAGAGAGAA ACAGAGATAAAG	Promoter – CDS
AA 1004	Reverse	<i>pAthETT-AfiARF4</i>	TCTCTCTTTAATGGAAATTGATC TGAATGATGATG	Promoter – CDS
AA 0508	Reverse	<i>pAthETT-AthETT</i>	AACCACCCATTAAGAGAGAGA AACAGAGATAAAG	Promoter – CDS
AA 0425	Reverse	<i>pAthETT-AthARF4</i>	CAAATTCATTAAGAGAGAGAA ACAGAGATAAAG	Promoter – CDS
AA 0431	Reverse	<i>pAthETT-SlyETT</i>	CACACATCATTAAGAGAGAGAA ACAGAGATAAAG	Promoter – CDS
AA 0433	Reverse	<i>pAthETT-SlyARF4</i>	CAATTTCCATTAAGAGAGAGAA ACAGAGATAAAG	Promoter – CDS
AA 0513	Forward	<i>pAthETT-MpoARF2</i>	TCTCTCTTTAATGTCAGAAGCAT CTTCCATCAC	Promoter – CDS
AA 0495	Forward	<i>pAthETT-CriARF3/4</i>	TCTCTCTTTAATGCATCTCGACT CGCAGC	Promoter – CDS
AA 0436	Forward	<i>pAthETT-GbiARF3/4</i>	TCTCTCTTTAATGGAAATTGATC TCAACAGTCC	Promoter – CDS
AA 0428	Forward	<i>pAthETT-AtrETT</i>	TCTCTCTTTAATGGGCATTGATC TGAACCGG	Promoter – CDS
AA 0430	Forward	<i>pAthETT-AtrARF4</i>	TCTCTCTTTAATGGAAATTGATC TCAACTGCG	Promoter – CDS
AA 0488	Forward	<i>pAthETT-NthETT</i>	TCTCTCTTTAATGGAGATCGATC TAAACAGGGTCCG	Promoter – CDS
AA 0490	Forward	<i>pAthETT-NthARF4</i>	TCTCTCTTTAATGGAAATTGATC TCAACAGTGC	Promoter – CDS
AA 1002	Forward	<i>pAthETT-AfiETT</i>	TCTCTCTTTAATGGAAATCGATC TGAACGCCA	Promoter – CDS
AA 0429*	Forward	<i>pAthETT-AfiARF4</i>	CAATTTCCATTAAGAGAGAGAA ACAGAGATAAAG	Promoter – CDS
AA 0509	Forward	<i>pAthETT-AthETT</i>	TCTCTCTTTAATGGGTGGTTTAA TCGATCTGAACG	Promoter – CDS
AA 0426	Forward	<i>pAthETT-AthARF4</i>	TCTCTCTTTAATGGAAATTTGACTT GAATACTGAGA	Promoter – CDS
AA 0432	Forward	<i>pAthETT-SlyETT</i>	TCTCTCTTTAATGATGTGTGGAC TTATTGATCTG	Promoter – CDS
AA 0434	Forward	<i>pAthETT-SlyARF4</i>	TCTCTCTTTAATGGAAATTGATC TGAATCATGCA	Promoter – CDS

AA 0514	Reverse	<i>MpoARF2</i>	ATGGTCTTTGTAGTCAAGCTTCT ACATGTCGTCGCC	Plasmid – CDS
AA 0496	Reverse	<i>CriARF3/4</i>	ATGGTCTTTGTAGTCAAGCTTTT AACCTGAGATGGA	Plasmid – CDS
AA 0273	Reverse	<i>GbiARF3/4</i>	ATGGTCTTTGTAGTCAAGCTTTT AAATTCTTGTGCTGGTGGAG	Plasmid – CDS
AA 0259	Reverse	<i>AtrETT</i>	ATGGTCTTTGTAGTCAAGCTTTT ACACAGCTCTAGCAAGGCC	Plasmid – CDS
AA 0389	Reverse	<i>AtrARF4</i>	ATGGTCTTTGTAGTCAAGCTTCT ATTCGAGTCCTCTTGTTAT	Plasmid – CDS
AA 0489	Reverse	<i>NthETT</i>	ATGGTCTTTGTAGTCAAGCTTTC AAGTCCTTGTTAC	Plasmid – CDS
AA 0491	Reverse	<i>NthARF4</i>	ATGGTCTTTGTAGTCAAGCTTCT AGATGTTGTTTTT	Plasmid – CDS
AA 1003	Reverse	<i>AfiETT</i>	ATGGTCTTTGTAGTCAAGCTTTC AATGGCCCTGCCTACAACA	Plasmid – CDS
AA 1005	Reverse	<i>AfiARF4</i>	ATGGTCTTTGTAGTCAAGCTTTT AAGGCCTCGTTACTGTCAAAG	Plasmid – CDS
AA 0510	Reverse	<i>AthETT</i>	ATGGTCTTTGTAGTCAAGCTTCT AGAGAGCAATGTC	Plasmid – CDS
AA 0388	Reverse	<i>AthARF4</i>	ATGGTCTTTGTAGTCAAGCTTTC AAACCCTAGTGATTGTA	Plasmid – CDS
AA 0279	Reverse	<i>SlyETT</i>	ATGGTCTTTGTAGTCAAGCTTCT ACAGAGCAATATCAAGAAGC	Plasmid – CDS
AA 0484	Reverse	<i>SlyARF4</i>	ATGGTCTTTGTAGTCAAGCTTTC AAATCCTGATTAC	Plasmid – CDS
AA 1204	Reverse	<i>AthETT- GbiARFL1</i>	ATGGTCTTTGTAGTCAAGCTTTT AAGGCCTCGTTACTGTCAAAG	Domain Swaps
AA 1205	Reverse	<i>AthETT- GbiARFL1</i>	ATGGTCTTTGTAGTCAAGCTTAC GCCCAAAGCTGGAAC	Domain Swaps
AA 1210	Reverse	<i>AthETT- AtrETT</i>	ATGGTCTTTGTAGTCAAGCTTTC AAACCCTAGTGATTGTA	Domain Swaps
AA 1211	Reverse	<i>AthETT- AtrETT</i>	ATGGTCTTTGTAGTCAAGCTTGC GGTTGGCTGTTTTATTCA	Domain Swaps
AA 1214	Reverse	<i>AthETT</i>	ATGGTCTTTGTAGTCAAGCTTGA GAGCAATGTCTAGCAACATGTC	Domain Swaps
AA 0101*	Forward	<i>arf4^{GE}</i>	AACAAGCACCTCCATTTAG	Genotyping – WT/mutant
AA 0132	Reverse	<i>arf4^{GE}</i>	TCCATTTACTCTGAGCTTTG	Genotyping – WT
AA 0598	Reverse	<i>arf4^{GE}</i>	ACACATCCCATAAACTCACA	Genotyping –mutant
AA 0438	Forward	<i>pAthETT 5'UTR</i>	AGAGGGTAAAAGTCATGAAG	Genotyping
AA 0284	Reverse	<i>pCambia 1305</i>	TCACTTATCGTCATCGTCCT	Genotyping
AA 0530	Reverse	<i>MpoARF2</i>	CTTTGGGTTGCAGTTGTT	Genotyping
AA 0536	Reverse	<i>CriARF3/4</i>	ACGATACTTTTGTATGGGGA	Genotyping
AA 0290	Forward	<i>GbiARF3/4</i>	GTGATTACCAGCAGCCTTTT	Genotyping
AA 0135	Forward	<i>AtrETT</i>	CGTTTTTCAGACTTTGGGGAA	Genotyping
AA 0192	Forward	<i>AtrARF4</i>	TTTTCTACAACCCAAGGGCA	Genotyping
AA 1077	Forward	<i>NthETT</i>	TGAATGCCAGAGTGTAGA	Genotyping
AA	Reverse	<i>NthARF4</i>	CATCCCAACGTACCATCA	Genotyping

0791				
AA 1019	Reverse	<i>AfiETT</i>	TGCATTGTCTCTCACACC	Genotyping
AA 1021	Reverse	<i>AfiARF4</i>	AACATCCAAACCCAGTCTA	Genotyping
AA 0100	Reverse	<i>AthETT</i>	CCCTCGCTTTAAATCTCATC	Genotyping
AA 0101*	Reverse	<i>AthARF4</i>	AACAAGCACCTCCATTTAG	Genotyping
AA 0302	Reverse	<i>SlyETT</i>	TCCTTCCATTTCTGCTCAAT	Genotyping
AA 0264	Forward	<i>SlyARF4</i>	TCAGACTGGGAATAAGAAGA	Genotyping
AA 0001	Forward	<i>UBQ10</i>	AGAACTCTTGCTGACTACAATAT CCAG	qPCR
AA 0002	Reverse	<i>UBQ10</i>	ATAGTTTTCCAGTCAACGTCTT AAC	qPCR
AA 0951	Forward	<i>AthETT</i>	CACCCTCTCCGTCTTGCTT	qPCR
AA 0952	Reverse	<i>AthETT</i>	TTGCTTTGAACAGCTGACGC	qPCR
AA 1186	Forward	<i>pCambia13 05 3'UTR</i>	AGTGAGGTGACCAGCTCGAA	qPCR
AA 1187	Reverse	<i>pCambia13 05 3'UTR</i>	AATCATCGCAAGACCGGCAA	qPCR
AK 205**	Forward	<i>PID</i>	ATTTACACTCTCTCCGTCATAGA CAAC	qPCR
AK 206**	Reverse	<i>PID</i>	ACATGTGTAGATATTCTAACGCC ACTA	qPCR

* indicates redundant primers used in multiple reactions.

** indicates primers obtained from Kuhn et al. (2020)

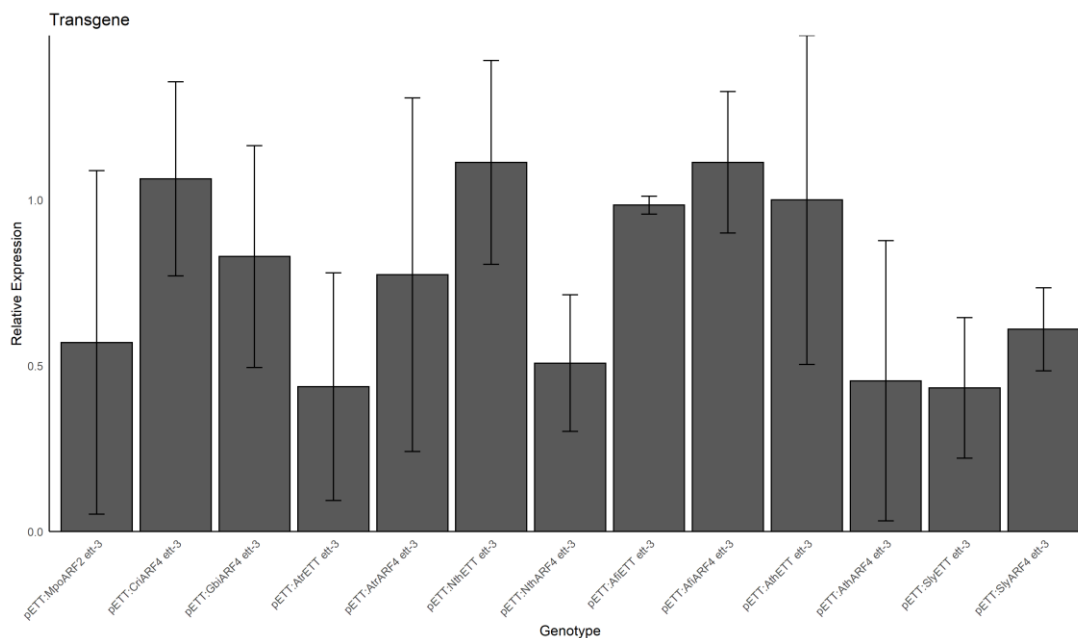


Figure S4.1: Expression level of ETT/ARF4-like orthologues in transgenic *ett-3* complementation lines. Relative transgene expression of all lines are normalised to the expression of the *pAthETT:AthETT ett-3* line. Bars plot the mean value and error bars represent the standard deviation of the mean ($n = 3$).

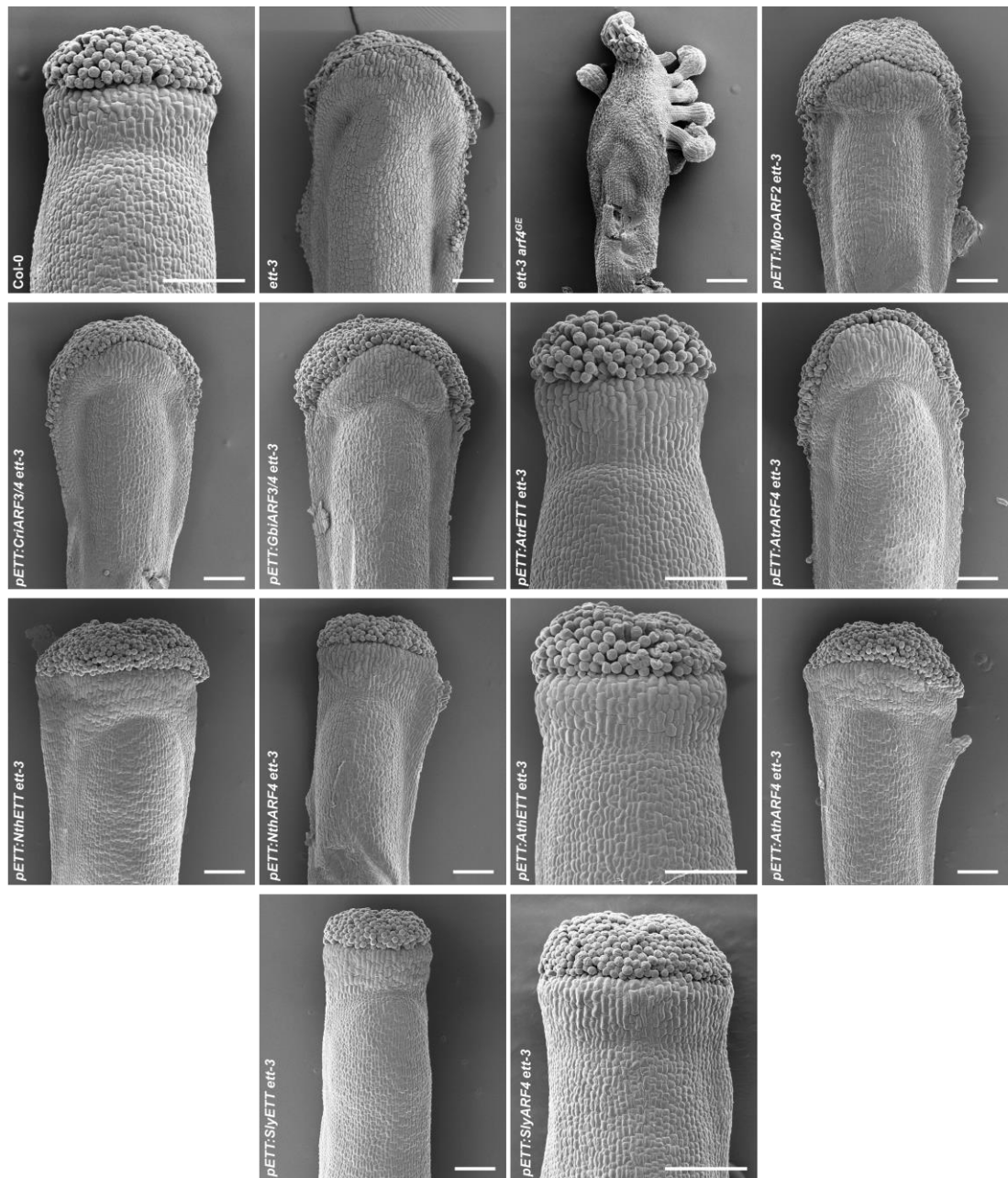


Figure S4.2: Lateral view of the gynoecium of wild-type, mutant and ETT/ARF4-like complementation lines. Scale bar represents 100 μ m.

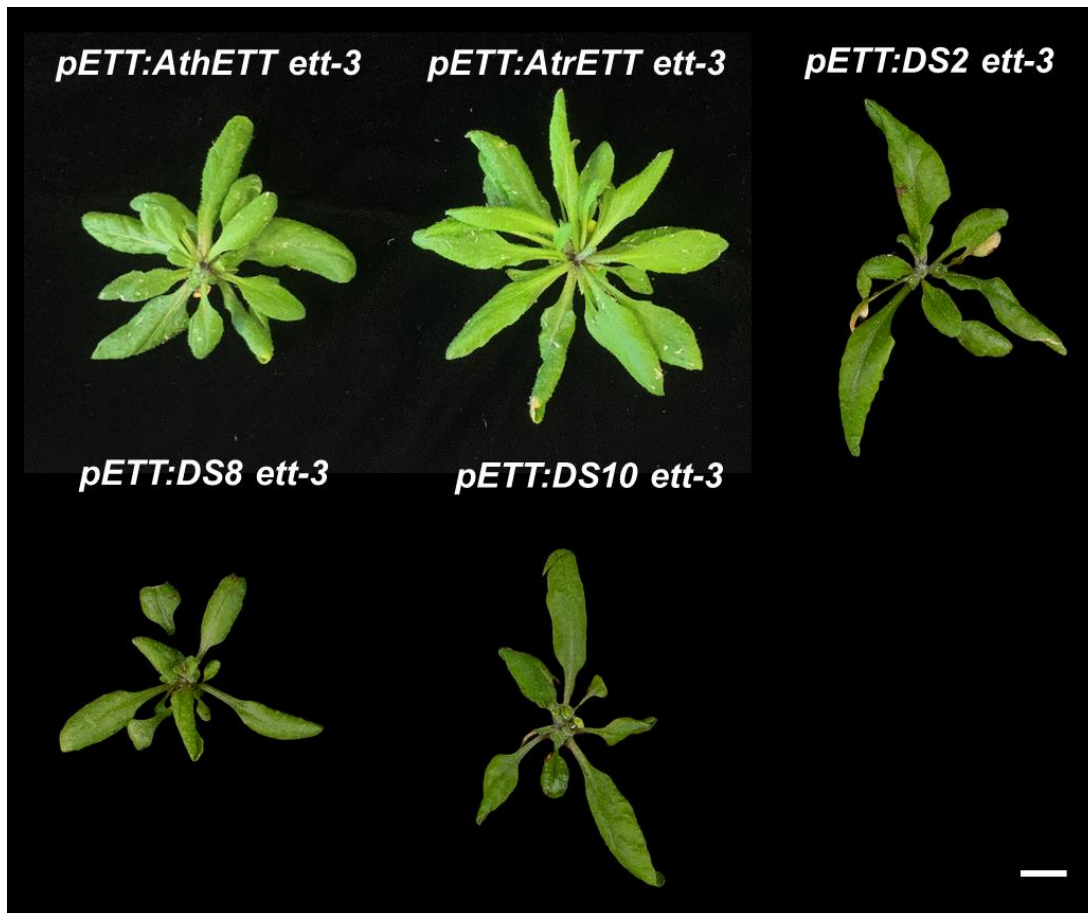


Figure S4.3: Rosette phenotypes of wild-type and *A. trichopoda* ETT-derived complementation lines. Scale bar represents 10 mm.

References

- Abel, S., and Theologis, A. (1996). Early genes and auxin action. *Plant Physiol* *111*, 9-17.
- Abley, K., De Reuille, P.B., Strutt, D., Bangham, A., Prusinkiewicz, P., Marée, A.F.M., Grieneisen, V.A., and Coen, E. (2013). An intracellular partitioning-based framework for tissue cell polarity in plants and animals. *Development* *140*, 2061-2074.
- Ahlmann-Eltze, C., and Patil, I. (2021). ggsignif: R Package for Displaying Significance Brackets for 'ggplot2'.
- Andres-Robin, A., Reymond, M.C., Dupire, A., Battu, V., Dubrulle, N., Mouille, G., Lefebvre, V., Pelloux, J., Boudaoud, A., Traas, J., *et al.* (2018). Evidence for the Regulation of Gynoecium Morphogenesis by ETTIN via Cell Wall Dynamics. *Plant Physiol* *178*, 1222-1232.
- Ang, A.C.H., and Østergaard, L. (2023). Save your TIRs – more to auxin than meets the eye. *New Phytologist* *238*, 971-976.
- Argout, X., Salse, J., Aury, J.-M., Guiltinan, M.J., Droc, G., Gouzy, J., Allegre, M., Chaparro, C., Legavre, T., Maximova, S.N., *et al.* (2011). The genome of *Theobroma cacao*. *Nature Genetics* *43*, 101-108.
- Arnault, G., Vialette, A.C.M., Andres-Robin, A., Fogliani, B., Gâteblé, G., and Scutt, C.P. (2018). Evidence for the Extensive Conservation of Mechanisms of Ovule Integument Development Since the Most Recent Common Ancestor of Living Angiosperms. *Frontiers in Plant Science* *9*.
- Arsuffi, G., and Braybrook, S.A. (2018). Acid growth: an ongoing trip. *J Exp Bot* *69*, 137-146.
- Ashe, H.L., and Briscoe, J. (2006). The interpretation of morphogen gradients. *Development* *133*, 385-394.
- Axtell, M.J., Snyder, J.A., and Bartel, D.P. (2007). Common functions for diverse small RNAs of land plants. *The Plant Cell* *19*, 1750-1769.
- Banks, J.A., Nishiyama, T., Hasebe, M., Bowman, J.L., Gribskov, M., dePamphilis, C., Albert, V.A., Aono, N., Aoyama, T., Ambrose, B.A., *et al.* (2011). The *Selaginella* Genome Identifies Genetic Changes Associated with the Evolution of Vascular Plants. *Science* *332*, 960-963.
- Barbez, E., Dünser, K., Gaidora, A., Lendl, T., and Busch, W. (2017). Auxin steers root cell expansion via apoplastic pH regulation in *Arabidopsis thaliana*. *Proceedings of the National Academy of Sciences* *114*, E4884-E4893.
- Bartlett, A., O'Malley, R.C., Huang, S.-s.C., Galli, M., Nery, J.R., Gallavotti, A., and Ecker, J.R. (2017). Mapping genome-wide transcription-factor binding sites using DAP-seq. *Nature Protocols* *12*, 1659-1672.
- Beavo, J.A., and Brunton, L.L. (2002). Cyclic nucleotide research—still expanding after half a century. *Nature reviews Molecular cell biology* *3*, 710-717.

Becker, A. (2020). A molecular update on the origin of the carpel. *Curr Opin Plant Biol* 53, 15-22.

Bellaoui, M., Pidkowich, M.S., Samach, A., Kushalappa, K., Kohalmi, S.E., Modrusan, Z., Crosby, W.L., and Haughn, G.W. (2001). The Arabidopsis BELL1 and KNOX TALE homeodomain proteins interact through a domain conserved between plants and animals. *The Plant Cell* 13, 2455-2470.

Benjamins, R., Quint, A., Weijers, D., Hooykaas, P., and Offringa, R. (2001). The PINOID protein kinase regulates organ development in Arabidopsis by enhancing polar auxin transport. *Development* 128, 4057-4067.

Benková, E., Michniewicz, M., Sauer, M., Teichmann, T., Seifertová, D., Jürgens, G., and Friml, J. (2003). Local, efflux-dependent auxin gradients as a common module for plant organ formation. *Cell* 115, 591-602.

Bennett, M.J., Marchant, A., Green, H.G., May, S.T., Ward, S.P., Millner, P.A., Walker, A.R., Schulz, B., and Feldmann, K.A. (1996). *Arabidopsis* AUX1 Gene: A Permease-Like Regulator of Root Gravitropism. *Science* 273, 948-950.

Bennett, T., Sieberer, T., Willett, B., Booker, J., Luschig, C., and Leyser, O. (2006). The Arabidopsis MAX Pathway Controls Shoot Branching by Regulating Auxin Transport. *Curr Biol* 16, 553-563.

Bennett, T.A., Liu, M.M., Aoyama, T., Bierfreund, N.M., Braun, M., Coudert, Y., Dennis, R.J., O'Connor, D., Wang, X.Y., and White, C.D. (2014). Plasma membrane-targeted PIN proteins drive shoot development in a moss. *Curr Biol* 24, 2776-2785.

Bhalerao, R.P., and Bennett, M.J. (2003). The case for morphogens in plants. *Nature Cell Biology* 5, 939-943.

Bharathan, G., Janssen, B.-J., Kellogg, E.A., and Sinha, N. (1999). Phylogenetic relationships and evolution of the KNOTTED class of plant homeodomain proteins. *Mol Biol Evol* 16, 553-563.

Bhatia, N., Åhl, H., Jönsson, H., and Heisler, M.G. (2019). Quantitative analysis of auxin sensing in leaf primordia argues against proposed role in regulating leaf dorsoventrality. *Elife* 8, e39298.

Binder, B.M. (2020). Ethylene signaling in plants. *J Biol Chem* 295, 7710-7725.

Birchler, J.A., and Yang, H. (2022). The multiple fates of gene duplications: Deletion, hypofunctionalization, subfunctionalization, neofunctionalization, dosage balance constraints, and neutral variation. *Plant Cell* 34, 2466-2474.

Blilou, I., Xu, J., Wildwater, M., Willemsen, V., Paponov, I., Friml, J., Heidstra, R., Aida, M., Palme, K., and Scheres, B. (2005). The PIN auxin efflux facilitator network controls growth and patterning in Arabidopsis roots. *Nature* 433, 39-44.

Boer, D.R., Freire-Rios, A., van den Berg, W.A., Saaki, T., Manfield, I.W., Kepinski, S., López-Vidriero, I., Franco-Zorrilla, J.M., de Vries, S.C., Solano, R., *et al.* (2014). Structural basis for DNA binding specificity by the auxin-dependent ARF transcription factors. *Cell* 156, 577-589.

- Bombarely, A., Moser, M., Amrad, A., Bao, M., Bapaume, L., Barry, C.S., Blied, M., Boersma, M.R., Borghi, L., Bruggmann, R., *et al.* (2016). Insight into the evolution of the Solanaceae from the parental genomes of *Petunia hybrida*. *Nat Plants* 2, 16074.
- Bowman, J.L. (2022). The origin of a land flora. *Nature Plants* 8, 1352-1369.
- Bowman, J.L., Kohchi, T., Yamato, K.T., Jenkins, J., Shu, S., Ishizaki, K., Yamaoka, S., Nishihama, R., Nakamura, Y., Berger, F., *et al.* (2017). Insights into Land Plant Evolution Garnered from the *Marchantia polymorpha* Genome. *Cell* 171, 287-304.e215.
- Branon, T.C., Bosch, J.A., Sanchez, A.D., Udeshi, N.D., Svinkina, T., Carr, S.A., Feldman, J.L., Perrimon, N., and Ting, A.Y. (2018). Efficient proximity labeling in living cells and organisms with TurbID. *Nature Biotechnology* 36, 880-887.
- Briginshaw, L.N., Flores-Sandoval, E., Dierschke, T., Alvarez, J.P., and Bowman, J.L. (2022). KANADI promotes thallus differentiation and FR-induced gametangioophore formation in the liverwort *Marchantia*. *New Phytologist* 234, 1377-1393.
- Briones-Moreno, A., Hernández-García, J., Vargas-Chávez, C., Blanco-Touriñán, N., Phokas, A., Úrbez, C., Cerdán, P.D., Coates, J.C., Alabadí, D., and Blázquez, M.A. (2023). DELLA functions evolved by rewiring of associated transcriptional networks. *Nature Plants* 9, 535-543.
- Brückner, A., Polge, C., Lentze, N., Auerbach, D., and Schlattner, U. (2009). Yeast two-hybrid, a powerful tool for systems biology. *Int J Mol Sci* 10, 2763-2788.
- Bui, L.T., Cordle, A.R., Irish, E.E., and Cheng, C.-L. (2015). Transient and stable transformation of *Ceratopteris richardii* gametophytes. *BMC Research Notes* 8, 214.
- Burian, A., Paszkiewicz, G., Nguyen, K.T., Meda, S., Raczyńska-Szajgin, M., and Timmermans, M.C.P. (2022). Specification of leaf dorsiventrality via a prepatterned binary readout of a uniform auxin input. *Nature Plants* 8, 269-280.
- Byrne, M.E., Barley, R., Curtis, M., Arroyo, J.M., Dunham, M., Hudson, A., and Martienssen, R.A. (2000). Asymmetric leaves1 mediates leaf patterning and stem cell function in *Arabidopsis*. *Nature* 408, 967-971.
- Cadigan, K.M., and Nusse, R. (1997). Wnt signaling: a common theme in animal development. *Genes Dev* 11, 3286-3305.
- Caggiano, M.P., Yu, X., Bhatia, N., Larsson, A., Ram, H., Ohno, C.K., Sappl, P., Meyerowitz, E.M., Jönsson, H., and Heisler, M.G. (2017). Cell type boundaries organize plant development. *Elife* 6, e27421.
- Cai, J., Liu, X., Vanneste, K., Proost, S., Tsai, W.-C., Liu, K.-W., Chen, L.-J., He, Y., Xu, Q., Bian, C., *et al.* (2015). The genome sequence of the orchid *Phalaenopsis equestris*. *Nature Genetics* 47, 65-72.
- Calderón Villalobos, L.I., Lee, S., De Oliveira, C., Ivetac, A., Brandt, W., Armitage, L., Sheard, L.B., Tan, X., Parry, G., Mao, H., *et al.* (2012). A combinatorial TIR1/AFB-Aux/IAA co-receptor system for differential sensing of auxin. *Nat Chem Biol* 8, 477-485.

- Cannell, N., Emms, D.M., Hetherington, A.J., MacKay, J., Kelly, S., Dolan, L., and Sweetlove, L.J. (2020). Multiple metabolic innovations and losses are associated with major transitions in land plant evolution. *Curr Biol* 30, 1783-1800. e1711.
- Cao, M., Chen, R., Li, P., Yu, Y., Zheng, R., Ge, D., Zheng, W., Wang, X., Gu, Y., Gelova, Z., *et al.* (2019). TMK1-mediated auxin signalling regulates differential growth of the apical hook. *Nature* 568, 240-243.
- Capella-Gutiérrez, S., Silla-Martínez, J.M., and Gabaldón, T. (2009). trimAl: a tool for automated alignment trimming in large-scale phylogenetic analyses. *Bioinformatics* 25, 1972-1973.
- Carey, S.B., Jenkins, J., Lovell, J.T., Maumus, F., Sreedasyam, A., Payton, A.C., Shu, S., Tiley, G.P., Fernandez-Pozo, N., Healey, A., *et al.* (2021). Gene-rich UV sex chromosomes harbor conserved regulators of sexual development. *Science Advances* 7, eabh2488.
- Carroll, S.B. (2001). Chance and necessity: the evolution of morphological complexity and diversity. *Nature* 409, 1102-1109.
- Castel, B., Tomlinson, L., Locci, F., Yang, Y., and Jones, J.D.G. (2019). Optimization of T-DNA architecture for Cas9-mediated mutagenesis in Arabidopsis. *PLOS ONE* 14, e0204778.
- Catarino, B., Hetherington, A.J., Emms, D.M., Kelly, S., and Dolan, L. (2016). The Stepwise Increase in the Number of Transcription Factor Families in the Precambrian Predated the Diversification of Plants On Land. *Mol Biol Evol* 33, 2815-2819.
- Causier, B., Lloyd, J., Stevens, L., and Davies, B. (2012). TOPLESS co-repressor interactions and their evolutionary conservation in plants. *Plant Signal Behav* 7, 325-328.
- Chan, A.P., Crabtree, J., Zhao, Q., Lorenzi, H., Orvis, J., Puiu, D., Melake-Berhan, A., Jones, K.M., Redman, J., Chen, G., *et al.* (2010). Draft genome sequence of the oilseed species *Ricinus communis*. *Nature Biotechnology* 28, 951-956.
- Chaw, S.-M., Liu, Y.-C., Wu, Y.-W., Wang, H.-Y., Lin, C.-Y.I., Wu, C.-S., Ke, H.-M., Chang, L.-Y., Hsu, C.-Y., Yang, H.-T., *et al.* (2019). Stout camphor tree genome fills gaps in understanding of flowering plant genome evolution. *Nature Plants* 5, 63-73.
- Chen, F., Dong, W., Zhang, J., Guo, X., Chen, J., Wang, Z., Lin, Z., Tang, H., and Zhang, L. (2018). The Sequenced Angiosperm Genomes and Genome Databases. *Frontiers in Plant Science* 9.
- Chen, J., Hao, Z., Guang, X., Zhao, C., Wang, P., Xue, L., Zhu, Q., Yang, L., Sheng, Y., Zhou, Y., *et al.* (2019). *Liriodendron* genome sheds light on angiosperm phylogeny and species–pair differentiation. *Nature Plants* 5, 18-25.
- Chen, J., Huang, Q., Gao, D., Wang, J., Lang, Y., Liu, T., Li, B., Bai, Z., Luis Goicoechea, J., Liang, C., *et al.* (2013). Whole-genome sequencing of *Oryza brachyantha* reveals mechanisms underlying *Oryza* genome evolution. *Nat Commun* 4, 1595.

Chen, M., Zhu, X., Liu, X., Wu, C., Yu, C., Hu, G., Chen, L., Chen, R., Bouzayen, M., Zouine, M., *et al.* (2021). Knockout of Auxin Response Factor SIARF4 Improves Tomato Resistance to Water Deficit. *Int J Mol Sci* 22.

Cheng, S., van den Bergh, E., Zeng, P., Zhong, X., Xu, J., Liu, X., Hofberger, J., de Bruijn, S., Bhide, A.S., Kuelahoglu, C., *et al.* (2013). The *Tarenaya hassleriana* Genome Provides Insight into Reproductive Trait and Genome Evolution of Crucifers. *The Plant Cell* 25, 2813-2830.

Cheng, S., Xian, W., Fu, Y., Marin, B., Keller, J., Wu, T., Sun, W., Li, X., Xu, Y., Zhang, Y., *et al.* (2019). Genomes of Subaerial Zygnematophyceae Provide Insights into Land Plant Evolution. *Cell* 179, 1057-1067.e1014.

Cheng, Y., Dai, X., and Zhao, Y. (2006). Auxin biosynthesis by the YUCCA flavin monooxygenases controls the formation of floral organs and vascular tissues in *Arabidopsis*. *Genes Dev* 20, 1790-1799.

Cheng, Y., Dai, X., and Zhao, Y. (2007). Auxin synthesized by the YUCCA flavin monooxygenases is essential for embryogenesis and leaf formation in *Arabidopsis*. *The Plant Cell* 19, 2430-2439.

Chitwood, D.H., Nogueira, F.T., Howell, M.D., Montgomery, T.A., Carrington, J.C., and Timmermans, M.C. (2009). Pattern formation via small RNA mobility. *Gene Dev* 23, 549-554.

Choi, H.-S., Seo, M., and Cho, H.-T. (2018). Two TPL-binding motifs of ARF2 are involved in repression of auxin responses. *Frontiers in Plant Science* 9, 372.

Clark, J.W. (2023). Genome evolution in plants and the origins of innovation. *New Phytologist* 240, 2204-2209.

Clough, S.J., and Bent, A.F. (1998). Floral dip: a simplified method for *Agrobacterium*-mediated transformation of *Arabidopsis thaliana*. *Plant J* 16, 735-743.

Consortium, T.I.W.G.S., Mayer, K.F.X., Rogers, J., Doležel, J., Pozniak, C., Eversole, K., Feuillet, C., Gill, B., Friebe, B., Lukaszewski, A.J., *et al.* (2014). A chromosome-based draft sequence of the hexaploid bread wheat (*Triticum aestivum*) genome. *Science* 345, 1251788.

Crane, P.R., and Kenrick, P. (1997). Diverted development of reproductive organs: A source of morphological innovation in land plants. *Plant Systematics and Evolution* 206, 161-174.

Crooks, G.E., Hon, G., Chandonia, J.M., and Brenner, S.E. (2004). WebLogo: a sequence logo generator. *Genome Res* 14, 1188-1190.

Cui, L., Wall, P.K., Leebens-Mack, J.H., Lindsay, B.G., Soltis, D.E., Doyle, J.J., Soltis, P.S., Carlson, J.E., Arumuganathan, K., and Barakat, A. (2006). Widespread genome duplications throughout the history of flowering plants. *Genome Res* 16, 738-749.

D'Hont, A., Denoeud, F., Aury, J.-M., Baurens, F.-C., Carreel, F., Garsmeur, O., Noel, B., Bocs, S., Droc, G., Rouard, M., *et al.* (2012). The banana (*Musa*

- acuminata) genome and the evolution of monocotyledonous plants. *Nature* **488**, 213-217.
- Daccord, N., Celton, J.-M., Linsmith, G., Becker, C., Choisine, N., Schijlen, E., van de Geest, H., Bianco, L., Micheletti, D., Velasco, R., *et al.* (2017). High-quality de novo assembly of the apple genome and methylome dynamics of early fruit development. *Nature Genetics* **49**, 1099-1106.
- Dassanayake, M., Oh, D.-H., Haas, J.S., Hernandez, A., Hong, H., Ali, S., Yun, D.-J., Bressan, R.A., Zhu, J.-K., Bohnert, H.J., *et al.* (2011). The genome of the extremophile crucifer *Thellungiella parvula*. *Nature Genetics* **43**, 913-918.
- De Vega, J.J., Ayling, S., Hegarty, M., Kudrna, D., Goicoechea, J.L., Ergon, Å., Rognli, O.A., Jones, C., Swain, M., Geurts, R., *et al.* (2015). Red clover (*Trifolium pratense* L.) draft genome provides a platform for trait improvement. *Sci Rep-Uk* **5**, 17394.
- de Vries, J., Curtis, B.A., Gould, S.B., and Archibald, J.M. (2018). Embryophyte stress signaling evolved in the algal progenitors of land plants. *Proc Natl Acad Sci U S A* **115**, E3471-e3480.
- de Vries, J., Fischer, A.M., Roettger, M., Rommel, S., Schlupepmann, H., Bräutigam, A., Carlsbecker, A., and Gould, S.B. (2016). Cytokinin-induced promotion of root meristem size in the fern *Azolla* supports a shoot-like origin of euphyllophyte roots. *New Phytologist* **209**, 705-720.
- Degnan, B.M., Vervoort, M., Larroux, C., and Richards, G.S. (2009). Early evolution of metazoan transcription factors. *Current opinion in genetics & development* **19**, 591-599.
- Denoëud, F., Carretero-Paulet, L., Dereeper, A., Droc, G., Guyot, R., Pietrella, M., Zheng, C., Alberti, A., Anthony, F., Aprea, G., *et al.* (2014). The coffee genome provides insight into the convergent evolution of caffeine biosynthesis. *Science* **345**, 1181-1184.
- Dharmasiri, N., Dharmasiri, S., Weijers, D., Lechner, E., Yamada, M., Hobbie, L., Ehrismann, J.S., Jürgens, G., and Estelle, M. (2005). Plant development is regulated by a family of auxin receptor F box proteins. *Dev Cell* **9**, 109-119.
- Dierschke, T., Flores-Sandoval, E., Rast-Somssich, M.I., Althoff, F., Zachgo, S., and Bowman, J.L. (2021). Gamete expression of TALE class HD genes activates the diploid sporophyte program in *Marchantia polymorpha*. *Elife* **10**, e57088.
- Ding, B., Xia, R., Lin, Q., Gurung, V., Sagawa, J.M., Stanley, L.E., Strobel, M., Diggle, P.K., Meyers, B.C., and Yuan, Y.W. (2020). Developmental Genetics of Corolla Tube Formation: Role of the tasiRNA-ARF Pathway and a Conceptual Model. *Plant Cell* **32**, 3452-3468.
- Ding, Y.L., Sun, T.J., Ao, K., Peng, Y.J., Zhang, Y.X., Li, X., and Zhang, Y.L. (2018). Opposite Roles of Salicylic Acid Receptors NPR1 and NPR3/NPR4 in Transcriptional Regulation of Plant Immunity. *Cell* **173**, 1454-+.
- Diop, S.I., Subotic, O., Giraldo-Fonseca, A., Waller, M., Kirbis, A., Neubauer, A., Potente, G., Murray-Watson, R., Boskovic, F., Bont, Z., *et al.* (2020). A

pseudomolecule-scale genome assembly of the liverwort *Marchantia polymorpha*. *The Plant Journal* *101*, 1378-1396.

Dohm, J.C., Minoche, A.E., Holtgräwe, D., Capella-Gutiérrez, S., Zakrzewski, F., Tafer, H., Rupp, O., Sörensen, T.R., Stracke, R., Reinhardt, R., *et al.* (2014). The genome of the recently domesticated crop plant sugar beet (*Beta vulgaris*). *Nature* *505*, 546-549.

Dong, X., Li, Y., Guan, Y., Wang, S., Luo, H., Li, X., Li, H., and Zhang, Z. (2021). Auxin-induced AUXIN RESPONSE FACTOR4 activates APETALA1 and FRUITFULL to promote flowering in woodland strawberry. *Horticulture Research* *8*, 115.

Douglas, R.N., Wiley, D., Sarkar, A., Springer, N., Timmermans, M.C.P., and Scanlon, M.J. (2010). ragged seedling2 Encodes an ARGONAUTE7-Like Protein Required for Mediolateral Expansion, but Not Dorsiventrality, of Maize Leaves *The Plant Cell* *22*, 1441-1451.

Driever, W., and Nüsslein-Volhard, C. (1988). The bicoid protein determines position in the *Drosophila* embryo in a concentration-dependent manner. *Cell* *54*, 95-104.

Driever, W., Thoma, G., and Nüsslein-Volhard, C. (1989). Determination of spatial domains of zygotic gene expression in the *Drosophila* embryo by the affinity of binding sites for the bicoid morphogen. *Nature* *340*, 363-367.

Dubreuil, B., Matalon, O., and Levy, E.D. (2019). Protein Abundance Biases the Amino Acid Composition of Disordered Regions to Minimize Non-functional Interactions. *J Mol Biol* *431*, 4978-4992.

Dupré, P., Lacoux, J., Neutelings, G., Mattar-Laurain, D., Fliniaux, M.-A., David, A., and Jacquín-Dubreuil, A. (2000). Genetic transformation of *Ginkgo biloba* by *Agrobacterium tumefaciens*. *Physiologia Plantarum* *108*, 413-419.

Edwards, D., Morris, J.L., Richardson, J.B., and Kenrick, P. (2014). Cryptospores and cryptophytes reveal hidden diversity in early land floras. *New Phytologist* *202*, 50-78.

Egea-Cortines, M., Saedler, H., and Sommer, H. (1999). Ternary complex formation between the MADS-box proteins SQUAMOSA, DEFICIENS and GLOBOSA is involved in the control of floral architecture in *Antirrhinum majus*. *EMBO J* *18*, 5370-5379.

Emery, J.F., Floyd, S.K., Alvarez, J., Eshed, Y., Hawker, N.P., Izhaki, A., Baum, S.F., and Bowman, J.L. (2003). Radial Patterning of *Arabidopsis* Shoots by Class III HD-ZIP and KANADI Genes. *Curr Biol* *13*, 1768-1774.

Endress, P.K., and Doyle, J.A. (2015). Ancestral traits and specializations in the flowers of the basal grade of living angiosperms. *TAXON* *64*, 1093-1116.

Endress, P.K., and Igersheim, A. (2000). Gynoecium structure and evolution in basal angiosperms. *International Journal of Plant Sciences* *161*, S211-S223.

Engler, C., and Marillonnet, S. (2014). Golden Gate cloning. *Methods Mol Biol* *1116*, 119-131.

- Fahlgren, N., Montgomery, T.A., Howell, M.D., Allen, E., Dvorak, S.K., Alexander, A.L., and Carrington, J.C. (2006). Regulation of AUXIN RESPONSE FACTOR3 by TAS3 ta-siRNA affects developmental timing and patterning in Arabidopsis. *Curr Biol* 16, 939-944.
- Fang, Y., Qin, X., Liao, Q., Du, R., Luo, X., Zhou, Q., Li, Z., Chen, H., Jin, W., Yuan, Y., *et al.* (2022). The genome of homosporous maidenhair fern sheds light on the euphyllophyte evolution and defences. *Nature Plants* 8, 1024-1037.
- Fendrych, M., Akhmanova, M., Merrin, J., Glanc, M., Hagihara, S., Takahashi, K., Uchida, N., Torii, K.U., and Friml, J. (2018). Rapid and reversible root growth inhibition by TIR1 auxin signalling. *Nature Plants* 4, 453-459.
- Fendrych, M., Leung, J., and Friml, J. (2016). TIR1/AFB-Aux/IAA auxin perception mediates rapid cell wall acidification and growth of Arabidopsis hypocotyls. *Elife* 5, e19048.
- Finet, C., Berne-Dedieu, A., Scutt, C.P., and Marletaz, F. (2013). Evolution of the ARF Gene Family in Land Plants: Old Domains, New Tricks. *Mol Biol Evol* 30, 45-56.
- Finet, C., Floyd, S.K., Conway, S.J., Zhong, B., Scutt, C.P., and Bowman, J.L. (2016). Evolution of the YABBY gene family in seed plants. *Evolution & Development* 18, 116-126.
- Finet, C., Fourquin, C., Vinauger, M., Berne-Dedieu, A., Chambrier, P., Paindavoine, S., and Scutt, C.P. (2010). Parallel structural evolution of auxin response factors in the angiosperms. *Plant J* 63, 952-959.
- Finn, R.D., Clements, J., and Eddy, S.R. (2011). HMMER web server: interactive sequence similarity searching. *Nucleic Acids Res* 39, W29-37.
- Flores-Sandoval, E., Eklund, D.M., and Bowman, J.L. (2015). A simple auxin transcriptional response system regulates multiple morphogenetic processes in the liverwort *Marchantia polymorpha*. *Plos Genet* 11, e1005207.
- Flores-Sandoval, E., Eklund, D.M., Hong, S.-F., Alvarez, J.P., Fisher, T.J., Lampugnani, E.R., Golz, J.F., Vázquez-Lobo, A., Dierschke, T., Lin, S.-S., *et al.* (2018). Class C ARFs evolved before the origin of land plants and antagonize differentiation and developmental transitions in *Marchantia polymorpha*. *New Phytologist* 218, 1612-1630.
- Floyd, Sandra K., and Bowman, John L. (2007). The Ancestral Developmental Tool Kit of Land Plants. *International Journal of Plant Sciences* 168, 1-35.
- Floyd, S.K., Zalewski, C.S., and Bowman, J.L. (2006). Evolution of Class III Homeodomain–Leucine Zipper Genes in Streptophytes. *Genetics* 173, 373-388.
- Fourquin, C., Vinauger-Douard, M., Chambrier, P., Berne-Dedieu, A., and Scutt, C.P. (2007). Functional Conservation between CRABS CLAW Orthologues from Widely Diverged Angiosperms. *Annals of Botany* 100, 651-657.
- Freire-Rios, A., Tanaka, K., Crespo, I., van der Wijk, E., Sizentsova, Y., Levitsky, V., Lindhoud, S., Fontana, M., Hohlbein, J., Boer, D.R., *et al.* (2020). Architecture of DNA elements mediating ARF transcription factor binding and auxin-responsive

gene expression in *Arabidopsis*. Proceedings of the National Academy of Sciences 117, 24557-24566.

Friml, J., Gallei, M., Gelova, Z., Johnson, A., Mazur, E., Monzer, A., Rodriguez, L., Roosjen, M., Verstraeten, I., Zivanovic, B.D., *et al.* (2022). ABP1-TMK auxin perception for global phosphorylation and auxin canalization. Nature 609, 575-581.

Friml, J., Vieten, A., Sauer, M., Weijers, D., Schwarz, H., Hamann, T., Offringa, R., and Jürgens, G. (2003). Efflux-dependent auxin gradients establish the apical-basal axis of Arabidopsis. Nature 426, 147-153.

Friml, J., Wiśniewska, J., Benková, E., Mendgen, K., and Palme, K. (2002). Lateral relocation of auxin efflux regulator PIN3 mediates tropism in Arabidopsis. Nature 415, 806-809.

Friml, J., Yang, X., Michniewicz, M., Weijers, D., Quint, A., Tietz, O., Benjamins, R., Ouwerkerk, P.B.F., Ljung, K., Sandberg, G., *et al.* (2004). A PINOID-Dependent Binary Switch in Apical-Basal PIN Polar Targeting Directs Auxin Efflux. Science 306, 862-865.

Frohnhofer, H.G., and Nüsslein-Volhard, C. (1986). Organization of anterior pattern in the Drosophila embryo by the maternal gene bicoid. Nature 324, 120-125.

Furumizu, C., Alvarez, J.P., Sakakibara, K., and Bowman, J.L. (2015). Antagonistic roles for KNOX1 and KNOX2 genes in patterning the land plant body plan following an ancient gene duplication. Plos Genet 11, e1004980.

Gade, P., and Kalvakolanu, D.V. (2012). Chromatin immunoprecipitation assay as a tool for analyzing transcription factor activity. Methods Mol Biol 809, 85-104.

Galli, M., Khakhar, A., Lu, Z., Chen, Z., Sen, S., Joshi, T., Nemhauser, J.L., Schmitz, R.J., and Gallavotti, A. (2018). The DNA binding landscape of the maize AUXIN RESPONSE FACTOR family. Nat Commun 9, 4526.

Galvan-Ampudia, C.S., Cerutti, G., Legrand, J., Brunoud, G., Martin-Arevalillo, R., Azais, R., Bayle, V., Moussu, S., Wenzl, C., Jaillais, Y., *et al.* (2020). Temporal integration of auxin information for the regulation of patterning. Elife 9, e55832.

Gälweiler, L., Guan, C., Müller, A., Wisman, E., Mendgen, K., Yephremov, A., and Palme, K. (1998). Regulation of polar auxin transport by AtPIN1 in Arabidopsis vascular tissue. Science 282, 2226-2230.

Gammons, M., and Bienz, M. (2018). Multiprotein complexes governing Wnt signal transduction. Current Opinion in Cell Biology 51, 42-49.

Gao, B., Wang, L., Oliver, M., Chen, M., and Zhang, J. (2020). Phylogenomic synteny network analyses reveal ancestral transpositions of auxin response factor genes in plants. Plant Methods 16, 70.

Gao, Q., and Finkelstein, R. (1998). Targeting gene expression to the head: the Drosophila orthodenticle gene is a direct target of the Bicoid morphogen. Development 125, 4185-4193.

Gao, Y., Zhang, Y., Zhang, D., Dai, X., Estelle, M., and Zhao, Y. (2015). Auxin binding protein 1 (ABP1) is not required for either auxin signaling or

Arabidopsis development. Proceedings of the National Academy of Sciences *112*, 2275-2280.

Garcia-Mas, J., Benjak, A., Sanseverino, W., Bourgeois, M., Mir, G., González, V.M., Hénaff, E., Câmara, F., Cozzuto, L., Lowy, E., *et al.* (2012). The genome of melon (*Cucumis melo* L.). Proceedings of the National Academy of Sciences *109*, 11872-11877.

Garcia, D., Collier, S.A., Byrne, M.E., and Martienssen, R.A. (2006). Specification of Leaf Polarity in *Arabidopsis* via the trans-Acting siRNA Pathway. *Curr Biol* *16*, 933-938.

Geldner, N., Friml, J., Stierhof, Y.-D., Jürgens, G., and Palme, K. (2001). Auxin transport inhibitors block PIN1 cycling and vesicle trafficking. *Nature* *413*, 425-428.

Gil-Garcia, M., Iglesias, V., Pallarès, I., and Ventura, S. (2021). Prion-like proteins: from computational approaches to proteome-wide analysis. *FEBS Open Bio* *11*, 2400-2417.

Goodstein, D.M., Shu, S., Howson, R., Neupane, R., Hayes, R.D., Fazo, J., Mitros, T., Dirks, W., Hellsten, U., Putnam, N., *et al.* (2011). Phytozome: a comparative platform for green plant genomics. *Nucleic Acids Res* *40*, D1178-D1186.

Gorelova, V. (2023). Gateway to morphogenesis: TIR1 auxin receptor is essential for cellular differentiation and organ formation in *Marchantia polymorpha*. *The Plant Cell* *35*, 965-966.

Gray, W.M., Kepinski, S., Rouse, D., Leyser, O., and Estelle, M. (2001). Auxin regulates SCFTIR1-dependent degradation of AUX/IAA proteins. *Nature* *414*, 271-276.

Gremski, K., Ditta, G., and Yanofsky, M.F. (2007). The HECATE genes regulate female reproductive tract development in *Arabidopsis thaliana*.

Gu, B., Dong, H., Smith, C., Cui, G., Li, Y., and Bevan, M.W. (2022). Modulation of receptor-like transmembrane kinase 1 nuclear localization by DA1 peptidases in *Arabidopsis*. *Proc Natl Acad Sci U S A* *119*, e2205757119.

Guan, C., Du, F., and Jiao, Y. (2018). Uniform distribution of 35S promoter-driven mDII auxin control sensor in leaf primordia. *bioRxiv*, 293753.

Guan, C., Wu, B., Yu, T., Wang, Q., Krogan, N.T., Liu, X., and Jiao, Y. (2017). Spatial Auxin Signaling Controls Leaf Flattening in *Arabidopsis*. *Curr Biol* *27*, 2940-2950.e2944.

Guan, R., Zhao, Y., Zhang, H., Fan, G., Liu, X., Zhou, W., Shi, C., Wang, J., Liu, W., Liang, X., *et al.* (2016). Draft genome of the living fossil *Ginkgo biloba*. *Gigascience* *5*, 49.

Guilfoyle, T.J., and Hagen, G. (2001). Auxin response factors. *Journal of Plant Growth Regulation* *20*.

Guo, C., Luo, Y., Gao, L.-M., Yi, T.-S., Li, H.-T., Yang, J.-B., and Li, D.-Z. (2023). Phylogenomics and the flowering plant tree of life. *J Integr Plant Biol* *65*, 299-323.

- Guo, H., and Ecker, J.R. (2003). Plant responses to ethylene gas are mediated by SCF(EBF1/EBF2)-dependent proteolysis of EIN3 transcription factor. *Cell* 115, 667-677.
- Guo, S., Zhang, J., Sun, H., Salse, J., Lucas, W.J., Zhang, H., Zheng, Y., Mao, L., Ren, Y., Wang, Z., *et al.* (2013). The draft genome of watermelon (*Citrullus lanatus*) and resequencing of 20 diverse accessions. *Nature Genetics* 45, 51-58.
- Hager, A., Menzel, H., and Krauss, A. (1971). [Experiments and hypothesis concerning the primary action of auxin in elongation growth]. *Planta* 100, 47-75.
- Han, X., Rong, H., Feng, Y., Xin, Y., Luan, X., Zhou, Q., Xu, M., and Xu, L.A. (2023). Protoplast isolation and transient transformation system for *Ginkgo biloba* L. *Front Plant Sci* 14, 1145754.
- Harkess, A., Zhou, J., Xu, C., Bowers, J.E., Van der Hulst, R., Ayyampalayam, S., Mercati, F., Riccardi, P., McKain, M.R., Kakrana, A., *et al.* (2017). The asparagus genome sheds light on the origin and evolution of a young Y chromosome. *Nat Commun* 8, 1279.
- Harrison, C.J., Corley, S.B., Moylan, E.C., Alexander, D.L., Scotland, R.W., and Langdale, J.A. (2005). Independent recruitment of a conserved developmental mechanism during leaf evolution. *Nature* 434, 509-514.
- Harrison, C.J., and Morris, J.L. (2018). The origin and early evolution of vascular plant shoots and leaves. *Philos Trans R Soc Lond B Biol Sci* 373.
- Harrison, C.J., Rezvani, M., and Langdale, J.A. (2007). Growth from two transient apical initials in the meristem of *Selaginella kraussiana*.
- Hawkins, C., and Liu, Z. (2014). A model for an early role of auxin in *Arabidopsis* gynoecium morphogenesis. *Frontiers in Plant Science* 5.
- Hay, A., Barkoulas, M., and Tsiantis, M. (2006). ASYMMETRIC LEAVES1 and auxin activities converge to repress BREVIPEDICELLUS expression and promote leaf development in *Arabidopsis*. *Development* 133, 3955-3961.
- He, Q., Tang, S., Zhi, H., Chen, J., Zhang, J., Liang, H., Alam, O., Li, H., Zhang, H., Xing, L., *et al.* (2023). A graph-based genome and pan-genome variation of the model plant *Setaria*. *Nature Genetics* 55, 1232-1242.
- Healey, A.L., Piatkowski, B., Lovell, J.T., Sreedasyam, A., Carey, S.B., Mamidi, S., Shu, S., Plott, C., Jenkins, J., Lawrence, T., *et al.* (2023). Newly identified sex chromosomes in the *Sphagnum* (peat moss) genome alter carbon sequestration and ecosystem dynamics. *Nature Plants* 9, 238-254.
- Heisler, M.G., Atkinson, A., Bylstra, Y.H., Walsh, R., and Smyth, D.R. (2001). SPATULA, a gene that controls development of carpel margin tissues in *Arabidopsis*, encodes a bHLH protein. *Development* 128, 1089-1098.
- Heisler, M.G., Ohno, C., Das, P., Sieber, P., Reddy, G.V., Long, J.A., and Meyerowitz, E.M. (2005). Patterns of auxin transport and gene expression during primordium development revealed by live imaging of the *Arabidopsis* inflorescence meristem. *Curr Biol* 15, 1899-1911.

- Hellsten, U., Wright, K.M., Jenkins, J., Shu, S., Yuan, Y., Wessler, S.R., Schmutz, J., Willis, J.H., and Rokhsar, D.S. (2013). Fine-scale variation in meiotic recombination in *Mimulus* inferred from population shotgun sequencing. *Proc Natl Acad Sci U S A* *110*, 19478-19482.
- Hertel, R., Thomson, K.S., and Russo, V.E.A. (1972). In-vitro auxin binding to particulate cell fractions from corn coleoptiles. *Planta* *107*, 325-340.
- Hesse, T., Feldwisch, J., Balshüsemann, D., Bauw, G., Puype, M., Vandekerckhove, J., Löbner, M., Klämbt, D., Schell, J., and Palme, K. (1989). Molecular-cloning and structural-analysis of a gene from *Zea-Mays* (L) coding for a putative receptor for the plant hormone auxin. *EMBO J* *8*, 2453-2461.
- Hetherington, A.J., and Dolan, L. (2018). Stepwise and independent origins of roots among land plants. *Nature* *561*, 235-238.
- Hirsch, C.N., Hirsch, C.D., Brohammer, A.B., Bowman, M.J., Soifer, I., Barad, O., Shem-Tov, D., Baruch, K., Lu, F., Hernandez, A.G., *et al.* (2016). Draft Assembly of Elite Inbred Line PH207 Provides Insights into Genomic and Transcriptome Diversity in Maize. *The Plant Cell* *28*, 2700-2714.
- Hisanaga, T., Fujimoto, S., Cui, Y., Sato, K., Sano, R., Yamaoka, S., Kohchi, T., Berger, F., and Nakajima, K. (2021). Deep evolutionary origin of gamete-directed zygote activation by KNOX/BELL transcription factors in green plants. *Elife* *10*, e57090.
- Hofmeister, W. (1862). On the germination, development, and fructification of the higher Cryptogamia: and on the fructification of the coniferae (Corinthian Press).
- Hori, K., Maruyama, F., Fujisawa, T., Togashi, T., Yamamoto, N., Seo, M., Sato, S., Yamada, T., Mori, H., Tajima, N., *et al.* (2014). Klebsormidium flaccidum genome reveals primary factors for plant terrestrial adaptation. *Nat Commun* *5*, 3978.
- Horst, N.A., Katz, A., Pereman, I., Decker, E.L., Ohad, N., and Reski, R. (2016). A single homeobox gene triggers phase transition, embryogenesis and asexual reproduction. *Nature Plants* *2*, 1-6.
- Hu, L., Xu, Z., Wang, M., Fan, R., Yuan, D., Wu, B., Wu, H., Qin, X., Yan, L., Tan, L., *et al.* (2019). The chromosome-scale reference genome of black pepper provides insight into piperine biosynthesis. *Nat Commun* *10*, 4702.
- Hu, T.T., Pattyn, P., Bakker, E.G., Cao, J., Cheng, J.-F., Clark, R.M., Fahlgren, N., Fawcett, J.A., Grimwood, J., Gundlach, H., *et al.* (2011). The *Arabidopsis lyrata* genome sequence and the basis of rapid genome size change. *Nature Genetics* *43*, 476-481.
- Huang, R., Zheng, R., He, J., Zhou, Z., Wang, J., Xiong, Y., and Xu, T. (2019). Noncanonical auxin signaling regulates cell division pattern during lateral root development. *Proc Natl Acad Sci U S A* *116*, 21285-21290.
- Huang, S., Ding, J., Deng, D., Tang, W., Sun, H., Liu, D., Zhang, L., Niu, X., Zhang, X., Meng, M., *et al.* (2013a). Draft genome of the kiwifruit *Actinidia chinensis*. *Nat Commun* *4*, 2640.

Huang, X., Wang, W., Gong, T., Wickell, D., Kuo, L.-Y., Zhang, X., Wen, J., Kim, H., Lu, F., Zhao, H., *et al.* (2022). The flying spider-monkey tree fern genome provides insights into fern evolution and arborescence. *Nature Plants* 8, 500-512.

Huang, Z., Van Houten, J., Gonzalez, G., Xiao, H., and van der Knaap, E. (2013b). Genome-wide identification, phylogeny and expression analysis of SUN, OFP and YABBY gene family in tomato. *Mol Genet Genomics* 288, 111-129.

Husbands, A.Y., Benkovics, A.H., Nogueira, F.T., Lodha, M., and Timmermans, M.C. (2015). The ASYMMETRIC LEAVES complex employs multiple modes of regulation to affect adaxial-abaxial patterning and leaf complexity. *The Plant Cell* 27, 3321-3335.

Ibarra-Laclette, E., Lyons, E., Hernández-Guzmán, G., Pérez-Torres, C.A., Carretero-Paulet, L., Chang, T.-H., Lan, T., Welch, A.J., Juárez, M.J.A., Simpson, J., *et al.* (2013). Architecture and evolution of a minute plant genome. *Nature* 498, 94-98.

Iorizzo, M., Ellison, S., Senalik, D., Zeng, P., Satapoomin, P., Huang, J., Bowman, M., Iovene, M., Sanseverino, W., Cavagnaro, P., *et al.* (2016). A high-quality carrot genome assembly provides new insights into carotenoid accumulation and asterid genome evolution. *Nature Genetics* 48, 657-666.

Islam, M.S., Saito, J.A., Emdad, E.M., Ahmed, B., Islam, M.M., Halim, A., Hossen, Q.M.M., Hossain, M.Z., Ahmed, R., Hossain, M.S., *et al.* (2017). Comparative genomics of two jute species and insight into fibre biogenesis. *Nature Plants* 3, 16223.

Iwasaki, M., Takahashi, H., Iwakawa, H., Nakagawa, A., Ishikawa, T., Tanaka, H., Matsumura, Y., Pekker, I., Eshed, Y., Vial-Pradel, S., *et al.* (2013). Dual regulation of ETTIN (ARF3) gene expression by AS1-AS2, which maintains the DNA methylation level, is involved in stabilization of leaf adaxial-abaxial partitioning in *Arabidopsis*. *Development* 140, 1958-1969.

Jackson, D., Veit, B., and Hake, S. (1994). Expression of maize KNOTTED1 related homeobox genes in the shoot apical meristem predicts patterns of morphogenesis in the vegetative shoot. *Development* 120, 405-413.

Jaillon, O., Aury, J.-M., Noel, B., Policriti, A., Clepet, C., Casagrande, A., Choisne, N., Aubourg, S., Vitulo, N., Jubin, C., *et al.* (2007). The grapevine genome sequence suggests ancestral hexaploidization in major angiosperm phyla. *Nature* 449, 463-467.

Jarvis, D.E., Ho, Y.S., Lightfoot, D.J., Schmöckel, S.M., Li, B., Borm, T.J.A., Ohyanagi, H., Mineta, K., Mitchell, C.T., Saber, N., *et al.* (2017). The genome of *Chenopodium quinoa*. *Nature* 542, 307-312.

Jiao, C., Sørensen, I., Sun, X., Sun, H., Behar, H., Alseekh, S., Philippe, G., Palacio Lopez, K., Sun, L., Reed, R., *et al.* (2020). The *Penium margaritaceum* Genome: Hallmarks of the Origins of Land Plants. *Cell* 181, 1097-1111.e1012.

Jiao, Y., Leebens-Mack, J., Ayyampalayam, S., Bowers, J.E., McKain, M.R., McNeal, J., Rolf, M., Ruzicka, D.R., Wafula, E., Wickett, N.J., *et al.* (2012). A genome triplication associated with early diversification of the core eudicots. *Genome Biol* 13, R3.

Jill Harrison, C. (2017). Development and genetics in the evolution of land plant body plans. *Philosophical Transactions of the Royal Society B: Biological Sciences* 372, 20150490.

Jin, Q., Scherp, P., Heimann, K., and Hasenstein, K.H. (2008). Auxin and cytoskeletal organization in algae. *Cell Biology International* 32, 542-545.

Jin, R., Klasfeld, S., Zhu, Y., Fernandez Garcia, M., Xiao, J., Han, S.-K., Konkol, A., and Wagner, D. (2021). LEAFY is a pioneer transcription factor and licenses cell reprogramming to floral fate. *Nat Commun* 12, 626.

Juarez, M.T., Kui, J.S., Thomas, J., Heller, B.A., and Timmermans, M.C. (2004). microRNA-mediated repression of rolled leaf1 specifies maize leaf polarity. *Nature* 428, 84-88.

Jumper, J., Evans, R., Pritzel, A., Green, T., Figurnov, M., Ronneberger, O., Tunyasuvunakool, K., Bates, R., Žídek, A., Potapenko, A., *et al.* (2021). Highly accurate protein structure prediction with AlphaFold. *Nature* 596, 583-589.

Kalyaanamoorthy, S., Minh, B.Q., Wong, T.K.F., von Haeseler, A., and Jermini, L.S. (2017). ModelFinder: fast model selection for accurate phylogenetic estimates. *Nature Methods* 14, 587-589.

Kang, Y.J., Kim, S.K., Kim, M.Y., Lestari, P., Kim, K.H., Ha, B.-K., Jun, T.H., Hwang, W.J., Lee, T., Lee, J., *et al.* (2014). Genome sequence of mungbean and insights into evolution within *Vigna* species. *Nat Commun* 5, 5443.

Kato, H., Ishizaki, K., Kouno, M., Shirakawa, M., Bowman, J.L., Nishihama, R., and Kohchi, T. (2015). Auxin-Mediated Transcriptional System with a Minimal Set of Components Is Critical for Morphogenesis through the Life Cycle in *Marchantia polymorpha*. *Plos Genet* 11, e1005084.

Kato, H., Mutte, S.K., Suzuki, H., Crespo, I., Das, S., Radoeva, T., Fontana, M., Yoshitake, Y., Hainiwa, E., van den Berg, W., *et al.* (2020). Design principles of a minimal auxin response system. *Nature Plants* 6, 473-482.

Katoh, K., Misawa, K., Kuma, K., and Miyata, T. (2002). MAFFT: a novel method for rapid multiple sequence alignment based on fast Fourier transform. *Nucleic Acids Res* 30, 3059-3066.

Kaya-Okur, H.S., Janssens, D.H., Henikoff, J.G., Ahmad, K., and Henikoff, S. (2020). Efficient low-cost chromatin profiling with CUT&Tag. *Nature Protocols* 15, 3264-3283.

Kelley, D.R., Arreola, A., Gallagher, T.L., and Gasser, C.S. (2012). ETTIN (ARF3) physically interacts with KANADI proteins to form a functional complex essential for integument development and polarity determination in *Arabidopsis*. *Development* 139, 1105-1109.

Kelley, D.R., and Estelle, M. (2012). Ubiquitin-Mediated Control of Plant Hormone Signaling. *Plant Physiol* 160, 47-55.

Kenrick, P., and Crane, P.R. (1997). The origin and early evolution of plants on land. *Nature* 389, 33-39.

- Kepinski, S., and Leyser, O. (2005). The Arabidopsis F-box protein TIR1 is an auxin receptor. *Nature* 435, 446-451.
- Kerstetter, R., Vollbrecht, E., Lowe, B., Veit, B., Yamaguchi, J., and Hake, S. (1994). Sequence analysis and expression patterns divide the maize knotted1-like homeobox genes into two classes. *The Plant Cell* 6, 1877-1887.
- Kerstetter, R.A., Bollman, K., Taylor, R.A., Bomblies, K., and Poethig, R.S. (2001). KANADI regulates organ polarity in Arabidopsis. *Nature* 411, 706-709.
- Khanday, I., Yadav, S.R., and Vijayraghavan, U. (2013). Rice LHS1/OsMADS1 Controls Floret Meristem Specification by Coordinated Regulation of Transcription Factors and Hormone Signaling Pathways *Plant Physiol* 161, 1970-1983.
- Kieber, J.J., and Schaller, G.E. (2018). Cytokinin signaling in plant development. *Development* 145.
- Kim, S., Park, M., Yeom, S.-I., Kim, Y.-M., Lee, J.M., Lee, H.-A., Seo, E., Choi, J., Cheong, K., Kim, K.-T., *et al.* (2014). Genome sequence of the hot pepper provides insights into the evolution of pungency in Capsicum species. *Nature Genetics* 46, 270-278.
- Kim, S.T., Yoo, M.J., Albert, V.A., Farris, J.S., Soltis, P.S., and Soltis, D.E. (2004). Phylogeny and diversification of B-function MADS-box genes in angiosperms: Evolutionary and functional implications of a 260-million-year-old duplication. *Am J Bot* 91, 2102-2118.
- Klämbt, D., Knauth, B., and Dittmann, I. (1992). Auxin dependent growth of rhizoids of Chara globularis. *Physiologia Plantarum* 85, 537-540.
- Kleine-Vehn, J.r., Dhonukshe, P., Swarup, R., Bennett, M., and Friml, J.i. (2006). Subcellular Trafficking of the Arabidopsis Auxin Influx Carrier AUX1 Uses a Novel Pathway Distinct from PIN1. *The Plant Cell* 18, 3171-3181.
- Knoll, A.H. (2011). The Multiple Origins of Complex Multicellularity. *Annu Rev Earth PI Sc* 39, 217-239.
- Korasick, D.A., Westfall, C.S., Lee, S.G., Nanao, M.H., Dumas, R., Hagen, G., Guilfoyle, T.J., Jez, J.M., and Strader, L.C. (2014). Molecular basis for AUXIN RESPONSE FACTOR protein interaction and the control of auxin response repression. *Proceedings of the National Academy of Sciences* 111, 5427-5432.
- Kuhn, A., Ramans Harborough, S., McLaughlin, H.M., Natarajan, B., Verstraeten, I., Friml, J., Kepinski, S., and Østergaard, L. (2020). Direct ETTIN-auxin interaction controls chromatin states in gynoecium development. *Elife* 9, e51787.
- Kuhn, A., Roosjen, M., Mutte, S., Dubey, S.M., Carrillo Carrasco, V.P., Boeren, S., Monzer, A., Koehorst, J., Kohchi, T., Nishihama, R., *et al.* (2024). RAF-like protein kinases mediate a deeply conserved, rapid auxin response. *Cell* 187, 130-148.e117.
- Kutschera, U. (1994). The current status of the acid-growth hypothesis. *New Phytologist* 126, 549-569.

- Labun, K., Montague, T.G., Krause, M., Torres Cleuren, Y.N., Tjeldnes, H., and Valen, E. (2019). CHOPCHOP v3: expanding the CRISPR web toolbox beyond genome editing. *Nucleic Acids Res* 47, W171-W174.
- Lang, D., Ullrich, K.K., Murat, F., Fuchs, J., Jenkins, J., Haas, F.B., Piednoel, M., Gundlach, H., Van Bel, M., Meyberg, R., *et al.* (2018). The *Physcomitrella patens* chromosome-scale assembly reveals moss genome structure and evolution. *Plant J* 93, 515-533.
- Larsson, E., Franks, R.G., and Sundberg, E. (2013). Auxin and the *Arabidopsis thaliana* gynoecium. *J Exp Bot* 64, 2619-2627.
- Larsson, E., Roberts, C.J., Claes, A.R., Franks, R.G., and Sundberg, E. (2014). Polar auxin transport is essential for medial versus lateral tissue specification and vascular-mediated valve outgrowth in *Arabidopsis* gynoecia. *Plant Physiol* 166, 1998-2012.
- Lee, J.-H., Lin, H., Joo, S., and Goodenough, U. (2008). Early Sexual Origins of Homeoprotein Heterodimerization and Evolution of the Plant KNOX/BELL Family. *Cell* 133, 829-840.
- Leebens-Mack, J.H., Barker, M.S., Carpenter, E.J., Deyholos, M.K., Gitzendanner, M.A., Graham, S.W., Grosse, I., Li, Z., Melkonian, M., Mirarab, S., *et al.* (2019). One thousand plant transcriptomes and the phylogenomics of green plants. *Nature* 574, 679-685.
- Letunic, I., and Bork, P. (2021). Interactive Tree Of Life (iTOL) v5: an online tool for phylogenetic tree display and annotation. *Nucleic Acids Res* 49, W293-W296.
- Leyser, O. (2017). Auxin Signaling. *Plant Physiol* 176, 465-479.
- Li, D., Flores-Sandoval, E., Ahtesham, U., Coleman, A., Clay, J.M., Bowman, J.L., and Chang, C. (2020a). Ethylene-independent functions of the ethylene precursor ACC in *Marchantia polymorpha*. *Nature Plants* 6, 1335-1344.
- Li, F.-W., Brouwer, P., Carretero-Paulet, L., Cheng, S., de Vries, J., Delaux, P.-M., Eily, A., Koppers, N., Kuo, L.-Y., Li, Z., *et al.* (2018). Fern genomes elucidate land plant evolution and cyanobacterial symbioses. *Nature Plants* 4, 460-472.
- Li, F.-W., Nishiyama, T., Waller, M., Frangedakis, E., Keller, J., Li, Z., Fernandez-Pozo, N., Barker, M.S., Bennett, T., Blázquez, M.A., *et al.* (2020b). *Anthoceros* genomes illuminate the origin of land plants and the unique biology of hornworts. *Nature Plants* 6, 259-272.
- Li, L., Verstraeten, I., Roosjen, M., Takahashi, K., Rodriguez, L., Merrin, J., Chen, J., Shabala, L., Smet, W., Ren, H., *et al.* (2021). Cell surface and intracellular auxin signalling for H(+) fluxes in root growth. *Nature* 599, 273-277.
- Li, Y., Liu, Z.-B., Shi, X., Hagen, G., and Guilfoyle, T.J. (1994). An auxin-inducible element in soybean SAUR promoters. *Plant Physiol* 106, 37-43.
- Liang, G.Z., and Li, S.Z. (2007). A new sequence representation as applied in better specificity elucidation for human immunodeficiency virus type 1 protease. *Peptide Science* 88, 401-412.

- Lieberman-Lazarovich, M., Yahav, C., Israeli, A., and Efroni, I. (2019). Deep Conservation of cis-Element Variants Regulating Plant Hormonal Responses. *Plant Cell* 31, 2559-2572.
- Lin, W., Zhou, X., Tang, W., Takahashi, K., Pan, X., Dai, J., Ren, H., Zhu, X., Pan, S., Zheng, H., *et al.* (2021). TMK-based cell-surface auxin signalling activates cell-wall acidification. *Nature* 599, 278-282.
- Linkies, A., Graeber, K., Knight, C., and Leubner-Metzger, G. (2010). The evolution of seeds. *New Phytologist* 186, 817-831.
- Liu, H., Wang, X., Wang, G., Cui, P., Wu, S., Ai, C., Hu, N., Li, A., He, B., Shao, X., *et al.* (2021). The nearly complete genome of *Ginkgo biloba* illuminates gymnosperm evolution. *Nature Plants* 7, 748-756.
- Liu, J., Hua, W., Hu, Z., Yang, H., Zhang, L., Li, R., Deng, L., Sun, X., Wang, X., and Wang, H. (2015). Natural variation in ARF18 gene simultaneously affects seed weight and silique length in polyploid rapeseed. *Proceedings of the National Academy of Sciences* 112, E5123-E5132.
- Liu, M.-J., Zhao, J., Cai, Q.-L., Liu, G.-C., Wang, J.-R., Zhao, Z.-H., Liu, P., Dai, L., Yan, G., Wang, W.-J., *et al.* (2014a). The complex jujube genome provides insights into fruit tree biology. *Nat Commun* 5, 5315.
- Liu, S., Liu, Y., Yang, X., Tong, C., Edwards, D., Parkin, I.A.P., Zhao, M., Ma, J., Yu, J., Huang, S., *et al.* (2014b). The *Brassica oleracea* genome reveals the asymmetrical evolution of polyploid genomes. *Nat Commun* 5, 3930.
- Liu, X., Kim, Y.J., Müller, R., Yumul, R.E., Liu, C., Pan, Y., Cao, X., Goodrich, J., and Chen, X. (2011). AGAMOUS terminates floral stem cell maintenance in *Arabidopsis* by directly repressing WUSCHEL through recruitment of Polycomb Group proteins. *Plant Cell* 23, 3654-3670.
- Liu, X.G., Dinh, T.T., Li, D.M., Shi, B.H., Li, Y.P., Cao, X.W., Guo, L., Pan, Y.Y., Jiao, Y.L., and Chen, X.M. (2014c). AUXIN RESPONSE FACTOR 3 integrates the functions of AGAMOUS and APETALA2 in floral meristem determinacy. *Plant J* 80, 629-641.
- Livak, K.J., and Schmittgen, T.D. (2001). Analysis of relative gene expression data using real-time quantitative PCR and the 2(-Delta Delta C(T)) Method. *Methods* 25, 402-408.
- Lohmann, J.U., Hong, R.L., Hobe, M., Busch, M.A., Parcy, F., Simon, R., and Weigel, D. (2001). A molecular link between stem cell regulation and floral patterning in *Arabidopsis*. *Cell* 105, 793-803.
- Long, J.A., Moan, E.I., Medford, J.I., and Barton, M.K. (1996). A member of the KNOTTED class of homeodomain proteins encoded by the STM gene of *Arabidopsis*. *Nature* 379, 66-69.
- Long, J.A., Ohno, C., Smith, Z.R., and Meyerowitz, E.M. (2006). TOPLESS regulates apical embryonic fate in *Arabidopsis*. *Science* 312, 1520-1523.
- Lopez-Obando, M., Landberg, K., Sundberg, E., and Thelander, M. (2022). Dependence on clade II bHLH transcription factors for nursing of haploid products

by tapetal-like cells is conserved between moss sporangia and angiosperm anthers. *New Phytologist* 235, 718-731.

Lora, J., Hormaza, J.I., Herrero, M., and Gasser, C.S. (2011). Seedless fruits and the disruption of a conserved genetic pathway in angiosperm ovule development. *Proceedings of the National Academy of Sciences* 108, 5461-5465.

Lu, Q., Li, H., Hong, Y., Zhang, G., Wen, S., Li, X., Zhou, G., Li, S., Liu, H., Liu, H., *et al.* (2018). Genome Sequencing and Analysis of the Peanut B-Genome Progenitor (*Arachis ipaensis*). *Frontiers in Plant Science* 9.

Lv, Q., Qiu, J., Liu, J., Li, Z., Zhang, W., Wang, Q., Fang, J., Pan, J., Chen, Z., Cheng, W., *et al.* (2020). The *Chimonanthus salicifolius* genome provides insight into magnoliid evolution and flavonoid biosynthesis. *Plant J* 103, 1910-1923.

Maccaferri, M., Harris, N.S., Twardziok, S.O., Pasam, R.K., Gundlach, H., Spannagl, M., Ormanbekova, D., Lux, T., Prade, V.M., Milner, S.G., *et al.* (2019). Durum wheat genome highlights past domestication signatures and future improvement targets. *Nature Genetics* 51, 885-895.

Maere, S., De Bodt, S., Raes, J., Casneuf, T., Van Montagu, M., Kuiper, M., and Van de Peer, Y. (2005). Modeling gene and genome duplications in eukaryotes. *Proceedings of the National Academy of Sciences* 102, 5454-5459.

Maizel, A., Busch, M.A., Tanahashi, T., Perkovic, J., Kato, M., Hasebe, M., and Weigel, D. (2005). The Floral Regulator *LEAFY* Evolves by Substitutions in the DNA Binding Domain. *Science* 308, 260-263.

Mallory, A.C., Bartel, D.P., and Bartel, B. (2005). MicroRNA-directed regulation of *Arabidopsis* *AUXIN RESPONSE FACTOR17* is essential for proper development and modulates expression of early auxin response genes. *Plant Cell* 17, 1360-1375.

Maraschin Fdos, S., Memelink, J., and Offringa, R. (2009). Auxin-induced, SCF(TIR1)-mediated poly-ubiquitination marks *AUX/IAA* proteins for degradation. *Plant J* 59, 100-109.

Marchant, A., Bhalerao, R., Casimiro, I., Eklöf, J., Casero, P.J., Bennett, M., and Sandberg, G. (2002). *AUX1* promotes lateral root formation by facilitating indole-3-acetic acid distribution between sink and source tissues in the *Arabidopsis* seedling. *The Plant Cell* 14, 589-597.

Marchant, A., Kargul, J., May, S.T., Muller, P., Delbarre, A., Perrot-Rechenmann, C., and Bennett, M.J. (1999). *AUX1* regulates root gravitropism in *Arabidopsis* by facilitating auxin uptake within root apical tissues. *EMBO J* 18, 2066-2073.

Marchant, D.B., Chen, G., Cai, S., Chen, F., Schafran, P., Jenkins, J., Shu, S., Plott, C., Webber, J., Lovell, J.T., *et al.* (2022). Dynamic genome evolution in a model fern. *Nature Plants* 8, 1038-1051.

Marchant, D.B., Sessa, E.B., Wolf, P.G., Heo, K., Barbazuk, W.B., Soltis, P.S., and Soltis, D.E. (2019). The C-Fern (*Ceratopteris richardii*) genome: insights into plant genome evolution with the first partial homosporous fern genome assembly. *Sci Rep-Uk* 9, 18181.

- Marin, E., Jouannet, V., Herz, A., Lokerse, A.S., Weijers, D., Vaucheret, H., Nussaume, L., Crespi, M.D., and Maizel, A. (2010). miR390, Arabidopsis TAS3 tasiRNAs, and Their AUXIN RESPONSE FACTOR Targets Define an Autoregulatory Network Quantitatively Regulating Lateral Root Growth. *The Plant Cell* 22, 1104-1117.
- Marks, R.A., Hotaling, S., Frandsen, P.B., and VanBuren, R. (2021). Representation and participation across 20 years of plant genome sequencing. *Nature Plants* 7, 1571-1578.
- Marques-Bueno, M.M., Armengot, L., Noack, L.C., Bareille, J., Rodriguez, L., Platre, M.P., Bayle, V., Liu, M., Opdenacker, D., Vanneste, S., *et al.* (2021). Auxin-Regulated Reversible Inhibition of TMK1 Signaling by MAKR2 Modulates the Dynamics of Root Gravitropism. *Curr Biol* 31, 228-237 e210.
- Martin-Arevalillo, R., Thevenon, E., Jégu, F., Vinos-Poyo, T., Vernoux, T., Parcy, F., and Dumas, R. (2019). Evolution of the auxin response factors from charophyte ancestors. *Plos Genet* 15, e1008400.
- Mascher, M., Gundlach, H., Himmelbach, A., Beier, S., Twardziok, S.O., Wicker, T., Radchuk, V., Dockter, C., Hedley, P.E., Russell, J., *et al.* (2017). A chromosome conformation capture ordered sequence of the barley genome. *Nature* 544, 427-433.
- Mashiguchi, K., Seto, Y., and Yamaguchi, S. (2021). Strigolactone biosynthesis, transport and perception. *The Plant Journal* 105, 335-350.
- McClure, B.A., Hagen, G., Brown, C.S., Gee, M.A., and Guilfoyle, T.J. (1989). Transcription, organization, and sequence of an auxin-regulated gene cluster in soybean. *Plant Cell* 1, 229-239.
- McConnell, J.R., Emery, J., Eshed, Y., Bao, N., Bowman, J., and Barton, M.K. (2001). Role of PHABULOSA and PHAVOLUTA in determining radial patterning in shoots. *Nature* 411, 709-713.
- Mellerowicz, E.J., Horgan, K., Walden, A., Coker, A., and Walter, C. (1998). PRFLL—a *Pinus radiata* homologue of FLORICAULA and LEAFY is expressed in buds containing vegetative shoot and undifferentiated male cone primordia. *Planta* 206, 619-629.
- Merchant, S.S., Prochnik, S.E., Vallon, O., Harris, E.H., Karpowicz, S.J., Witman, G.B., Terry, A., Salamov, A., Fritz-Laylin, L.K., Maréchal-Drouard, L., *et al.* (2007). The *Chlamydomonas* genome reveals the evolution of key animal and plant functions. *Science* 318, 245-250.
- Meyerowitz, E.M., Smyth, D.R., and Bowman, J.L. (1989). Abnormal flowers and pattern formation in floral development. *Development* 106, 209-217.
- Michalko, J., Dravecká, M., Bollenbach, T., and Friml, J. (2015). Embryo-lethal phenotypes in early *abp1* mutants are due to disruption of the neighboring BSM gene [version 1; peer review: 3 approved]. *F1000Research* 4.
- Michniewicz, M., Zago, M.K., Abas, L., Weijers, D., Schweighofer, A., Meskiene, I., Heisler, M.G., Ohno, C., Zhang, J., Huang, F., *et al.* (2007). Antagonistic Regulation

of PIN Phosphorylation by PP2A and PINOID Directs Auxin Flux. *Cell* 130, 1044-1056.

Ming, R., Hou, S., Feng, Y., Yu, Q., Dionne-Laporte, A., Saw, J.H., Senin, P., Wang, W., Ly, B.V., Lewis, K.L.T., *et al.* (2008). The draft genome of the transgenic tropical fruit tree papaya (*Carica papaya* Linnaeus). *Nature* 452, 991-996.

Ming, R., VanBuren, R., Liu, Y., Yang, M., Han, Y., Li, L.-T., Zhang, Q., Kim, M.-J., Schatz, M.C., Campbell, M., *et al.* (2013). Genome of the long-living sacred lotus (*Nelumbo nucifera* Gaertn.). *Genome Biology* 14, R41.

Ming, R., VanBuren, R., Wai, C.M., Tang, H., Schatz, M.C., Bowers, J.E., Lyons, E., Wang, M.-L., Chen, J., Biggers, E., *et al.* (2015). The pineapple genome and the evolution of CAM photosynthesis. *Nature Genetics* 47, 1435-1442.

Minh, B.Q., Schmidt, H.A., Chernomor, O., Schrempf, D., Woodhams, M.D., von Haeseler, A., and Lanfear, R. (2020). IQ-TREE 2: New Models and Efficient Methods for Phylogenetic Inference in the Genomic Era. *Mol Biol Evol* 37, 1530-1534.

Moubayidin, L., and Østergaard, L. (2014). Dynamic control of auxin distribution imposes a bilateral-to-radial symmetry switch during gynoecium development. *Curr Biol* 24, 2743-2748.

Moyroud, E., Monniaux, M., Thévenon, E., Dumas, R., Scutt, C.P., Frohlich, M.W., and Parcy, F. (2017). A link between LEAFY and B-gene homologues in *Welwitschia mirabilis* sheds light on ancestral mechanisms prefiguring floral development. *New Phytologist* 216, 469-481.

Müller, C.J., Larsson, E., Spíchal, L., and Sundberg, E. (2017). Cytokinin-auxin crosstalk in the gynoecial primordium ensures correct domain patterning. *Plant Physiol* 175, 1144-1157.

Mutte, S.K., Kato, H., Rothfels, C., Melkonian, M., Wong, G.K.-S., and Weijers, D. (2018). Origin and evolution of the nuclear auxin response system. *Elife* 7, e33399.

Mutte, S.K., and Weijers, D. (2020). Deep Evolutionary History of the Phox and Bem1 (PB1) Domain Across Eukaryotes. *Sci Rep-Uk* 10, 3797.

Myburg, A.A., Grattapaglia, D., Tuskan, G.A., Hellsten, U., Hayes, R.D., Grimwood, J., Jenkins, J., Lindquist, E., Tice, H., Bauer, D., *et al.* (2014). The genome of *Eucalyptus grandis*. *Nature* 510, 356-362.

Nagawa, S., Xu, T., Lin, D., Dhonukshe, P., Zhang, X., Friml, J., Scheres, B., Fu, Y., and Yang, Z. (2012). ROP GTPase-dependent actin microfilaments promote PIN1 polarization by localized inhibition of clathrin-dependent endocytosis. *Plos Biol* 10, e1001299.

Nagy, I., Veeckman, E., Liu, C., Bel, M.V., Vandepoele, K., Jensen, C.S., Ruttink, T., and Asp, T. (2022). Chromosome-scale assembly and annotation of the perennial ryegrass genome. *BMC Genomics* 23, 505.

Nakata, M., Matsumoto, N., Tsugeki, R., Rikirsch, E., Laux, T., and Okada, K. (2012). Roles of the Middle Domain-Specific WUSCHEL-RELATED HOMEBOX Genes in Early Development of Leaves in *Arabidopsis*. *The Plant Cell* 24, 519-535.

- Nanao, M.H., Vinos-Poyo, T., Brunoud, G., Thévenon, E., Mazzoleni, M., Mast, D., Lainé, S., Wang, S., Hagen, G., and Li, H. (2014). Structural basis for oligomerization of auxin transcriptional regulators. *Nat Commun* 5, 3617.
- Napier, R. (2021). The Story of Auxin-Binding Protein 1 (ABP1). *Cold Spring Harb Perspect Biol* 13.
- Nellen, D., Burke, R., Struhl, G., and Basler, K. (1996). Direct and long-range action of a DPP morphogen gradient. *Cell* 85, 357-368.
- Nemhauser, J.L., Feldman, L.J., and Zambryski, P.C. (2000). Auxin and ETTIN in Arabidopsis gynoecium morphogenesis. *Development* 127, 3877-3888.
- Nishiyama, T., Sakayama, H., de Vries, J., Buschmann, H., Saint-Marcoux, D., Ullrich, K.K., Haas, F.B., Vanderstraeten, L., Becker, D., Lang, D., *et al.* (2018). The Chara Genome: Secondary Complexity and Implications for Plant Terrestrialization. *Cell* 174, 448-464.e424.
- Nogueira, F.T., Madi, S., Chitwood, D.H., Juarez, M.T., and Timmermans, M.C. (2007). Two small regulatory RNAs establish opposing fates of a developmental axis. *Gene Dev* 21, 750-755.
- Nüsslein-Volhard, C., and Wieschaus, E. (1980). Mutations affecting segment number and polarity in Drosophila. *Nature* 287, 795-801.
- Nystedt, B., Street, N.R., Wetterbom, A., Zuccolo, A., Lin, Y.-C., Scofield, D.G., Vezzi, F., Delhomme, N., Giacomello, S., Alexeyenko, A., *et al.* (2013). The Norway spruce genome sequence and conifer genome evolution. *Nature* 497, 579-584.
- Ó'Maoiléidigh, D.S., Stewart, D., Zheng, B., Coupland, G., and Wellmer, F. (2018). Floral homeotic proteins modulate the genetic program for leaf development to suppress trichome formation in flowers. *Development* 145.
- O'Malley, R.C., Huang, S.-s.C., Song, L., Lewsey, M.G., Bartlett, A., Nery, J.R., Galli, M., Gallavotti, A., and Ecker, J.R. (2016). Cistrome and episcistrome features shape the regulatory DNA landscape. *Cell* 165, 1280-1292.
- Ohtaka, K., Hori, K., Kanno, Y., Seo, M., and Ohta, H. (2017). Primitive Auxin Response without TIR1 and Aux/IAA in the Charophyte Alga Klebsormidium nitens. *Plant Physiol* 174, 1621-1632.
- Okada, K., Ueda, J., Komaki, M.K., Bell, C.J., and Shimura, Y. (1991). Requirement of the Auxin Polar Transport System in Early Stages of Arabidopsis Floral Bud Formation. *Plant Cell* 3, 677-684.
- Olsen, J.L., Rouzé, P., Verhelst, B., Lin, Y.-C., Bayer, T., Collen, J., Dattolo, E., De Paoli, E., Dittami, S., Maumus, F., *et al.* (2016). The genome of the seagrass *Zostera marina* reveals angiosperm adaptation to the sea. *Nature* 530, 331-335.
- Ori, N., Eshed, Y., Chuck, G., Bowman, J.L., and Hake, S. (2000). Mechanisms that control knox gene expression in the Arabidopsis shoot. *Development* 127, 5523-5532.
- Osorio, D., Rondón-Villarreal, P., and Torres, R. (2015). Peptides: a package for data mining of antimicrobial peptides. *Small* 12, 44-444.

- Pabón-Mora, N., Suárez-Baron, H., Ambrose, B.A., and González, F. (2015). Flower Development and Perianth Identity Candidate Genes in the Basal Angiosperm *Aristolochia fimbriata* (Piperales: Aristolochiaceae). *Front Plant Sci* 6, 1095.
- Parcy, F., Nilsson, O., Busch, M.A., Lee, I., and Weigel, D. (1998). A genetic framework for floral patterning. *Nature* 395, 561-566.
- Parry, G., Calderon-Villalobos, L.I., Prigge, M., Peret, B., Dharmasiri, S., Itoh, H., Lechner, E., Gray, W.M., Bennett, M., and Estelle, M. (2009). Complex regulation of the TIR1/AFB family of auxin receptors. *Proceedings of the National Academy of Sciences* 106, 22540-22545.
- Paterson, A.H., Bowers, J.E., Bruggmann, R., Dubchak, I., Grimwood, J., Gundlach, H., Haberler, G., Hellsten, U., Mitros, T., Poliakov, A., *et al.* (2009). The *Sorghum bicolor* genome and the diversification of grasses. *Nature* 457, 551-556.
- Pekker, I., Alvarez, J.P., and Eshed, Y. (2005). Auxin response factors mediate Arabidopsis organ asymmetry via modulation of KANADI activity. *Plant Cell* 17, 2899-2910.
- Pelaz, S., Ditta, G.S., Baumann, E., Wisman, E., and Yanofsky, M.F. (2000). B and C floral organ identity functions require SEPALLATA MADS-box genes. *Nature* 405, 200-203.
- Péret, B., Swarup, K., Ferguson, A., Seth, M., Yang, Y., Dhondt, S., James, N., Casimiro, I., Perry, P., and Syed, A. (2012). AUX/LAX genes encode a family of auxin influx transporters that perform distinct functions during Arabidopsis development. *The Plant Cell* 24, 2874-2885.
- Peréz-Mesa, P., Ortíz-Ramírez, C.I., González, F., Ferrándiz, C., and Pabón-Mora, N. (2020). Expression of gynoecium patterning transcription factors in *Aristolochia fimbriata* (Aristolochiaceae) and their contribution to gynostemium development. *EvoDevo* 11, 4.
- Petrásek, J., Mravec, J., Bouchard, R., Blakeslee, J.J., Abas, M., Seifertová, D., Wisniewska, J., Tadele, Z., Kubes, M., Covanová, M., *et al.* (2006). PIN proteins perform a rate-limiting function in cellular auxin efflux. *Science* 312, 914-918.
- Philipson, W. (1990). The significance of apical meristems in the phylogeny of land plants. *Plant Systematics and Evolution* 173, 17-38.
- Piya, S., Shrestha, S.K., Binder, B., Stewart, C.N., Jr., and Hewezi, T. (2014). Protein-protein interaction and gene co-expression maps of ARFs and Aux/IAAs in Arabidopsis. *Front Plant Sci* 5, 744.
- Plackett, A.R.G., Conway, S.J., Hewett Hazelton, K.D., Rabinowitsch, E.H., Langdale, J.A., and Di Stilio, V.S. (2018). LEAFY maintains apical stem cell activity during shoot development in the fern *Ceratopteris richardii* *Elife* 7, e39625.
- Plackett, A.R.G., Rabinowitsch, E.H., and Langdale, J.A. (2015). Protocol: genetic transformation of the fern *Ceratopteris richardii* through microparticle bombardment. *Plant Methods* 11, 37.

Planas-Riverola, A., Gupta, A., Betegón-Putze, I., Bosch, N., Ibañes, M., and Caño-Delgado, A.I. (2019). Brassinosteroid signaling in plant development and adaptation to stress. *Development* 146.

Plant, A.R., Larrieu, A., and Causier, B. (2021). Repressor for hire! The vital roles of TOPLESS-mediated transcriptional repression in plants. *New Phytologist* 231, 963-973.

Povilus, R.A., DaCosta, J.M., Grassa, C., Satyaki, P.R.V., Moeglein, M., Jaenisch, J., Xi, Z., Mathews, S., Gehring, M., Davis, C.C., *et al.* (2020). Water lily (*Nymphaea thermarum*) genome reveals variable genomic signatures of ancient vascular cambium losses. *Proceedings of the National Academy of Sciences* 117, 8649-8656.

Povilus, R.A., Losada, J.M., and Friedman, W.E. (2015). Floral biology and ovule and seed ontogeny of *Nymphaea thermarum*, a water lily at the brink of extinction with potential as a model system for basal angiosperms. *Ann Bot* 115, 211-226.

Prigge, M.J., and Clark, S.E. (2006). Evolution of the class III HD-Zip gene family in land plants. *Evolution & Development* 8, 350-361.

Prigge, M.J., Lavy, M., Ashton, N.W., and Estelle, M. (2010). *Physcomitrella patens* auxin-resistant mutants affect conserved elements of an auxin-signaling pathway. *Curr Biol* 20, 1907-1912.

Prigge, M.J., Otsuga, D., Alonso, J.M., Ecker, J.R., Drews, G.N., and Clark, S.E. (2005). Class III homeodomain-leucine zipper gene family members have overlapping, antagonistic, and distinct roles in *Arabidopsis* development. *Plant Cell* 17, 61-76.

Prigge, M.J., Platre, M., Kadakia, N., Zhang, Y., Greenham, K., Szutu, W., Pandey, B.K., Bhosale, R.A., Bennett, M.J., Busch, W., *et al.* (2020). Genetic analysis of the *Arabidopsis* TIR1/AFB auxin receptors reveals both overlapping and specialized functions. *Elife* 9, e54740.

Prince, V.E., and Pickett, F.B. (2002). Splitting pairs: the diverging fates of duplicated genes. *Nat Rev Genet* 3, 827-837.

Project, A.G., Albert, V.A., Barbazuk, W.B., dePamphilis, C.W., Der, J.P., Leebens-Mack, J., Ma, H., Palmer, J.D., Rounsley, S., Sankoff, D., *et al.* (2013). The *Amborella* Genome and the Evolution of Flowering Plants. *Science* 342, 1241089.

Prunet, N., Morel, P., Thierry, A.-M., Eshed, Y., Bowman, J.L., Negrutiu, I., and Trehin, C. (2008). REBELOTE, SQUINT, and ULTRAPETALA1 function redundantly in the temporal regulation of floral meristem termination in *Arabidopsis thaliana*. *The Plant Cell* 20, 901-919.

Prusinkiewicz, P., Crawford, S., Smith, R.S., Ljung, K., Bennett, T., Ongaro, V., and Leyser, O. (2009). Control of bud activation by an auxin transport switch. *Proc Natl Acad Sci U S A* 106, 17431-17436.

Qi, J., Wang, Y., Yu, T., Cunha, A., Wu, B., Vernoux, T., Meyerowitz, E., and Jiao, Y. (2014). Auxin depletion from leaf primordia contributes to organ patterning. *Proceedings of the National Academy of Sciences* 111, 18769-18774.

- Qi, L., Kwiatkowski, M., Chen, H., Hoermayer, L., Sinclair, S., Zou, M., del Genio, C.I., Kubeš, M.F., Napier, R., Jaworski, K., *et al.* (2022). Adenylate cyclase activity of TIR1/AFB auxin receptors in plants. *Nature* 611, 133-138.
- Qin, L., Hu, Y., Wang, J., Wang, X., Zhao, R., Shan, H., Li, K., Xu, P., Wu, H., Yan, X., *et al.* (2021). Insights into angiosperm evolution, floral development and chemical biosynthesis from the *Aristolochia fimbriata* genome. *Nature Plants* 7, 1239-1253.
- Rademacher, E.H., Lokerse, A.S., Schlereth, A., Llavata-Peris, C.I., Bayer, M., Kientz, M., Freire Rios, A., Borst, J.W., Lukowitz, W., Jürgens, G., *et al.* (2012). Different auxin response machineries control distinct cell fates in the early plant embryo. *Dev Cell* 22, 211-222.
- Rademacher, E.H., Möller, B., Lokerse, A.S., Llavata-Peris, C.I., van den Berg, W., and Weijers, D. (2011). A cellular expression map of the *Arabidopsis* AUXIN RESPONSE FACTOR gene family. *Plant J* 68, 597-606.
- Ramos, J.A., Zenser, N., Leyser, O., and Callis, J. (2001). Rapid Degradation of Auxin/Indoleacetic Acid Proteins Requires Conserved Amino Acids of Domain II and Is Proteasome Dependent. *The Plant Cell* 13, 2349-2360.
- Reinhardt, D., Mandel, T., and Kuhlemeier, C. (2000). Auxin regulates the initiation and radial position of plant lateral organs. *The Plant Cell* 12, 507-518.
- Reinhardt, D., Pesce, E.-R., Stieger, P., Mandel, T., Baltensperger, K., Bennett, M., Traas, J., Friml, J., and Kuhlemeier, C. (2003). Regulation of phyllotaxis by polar auxin transport. *Nature* 426, 255-260.
- Ren, H., Park, M.Y., Spartz, A.K., Wong, J.H., and Gray, W.M. (2018). A subset of plasma membrane-localized PP2C.D phosphatases negatively regulate SAUR-mediated cell expansion in *Arabidopsis*. *Plos Genet* 14, e1007455.
- Rendón-Anaya, M., Ibarra-Laclette, E., Méndez-Bravo, A., Lan, T., Zheng, C., Carretero-Paulet, L., Perez-Torres, C.A., Chacón-López, A., Hernandez-Guzmán, G., Chang, T.-H., *et al.* (2019). The avocado genome informs deep angiosperm phylogeny, highlights introgressive hybridization, and reveals pathogen-influenced gene space adaptation. *Proceedings of the National Academy of Sciences* 116, 17081-17089.
- Rensing, S.A., Lang, D., Zimmer, A.D., Terry, A., Salamov, A., Shapiro, H., Nishiyama, T., Perroud, P.-F., Lindquist, E.A., and Kamisugi, Y. (2008). The *Physcomitrella* genome reveals evolutionary insights into the conquest of land by plants. *Science* 319, 64-69.
- Reyes-Olalde, J.I., Zuñiga-Mayo, V.M., Montes, R.A.C., Marsch-Martínez, N., and de Folter, S. (2013). Inside the gynoecium: at the carpel margin. *Trends in plant science* 18, 644-655.
- Reyes-Olalde, J.I., Zúñiga-Mayo, V.M., Serwatowska, J., Chavez Montes, R.A., Lozano-Sotomayor, P., Herrera-Ubaldo, H., Gonzalez-Aguilera, K.L., Ballester, P., Ripoll, J.J., and Ezquer, I. (2017). The bHLH transcription factor SPATULA enables cytokinin signaling, and both activate auxin biosynthesis and transport genes at the medial domain of the gynoecium. *Plos Genet* 13, e1006726.

- Roosjen, M., Paque, S., and Weijers, D. (2017). Auxin Response Factors: output control in auxin biology. *J Exp Bot* 69, 179-188.
- Ruan, J., Zhou, Y., Zhou, M., Yan, J., Khurshid, M., Weng, W., Cheng, J., and Zhang, K. (2019). Jasmonic Acid Signaling Pathway in Plants. *International Journal of Molecular Sciences* 20, 2479.
- Rutjens, B., Bao, D., Van Eck-Stouten, E., Brand, M., Smeekens, S., and Proveniers, M. (2009). Shoot apical meristem function in Arabidopsis requires the combined activities of three BEL1-like homeodomain proteins. *The Plant Journal* 58, 641-654.
- Sabatini, S., Beis, D., Wolkenfelt, H., Murfett, J., Guilfoyle, T., Malamy, J., Benfey, P., Leyser, O., Bechtold, N., Weisbeek, P., *et al.* (1999). An auxin-dependent distal organizer of pattern and polarity in the Arabidopsis root. *Cell* 99, 463-472.
- Sagar, M., Chervin, C., Mila, I., Hao, Y., Roustan, J.-P., Benichou, M., Gibon, Y., Biais, B., Maury, P., Latché, A., *et al.* (2013). SIARF4, an Auxin Response Factor Involved in the Control of Sugar Metabolism during Tomato Fruit Development *Plant Physiol* 161, 1362-1374.
- Sakakibara, K., Ando, S., Yip, H.K., Tamada, Y., Hiwatashi, Y., Murata, T., Deguchi, H., Hasebe, M., and Bowman, J.L. (2013). KNOX2 genes regulate the haploid-to-diploid morphological transition in land plants. *Science* 339, 1067-1070.
- Sakakibara, K., Nishiyama, T., Deguchi, H., and Hasebe, M. (2008). Class 1 KNOX genes are not involved in shoot development in the moss *Physcomitrella patens* but do function in sporophyte development. *Evolution & development* 10, 555-566.
- Sanders, H.L., Darrah, P.R., and Langdale, J.A. (2011). Sector analysis and predictive modelling reveal iterative shoot-like development in fern fronds. *Development* 138, 2925-2934.
- Sanders, H.L., and Langdale, J.A. (2013). Conserved transport mechanisms but distinct auxin responses govern shoot patterning in *Selaginella kraussiana*. *New Phytologist* 198, 419-428.
- Santner, A., Calderon-Villalobos, L.I., and Estelle, M. (2009). Plant hormones are versatile chemical regulators of plant growth. *Nat Chem Biol* 5, 301-307.
- Sarojam, R., Sappl, P.G., Goldshmidt, A., Efroni, I., Floyd, S.K., Eshed, Y., and Bowman, J.L. (2010). Differentiating Arabidopsis shoots from leaves by combined YABBY activities. *The Plant Cell* 22, 2113-2130.
- Sasaki, T., and International Rice Genome Sequencing, P. (2005). The map-based sequence of the rice genome. *Nature* 436, 793-800.
- Sato, A., and Yamamoto, K.T. (2008). What's the physiological role of domain II-less Aux/IAA proteins? *Plant Signal Behav* 3, 496-497.
- Sato, S., Tabata, S., Hirakawa, H., Asamizu, E., Shirasawa, K., Isobe, S., Kaneko, T., Nakamura, Y., Shibata, D., Aoki, K., *et al.* (2012). The tomato genome sequence provides insights into fleshy fruit evolution. *Nature* 485, 635-641.

- Sayou, C., Monniaux, M., Nanao, M.H., Moyroud, E., Brockington, S.F., Thévenon, E., Chahtane, H., Warthmann, N., Melkonian, M., Zhang, Y., *et al.* (2014). A Promiscuous Intermediate Underlies the Evolution of LEAFY DNA Binding Specificity. *Science* 343, 645-648.
- Scarpella, E., Marcos, D., Friml, J., and Berleth, T. (2006). Control of leaf vascular patterning by polar auxin transport. *Genes Dev* 20, 1015-1027.
- Scheres, B. (2007). Stem-cell niches: nursery rhymes across kingdoms. *Nature Reviews Molecular Cell Biology* 8, 345-354.
- Scheres, B., Wolkenfelt, H., Willemsen, V., Terlouw, M., Lawson, E., Dean, C., and Weisbeek, P. (1994). Embryonic origin of the Arabidopsis primary root and root meristem initials. *Development* 120, 2475-2487.
- Schmutz, J., Cannon, S.B., Schlueter, J., Ma, J., Mitros, T., Nelson, W., Hyten, D.L., Song, Q., Thelen, J.J., Cheng, J., *et al.* (2010). Genome sequence of the palaeopolyploid soybean. *Nature* 463, 178-183.
- Schnable, P.S., Ware, D., Fulton, R.S., Stein, J.C., Wei, F., Pasternak, S., Liang, C., Zhang, J., Fulton, L., Graves, T.A., *et al.* (2009). The B73 maize genome: complexity, diversity, and dynamics. *Science* 326, 1112-1115.
- Schultz, E.A., and Haughn, G.W. (1991). LEAFY, a homeotic gene that regulates inflorescence development in Arabidopsis. *The Plant Cell* 3, 771-781.
- Schuster, C., Gaillochet, C., and Lohmann, J.U. (2015). Arabidopsis HECATE genes function in phytohormone control during gynoecium development. *Development* 142, 3343-3350.
- Schwechheimer, C. (2012). Gibberellin Signaling in Plants – The Extended Version. *Frontiers in Plant Science* 2.
- Semiarti, E., Ueno, Y., Tsukaya, H., Iwakawa, H., Machida, C., and Machida, Y. (2001). The ASYMMETRIC LEAVES2 gene of Arabidopsis thaliana regulates formation of a symmetric lamina, establishment of venation and repression of meristem-related homeobox genes in leaves. *Development* 128, 1771-1783.
- Serre, N.B.C., Kralík, D., Yun, P., Slouka, Z., Shabala, S., and Fendrych, M. (2021). AFB1 controls rapid auxin signalling through membrane depolarization in Arabidopsis thaliana root. *Nat Plants* 7, 1229-1238.
- Sessa, E.B., and Der, J.P. (2016). Chapter Seven - Evolutionary Genomics of Ferns and Lycophytes. In *Advances in Botanical Research*, S.A. Rensing, ed. (Academic Press), pp. 215-254.
- Sessions, A., Nemhauser, J.L., McCall, A., Roe, J.L., Feldmann, K.A., and Zambryski, P.C. (1997a). ETTIN patterns the Arabidopsis floral meristem and reproductive organs. *Development* 124, 4481-4491.
- Sessions, A., Nemhauser, J.L., McColl, A., Roe, J.L., Feldmann, K.A., and Zambryski, P.C. (1997b). ETTIN patterns the Arabidopsis floral meristem and reproductive organs. *Development* 124, 4481-4491.

- Shindo, S., Sakakibara, K., Sano, R., Ueda, K., and Hasebe, M. (2001). Characterization of a FLORICAULA/LEAFY homologue of *Gnetum parvifolium* and its implications for the evolution of reproductive organs in seed plants. *International Journal of Plant Sciences* 162, 1199-1209.
- Shulaev, V., Sargent, D.J., Crowhurst, R.N., Mockler, T.C., Folkerts, O., Delcher, A.L., Jaiswal, P., Mockaitis, K., Liston, A., Mane, S.P., *et al.* (2011). The genome of woodland strawberry (*Fragaria vesca*). *Nature Genetics* 43, 109-116.
- Si, F., Yang, C., Yan, B., Yan, W., Tang, S., Yan, Y., Cao, X., and Song, X. (2022). Control of OsARF3a by OsKANADI1 contributes to lemma development in rice. *The Plant Journal* 110, 1717-1730.
- Siegfried, K.R., Eshed, Y., Baum, S.F., Otsuga, D., Drews, G.N., and Bowman, J.L. (1999). Members of the YABBY gene family specify abaxial cell fate in *Arabidopsis*. *Development* 126, 4117-4128.
- Simonini, S., Bencivenga, S., Trick, M., and Ostergaard, L. (2017). Auxin-Induced Modulation of ETTIN Activity Orchestrates Gene Expression in *Arabidopsis*. *Plant Cell* 29, 1864-1882.
- Simonini, S., Deb, J., Moubayidin, L., Stephenson, P., Valluru, M., Freire-Rios, A., Sorefan, K., Weijers, D., Friml, J., and Ostergaard, L. (2016). A noncanonical auxin-sensing mechanism is required for organ morphogenesis in *Arabidopsis*. *Gene Dev* 30, 2286-2296.
- Simonini, S., Mas, P.J., Mas, C.M.V.S., Ostergaard, L., and Hart, D.J. (2018a). Auxin sensing is a property of an unstructured domain in the Auxin Response Factor ETTIN of *Arabidopsis thaliana*. *Sci Rep-Uk* 8.
- Simonini, S., Stephenson, P., and Ostergaard, L. (2018b). A molecular framework controlling style morphology in Brassicaceae. *Development* 145.
- Singh, R., Ong-Abdullah, M., Low, E.-T.L., Manaf, M.A.A., Rosli, R., Nookiah, R., Ooi, L.C.-L., Ooi, S.E., Chan, K.-L., Halim, M.A., *et al.* (2013). Oil palm genome sequence reveals divergence of interfertile species in Old and New worlds. *Nature* 500, 335-339.
- Skokan, R., Medvecká, E., Viaene, T., Vosolsobě, S., Zwiewka, M., Müller, K., Skůpa, P., Karady, M., Zhang, Y., Janacek, D.P., *et al.* (2019). PIN-driven auxin transport emerged early in streptophyte evolution. *Nature Plants* 5, 1114-1119.
- Slotte, T., Hazzouri, K.M., Ågren, J.A., Koenig, D., Maumus, F., Guo, Y.-L., Steige, K., Platts, A.E., Escobar, J.S., Newman, L.K., *et al.* (2013). The *Capsella rubella* genome and the genomic consequences of rapid mating system evolution. *Nature Genetics* 45, 831-835.
- Song, X., Wang, D., Ma, L., Chen, Z., Li, P., Cui, X., Liu, C., Cao, S., Chu, C., Tao, Y., *et al.* (2012). Rice RNA-dependent RNA polymerase 6 acts in small RNA biogenesis and spikelet development. *The Plant Journal* 71, 378-389.
- Sorefan, K., Girin, T., Liljegren, S.J., Ljung, K., Robles, P., Galvan-Ampudia, C.S., Offringa, R., Friml, J., Yanofsky, M.F., and Ostergaard, L. (2009). A regulated auxin minimum is required for seed dispersal in *Arabidopsis*. *Nature* 459, 583-U114.

Spartz, A.K., Ren, H., Park, M.Y., Grandt, K.N., Lee, S.H., Murphy, A.S., Sussman, M.R., Overvoorde, P.J., and Gray, W.M. (2014). SAUR Inhibition of PP2C-D Phosphatases Activates Plasma Membrane H⁺-ATPases to Promote Cell Expansion in Arabidopsis. *Plant Cell* 26, 2129-2142.

Steeves, T.A., and Sussex, I.M. (1989). *Patterns in plant development* (Cambridge University Press).

Stepanova, A.N., Robertson-Hoyt, J., Yun, J., Benavente, L.M., Xie, D.-Y., Doležal, K., Schlereth, A., Jürgens, G., and Alonso, J.M. (2008). TAA1-mediated auxin biosynthesis is essential for hormone crosstalk and plant development. *Cell* 133, 177-191.

Steward, R., Zusman, S.B., Huang, L.H., and Schedl, P. (1988). The dorsal protein is distributed in a gradient in early drosophila embryos. *Cell* 55, 487-495.

Stumpf, H.F. (1966). Mechanism by which Cells estimate their Location within the Body. *Nature* 212, 430-431.

Sun, B., Xu, Y., Ng, K.-H., and Ito, T. (2009). A timing mechanism for stem cell maintenance and differentiation in the Arabidopsis floral meristem. *Gene Dev* 23, 1791-1804.

Sun, J., and Li, G.S. (2020). Leaf dorsoventrality candidate gene CpARF4 has conserved expression pattern but divergent tasiR-ARF regulation in the water fern *Ceratopteris pteridoides*. *Am J Bot* 107, 1470-1480.

Suzuki, H., Kato, H., Iwano, M., Nishihama, R., and Kohchi, T. (2023). Auxin signaling is essential for organogenesis but not for cell survival in the liverwort *Marchantia polymorpha*. *The Plant Cell* 35, 1058-1075.

Swarup, R., Kramer, E.M., Perry, P., Knox, K., Leyser, H.M.O., Haseloff, J., Beemster, G.T.S., Bhalerao, R., and Bennett, M.J. (2005). Root gravitropism requires lateral root cap and epidermal cells for transport and response to a mobile auxin signal. *Nature Cell Biology* 7, 1057-1065.

Szemenyei, H., Hannon, M., and Long, J.A. (2008). TOPLESS mediates auxin-dependent transcriptional repression during Arabidopsis embryogenesis. *Science* 319, 1384-1386.

Takahashi, K., Hayashi, K.-i., and Kinoshita, T. (2012). Auxin Activates the Plasma Membrane H⁺-ATPase by Phosphorylation during Hypocotyl Elongation in Arabidopsis. *Plant Physiol* 159, 632-641.

Tan, X., Calderon-Villalobos, L.I., Sharon, M., Zheng, C., Robinson, C.V., Estelle, M., and Zheng, N. (2007). Mechanism of auxin perception by the TIR1 ubiquitin ligase. *Nature* 446, 640-645.

Tanabe, Y., Hasebe, M., Sekimoto, H., Nishiyama, T., Kitani, M., Henschel, K., Münster, T., Theissen, G., Nozaki, H., and Ito, M. (2005). Characterization of MADS-box genes in charophycean green algae and its implication for the evolution of MADS-box genes. *Proceedings of the National Academy of Sciences* 102, 2436-2441.

- Tanahashi, T., Sumikawa, N., Kato, M., and Hasebe, M. (2005). Diversification of gene function: homologs of the floral regulator FLO/LFY control the first zygotic cell division in the moss *Physcomitrella patens*.
- Tanaka, H., Hirakawa, H., Kosugi, S., Nakayama, S., Ono, A., Watanabe, A., Hashiguchi, M., Gondo, T., Ishigaki, G., Muguera, M., *et al.* (2016). Sequencing and comparative analyses of the genomes of zoysiagrasses. *DNA Res* 23, 171-180.
- Tang, C., Yang, M., Fang, Y., Luo, Y., Gao, S., Xiao, X., An, Z., Zhou, B., Zhang, B., Tan, X., *et al.* (2016). The rubber tree genome reveals new insights into rubber production and species adaptation. *Nature Plants* 2, 16073.
- Tao, Y., Ferrer, J.-L., Ljung, K., Pojer, F., Hong, F., Long, J.A., Li, L., Moreno, J.E., Bowman, M.E., and Ivans, L.J. (2008). Rapid synthesis of auxin via a new tryptophan-dependent pathway is required for shade avoidance in plants. *Cell* 133, 164-176.
- The Arabidopsis Genome, I. (2000). Analysis of the genome sequence of the flowering plant *Arabidopsis thaliana*. *Nature* 408, 796-815.
- Theissen, G., and Melzer, R. (2007). Molecular mechanisms underlying origin and diversification of the angiosperm flower. *Ann Bot* 100, 603-619.
- Thimann, K.V., and Koepfli, J. (1935). Identity of the Growth-Promoting and Root-Forming Substances of Plants. *Nature* 135.
- Tidy, A., Abu Bakar, N., Carrier, D., Kerr, I.D., Hodgman, C., Bennett, M.J., and Swarup, R. (2023). Mechanistic insight into the role of AUXIN RESISTANCE4 in trafficking of AUXIN1 and LIKE AUX1-2. *Plant Physiol.*
- Tiwari, S.B., Hagen, G., and Guilfoyle, T. (2003). The roles of auxin response factor domains in auxin-responsive transcription. *Plant Cell* 15, 533-543.
- Tiwari, S.B., Hagen, G., and Guilfoyle, T.J. (2004). Aux/IAA proteins contain a potent transcriptional repression domain. *Plant Cell* 16, 533-543.
- Tomescu, A.M. (2009). Megaphylls, microphylls and the evolution of leaf development. *Trends in plant science* 14, 5-12.
- Toriba, T., and Hirano, H.-Y. (2014). The DROOPING LEAF and OsETTIN2 genes promote awn development in rice. *The Plant Journal* 77, 616-626.
- Tomas, A., Paponov, I., and Perrot-Rechenmann, C. (2010). AUXIN BINDING PROTEIN 1: functional and evolutionary aspects. *Trends in Plant Science* 15, 436-446.
- Tsiantis, M., Schneeberger, R., Golz, J.F., Freeling, M., and Langdale, J.A. (1999). The maize rough sheath2 gene and leaf development programs in monocot and dicot plants. *Science* 284, 154-156.
- Tuskan, G.A., Difazio, S., Jansson, S., Bohlmann, J., Grigoriev, I., Hellsten, U., Putnam, N., Ralph, S., Rombauts, S., Salamov, A., *et al.* (2006). The genome of black cottonwood, *Populus trichocarpa* (Torr. & Gray). *Science* 313, 1596-1604.

Uemura, A., Yamaguchi, N., Xu, Y., Wee, W., Ichihashi, Y., Suzuki, T., Shibata, A., Shirasu, K., and Ito, T. (2018). Regulation of floral meristem activity through the interaction of AGAMOUS, SUPERMAN, and CLAVATA3 in Arabidopsis. *Plant reproduction* 31, 89-105.

Ulmasov, T., Hagen, G., and Guilfoyle, T.J. (1999a). Activation and repression of transcription by auxin-response factors. *Proceedings of the National Academy of Sciences* 96, 5844-5849.

Ulmasov, T., Hagen, G., and Guilfoyle, T.J. (1999b). Dimerization and DNA binding of auxin response factors. *Plant J* 19, 309-319.

Ulmasov, T., Liu, Z.-B., Hagen, G., and Guilfoyle, T.J. (1995). Composite structure of auxin response elements. *The Plant Cell* 7, 1611-1623.

Ulmasov, T., Murfett, J., Hagen, G., and Guilfoyle, T.J. (1997). Aux/IAA proteins repress expression of reporter genes containing natural and highly active synthetic auxin response elements. *Plant Cell* 9, 1963-1971.

Van Bel, M., Silvestri, F., Weitz, E.M., Kreft, L., Botzki, A., Coppens, F., and Vandepoele, K. (2021). PLAZA 5.0: extending the scope and power of comparative and functional genomics in plants. *Nucleic Acids Res* 50, D1468-D1474.

VanBuren, R., Wai, C.M., Keilwagen, J., and Pardo, J. (2018). A chromosome-scale assembly of the model desiccation tolerant grass *Oropetium thomaeum*. *Plant Direct* 2, e00096.

Vandenbussche, M., Horstman, A., Zethof, J., Koes, R., Rijpkema, A.S., and Gerats, T. (2009). Differential recruitment of WOX transcription factors for lateral development and organ fusion in *Petunia* and *Arabidopsis*. *The Plant Cell* 21, 2269-2283.

Vanneste, S., and Friml, J. (2009). Auxin: a trigger for change in plant development. *Cell* 136, 1005-1016.

Varshney, R.K., Chen, W., Li, Y., Bharti, A.K., Saxena, R.K., Schlueter, J.A., Donoghue, M.T.A., Azam, S., Fan, G., Whaley, A.M., *et al.* (2012). Draft genome sequence of pigeonpea (*Cajanus cajan*), an orphan legume crop of resource-poor farmers. *Nature Biotechnology* 30, 83-89.

Varshney, R.K., Shi, C., Thudi, M., Mariac, C., Wallace, J., Qi, P., Zhang, H., Zhao, Y., Wang, X., Rathore, A., *et al.* (2017). Pearl millet genome sequence provides a resource to improve agronomic traits in arid environments. *Nat Biotechnol* 35, 969-976.

Varshney, R.K., Song, C., Saxena, R.K., Azam, S., Yu, S., Sharpe, A.G., Cannon, S., Baek, J., Rosen, B.D., Tar'an, B., *et al.* (2013). Draft genome sequence of chickpea (*Cicer arietinum*) provides a resource for trait improvement. *Nature Biotechnology* 31, 240-246.

Vasco, A., Smalls, T.L., Graham, S.W., Cooper, E.D., Wong, G.K., Stevenson, D.W., Moran, R.C., and Ambrose, B.A. (2016). Challenging the paradigms of leaf evolution: Class III HD-Zips in ferns and lycophytes. *New Phytol* 212, 745-758.

Verde, I., Abbott, A.G., Scalabrin, S., Jung, S., Shu, S., Marroni, F., Zhebentyayeva, T., Dettori, M.T., Grimwood, J., Cattonaro, F., *et al.* (2013). The high-quality draft genome of peach (*Prunus persica*) identifies unique patterns of genetic diversity, domestication and genome evolution. *Nature Genetics* **45**, 487-494.

Verma, V., Ravindran, P., and Kumar, P.P. (2016). Plant hormone-mediated regulation of stress responses. *Bmc Plant Biol* **16**.

Vernoux, T., Brunoud, G., Farcot, E., Morin, V., Van den Daele, H., Legrand, J., Oliva, M., Das, P., Larrieu, A., Wells, D., *et al.* (2011). The auxin signalling network translates dynamic input into robust patterning at the shoot apex. *Mol Syst Biol* **7**, 508.

Vogel, J.P., Garvin, D.F., Mockler, T.C., Schmutz, J., Rokhsar, D., Bevan, M.W., Barry, K., Lucas, S., Harmon-Smith, M., Lail, K., *et al.* (2010). Genome sequencing and analysis of the model grass *Brachypodium distachyon*. *Nature* **463**, 763-768.

Waites, R., Selvadurai, H.R., Oliver, I.R., and Hudson, A. (1998). The PHANTASTICA gene encodes a MYB transcription factor involved in growth and dorsoventrality of lateral organs in *Antirrhinum*. *Cell* **93**, 779-789.

Wan, T., Liu, Z.-M., Li, L.-F., Leitch, A.R., Leitch, I.J., Lohaus, R., Liu, Z.-J., Xin, H.-P., Gong, Y.-B., Liu, Y., *et al.* (2018). A genome for gnetophytes and early evolution of seed plants. *Nature Plants* **4**, 82-89.

Wang, K., Wang, Z., Li, F., Ye, W., Wang, J., Song, G., Yue, Z., Cong, L., Shang, H., Zhu, S., *et al.* (2012). The draft genome of a diploid cotton *Gossypium raimondii*. *Nature Genetics* **44**, 1098-1103.

Wang, L., Kim, J., and Somers, D.E. (2013). Transcriptional corepressor TOPLESS complexes with pseudoresponse regulator proteins and histone deacetylases to regulate circadian transcription. *Proc Natl Acad Sci U S A* **110**, 761-766.

Wang, S., Li, L., Li, H., Sahu, S.K., Wang, H., Xu, Y., Xian, W., Song, B., Liang, H., Cheng, S., *et al.* (2020). Genomes of early-diverging streptophyte algae shed light on plant terrestrialization. *Nature Plants* **6**, 95-106.

Wang, W., Feng, B., Xiao, J., Xia, Z., Zhou, X., Li, P., Zhang, W., Wang, Y., Møller, B.L., Zhang, P., *et al.* (2014a). Cassava genome from a wild ancestor to cultivated varieties. *Nat Commun* **5**, 5110.

Wang, W., Haberer, G., Gundlach, H., Gläßer, C., Nussbaumer, T., Luo, M.C., Lomsadze, A., Borodovsky, M., Kerstetter, R.A., Shanklin, J., *et al.* (2014b). The *Spirodela polyrhiza* genome reveals insights into its neotenus reduction fast growth and aquatic lifestyle. *Nat Commun* **5**, 3311.

Wang, X., Wang, H., Wang, J., Sun, R., Wu, J., Liu, S., Bai, Y., Mun, J.-H., Bancroft, I., Cheng, F., *et al.* (2011). The genome of the mesopolyploid crop species *Brassica rapa*. *Nature Genetics* **43**, 1035-1039.

Waterhouse, A.M., Procter, J.B., Martin, D.M.A., Clamp, M., and Barton, G.J. (2009). Jalview Version 2—a multiple sequence alignment editor and analysis workbench. *Bioinformatics* **25**, 1189-1191.

- Weigel, D., Alvarez, J., Smyth, D.R., Yanofsky, M.F., and Meyerowitz, E.M. (1992). LEAFY controls floral meristem identity in Arabidopsis. *Cell* 69, 843-859.
- Weigel, D., and Glazebrook, J. (2006). Setting up Arabidopsis crosses. *CSH Protoc* 2006.
- Weigel, D., and Jürgens, G. (2002). Stem cells that make stems. *Nature* 415, 751-754.
- Weigel, D., and Nilsson, O. (1995). A developmental switch sufficient for flower initiation in diverse plants. *Nature* 377, 495-500.
- Weijers, D., Benkova, E., Jäger, K.E., Schlereth, A., Hamann, T., Kientz, M., Wilmoth, J.C., Reed, J.W., and Jürgens, G. (2005). Developmental specificity of auxin response by pairs of ARF and Aux/IAA transcriptional regulators. *EMBO J* 24, 1874-1885.
- Weijers, D., Schlereth, A., Ehrismann, J.S., Schwank, G., Kientz, M., and Jürgens, G. (2006). Auxin triggers transient local signaling for cell specification in Arabidopsis embryogenesis. *Dev Cell* 10, 265-270.
- Wickham, H. (2011). ggplot2. *Wiley interdisciplinary reviews: computational statistics* 3, 180-185.
- Wolpert, L. (1969). Positional information and the spatial pattern of cellular differentiation. *Journal of Theoretical Biology* 25, 1-47.
- Worden, A.Z., Lee, J.H., Mock, T., Rouzé, P., Simmons, M.P., Aerts, A.L., Allen, A.E., Cuvelier, M.L., Derelle, E., Everett, M.V., *et al.* (2009). Green evolution and dynamic adaptations revealed by genomes of the marine picoeukaryotes *Micromonas*. *Science* 324, 268-272.
- Wu, G., Lin, W.-c., Huang, T., Poethig, R.S., Springer, P.S., and Kerstetter, R.A. (2008). KANADI1 regulates adaxial–abaxial polarity in Arabidopsis by directly repressing the transcription of ASYMMETRIC LEAVES2. *Proceedings of the National Academy of Sciences* 105, 16392-16397.
- Wu, G.A., Prochnik, S., Jenkins, J., Salse, J., Hellsten, U., Murat, F., Perrier, X., Ruiz, M., Scalabrin, S., Terol, J., *et al.* (2014). Sequencing of diverse mandarin, pummelo and orange genomes reveals complex history of admixture during citrus domestication. *Nature Biotechnology* 32, 656-662.
- Wu, J., Wang, Z., Shi, Z., Zhang, S., Ming, R., Zhu, S., Khan, M.A., Tao, S., Korban, S.S., Wang, H., *et al.* (2013). The genome of the pear (*Pyrus bretschneideri* Rehd.). *Genome Res* 23, 396-408.
- Xia, R., Xu, J., and Meyers, B.C. (2017). The Emergence, Evolution, and Diversification of the miR390-TAS3-ARF Pathway in Land Plants. *Plant Cell* 29, 1232-1247.
- Xiao, N., Cao, D.S., Zhu, M.F., and Xu, Q.S. (2015). protr/ProtrWeb: R package and web server for generating various numerical representation schemes of protein sequences. *Bioinformatics* 31, 1857-1859.

- Xu, L., Xu, Y., Dong, A., Sun, Y., Pi, L., Xu, Y., and Huang, H. (2003). Novel *as1* and *as2* defects in leaf adaxial-abaxial polarity reveal the requirement for *ASYMMETRIC LEAVES1* and *2* and *ERECTA* functions in specifying leaf adaxial identity.
- Xu, T., Dai, N., Chen, J., Nagawa, S., Cao, M., Li, H., Zhou, Z., Chen, X., De Rycke, R., Rakusova, H., *et al.* (2014). Cell surface ABP1-TMK auxin-sensing complex activates ROP GTPase signaling. *Science* **343**, 1025-1028.
- Xu, T., Wen, M., Nagawa, S., Fu, Y., Chen, J.G., Wu, M.J., Perrot-Rechenmann, C., Friml, J., Jones, A.M., and Yang, Z. (2010). Cell surface- and rho GTPase-based auxin signaling controls cellular interdigitation in *Arabidopsis*. *Cell* **143**, 99-110.
- Xu, X., Pan, S., Cheng, S., Zhang, B., Mu, D., Ni, P., Zhang, G., Yang, S., Li, R., Wang, J., *et al.* (2011). Genome sequence and analysis of the tuber crop potato. *Nature* **475**, 189-195.
- Yamada, T., Yokota, S., Hirayama, Y., Imaichi, R., Kato, M., and Gasser, C.S. (2011). Ancestral expression patterns and evolutionary diversification of *YABBY* genes in angiosperms. *Plant J* **67**, 26-36.
- Yamaguchi, N., Huang, J., Xu, Y., Tanoi, K., and Ito, T. (2017). Fine-tuning of auxin homeostasis governs the transition from floral stem cell maintenance to gynoecium formation. *Nat Commun* **8**, 1125.
- Yang, J., He, H., He, Y., Zheng, Q., Li, Q., Feng, X., Wang, P., Qin, G., Gu, Y., Wu, P., *et al.* (2021). TMK1-based auxin signaling regulates abscisic acid responses via phosphorylating ABI1/2 in *Arabidopsis*. *Proc Natl Acad Sci U S A* **118**.
- Yang, Y., Hammes, U.Z., Taylor, C.G., Schachtman, D.P., and Nielsen, E. (2006). High-affinity auxin transport by the *AUX1* influx carrier protein. *Curr Biol* **16**, 1123-1127.
- Yifhar, T., Pekker, I., Peled, D., Friedlander, G., Pistunov, A., Sabban, M., Wachsman, G., Alvarez, J.P., Amsellem, Z., and Eshed, Y. (2012). Failure of the Tomato Trans-Acting Short Interfering RNA Program to Regulate *AUXIN RESPONSE FACTOR3* and *ARF4* Underlies the Wiry Leaf Syndrome. *Plant Cell* **24**, 3575-3589.
- Yip, H.K., Floyd, S.K., Sakakibara, K., and Bowman, J.L. (2016). Class III HD-Zip activity coordinates leaf development in *Physcomitrella patens*. *Dev Biol* **419**, 184-197.
- Young, N.D., Debellé, F., Oldroyd, G.E.D., Geurts, R., Cannon, S.B., Udvardi, M.K., Benedito, V.A., Mayer, K.F.X., Gouzy, J., Schoof, H., *et al.* (2011). The *Medicago* genome provides insight into the evolution of rhizobial symbioses. *Nature* **480**, 520-524.
- Yu, C., Qiao, G., Qiu, W., Yu, D., Zhou, S., Shen, Y., Yu, G., Jiang, J., Han, X., Liu, M., *et al.* (2018). Molecular breeding of water lily: engineering cold stress tolerance into tropical water lily. *Horticulture Research* **5**, 73.
- Yu, J., Hu, S., Wang, J., Wong, G.K., Li, S., Liu, B., Deng, Y., Dai, L., Zhou, Y., Zhang, X., *et al.* (2002). A draft sequence of the rice genome (*Oryza sativa* L. ssp. *indica*). *Science* **296**, 79-92.

Yu, Y., Tang, W., Lin, W., Li, W., Zhou, X., Li, Y., Chen, R., Zheng, R., Qin, G., Cao, W., *et al.* (2023). ABLs and TMKs are co-receptors for extracellular auxin. *Cell* 186, 5457-5471.e5417.

Zadnikova, P., Petrasek, J., Marhavy, P., Raz, V., Vandenbussche, F., Ding, Z., Schwarzerova, K., Morita, M.T., Tasaka, M., Hejatko, J., *et al.* (2010). Role of PIN-mediated auxin efflux in apical hook development of *Arabidopsis thaliana*. *Development* 137, 607-617.

Zadnikova, P., Wabnik, K., Abuzeineh, A., Gallemi, M., Van Der Straeten, D., Smith, R.S., Inze, D., Friml, J., Prusinkiewicz, P., and Benkova, E. (2016). A Model of Differential Growth-Guided Apical Hook Formation in Plants. *Plant Cell* 28, 2464-2477.

Zazimalová, E., Murphy, A.S., Yang, H., Hoyerová, K., and Hosek, P. (2010). Auxin transporters--why so many? *Cold Spring Harb Perspect Biol* 2, a001552.

Zemlyanskaya, E.V., Wiebe, D.S., Omelyanchuk, N.A., Levitsky, V.G., and Mironova, V.V. (2016). Meta-analysis of transcriptome data identified TGTCNN motif variants associated with the response to plant hormone auxin in *Arabidopsis thaliana* L. *Journal of bioinformatics and computational biology* 14, 1641009.

Zhang, G.-Q., Liu, K.-W., Li, Z., Lohaus, R., Hsiao, Y.-Y., Niu, S.-C., Wang, J.-Y., Lin, Y.-C., Xu, Q., Chen, L.-J., *et al.* (2017). The *Apostasia* genome and the evolution of orchids. *Nature* 549, 379-383.

Zhang, J., Mazur, E., Balla, J., Gallei, M., Kalousek, P., Medved'ová, Z., Li, Y., Wang, Y., Prát, T., Vasileva, M., *et al.* (2020a). Strigolactones inhibit auxin feedback on PIN-dependent auxin transport canalization. *Nat Commun* 11, 3508.

Zhang, J., Zhang, X., Tang, H., Zhang, Q., Hua, X., Ma, X., Zhu, F., Jones, T., Zhu, X., Bowers, J., *et al.* (2018a). Allele-defined genome of the autopolyploid sugarcane *Saccharum spontaneum* L. *Nature Genetics* 50, 1565-1573.

Zhang, K., Wang, R., Zi, H., Li, Y., Cao, X., Li, D., Guo, L., Tong, J., Pan, Y., and Jiao, Y. (2018b). AUXIN RESPONSE FACTOR3 regulates floral meristem determinacy by repressing cytokinin biosynthesis and signaling. *The Plant Cell* 30, 324-346.

Zhang, K., Zhang, H., Pan, Y., Niu, Y., Guo, L., Ma, Y., Tian, S., Wei, J., Wang, C., Yang, X., *et al.* (2022). Cell- and noncell-autonomous AUXIN RESPONSE FACTOR3 controls meristem proliferation and phyllotactic patterns. *Plant Physiol.*

Zhang, Y., Rodriguez, L., Li, L., Zhang, X., and Friml, J. (2020b). Functional innovations of PIN auxin transporters mark crucial evolutionary transitions during rise of flowering plants. *Science Advances* 6, eabc8895.

Zhang, Z., Runions, A., Mentink, R.A., Kierzkowski, D., Karady, M., Hashemi, B., Huijser, P., Strauss, S., Gan, X., Ljung, K., *et al.* (2020c). A WOX/Auxin Biosynthesis Module Controls Growth to Shape Leaf Form. *Curr Biol* 30, 4857-4868.e4856.

Zhao, H., Gao, Z., Wang, L., Wang, J., Wang, S., Fei, B., Chen, C., Shi, C., Liu, X., Zhang, H., *et al.* (2018a). Chromosome-level reference genome and alternative splicing atlas of moso bamboo (*Phyllostachys edulis*). *GigaScience* 7.

Zhao, H., Wang, S., Wang, J., Chen, C., Hao, S., Chen, L., Fei, B., Han, K., Li, R., Shi, C., *et al.* (2018b). The chromosome-level genome assemblies of two rattans (*Calamus simplicifolius* and *Daemonorops jenkinsiana*). *Gigascience* 7.

Zhou, C., Han, L., Fu, C., Wen, J., Cheng, X., Nakashima, J., Ma, J., Tang, Y., Tan, Y., Tadege, M., *et al.* (2013). The Trans-Acting Short Interfering RNA3 Pathway and NO APICAL MERISTEM Antagonistically Regulate Leaf Margin Development and Lateral Organ Separation, as Revealed by Analysis of an *argonaute7/lobed leaflet1* Mutant in *Medicago truncatula*. *The Plant Cell* 25, 4845-4862.

Zimin, A.V., Stevens, K.A., Crepeau, M.W., Puiu, D., Wegrzyn, J.L., Yorke, J.A., Langley, C.H., Neale, D.B., and Salzberg, S.L. (2017). An improved assembly of the loblolly pine mega-genome using long-read single-molecule sequencing. *Gigascience* 6, 1-4.

Zimmermann, W. (1952). Main results of the "Telome Theory".

Zumajo-Cardona, C., and Ambrose, B.A. (2020). Phylogenetic analyses of key developmental genes provide insight into the complex evolution of seeds. *Molecular Phylogenetics and Evolution* 147, 106778.

Zumajo-Cardona, C., Vasco, A., and Ambrose, B.A. (2019). The Evolution of the KANADI Gene Family and Leaf Development in Lycophytes and Ferns. In *Plants*.